



# **TEABAG TECHNOLOGY IN LONG CHAIN ALKANE SELECTIVE OXIDATION**

A Thesis Submitted to the University of Cardiff for the  
Degree of Doctor in Philosophy

By

Yuan Shang

Chemistry Department,  
University of Cardiff

April 2014

---

## ACKNOWLEDGMENTS

---

I would like to take the opportunity to thank many people who directly or otherwise, made the writing of this thesis possible:

First of all, I would like to thank my academic supervisors Prof. Graham Hutchings and Dr. Jonathan Bartley for offering me the opportunity to pursue the research, and for their warm encouragement when I felt embarrassed and even gave up. Without their generous help, I would not be able to complete this thesis.

I would like to thank Johnson Matthey and Sasol for funding the collaborative project. I would like to thank my industrial supervisor Xavier Baucherel, and his colleague Mike Watson for their help from Johnson Matthey in both my research and the financial support.

I would also like to thank Frans Prinsloo, Nishlan Govender from Sasol. The travel to South Africa is very memorable. I would like to specially thank Chris Nicolaides, who unfortunately left us forever. He is so nice and friendly to me.

I would like to thank Don Bethell, Matt House, Rhys Lloyd, Tom Davies, who gave me great assistance and guidance in the study and technical analysis.

I would like to thank all my lab mates from lab 0.76 and lab 1.88, especially my colleagues Edouard Huguet and Sivaram Pradhan. They are so amazing and gave me so many help. They enlightened my life these years.

Outside the university I would also like to thank my family for their endless support both financial and emotional throughout. I love them.

---

## ABSTRACT

---

This thesis describes the searching, preparation, characterization and catalytic evaluation of active catalysts for the terminal selectivity of long chain linear alkanes. The focus of the thesis is the study of shape selective materials, including the organic material cyclodextrins, and the inorganic material, zeolite and zeolitic membranes. Prepared catalysts were performed with *n*-decane or *n*-hexane as models to produce the terminal oxidation products 1-decanol, 1-hexanol, decanoic acid and hexanoic acid.

Studies with the Andrews glass reactor showed a stable terminal selectivity of 5%-9% in the autoxidation of *n*-hexane in short time reactions. A comparison between the Andrews glass reactor and Parr stainless steel reactor showed that the autoxidation reactions can get higher conversion but lower terminal selectivity in the stainless steel reactor than the glass reactor.

Most of the metal/support catalysts showed very low conversion and very poor terminal selectivity. Increasing the temperature leads to higher conversion but results in more cracked products and less selectivity for oxygenated C<sub>10</sub> products. The most active catalyst was 5 w.t.% Au/TiO<sub>2</sub>. However, these catalysts did not show good terminal alcohol selectivity (<3%); whereas the cracked acid selectivity was high (32.0%). Cyclodextrin covered Au/SiO<sub>2</sub> catalysts showed limited changes in terminal selectivities (1-2%).

Zeolite 4A, silicalite-1, ZSM-5, zeolite X/Y coated catalysts were successfully synthesized with alumina and silica sphere supports. The most attractive oxidation results were performed by zeolite X/Y and zeolite 4A coated silica catalysts in *n*-hexane liquid phase oxidation,

especially for with short reaction time. With zeolite X/Y membrane, in a 30 min reaction, the terminal selectivity was 16%, while the terminal selectivity for the blank reactions was 0-9%. With longer reaction time, the terminal selectivity decreased to 6-7%. Zeolite 4A membrane can produce a terminal selectivity of 13% in 4 h reactions.

---

# CONTENTS

---

<b>Chapter 1: Introduction</b>	<b>1</b>
1.1 Significance of the thesis	2
1.2 Aim of the thesis	2
1.3 Catalysis	3
1.4 Challenges in the selective oxidation	4
1.5 Industrial applications of long chain linear alcohols	5
1.6 Current manufacture of long linear alcohols in industry	6
1.7 Alkane oxidation in literature	8
1.8 Zeolites	10
1.8.1 Zeolite composition	10
1.8.2 Shape selective application of zeolite	11
1.8.3 Synthesis of the zeolite membrane	12
1.9 The model reactions in this research	14
1.10 The research branches in this project	15
1.10.1 Supported catalyst investigations for shape selective catalysts	15
1.10.2 Teabag technology	15
1.11 References	16
<b>Chapter 2: Experimental Techniques</b>	<b>19</b>
2.1 Introduction	20
2.2 Catalyst preparation	20
2.2.1 Preparation of supported metal catalysts	20
2.2.2 Preparation of zeolite and zeolitic coated catalysts	23
2.2.3 Preparation of cyclodextrin modified catalysts	25

2.3	Catalyst characterization technique	25
2.3.1	X-ray powder diffraction	25
2.3.2	Scanning electron microscopy	27
2.3.3	Surface area method (BET)	29
2.3.4	Atomic absorption spectroscopy	30
2.3.5	X-ray photoelectron spectroscopy	31
2.4	Reactors used in the project	32
2.4.1	The Parr multiple stainless steel reactor system	32
2.4.2	The Andrews glass reactor system	34
2.5	Analysis and qualification of reaction products	35
2.5.1	Analysis by Gas Chromatography	35
2.5.2	Quantification of the products via response factor	36
2.5.2.1	Use of internal standard	36
2.5.2.2	Calculations of relative response factors of each compound	36
2.5.2.3	Quantification and analysis of the reaction	39
2.6	References	41
	<b>Chapter 3: Andrews Glass Reactor</b>	<b>42</b>
3.1	Introduction	43
3.2	Experimental	44
3.2.1	Apparatus and reaction	44
3.2.2	Safety operating procedure	45
3.2.3	Characterization technique	48
3.3	Results	48
3.3.1	Andrews glass reactor in blank hexane oxidation	48

3.3.1.1	Comparison between Andrews glass reactor and stainless steel reactor	49
3.3.1.2	Repeat Iglesia's blank reaction	51
3.3.1.3	The unknown products in analysis	51
3.3.1.4	Application of aqua regia as washing agent	52
3.3.1.5	Time on-line reactions	53
3.3.1.6	Discussion	55
3.3.2	Reaction with Mn-ZSM5	56
3.4	Conclusion	57
3.5	References	58
<b>Chapter 4: Catalytic investigation for teabag coating</b>		<b>60</b>
4.1	Introduction	61
4.2	Experimental	62
4.2.1	Metal/support catalysts	62
4.2.2	Rh/Ru loaded catalysts	63
4.3	Results	64
4.3.1	Pd, Au, Pt loaded supported catalysts	64
4.3.2	Higher temperature reactions	66
4.3.3	Discussion	68
4.3.4	Use of a radical scavenger	68
4.3.5	Development of the catalyst preparation method	70
4.3.6	Ru and Rh loaded catalysts	75
4.3.6.1	$\alpha$ -phase alumina powder support	76
4.3.6.2	$\gamma$ -phase alumina powder support	78
4.3.6.3	Loading with alumina spheres	83
4.4	Conclusion	85

4.5	References	87
<b>Chapter 5: Cyclodextrin covered catalysts</b>		<b>88</b>
5.1	Introduction	89
5.2	Cyclodextrins as catalyst modifiers	91
5.3	Experimental	95
	5.3.1 Preparation of CD covered catalysts	95
	5.3.2 Catalyst testing	96
5.4	Results	97
	5.4.1 BET analysis	97
	5.4.2 Activity of CDs	98
	5.4.2.1 Activity of CDs under reaction conditions	98
	5.4.2.2 Activity of CDs with the addition of radical scavenger	100
	5.4.3 CD modified Au/SiO <sub>2</sub>	101
	5.4.3.1 The fully covered Au/SiO <sub>2</sub>	101
	5.4.3.2 Different level of CD coverage over catalysts	102
	5.4.3.3 Cyclodextrin modified catalyst recycling	104
	5.4.4 CD modified Au/HCl treated SiO <sub>2</sub>	105
5.5	Conclusion	107
5.6	References	107
<b>Chapter 6: Teabag Technology</b>		<b>109</b>
6.1	Introduction	110
6.2	The teabag technology project	110
6.3	Zeolite membrane synthesis	112
	6.3.1 Preparation method	112

6.3.2	Supports in zeolite coating	116
6.3.3	Other factors for preparation	119
6.3.4	Deactivation	123
6.4	Experimental	124
6.4.1	Preparation of coated catalysts	124
6.4.1.1	Zeolite A coated samples with silica powder support	125
6.4.1.2	Zeolite 4A coated samples with sphere supports	126
6.4.1.3	Silicalite-1 coating with sphere supports	127
6.4.1.4	ZSM-5 coating with $\alpha$ - and $\gamma$ -Al <sub>2</sub> O <sub>3</sub>	128
6.4.2	Reaction conditions	129
6.4.3	Characterization	130
6.5	Results	130
6.5.1	Zeolite A coating with powder support	130
6.5.1.1	Coated SiO <sub>2</sub> in liquid phase reaction	130
6.5.1.2	Discussion	147
6.5.1.3	Coated MgO in gas phase reaction	147
6.5.1.4	Discussion	156
6.5.1.5	Conclusion	157
6.5.2	Zeolite A coating with sphere support	158
6.5.2.1	Results	159
6.5.2.2	Results and discussion	161
6.5.3	Silicalite-1 coating with sphere support	162
6.5.3.1	S1 coating with $\alpha$ -alumina spheres	162
6.5.3.2	S1 coating with $\gamma$ -alumina spheres	167
6.5.3.3	Discussion and conclusion	172
6.5.4	ZSM-5 coating with alumina sphere support	173

6.5.4.1 ZSM-5 coating with $\alpha$ -alumina spheres	173
6.5.4.2 ZSM-5 coating with $\beta$ -alumina spheres	182
6.5.4.3 Discussion	189
6.5.5 Zeolite X/Y coating with silica sphere support	191
6.5.5.1 Results	191
6.5.5.2 Discussion	192
6.5.6 Zeolite A coating in hexane oxidation	193
6.6 Conclusion	196
6.7 References	198
<b>Chapter 7: Conclusions</b>	<b>201</b>

---

## ABBREVIATIONS

---

°C	Degrees centigrade
Å	Angstrom
AAS	Atomic Absorption Spectroscopy
Al <sub>2</sub> O <sub>3</sub>	Alumina
Bar	Unit of Pressure
BET	Brunauer Emmett Teller
cm	Centimetre
EDX	Energy Dispersive X-ray Spectroscopy
FID	Flame Ionisation Detector
NMR	Nuclear Magnetic Resonance
g	Grams
GC	Gas Chromatography
GC-MS	Gas Chromatography Mass-Spectrometer
MgO	Magnesium Oxide
m	Metre
min	Minute
mL	Millilitre
ppm	Parts Per Million
psi	Pounds Per Square Inch
S1	Silicalite-1
SEM	Scanning Electron Microscopy
SiO <sub>2</sub>	Silica
TEM	Transmission Electron Microscopy
VMgO	Vanadium-Magnesium Mixed Oxides

XPS	X-Ray Photoelectron Spectroscopy
XRD	X-Ray Diffraction
XRF	X-ray Fluorescence
ZSM-5	Zeolite Socony Mobil – 5

# *CHAPTER 1*

## *Introduction*

---

# INTRODUCTION

---

## 1.1 Significance of the thesis

Organic compounds, such as alcohols, aldehydes, ketones, epoxides and acids, are widely used in everyday life and industry. Therefore, the production of these compounds is of key importance in modern chemistry research and to the chemical industry. There are many ways to produce these oxygen-containing organic compounds, but oxidation of saturated hydrocarbons is one of the most significant. It is widely known that there are large quantities saturated hydrocarbons obtained from natural gas and petroleum [1]; in fact in South Africa, Sasol (one of the sponsors of this thesis) produces large amount of alkanes in its Fischer Tropsch process [2]. Alkanes, as a relatively environmentally friendly and low cost feedstock, are ideal for the production of those valuable organic compounds. Various products can be obtained by oxidation of alkanes. In this thesis, the study focused on the terminal oxidation of long chain alkanes, whose products can be used in the manufacture of plasticizers, lubricants, solvents, surfactants and materials for further chemical functionalization.

## 1.2 Aim of the thesis

The thesis is a fundamental study into the terminal oxidation of long chain *n*-alkanes, using *n*-decane and *n*-hexane as model compounds to produce 1-decanol, decanoic acid or 1-hexanol and hexanoic acid (**Figure 1.1**) in liquid phase reactions. There are two challenges in this study: how to enhance the activity of the reaction and how to control the regioselectivity of the oxidation. To overcome the challenges, catalysis was introduced into the project. The project was collaboration between Cardiff University, Johnson Matthey and Sasol.

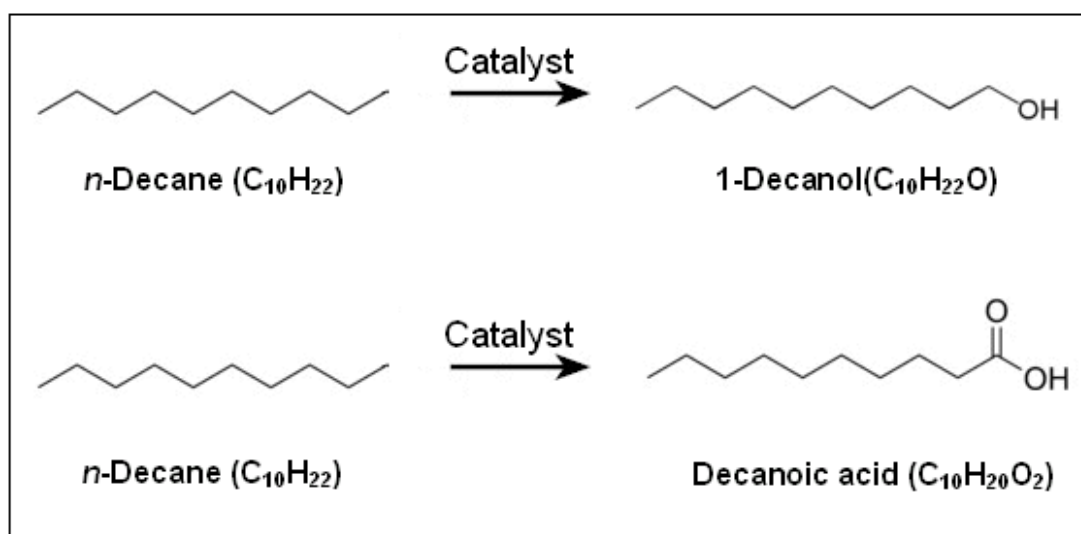


**Figure 1.1 Aim of the thesis – terminal oxidation of decane**

### 1.3 Catalysis

Catalysis is the change in rate of a chemical reaction due to the participation of a catalyst. Unlike other reagents that participate in the chemical reaction, a catalyst is not consumed by the reaction itself. A catalyst may participate in multiple chemical transformations. Catalysts that speed the reaction are called positive catalysts. Substances that interact with catalysts to slow the reaction are called inhibitors (or negative catalysts). Substances that increase the activity of catalysts are called promoters, and substances that deactivate catalysts are called catalytic poisons. A catalyst does not change the thermodynamics of the reaction, but simply provides a new and easier pathway by lowering the activation energy. A good catalyst must possess both high activity and long-term stability. But its single most important attribute is its selectivity, which reflects its ability to direct conversion of the reactant(s) along one specific pathway [3].

Catalysis can be divided into three categories: homogeneous catalysis, heterogeneous catalysis

and biocatalysis. Homogeneous catalysis covers all the cases where catalysts and reactants are in the same phase, while heterogeneous catalysis covers all the cases where catalysts and reactants are in different phases. Homogeneous catalysts exhibit a higher activity per unit mass of metal than heterogeneous catalysts [4], however, it is difficult to recover the catalyst. In heterogeneous catalysis, there is little difficulty in separating and recycling the catalyst. Biocatalysis is a rather special case, somewhere between the homogeneous and heterogeneous catalysis. In most cases, biocatalysts are enzymes, which are often seen as a separate catalyst group [5].

#### **1.4 Challenges in the selective oxidation of alkanes**

Economic factors and technological innovations often induce changes in the chemical feedstocks used to produce commodity organic chemicals. These reasons caused alkanes to replace acetylene in many commercial processes several decades ago. Alkanes, as the least expensive and most abundant hydrocarbon resource, have a very important potential role in the chemical industry. However, very few selective methods are available for converting alkanes into more valuable products. Furthermore, several desirable reactions utilizing alkanes are not thermodynamically favourable at reasonable temperatures. Even where alkanes are used, their transformations are often inefficient. This is because alkanes are saturated and lack functional groups. Hydrocarbons can only undergo reaction after cleavage of C-H or C-C bonds. In most instances, the strength of the C-H bonds involved controls the rate and selectivity of oxidation turnovers [6, 7]. As a result, preferential oxidation specific C-H bonds, except as dictated by their relative bond strengths, remains a formidable challenge. C-H bonds at terminal positions in *n*-alkanes are  $\sim 13$  kJ/mol stronger than secondary C-H bonds (e.g., 410 kJ/mol vs. 397 kJ/mol for propane) [8]; thus, terminal oxidation selectivities are typically below 10% in C<sub>10</sub>-

alkanes, unless spatial constraints, imposed by the H-abstractor or by the structure of the voids around active sites, favour terminal attachment or inhibit access to secondary or tertiary carbons.

Another problem in the selective oxidation of alkanes is the initial product of alkane oxidation is often more reactive toward the oxidant than the alkane itself. Overoxidation of the initial product will dramatically reduce the desired product yield.

### **1.5 Industrial applications of long chain linear alcohols**

Linear primary alcohols are amphiphiles composed of a polar part (hydroxyl group) and an apolar part (alkane chain). The amphiphile molecules can be utilized as surfactants. The limited solubility makes them aggregate in the interface between two phases to form micelles. Therefore, linear primary alcohols are good detergents. They are also used in the composition of plastics and cement, where they can increase the fluidity of the material. Another industrial application of linear alcohols is that they are very important materials for further chemical functionalization, based on the large number of reactions the hydroxyl group may undergo (**Figure 1.2** [9]). The resulting products are important commercial intermediates.

Terminal Linear alcohol	+ Oxygen	→ Aldehyde + carboxylic acid
	+ Alkali Melt	→ carboxylic acid
	+ Alkali	→ Dimeric Alcohol
	+ Proton	→ Ether, Olefin
	+ Alkyne	→ Vinyl Ether
	+ Carboxylic acid	→ Ester
	+ Hydrogen Halide	→ Alkyl Halide
	+ Ammonia/Amine	→ Amine
	+ Aldehyde/Ketone	→ Acetal
	+ Sulfide	→ Thiol
	+Alcoholate/H <sub>2</sub> S	→ Xanthate
	+Metal	→ Metal alkoxide

**Figure 1.2 Typical examples of reactions that can undergo terminal alcohols [9]**

### **1.6 Current manufacture of long linear alcohols in industry**

Two basic dominating industrial-scale processes are used to manufacture linear alcohols: the Ziegler process and the oxo synthesis (hydroformylation) starting from petrochemical feedstocks [10]. The Ziegler chemistry process contains five steps: hydrogenation, ethylation, growth reaction, oxidation and hydrolysis. The starting material is ethylene (**Figure 1.3**).

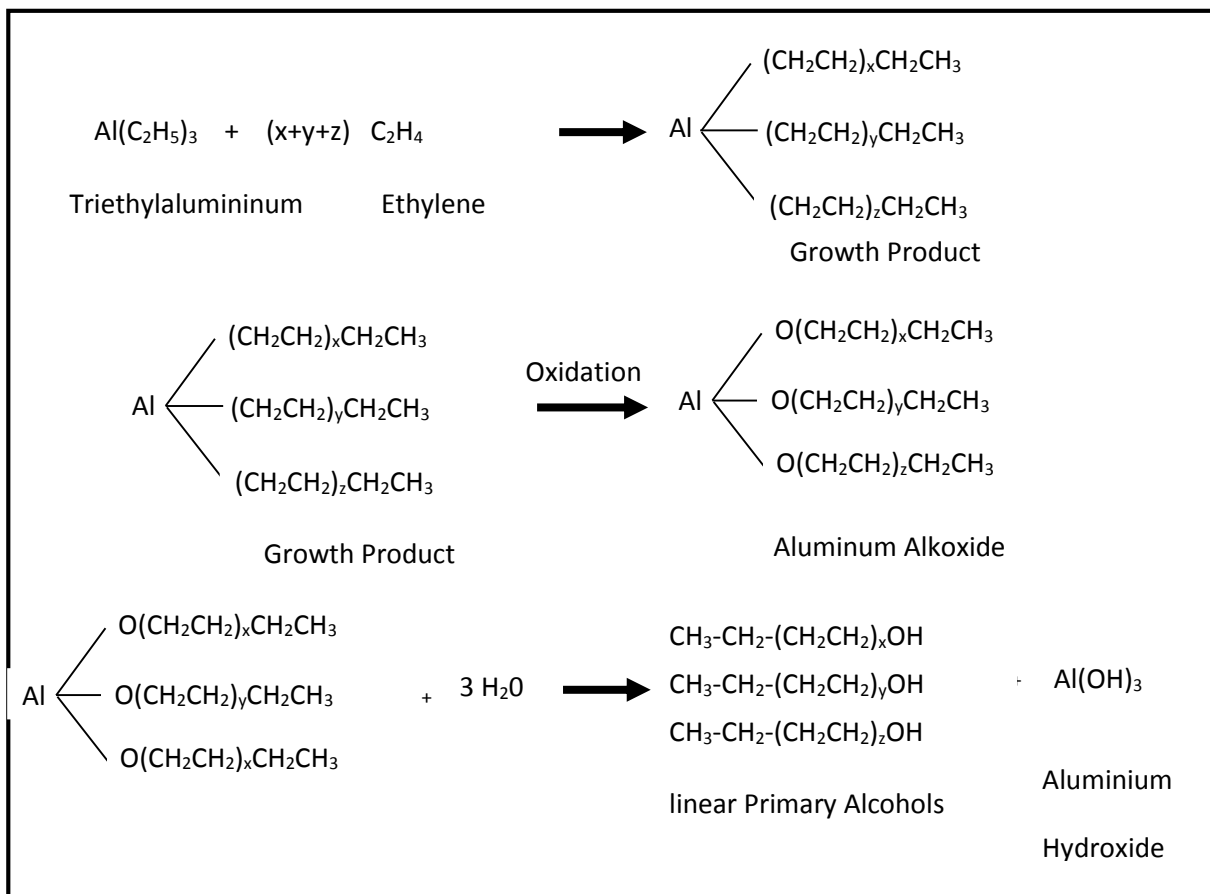


**Figure 1.3 The multi-step Ziegler process**

$\text{Al}_2\text{O}_3$  is not recycled during the reaction so it is not a catalytic process.

The second industrial route is hydroformylation, also known as the oxo process (**Figure 1.4**).

The process typically is accomplished by treatment of an alkene with high pressures (10-100 atm) of carbon monoxide and hydrogen at temperatures between 40 and 200°C [11]. Transition metal catalysts are required. It is a heterogeneous catalytic process.

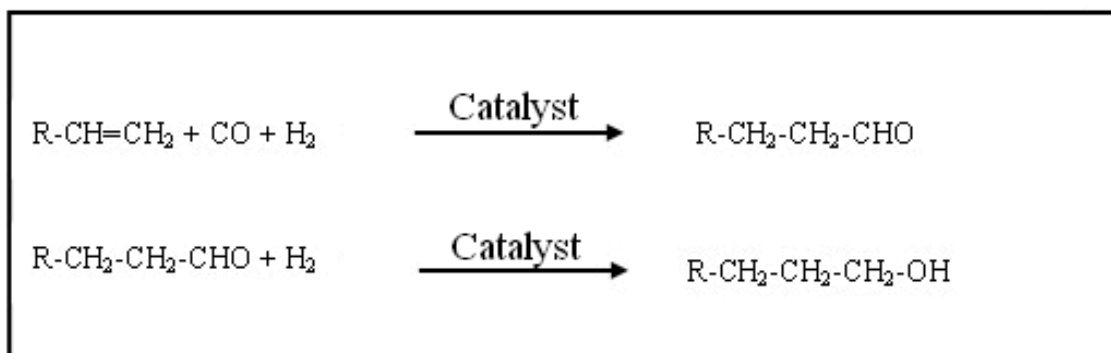


**Figure 1.4 Two-step oxo processes**

Both the Ziegler process and the oxo process use alkenes as the feedstocks and require multi-step reactions. A process using long chain linear alkanes as the feed would be less expensive and more environmentally friendly.

### 1.7. Alkane oxidation in literature

Literature covering long chain alkane oxidation is limited. Most of the literature discussing alkane activation relates to short chain linear alkanes (e.g., methane to butane) or cyclic hydrocarbons (e.g., cyclohexane), in which different catalytic approaches were presented.

A bio-catalytic approach has been used for the alkane oxidation. It was reported that enzymes (mono-oxygenase) can oxidize the terminal group of linear alkane with oxygen [12]. The catalytic active centre of the mono-oxygenase (Fe) is surrounded by a large protein structure, which controls the substrate to the oxidation centre.

Homogeneous catalysts were also reported in the terminal selective oxidation of alkanes. In the literature, in the presence of tetra-*n*-butylammonium salts of vanadium-containing polyphosphomolybdates  $[PMo_{11}VO_{40}]^{4-}$  and  $[PMo_6V_5O_{39}]^{12-}$ , *n*-Octane can be efficiently oxidized by hydrogen peroxide in acetonitrile. The terminal selectivity was reported to be 8.2%

[13].

However, due to the scope of this project, only heterogeneous catalysts were available to be coated by shape selective materials. Therefore, this review is focused on heterogeneous catalysts. Compared with biocatalysis and homogeneous catalysis, heterogeneous catalysis is preferred in industry because it is easier to operate and less expensive. There have been some attractive catalysts reported in the terminal oxidation of alkanes using heterogeneous catalysts. In gas phase studies, Mathebula reported a dehydrogenation process to produce the terminal alcohol using *n*-hexane as the reactant [14]. Following this method, VMgO was employed as the catalyst for the dehydrogenation of *n*-hexane to the terminal hexene. The conversion was reported to be 5% with a terminal selectivity less than 2%. Then, hydroxylation of alkene was applied by a two-step process, using sodium perborate followed by oxidation over H<sub>2</sub>O<sub>2</sub>/NaOH to obtain the terminal alcohol.

In liquid phase studies, the key results were reported by Thomas for *n*-hexane oxidation in liquid phase [15-21]. In his study, Thomas used ALPO catalysts with air as the oxidant. The terminal selectivity can be extremely high (up to 8.7% conversion, 65.5% selectivity with Co-ALPO-18). Iglesia [22] tried to reproduce Thomas's results under similar experimental conditions using Mn-ALPO catalysts. However the conversion was quite low (0.02-0.05%), while the terminal selectivity was 7% only. Iglesia concluded that Mn-ALPO did not lead to any preference for terminal selectivity, in contradiction with Thomas' results. Iglesia published his own results using Mn-ZSM5 as the catalyst (**Table 1.1**) [23].

Unlike Thomas's study, Iglesia noticed the autoxidation reaction and demonstrated a clear

difference in the terminal selectivity in the presence of catalysts. It was clear that when the catalyst was present, the terminal selectivity was initially high (24%), but the selectivity declined when conversion increased. In contrast the terminal selectivity in the autoxidation was always 7-8%.

**Table 1.1 Iglesia's results for oxidation of *n*-hexane with Mn-ZSM-5 catalysts**

<b>Time (hours)</b>	<b>Conversion (%)</b>	<b>Terminal selectivity (%) with Mn-ZSM-5</b>	<b>Terminal selectivity (%) Autoxidation</b>
0.5	0.007	24	7
2.5	0.013	18.5	8
4	0.047	15	8
7	0.1	10	7

## **1.8. Zeolites**

### **1.8.1 Zeolite composition.**

Zeolites are microporous crystalline solids with well-defined structures. Generally they contain silicon, aluminium and oxygen in their framework. Structurally, they are complex, crystalline inorganic polymers based on an infinitely extending three-dimensional, four-connected framework of  $\text{AlO}_4$  and  $\text{SiO}_4$  tetrahedra linked to each other by the sharing of oxygen ions (**Figure 1.5**). Each  $\text{AlO}_4$  tetrahedron in the framework bears a net negative charge which is balanced by an extra-framework cation. The framework structure contains channels or interconnected voids that are occupied by the cations and water molecules. The cations are mobile and ordinarily undergo ion exchange. The water may be removed reversibly, generally by the application of heat, which leaves intact a crystalline host structure permeated by the

micropores and voids which may amount to 50% of the crystals by volume [24].

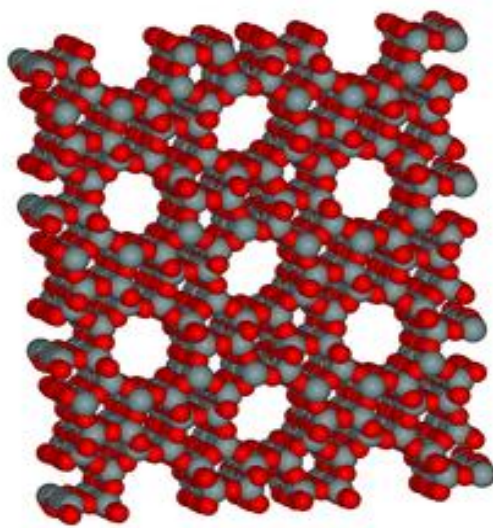


**Figure 1.5** The microporous molecular structure of a zeolite (ZSM-5)

### 1.8. 2 Shape selective application of zeolite

Due to the very regular pore structure of molecular dimensions, zeolites are well-known as a shape selective material. The maximum size of the molecular or ionic species that can enter the pores of a zeolite is controlled by the dimensions of the channels, which is usually less than 10 Å.

Zeolite shape selectivities can be distinguished into three types, depending on whether pore size limits the entrance of the reacting molecule, or the departure of the product molecule, or the formation of certain transition states (**Figure 1.6**).

- Reactant selectivity occurs when only parts of the reactant molecules are small enough to diffuse through the catalyst.
- Product selectivity occurs when some of the products formed within the pores are too bulky to diffuse out as observed products. They are either converted to less bulky

molecules (e.g., by equilibration) or eventually deactivate the catalyst by blocking the pores.

- Restricted transition state selectivity occurs when certain reactions are prevented because the corresponding transition state would require more space than available in the cavities. Neither reactant nor potential product molecules are prevented from diffusing through the pores. Reactions requiring smaller transition states proceed unhindered.

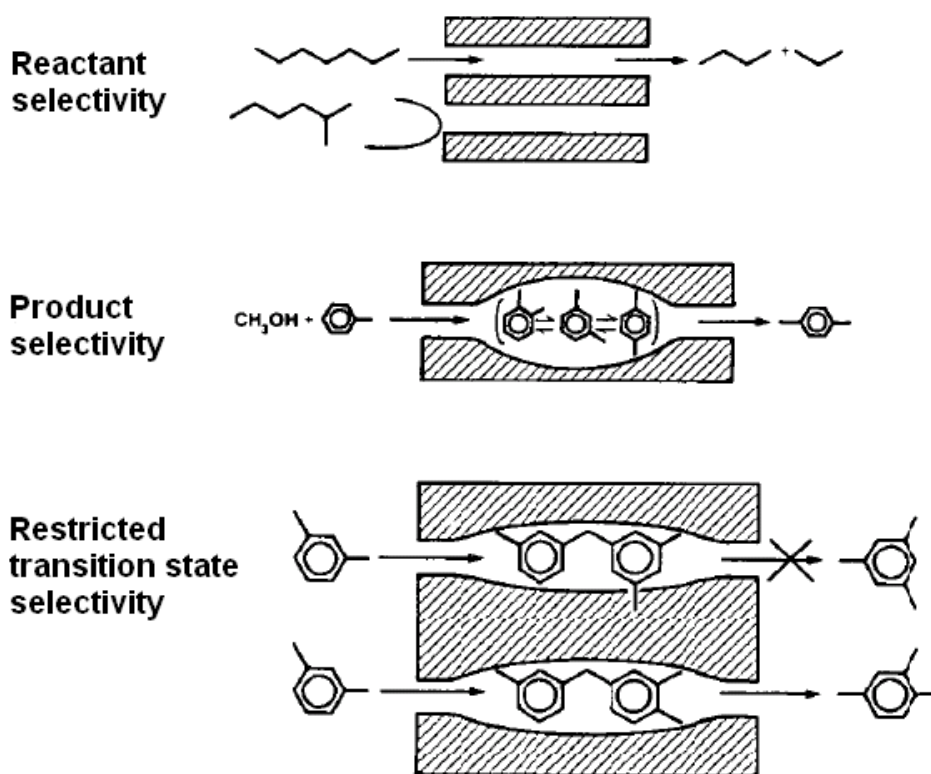


Figure 1.6 The type of shape selectivities [25]

### 1.8.3 Synthesis of the zeolite membrane

As a well-known shape selective catalyst, zeolites can be synthesized as membrane for the purpose of separation, adsorption or for the selective reaction. An ideal zeolite membrane

combines the general advantages of inorganic membranes (temperature stability, solvent resistance) with perfect shape selectivity. A continuous zeolite membrane can principally discriminate the components of gaseous or liquid mixtures dependent on their molecular size.

Several methods for the preparation of the zeolite coatings can be found in the literature.

1) Slurry coating or wash-coating, in which the zeolite is brought onto the support from a wash-coat solution, containing precursors of binders based on alumina, zirconia, silica, titania or silica-alumina. The coatings are calcined to obtain bonding of the crystallites to the support surface [26]. This method yields crystal layers which have a low continuity and a limited accessibility, since they are partly covered by the macroporous wash-coating.

2) Dry gel conversion, in which a gel containing the alumino-silicate precursor, water and template, is brought onto the support, dried and subsequently crystallized by contacting with steam at 105-150°C [27]

3) *In situ* coating, the most widely used method recently, in which the crystals are directly grown close to, or on the support either from a gel or a solution[28-41]. In this way, coatings may be grown that have a high continuity and can be optimized for use as either a membrane or a catalyst.

Although typical zeolite coating synthesis can be carried out in a dry gel, it is more common today to synthesize zeolite coatings by a hydrothermal method in dilute aluminosilicate systems in which the amorphous gel phase is not present. The first so called ‘clear solution’ (or ‘clear to eye solution’) system that produced zeolite NaA was reported at the International Zeolite Association (IZA) meeting in Tokyo in 1986 [28]. The batch composition in it formed the starting point of the present work in clear solution. One of the advantages of the clear solution

is it permits the use of *in situ* observations using light scattering techniques to study the synthesis[29], especially the nucleation and crystal growth processes occurring within the solution phase.

Another important factor in the zeolite membrane synthesis is the selection of support. Generally support materials should be chosen that are readily available, attrition resistant and chemically stable. For the purposes of the reaction, the most widely used supports were alumina and silica. More details of the literature review are presented in **Chapter 6**.

### 1.9 The model reactions in this research

The basic idea of the project is using shape-selective materials (e.g., cyclodextrins and zeolites) to realize the terminal selective oxidation of long chain alkanes. In the studies, *n*-hexane and *n*-decane were selected as the models to produce the linear alcohols. Cyclodextrins were applied as an organic shape selective material, whereas zeolites were used as inorganic shape selective materials. The shape selective catalysts were built by the active supported catalyst substrate and a continuous shape-selective membrane layer composed of shape-selective materials (e.g., cyclodextrin or zeolite covered catalysts). An ideal catalyst system following the principle of the idea is shown in the **Figure 1.7**.

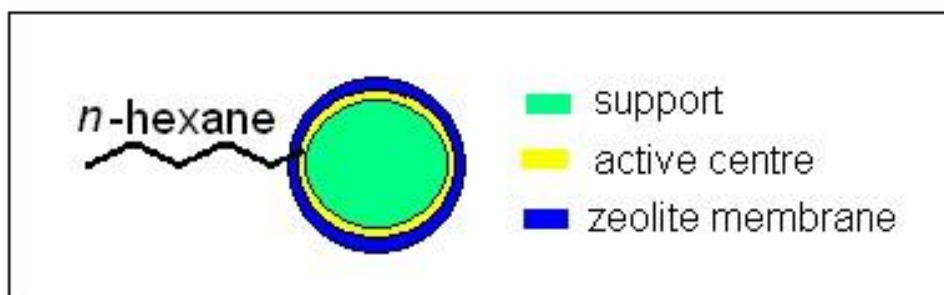


**Figure 1.7** The ideal shape-selective catalyst system

Therefore, the typical reactions were three phase reactions between gaseous (oxygen), liquid (*n*-hexane or *n*-decane) and solid catalysts, which are often encountered in the chemical industry. The advantages of liquid phase reactions are the relatively lower reaction temperatures and higher time-yields than gas phase reaction; the disadvantages are the products must be separated and purified afterwards, and the stability of catalysts also needs to be considered.

## **1.10 The research branches in the project**

### **1.10.1 Supported catalyst investigations for shape selective catalysts**

As shown in the **Figure 1.7**, the shape selective catalysts were built by the active supported catalyst substrate and a continuous shape-selective membrane layer composed by shape-selective materials (e.g., cyclodextrins or zeolites covered catalysts). Therefore, the first step of the research is to find the proper active supported catalysts.

### **1.10.2 Teabag technology**

Teabag catalysts prepared by teabag technology is an idea that zeolite coatings work as the teabag to control the diffusion of reactants to the active sites in a specific configuration that only allows the oxidation of the terminal position. Small aggregates of zeolite crystals as a coating on the surface of a catalyst have improved external mass transfer characteristics and a high internal accessibility, especially in fast liquid phase and gas/liquid phase reactions [42]. In the project zeolites with suitable pore size were selected, so that only the wanted reactant and product can pass through the outer coating to an oxidation catalyst underneath. The catalyst selectivity is determined by the molecules it will allow to diffusion through the zeolite coating

to the activate catalyst beneath. In **chapter 6**, the synthesis and reaction tests of catalysts with zeolite A, MFI, zeolite X coatings are discussed in details.

## 1.11 References

- [1] G. Centi, F. Cavani, F. Trifiro, *Selective Oxidation by Heterogeneous Catalysis*, Kluwer, Academic/Plenum Publishers, (2001), 26.
- [2] M.E. Dry, *Journal of Chemistry Technology and Biotechnology*, 77, (2002), 43.
- [3] *Principles and practice of heterogeneous catalysis*, J.M. Thomas, W.J. Thomas, VCH Publishers, (2005).
- [4] *Industrial catalysis*, J. Hagen, Wiley-VCH, (2006).
- [5] *Catalysis: concepts and green applications*, G. Rothenberg, Wiley-VCH, (2008).
- [6] C. Batiot, B.K. Hodnett, *Applied Catalysis A: General*, 127, (1996), 179.
- [7] J.A. Labinger, *Journal of Molecular Catalysis A: Chemical*, 220, (2004), 27.
- [8] D.F. McMillen, K.E. Lewis, G.P. Smith, D.M. Golden, *Journal of Physical Chemistry*, 86, (1982), 709.
- [9] *All about the fatty alcohols*, Condea, (2000).
- [10] U.R. Kreutzer, *Journal of the American Oil Chemists' Society*, 61, (1984), 343.
- [11] The Fischer-Tropsch archive, <http://www.fischer-tropsch.org/>
- [12] M. Baik, M. Newcomb, R.A. Friesner, S.J. Lippard, *Chemical Reviews*, 103, (2003), 2385.
- [13] B.R. Cook, T.J. Reinert, K.S. Suslick, *Journal of the American Chemical Society*, 108, (1986), 7281.
- [14] H.B. Friedrich, N. Govender, M.R. Mathebula, *Applied Catalysis A: General*, 297, (2006), 81.
- [15] J.M. Thomas, R. Raja, G. Sankar, R.G. Bell, *Nature*, (1999), 227.

- [16] R. Raja, J.M. Thomas, *Chemical Communications*, (1998), 1841.
- [17] R. Raja, G. Sankar, J.M. Thomas, *Journal of the American Chemistry Society*, 121, (1999), 119.
- [18] J.M. Thomas, R. Raja, G. Sankar, R. G. Bell, *Studies in Surface Science and Catalysis*, 130, (2000), 887.
- [19] R. Raja, G. Sankar, J.M. Thomas, *Angewandte Chemistry*, 39, (2000), 231.
- [20] J.M. Thomas, R. Raja, G. Sankar, R.G. Bell, *Accounts of Chemical Research*, 34, (2001), 191.
- [21] R. Raja, J.M. Thomas, *Journal of Molecular Catalysis A*, 3, (2002), 181.
- [22] B. Modén, B. Zhan, J. Dakka, J. G. Santiesteban, E. Iglesia, *Journal of Physical Chemistry*, 111, (2007), 1402.
- [23] B. Zhan, B. Modén, J. Dakka, J.G. Santiesteban, E. Iglesia, *Journal of Catalysis* 245, (2007), 316.
- [24] N. van der Puil, F.M. Dautzenberg, H. van Bekkum, J.C. Jansen, *Microporous and Mesoporous Materials*, 27, (1999), 95
- [25] Web: division of fuel chemistry American chemical society, [http://www.chemdex.org/chemistry\\_link/american\\_chemical\\_society\\_acs\\_division\\_fuel\\_chemistry](http://www.chemdex.org/chemistry_link/american_chemical_society_acs_division_fuel_chemistry)
- [26] E.R. Geus, A.E. Jansen, J. Schoonman, H. van Bekkum, *Studies in Surface Science and Catalysis*, Elsevier, (1991).
- [27] M. Matsukata, *Chemistry Communication*, (1996),1441.
- [28] P. Wenqin, S. Ueda and M. Koizumi, *Proceedings of the 7<sup>th</sup> International Zeolite Conference*(Eds. Y. Murakami, A. Lijima and J.W. Ward), Elsevier, (1986),177.
- [29] L. Gora, K. Streletzky, R.W. Thompson, G.D.J. Phillies, *Zeolites* 18, (1997),119.

- [30] T. Cetin, M. Tatlier, A. Erdem-Senatalar, U. Demirler, M. Urgen, *Microporous and Mesoporous Materials*, 47, (2001), 1
- [31] O. Andac, S.M.T elli, M. Tatlier, A. Erdem-Senatalar, *Microporous and Mesoporous Materials*, 88, (2006), 72.
- [32] Z. Zhou, J. Yang, Y. Zhang, L. Chang, W. Sun, J. Wang, *Separation and Purification Technology*, 55, (2007), 392.
- [33] Z. Wang, J. Hedlund, J. Sterte, *Microporous and Mesoporous Materials*, 52, (2002), 191.
- [34] M. Tatlier, M. Demir, B. Tokay, A. Erdem-Senatalar, L. Kiwi-Minsker, *Microporous and Mesoporous Materials*, 101, (2007), 274.
- [35] J.C. Jansen, J.H. Koegler, H. van Bekkum, H.P.A. Calis, C.M. van den Bleek, F. Kapteijn, J.A. Moulijn, E.R. Geus, N. van der Puil, *Microporous and Mesoporous Materials* 21, (1998), 273.
- [36] H. Kalipcilar, A. Culfaz, *Microporous and Mesoporous Materials* 52, (2002), 39
- [37] K. Aoki, K. Kusakabe, S. Morooka, *Journal of Membrane Science*, 141, (1998), 197.
- [38] Collier, Paul John, Golunskin, Stanislaw Edmund, U.S. Patent No.0032628, 2005.
- [39] P. Collier, S. Golunski, C. Malde, J. Breen, R. Burch, *Journal of the American. Chemistry. Society.*, 125, (2003), 12414.
- [40] N. Nishiyama, K. Ichioka, D. Park, Y. Egashira, K. Ueyama, L. Gora, W. Zhu, F. Kapteijn, J.A. Moulijn, *Industrial & Engineering Chemistry Research*, 43, (2004), 1211.
- [41] J.K. Edwards, B.E. Solsona, P. Landon, A.F. Carley, A. Herzing, C.J. Kiely, G.J. Hutchings, *Journal of Catalysis*, 235, (2005), 69.
- [42] *Introduction to zeolite science and practice*, Herman van Bekkum, New York: Elsevier Science B.V., (2001).

**CHAPTER 2**  
*Experimental  
Techniques*

---

# EXPERIMENTAL TECHNIQUES

---

## 2.1 Introduction

This chapter serves to describe: (i) the catalyst preparation methods, (ii) the basic principles of the characterization techniques used in this study, (iii) the reactors and reaction conditions used for catalyst testing, (iv) the methods to analyse and quantify the products.

## 2.2 Catalyst preparation

In this project, a large number of different types of catalysts were prepared and tested, including supported metal catalysts, oxide catalysts and zeolite and zeolitic membrane coated catalysts. The typical preparation methods are given in this chapter. The specific preparation methods are discussed in details in the appropriate chapters.

### 2.2.1 Preparation of supported metal catalysts

Various supported metal catalysts were prepared by impregnation methods using different metals and oxide or carbon supports. Depending on the nature of the supports, the impregnation methods were different. For powder supports, an incipient wetness method was used; while for the oxide sphere supports, a vacuum incipient wetness method was used.

The most commonly used supports were silica and alumina powder or alumina spheres, while the most commonly used metal was gold. Therefore, Au/alumina powder and Au/alumina sphere preparations are used as examples to introduce the typical preparation processes. The reagents for the preparation are given in **Table 2.1**.

**Table 2.1 Reagents for the preparation of Au/alumina powder or Au/alumina sphere catalysts.**

Reagent	Molar mass (g.mol <sup>-1</sup> )	Supplier	Purity
HAuCl <sub>4</sub> •3H <sub>2</sub> O	393.83	Aldrich	99.99 %
γ- alumina powder	101.96	Aldrich	>99 %
α- alumina sphere	101.96	Saint Gobian	-

To prepare a 5 wt.% Au/alumina powder catalyst by incipient wetness, an aqueous solution of H<sub>2</sub>AuCl<sub>4</sub>•3H<sub>2</sub>O was prepared by dissolving 5 g of H<sub>2</sub>AuCl<sub>4</sub>•3H<sub>2</sub>O in 50 ml distilled water. 10ml of the solution was then simultaneously added to 4.75 g of γ-Al<sub>2</sub>O<sub>3</sub> powder. The paste formed was dried at 110°C overnight and then calcined in static air, at 400°C for 3 h [1].

To prepare a 5 wt.% Au/alumina sphere catalyst by vacuum incipient wetness, an aqueous solution of H<sub>2</sub>AuCl<sub>4</sub>•3H<sub>2</sub>O was prepared by dissolving 5 g of H<sub>2</sub>AuCl<sub>4</sub>•3H<sub>2</sub>O in 50 ml distilled water. 1 g of alumina spheres were placed into a sealed two neck round bottom flask (**Figure 2.1**). The flask was heated to 80 °C using an oil bath and evacuated using a vacuum pump for 1 h. 1 ml of the H<sub>2</sub>AuCl<sub>4</sub>•3H<sub>2</sub>O solution was added into the flask through a syringe. The flask was shaken until all the solution was absorbed into the spheres. The spheres were then dried at 110 °C overnight, calcined at 400 °C for 3 h.

Other supported metal catalysts were synthesized by varying the starting reagents as shown in **Table 2.2**.



**Figure 2.1 Vacuum incipient wetness experimental set-up**

**Table 2.2 Summary of the supported metal catalysts prepared**

<b>Catalyst</b>	<b>Metal Reagent</b>	<b>Support</b>
5 wt.% Pd/SiO <sub>2</sub>	PdCl <sub>2</sub>	Silica gel
5 wt.% Pd/TiO <sub>2</sub>	PdCl <sub>2</sub>	Titania
5 wt.% Pt/SiO <sub>2</sub>	PtCl <sub>4</sub>	Silica gel
5 wt.% Pt/TiO <sub>2</sub>	PtCl <sub>4</sub>	Titania
2.5-2.5 wt.% Pd-Au/SiO <sub>2</sub>	PdCl <sub>2</sub> , HAuCl <sub>4</sub> •3H <sub>2</sub> O	Silica gel
3 wt.% Rh/Al <sub>2</sub> O <sub>3</sub>	RhCl <sub>3</sub> •xH <sub>2</sub> O	γ-Al <sub>2</sub> O <sub>3</sub>
3 wt.% Ru/Al <sub>2</sub> O <sub>3</sub>	RuCl <sub>3</sub> •xH <sub>2</sub> O	γ-Al <sub>2</sub> O <sub>3</sub>
5 wt.% Au/SiO <sub>2</sub>	HAuCl <sub>4</sub> •3H <sub>2</sub> O	Silica gel
5 wt.% Au/TiO <sub>2</sub>	HAuCl <sub>4</sub> •3H <sub>2</sub> O	Titania
5 wt.% Au/Al <sub>2</sub> O <sub>3</sub>	HAuCl <sub>4</sub> •3H <sub>2</sub> O	γ-Al <sub>2</sub> O <sub>3</sub>
5 wt.% Au/C <sub>60</sub>	HAuCl <sub>4</sub> •3H <sub>2</sub> O	C <sub>60</sub>
5 wt.% Au/graphite	HAuCl <sub>4</sub> •3H <sub>2</sub> O	Graphite
5 wt.% Rh/Al <sub>2</sub> O <sub>3</sub>	RhCl <sub>3</sub> •xH <sub>2</sub> O	α-Al <sub>2</sub> O <sub>3</sub> sphere
5 wt.% Au/Al <sub>2</sub> O <sub>3</sub>	RuCl <sub>3</sub> •xH <sub>2</sub> O	α-Al <sub>2</sub> O <sub>3</sub> sphere
3 wt.% Au/ Al <sub>2</sub> O <sub>3</sub>	HAuCl <sub>4</sub> •3H <sub>2</sub> O	γ-Al <sub>2</sub> O <sub>3</sub> sphere

### 2.2.2 Preparation of zeolite and zeolitic coated catalysts

Different zeolite and zeolitic materials were prepared and tested as catalysts, including zeolite 4A, silicalite-1, ZSM-5 and zeolite X. In addition to using these materials as catalysts they were also used as coatings for supported metal catalysts.

The zeolite coated catalysts were synthesized following the method reported by Collier *et al.* [2, 3]. For example, to prepare a zeolite 4A coated Au/alumina catalyst the following procedure was used. 5 g of Au/Al<sub>2</sub>O<sub>3</sub> spheres were added to a 5 wt.% solution of the polyelectrolyte (2-propen-1-ammonium N,N-dimethyl-N-2-propenyl chloride, known as magnafloc It35) containing dilute ammonia and stirred at room temperature for 20 min. An aqueous sodium aluminate solution (6.07 g sodium aluminate (Alfa Aesar) dissolved in 52 g distilled water) was rapidly added into an aqueous sodium metasilicate solution (15.51 g sodium metasilicate (Alfa Aesar, anhydrous) dissolved in 52 g distilled water) to make the zeolite precursor solution. The spheres were subsequently separated and washed with distilled water, and then added to the zeolite precursor solution. The mixture containing the spheres was stirred at room temperature for 2 h and then hydrothermally crystallized at 100 °C for 24 h in a 60 ml Teflon lined stainless steel autoclave. The Teflon liner was cleaned before and after each synthesis in NaOH solution for 24 h under the synthesis conditions. Finally the zeolite coated spheres were separated from the crystallization solution and washed with distilled water, dried at 110 °C and then calcined in air at 500 °C for 2 h.

The silicalite-1 coated catalysts were synthesized with a silicalite-1 precursor solution which consisted of TEOS (98%, Aldrich), tetrapropylammonium hydroxide (TPAOH) (1 M solution in water, Aldrich), ethanol (EtOH, Fluka) and distilled water with the molar ratios of 0.5

TPAOH: 120 H<sub>2</sub>O:8EtOH: 2 SiO<sub>2</sub>. Approximately 1.0 g of catalyst sphere was immersed in 15 g of the precursor solution. The crystallization was carried out under hydrothermal conditions at 180 °C for 24 h in a 60 ml stainless steel autoclave with Teflon liner. The Teflon liner was cleaned before and after each synthesis in NaOH solution for 24 h under the synthesis conditions. The coating procedure was repeated twice. The products were rinsed repeatedly by distilled water, separated by filtration and dried at 90 °C overnight, then calcined in air at 600 °C for 5 h with a heating rate of 1 °C/min [4].

The ZSM-5 coating synthesis method was adapted from the work of Deijger *et al.* [5], in which they investigated ZSM-5 zeolite coatings on ceramic foam supports with surface areas below 1 m<sup>2</sup>/g. The catalysts to be coated were cleaned by boiling in toluene for 1 h and dried overnight at 110 °C before being immersed in the zeolite precursor solution. The zeolite precursor solution was prepared by adding tetrapropylammonium hydroxide (TPAOH, Aldrich, 1 M solution in water), sodium aluminate (NaAlO<sub>2</sub>, Aldrich, Al 50-56%) to tetraethyl orthosilicate (TEOS, Aldrich, 98%) in a PTFE beaker. The molar ratio of the precursor solution was: 1 Al<sub>2</sub>O<sub>3</sub>: 40 SiO<sub>2</sub>: 10 TPAOH: 800 H<sub>2</sub>O. The precursor solution was stirred for 10 h at room temperature as an aging process before transferring the reaction mixture to an autoclave. In all experiments, 1 g of catalyst was added to the autoclave. The volume of precursor solution was varied (32 ml or 15 ml) to observe the influence of the amount of precursor. Syntheses were carried out under autogenous conditions at 160 °C for 24 h in Teflon-lined 60 ml autoclaves. Teflon liners were cleaned before and after each synthesis in NaOH solution for 24 h under synthesis conditions. The coated samples and the extra synthesized powder for the same batch were washed with deionised water and dried overnight at 110 °C. Finally the samples were calcined at 550 °C for 12 h using a heating rate of 5 °C/min.

### 2.2.3. Preparation of cyclodextrin modified catalysts

Cyclodextrin (CD) modified catalysts were prepared by an impregnation method. Using CD modified Au/SiO<sub>2</sub> as an example, the detailed steps of the preparation are as follows. The BET surface area of the Au/SiO<sub>2</sub> was determined. Assuming CD molecules cover the catalyst surface as a monolayer without gaps, the required mass of CDs to completely cover the surface of catalysts was calculated (e.g. to cover 1 g of Au/SiO<sub>2</sub>, 0.37 g of  $\alpha$ -CDs or 0.35 g of  $\beta$ -CDs is needed). Five times the calculated amount of CD was then dissolved in 25 ml of deionised water which was heated to 45°C with stirring. 5 ml of the CD solution was added to 1 g of Au/SiO<sub>2</sub> and the mixture heated to 45°C and stirred for 30 min and then put into an oven to dry overnight at 110°C.

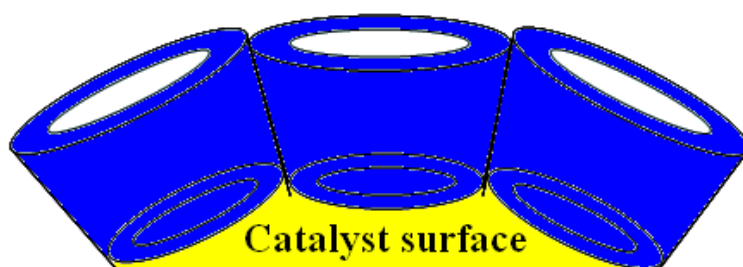


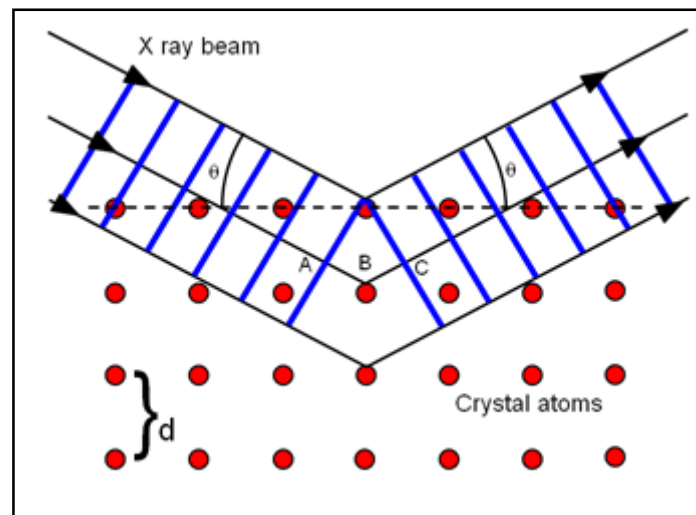
Figure 2.2 Ideal Au/ SiO<sub>2</sub> surface covered by cyclodextrin molecules

## 2.3 Catalyst characterization technique

### 2.3.1 X-ray powder diffraction

X-ray diffraction (XRD) is a versatile, non-destructive technique that reveals detailed information about the crystallographic structure of natural and manufactured materials [6].

To produce a powder XRD pattern, the sample must be crystalline. Bombarding a suitable target with electrons produces the X-rays. When the electrons hit the target, they excite electrons which return to their normal state shell with a consequent emission of X-rays. Diffraction occurs only when Bragg's Law is satisfied. The wavelengths of the X-rays produced by the powdered sample and diffracted by the analysed crystal obey the Bragg equation, which links the d-spacings on the powdered sample to the angle of incident of the X-rays on the sample (**Figure 2.3**) [7].



$$n\lambda = 2d\sin\theta$$

$\theta$  = angle between the crystal plane and the diffracted beam.

$\lambda$  = wavelength of incident X-rays beam.

$d$  = spacing between atomic layers in the powdered sample.

$n$  = integer.

**Figure 2.3 Bragg's Law of diffraction [7].**

The data obtained shows a series of lines of varying intensities at different  $2\theta$  values, obtained as the analyser crystal turns. A qualitative analysis of the sample is thus carried out. The schematic of an X-ray diffractometer is shown in **Figure 2.4**.

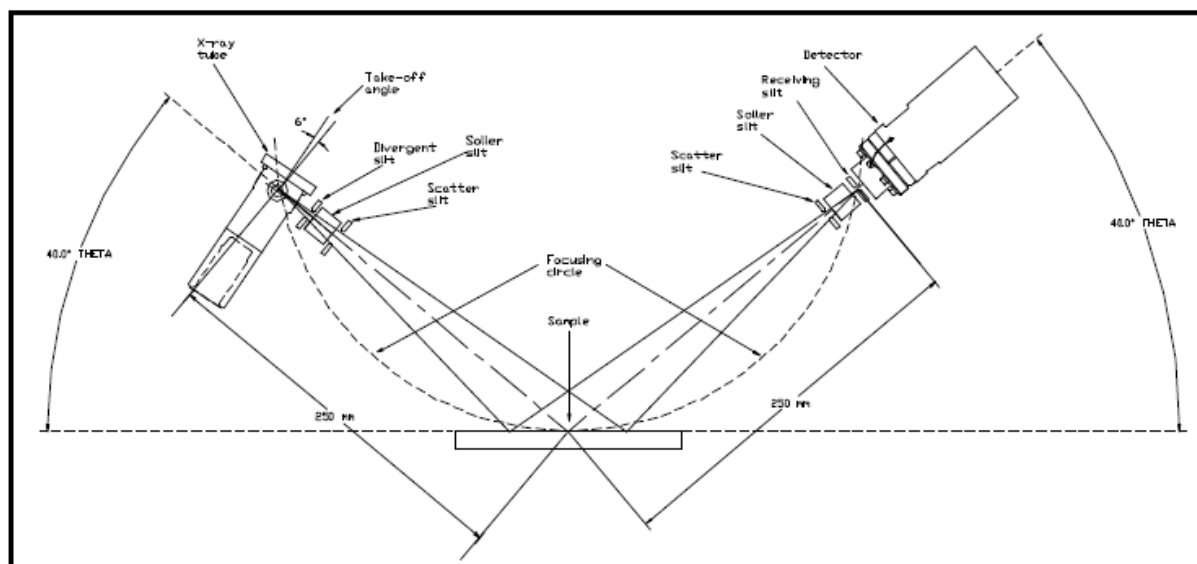


**Figure 2.4 Schematic of an X-ray diffractometer [8].**

In this project the XRD analysis was performed using a PANalytical Xpert Pro diffraction system with a monochromatic  $\text{Cu K}\alpha_1$  source operated at 40 keV and 30 mA. Catalysts analysed by XRD must be powders, therefore the catalysts prepared using preformed supports were ground into a very fine powder.

### **2.3.2 Scanning electron microscopy**

The Scanning electron microscope (SEM) is a microscope that uses electrons rather than light to form an image. The SEM has a large depth of field, which allows a large amount of the sample to be in focus at one time. The SEM also produces images of high resolution, which means that closely spaced features can be examined at a high magnification. Preparation of the samples is relatively easy since most SEMs only require the sample to be conductive. The

combination of higher magnification, larger depth of focus, greater resolution, and ease of sample observation makes the SEM one of the most heavily used instruments in research areas today [9]. When using the SEM, a beam of electrons is generated in the electron gun, which is located at the top of the SEM column. This beam is attracted through the anode, condensed by a condenser lens, and focused as a very fine point on the sample by the objective lens. The electron beam hits the sample, producing, among others, secondary and backscattered electrons from the sample. The electrons are collected by a secondary electron or a backscattered electron detector, converted to a voltage, and amplified. The scan coils are energized (by varying the voltage produced by the scan generator) and create a magnetic field which deflects the beam back and forth in a controlled pattern. The varying voltage is also applied to the coils around the neck of the cathode-ray tube (CRT) which produces a pattern of light deflected back and forth on the surface of the CRT. The pattern of deflection of the electron beam is the same as the pattern of deflection of the spot of light on the CRT. SEM must be run in vacuum. This is because if the sample is in a gas filled environment, an electron beam cannot be generated or maintained because of a high instability in the beam. Gases could react with the electron source, causing it to burn out, or cause electrons in the beam to ionize, which produces random discharges and leads to instability in the beam. **Figure 2.5** shows the schematic of an SEM instrument.

In this project the SEM images were taken by a Zeiss Evo-40 series scanning electron microscope. The method was widely used in the characterization of zeolite coated catalysts. The coated sphere samples were placed in the sample holder directly in the characterization.

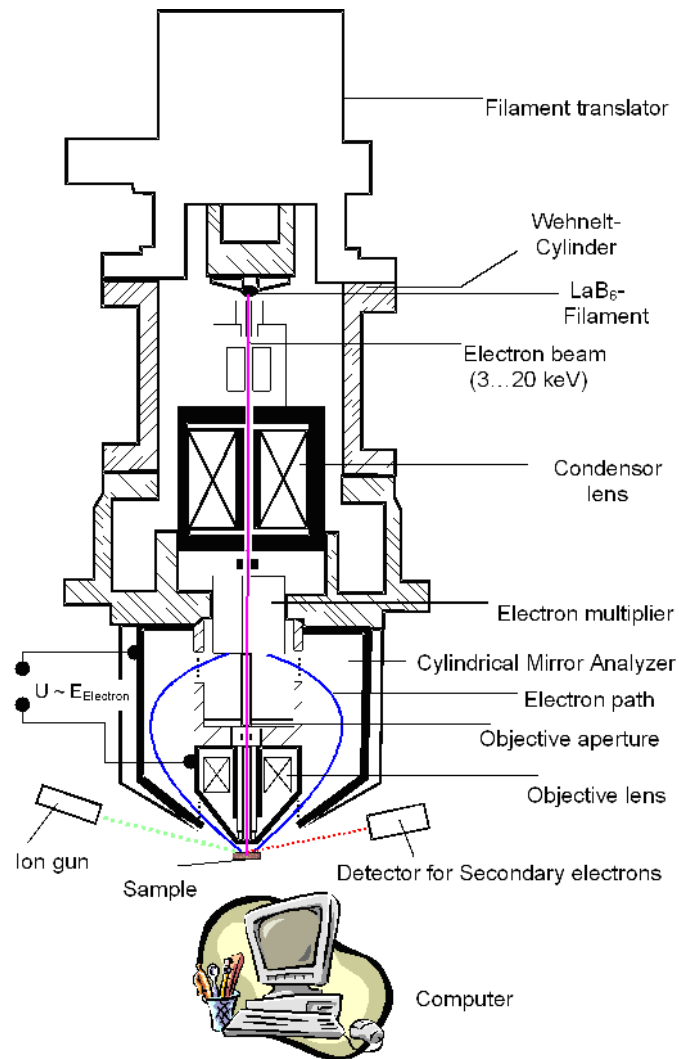


**Figure 2.5 Schematic of a Scanning electron microscope [10]**

### 2.3.3 Surface area method (BET)

Surface area is one of the key tools to characterize porous materials. The BET method is the most frequently used method to calculate the surface area. It provides precise specific surface area evaluation of materials by nitrogen multilayer adsorption measured as a function of relative pressure, using a fully automated analyser. The technique encompasses external area and pore area evaluations to determine the total specific surface area in  $\text{m}^2/\text{g}$  yielding important information in studying the effects of surface porosity and particle size. The concept of BET

theory is based on the extension of the Langmuir theory, which is a theory for monolayer molecular adsorption, to multilayer adsorption with the following hypotheses: (a) gas molecules physically adsorb on a solid in layers infinitely; (b) there is no interaction between each adsorption layer and (c) the Langmuir theory can be used for each layer. Therefore the BET equation is expressed in **Equation 2.1**.

$$1/v [(P_0/P) - 1] = (c-1)/(v_m c) * (P/P_0) + 1/(v_m c)$$

where P= equilibrium pressure

P<sub>0</sub>= saturation pressure of the gas

v= adsorbed gas quantify

v<sub>m</sub>= monolayer adsorbed gas quantity.

c=constant

### **Equation 2.1 The BET equation**

In this project, samples were analysed using the Quantachrome Autosorb-1 instrument. Before performing the analysis, samples were degassed by placing a 0.1 g sample in a glass tube (d = 12 mm) and heating under helium for an hour at 120°C. The sample filled glass tube is then placed into a Dewar flask containing liquid nitrogen and analysed by the machine.

#### **2.3.4. Atomic absorption spectroscopy**

Atomic absorption spectroscopy (AAS) is a technique for determining the concentration of a particular metal element in a sample. The technique can be used to analyse the concentration of over 70 different metals in a solution. The technique makes use of absorption spectrometry

to assess the concentration of an analyte in a sample. Therefore it relies heavily on the Beer-Lambert law.

In short, the electrons of the atoms in the atomizer can be promoted to higher orbitals for a short amount of time by absorbing a set quantity of energy (*i.e.* light of a given wavelength). This amount of energy (or wavelength) is specific to a particular electron transition in a particular element, and in general, each wavelength corresponds to only one element. This gives the technique its elemental selectivity.

As the quantity of energy (the power) put into the flame is known, and the quantity remaining at the other side (at the detector) can be measured, it is possible, from the Beer-Lambert law, to calculate how many of these transitions took place, and thus get a signal that is proportional to the concentration of the element being measured. A diagram of AAS is given in **Figure 2.6**.

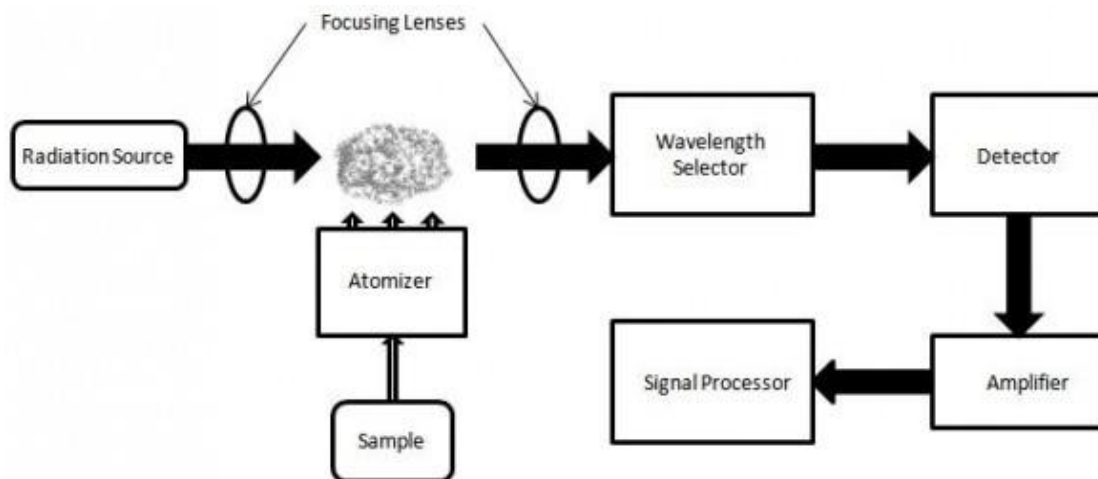


**Figure 2.6** Diagram of AAS [11]

### 2.3.5 X-ray Photoelectron Spectroscopy

X-ray Photoelectron Spectroscopy (XPS) is a quantitative spectroscopic technique that measures the elemental composition, empirical formula, chemical state and electronic state of the elements that exist within a material. XPS spectra are obtained by irradiating a material with a beam of X-rays while simultaneously measuring the kinetic energy and number of electrons that escape from the top 5 to 20 nm of the material being analysed. Because the energy of an X-ray with particular wavelength is known, the electron binding energy of each emitted electron can be determined by using an equation that is based on the work of Ernest Rutherford (**Equation 2.2**):

$$E_b = E_p - (E_k + \phi)$$

Where  $E_b$  = binding energy of the electron

$E_k$  = kinetic energy of the electron measured

$E_p$  = the energy of the X-ray photons being used

$\Phi$  = work function of the spectrometer (often ignored)

#### **Equation 2.2 XPS equation**

XPS analysis in this project was carried out with an ESCALAB 220 spectrometer using an achromatic AlK $\alpha$  source and analyser pass energy of 100 eV.

### 2.4 Reactors used in the project

Two types of reactors have been used in the project: the Parr multiple stainless steel reactor system and the Andrews glass reactor system.

#### **2.4.1 The Parr multiple stainless steel reactor system**

The Parr series 5000 multiple reactor system (**Figure 2.7**) has been used for the liquid phase oxidation of *n*-decane and *n*-hexane with oxygen. It is a system with six stainless steel vessels which can perform six reactions at different pressures and temperatures simultaneously. The volume of each vessel is 45 ml. Stirring with this system was operated by a single magnetic stirrer, therefore all six vessels have the same stirring speed during a single run. In the experiments, PTFE stirring seeds were the most frequently used, while glass stirring seeds were also applied in some reactions. The autoclaves can be operated up to 3000 psi and 275 °C [12]. The typical reactions performed with this system were always with 0.05 g of catalyst, 10 g *n*-decane or *n*-hexane, a stirring speed of 600 rpm, 15 bar O<sub>2</sub>, at different temperatures and reaction times. Before reactions, the autoclave was flushed twice with O<sub>2</sub> to remove all the air. Then the reactors were heated to the desired temperature (100°C, 110°C, 120°C or 130°C) for different runtimes. There was no sample tube with this reactor; therefore in order to exactly control the reaction time, ice water was used to cool down the autoclave at the end of the reaction.

#### **2.4.2 The Andrews glass reactor system**

The Andrews glass reactor system (**Figure 2.8**) has been used mainly for the liquid phase oxidation of *n*-hexane with oxygen. The three glass reactors (88.7ml, starter kit, Andrews Glass) were heated in separate oil baths by three separate hotplates. Oxygen pressure was controlled in each reactor. It was observed there were small temperature variations for the different reactors because of their separate heating controllers. Reactors A and B were found

to have quicker heating rates than reactor C. It always took reactor C several minutes more to reach the temperature set point.



**Figure 2.7 Multi reactor system and control box.**



**Figure 2.8 Andrews Glass Reactor System**

The volume of each glass vessel is 120 ml. Stirring with this system was always controlled to the same stirring speed and PTFE stirring seeds and glass stirring seeds were both employed. The reactors can be operated up to 225 psi [13]:

The typical reactions performed with this system were always with 0.05 g catalyst, 25 ml *n*-hexane, a stirring speed of 600 rpm, 3 bar O<sub>2</sub>, at different temperatures and reaction times. Before reaction, the vessel was flushed twice with O<sub>2</sub> to remove all the air. Then the reactors were heated to the desired temperature (110°C, 120°C, 130°C, 150°C) for different runtimes. A PTFE sample tube was used and in most cases, the samples were taken directly from this. In some specific cases, ice water was used to cool down the reactor at the end of the reaction.

## **2.5 Analysis and qualification of reaction products**

### **2.5.1 Analysis by Gas Chromatography**

The first step of reaction product analysis was through gas chromatography (GC). GC is a common type of chromatography for separating and analysing compounds that can be vaporized without decomposition, which was suitable in this project. After the oxidation of the long chain alkane, there was a mixture of various products. These can be separated in the GC as they have different boiling points. The higher the boiling point of the compound, the later the retention time of the compound.

Analysis were carried out using a Varian Star 3800 equipped with a Chrompack CP Wax 52CB, 25 m, 0.53 mm, 2.0 µm capillary column, and an FID detector. In the analysis, 0.2 µl sample was injected into the GC. Helium was the carrier gas employed in the system. Injection parameters on the GC used a split ratio of 10:1.

To achieve the best separation, the temperature programs in the GC were as follows:

(i) For *n*-decane products:

Start at 60 °C hold for 7 min.

Ramp at 35 °C/min to 115 °C hold for 12 min.

Ramp at 4 °C/min to 220 °C hold for 1 min.

Ramp at 50 °C/min to 240 °C hold for 2 min.

(ii) For *n*-hexane oxidation products:

Start at 35 °C hold for 7 min.

Ramp at 35 °C/min to 220 °C hold for 3 min.

## **2.5.2 Quantification of the products via response factor**

### **2.5.2.1 Use of internal standard**

To quantify the products, an internal standard was added to the reaction products. The internal standard used was 1,2,4-trichlorobenzene in both *n*-decane and *n*-hexane oxidation reactions. The advantage of this standard is that it did not interfere with the reaction and it is eluted from the column at a different retention time from the other compounds of interest (**Figure 2.3 and 2.4**). 0.15 ml of 1,2,4-trichlorobenzene was added to the reaction products mixture.

### **2.5.2.2 Calculations of relative response factors of each compound**

The relative response factor (K) of each product was determined using the ratio of the areas under the peak of a known amount of product and a constant amount of the internal standard (1,2,4-trichlorobenzene).

The anticipated compounds in the product mixture (e.g. 2-5 decanone, 1-5 decanol, *etc.*) were used to prepare five mixtures containing known amounts of products as well as the internal standard. For example, to calibrate *n*-decane oxidation products, the first to fifth calibrated solution should contain 10 g *n*-decane, 10/30/50/70/90 mg of each anticipated compound and 0.15 ml internal standard. The five mixtures were injected into the GC and the area of the peaks of the internal standard and the anticipated compounds measured. The mass of the compounds were known, therefore, the internal response factor can be calculated using **Equation 2.3**. The final internal response factor was the average value from the five solutions.

$$K = [(Area_{IS}) * (Mass_{AC})] / [(Mass_{IS}) * area_{AC}]$$

Where K = Relative Response Factor

Area<sub>IS</sub> = Area of Internal Standard in GC

Mass<sub>AC</sub> = Mass of specific anticipated compound

Mass<sub>IS</sub> = Mass of internal standard

Area<sub>AC</sub> = Area of specific anticipated compound

### **Equation 2.3 Calculation of internal standard**

All the relative response factors of the known products of *n*-dexane and *n*-hecane oxidation were calculated in this way. The retention time and response factor of each reaction product are given in **Table 2.3 and 2.4**.

**Table 2.3 Order, retention time and internal response factor of each product for *n*-decane reaction**

<b>Order on the GC trace</b>	<b>Compounds</b>	<b>Retention Time (min)</b>	<b>Internal Response Factor</b>
1	<i>n</i> -decane	3.44	0.498
2	5/4-decanone (5/4 one)	11.81	0.62
3	3-decanone (3 one)	12.54	0.59
4	2-decanone (2 one)	13.45	0.588
5	5/4-decanol (5/4 ol)	16.26	0.606
6	3-decanol (3 ol)	16.94	0.598
7	2-decanol (2 ol)	18.02	0.62
8	internal standard	20.44	N/A
9	pentanoic acid (C <sub>5</sub> OOH)	25.25	1
10	1-decanol (1 ol)	25.65	0.616
11	hexanoic acid (C <sub>6</sub> OOH)	29.30	0.904
12	heptanoic acid (C <sub>7</sub> OOH)	32.69	0.822
13	octanoic acid (C <sub>8</sub> OOH)	35.66	0.806
14	nonanoic acid (C <sub>9</sub> OOH)	38.38	0.8
15	decanoic acid (C <sub>10</sub> OOH)	40.85	0.788

**Table 2.4 Order, retention time and internal response factor of each product for *n*-hexane reaction**

<b>Order on the GC trace</b>	<b>Compounds</b>	<b>Retention Time (min)</b>	<b>Internal Response Factor</b>
1	n-hexane	0.858	0.894
2	3-hexanone (3 one)	8.75	0.762
3	2-hexanone (2 one)	10.12	0.69
4	hexanal	10.12	N/A
5	3-hexanol (3 ol)	16.92	0.684
6	2-hexanol (2 ol)	19.1	0.66
7	internal standard	23.325	N/A
8	1-hexanol (1 ol)	28.06	0.685
9	hexanoic acid (C <sub>6</sub> OOH)	40.66	0.9125

(The hexanal can not be separated as it has the same retention time as 2-hexanol )

### **2.5.2.3 Quantification and analysis of the reaction**

According to **Table 2.3 and 2.4**, all the response factors for the known compounds were determined. Hence, the amount of each known compounds in the product mixture can be calculated using **Equation 2.4**:

$$\text{Mass}_{\text{AC}} = (\text{Mass}_{\text{IS}} * \text{Area}_{\text{AC}} * K) / (\text{Area}_{\text{IS}})$$

Where K = Relative Response Factor

Area<sub>IS</sub> = Area of Internal Standard in GC

Mass<sub>AC</sub> = Mass of specific anticipated compound

Mass<sub>IS</sub> = Mass of internal standard

Area<sub>AC</sub> = Area of specific anticipated compound

### Equation 2.4 Calculation of amount of products

Then the yield, conversion and selectivity of the reaction can be calculated following the formula below:

Yield of each product (%) =

$$\frac{K \times (\text{Area of Product} / \text{Area}_{\text{IS}}) \times \text{Mass}_{\text{IS}}}{(\text{Mass of } n\text{-decane (10g)} / \text{Molar mass of decane} \times \text{Molar mass of product})} \times 100$$

Conversion (%) = Sum Yield of each product = Total Yield

Product Selectivity (%) = Yield of each product / Total Yield

Further experimental and characterisation details are discussed in the corresponding results chapters.

## 2.6 References

- [1] J.K. Edwards, B.E. Solsona, P. Landon, A.F. Carley, A. Herzing, C.J. Kiely, G.J. Hutchings, *Journal of Catalysis* 236, (2005), 69.
- [2] P. Collier, S. Golunski, C. Malde, J. Breen, R. Burch, *Journal of the American Chemistry Society* 125, (2003), 12414
- [3] Collier, Paul John, Golunskin, Stanislaw Edmund, U.S. Patent No.0032628, 2005.
- [4] D.C.Vu, M.Miyamoto, N.Nishiyama, S.Ichikawa, Y.Egashira, K.Ueyama, *Microporous and Mesoporous Materials* 115, (2008), 106
- [5] G.B.F. Seijger, O.L. Oudshoorn, W.E.J. van Kooten, J.C. Jansen, H. van Bekkum, C.M. van den Bleek, H.P.A. Calis, *Microporous and Mesoporous Materials* 39, (2000), 195
- [6] PANalytical <http://www.panalytical.com/index.cfm?pid=135>
- [7] <http://www.eserc.stonybrook.edu/ProjectJava/Bragg/>
- [8] *Providing Solutions To Your Diffraction Needs*, Cupertino: Scitag inc., (1999).
- [9] <http://mse.iastate.edu/microscopy/home.html>
- [10] <http://www.ifw-dresden.de/institutes/ikm/organisation/dep-31/equipment/aes-microprobe-phi660>
- [11] <http://www.universetoday.com/81974/atomic-absorption-spectroscopy/>
- [12] <http://www.parrinst.com>.
- [13] Andrews glass website, [http://www.andrewsglass.com/PRV\\_support.tpl](http://www.andrewsglass.com/PRV_support.tpl)

**CHAPTER 3**  
*Andrews Glass  
Reactor*

---

## ANDREWS GLASS REACTOR

---

### 3.1 Introduction

In liquid phase long chain alkane selective oxidation studies, the key results were reported by Thomas for *n*-hexane oxidation [1-7]. In his study, Thomas used ALPO catalysts with air as the oxidant. The terminal selectivity can be extremely high (up to 8.7% conversion, 65.5% selectivity with Co-ALPO-18). Iglesia [8] tried to reproduce Thomas's results under similar experimental conditions using Mn-ALPO catalysts. However the conversion was quite low (0.02-0.05%), while the terminal selectivity was 7% only. Iglesia concluded that Mn-ALPO did not lead to any preference for terminal selectivity in contradiction with Thomas' results. Iglesia published his own results using Mn-ZSM5 as the catalyst (**Table 3.1**) [9]. Unlike Thomas's study, Iglesia noticed the autoxidation reaction and demonstrated a clear difference in the terminal selectivity in the presence of catalysts. It was clear that when the catalyst was present, the terminal selectivity was initially high (24%), but the selectivity declined when conversion increased. In contrast the terminal selectivity in the autoxidation was always 7-8%. In this project, it was attempted to obtain the high level of terminal selectivity as Iglesia did.

Most of the reactions performed in this project were carried out in the Parr stainless steel reactor with or without a PTFE liner. However it was noticed that Iglesia *et al.* employed the Andrews glass reactor in their research. Hence the focus of this chapter was the comparison between the stainless steel reactor and the Andrews glass reactor. Studies using the Andrews glass reactor were also performed.

**Table 3.1 Iglesia's results for oxidation of *n*-hexane with Mn-ZSM-5 catalysts**

<b>Time (hours)</b>	<b>Conversion (%)</b>	<b>Terminal selectivity (%) with Mn-ZSM-5</b>	<b>Terminal selectivity (%) Autoxidation</b>
0.5	0.007	24	7
2.5	0.013	18.5	8
4	0.047	15	8
7	0.1	10	7

## **3.2 Experimental**

### **3.2.1 Apparatus and reaction**

The Andrews glass reactors system was set up as shown below in **Figure 3.1**. The three glass reactors (88.7 ml, starter kit, Andrews Glass) were heated in separate oil baths by three separate hotplates. Oxygen pressure was controlled in each reactor. Temperature variations were observed for the different reactors because of their separate heating controllers. Reactors A and B were found to have quicker heating rates than reactor C. It always took reactor C several minutes more to reach the temperature set point. Hexane oxidation reactions were performed under conditions equivalent to Iglesia's work [8]: 25 ml hexane, 3 bar oxygen, 130 °C for short time reactions.



**Figure 3.1 Andrews Glass Reactor System**

### **3.2.2 Safety operating procedure**

To avoid dangers of operation, the safety operating procedure for the reactor is given as follows:

#### To switch instruments on

Put beakers with silicon oil on top of the hotplates. Hold the wire-mesh covered glass reactors with clamps and immerse two-thirds of the glass reactor into the silicon oil baths. Switch on the power to the hotplates. Temperature and stirrer speed are controlled by and displayed on the hotplates. Pressure is displayed on a gauge on the head of the reactor and can be controlled by inlet and outlet valves also on the reactor head. The glass reactors should be handled gently.

#### Preparing a sample in the Andrews glass reactor

Place reactants in the glass cylinder. Reactants should occupy no more than two-thirds of the available space of the cylinder. The cylinder is then aligned with the head and joined. The

rubber ring in the head of the reactor should be well fitted into the top of the glass cylinder. Hold the head and the glass cylinder securely together and then tighten the head to the glass cylinder carefully.

#### Controlling the stirrer speed and temperature of the reactor

The stirrer speed and temperature can be set on the hotplate. The temperature detector must be immersed into the oil bath; the depth of the detector head should be kept in the same level in the glass cylinder.

#### Allowing gas flow into the reactor

The Andrews glass reactor set-up has inlet and outlet valves (on the head part). The inlet valve is connected to oxygen and is opened briefly to fill the reactor to the desired pressure. The outlet valve is kept closed during a reaction, but remains open at all other times. Both the inlet and outlet valves turn clockwise to close. Pressure in the cylinder is maintained when the outlet and inlet valves are closed. The pressure in the gas line is limited by a regular, therefore, normally the pressure in the glass line is not higher than 5 bar. However, to avoid any accidents, when releasing the gas into or out of the cylinder open the inlet or outlet valves is slowly.

#### Controlling the gas flow

Open the oxygen valve on the wall. The pressure inside the glass reactor is controlled by turning the glass inlet and outlet valves in the reactor head. To increase the pressure, turn the inlet valve anti-clockwise. To decrease the pressure, turn the outlet valve anti-clockwise. The gauge in the reactor head will show the pressure inside the reactor.

### Purging the glass reactor

Before starting any reaction it is necessary to evacuate the air present in the reactor and fill the reactor to the desired pressure with oxygen. Open the oxygen valve on wall behind the reactors. This will allow the gas to enter the glass reactor when the inlet on the reactor head is opened. Fill the reactor to the desired pressure by repeatedly briefly opening and closing in the inlet line. Then close the inlet valve and open the outlet valve on the head slowly to release the pressure. This is repeated three times, after which the reactor is pressurised and the inlet and outlet valves are closed. Close the gauge on the wall behind the reactors. Monitor the pressure in the reactor for approximately 5 minutes to ensure there are no leaks.

### Starting a reaction

After placing the sealed glass reactors and oil baths on the hotplate, put the temperature detector to the right position (as mentioned above). Purge the reactor and pressurise to the desired working pressure. Switch on the stirrer and set the desired temperature in the digital display connected to the hotplates.

### Ending a reaction

If the reaction is to be stopped for a required time, switch off the hotplate then put the reactor into ice bath for quick cooling. Once cool, the gas is evacuated from the reactor by slowly opening the outlet valve on the reactor head. The cylinder can then be disconnected, and the reaction mixture emptied. Always allow the reactor to cool before opening it.

### Cleaning the autoclave

After each reaction the reactor should be thoroughly washed and cleaned to remove all traces of the reactants. As well as cleaning the glass cylinders, it is also necessary to clean the stirrer bar.

### Instrument shutdown

Specified users will normally carry out instrument shutdown.

Ensure that the hotplate, especially the heating is switched off when the reaction is finish. The oxygen line to the equipment must also be closed when not used for filling the reactors and the instrument lines vented.

### Emergency shutdown procedure

1. Switch off electricity at the sockets.
2. O<sub>2</sub> gas supply should be shut off at the cylinder.
3. If it is safe to do so (i.e. no visible sign of leakage from the apparatus) remove the glass reactor(s) from the hotplate(s) (if applicable).
4. Do not allow anyone to touch the equipment or any contents of the reactor unless the person is a trained and competent user.

### **3.2.3 Characterization techniques**

Reaction samples were analysed by gas chromatography, with a CP Wax 52CB column, 25 m, 0.53 mm, 2.0 microns using a programmed temperature ramp. Each sample was injected at least twice.

## **3.3 Results**

### **3.3.1 Andrews glass reactor in blank hexane oxidation**

Hexane oxidation was carried out under the same conditions: 3 bar oxygen, 130 °C, with various amounts of hexane: 10g (the amount consistent with using the Parr stainless steel reactor) and 25ml (Iglesia's reported system), for 30 min and 1 hour.

### 3.3.1.1 Comparison between Andrews glass reactor and stainless steel reactor

Reactions were carried out over 30 min and 1h with 10 g hexane and repeated several times at a stir speed 3 in the hotplate. The oxidation results were given in **Table 3.2** and **Table 3.3**.

**Table 3.2 Glass reactor 130 °C, 3 bar O<sub>2</sub>, 10 g *n*-hexane, stir speed 3, 30 min**

Reactor	Conv. (%)	Selectivity (%)					
		3 one	2 one	3 ol	2 ol	1 ol	oic
A	<b>0.0017</b>	29	35	9	11	15	0
B	<b>0.0010</b>	33	36	9	13	7	0

**Table 3.3 Glass reactor 130 °C, 3 bar O<sub>2</sub>, 10 g *n*-hexane, stir speed 3, 1 h**

Reactor	Conv. (%)	Selectivity (%)					
		3 one	2 one	3 ol	2 ol	1 ol	oic
A	<b>0.0060</b>	34	34	7	12	11	0
B	<b>0.0050</b>	35	36	8	11	7	0

For the longer reaction time the 1-hexanol selectivity may have decreased slightly. Compared with the stainless steel reactor results reported previously (**Table 3.4**), the conversion in the glass reactor is lower.

**Table 3.4 Steel reactor 130 °C, 5 bar O<sub>2</sub>, 10g *n*-hexane, blank, 600 rpm, 30 min**

Reactor	Conv. (%)	Selectivity (%)					
		3 one	2 one	3 ol	2 ol	1 ol	oic
Stainless steel 30min	<b>0.0051</b>	20	34	13	15	18	0

A Further time on-line study was performed to compare the two reactors. The results were shown in **Table 3.5** and **Table 3.6**. From the results, the blank reactions gave higher conversion but lower terminal selectivity in the stainless steel reactor than the glass reactor, which indicates the stainless steel reactor itself may have some activity in the oxidation reaction.

**Table 3.5 Hexane auto-oxidation with glass reactor (reaction conditions: 130 °C, 3 bar O<sub>2</sub>, 25 ml *n*-hexane, 600 rpm, time-on-line)**

Time (h)	Reactor	Conv.(%)	Selectivity (%)				
			Ketones	Alcohols	Acid	Others	1-hexanol
0.5	A	0.0001	15	0	0	85	0
1	A	0.0002	16	13	1	70	5
2	A	0.0008	14	10	0	76	5
3	A	0.0118	13	11	0	76	6
4	A	0.0223	14	11	0	75	6

**Table 3.6 Hexane auto-oxidation with stainless steel reactor (reaction conditions: 130 °C, 3 bar O<sub>2</sub>, 25 ml *n*-hexane, 600 rpm, time-on-line)**

Time (h)	Conv. (%)	Selectivity (%)				
		Ketones	Alcohols	Hexanoic acid	Others	1-Hexanol
0	0					
1	0.001	72	15	0	12	0
2	0.002	65	24	0	8	2
3	0.008	56	24	0	20	3
4	0.022	63	18	0	19	1

### 3.3.1.2 Repeat Iglesia's blank reaction

A few reactions were performed under conditions equivalent to Iglesia's work, at 130°C, 3 bar O<sub>2</sub>, stir speed 2, for 30 min and 1 hour, however no products were detected. The GC sensitivity may also be a reason for products not being detected. It should be noted that the stir speed taken in these reactions was lower than before, the change is made because it was found when catalysts were added to the reactor at a high stir speed, the stirrer bar became trapped.

### 3.3.1.3 The unknown products in analysis

In a further analysis of GC traces, it was found that there were large quantities of unknown products in the hexane oxidation (as shown in **Figure 3.2**), which were not included in the calculated results. In order to have a clear product distribution, the results were calculated including these unknown products discussed in the following section in this chapter.

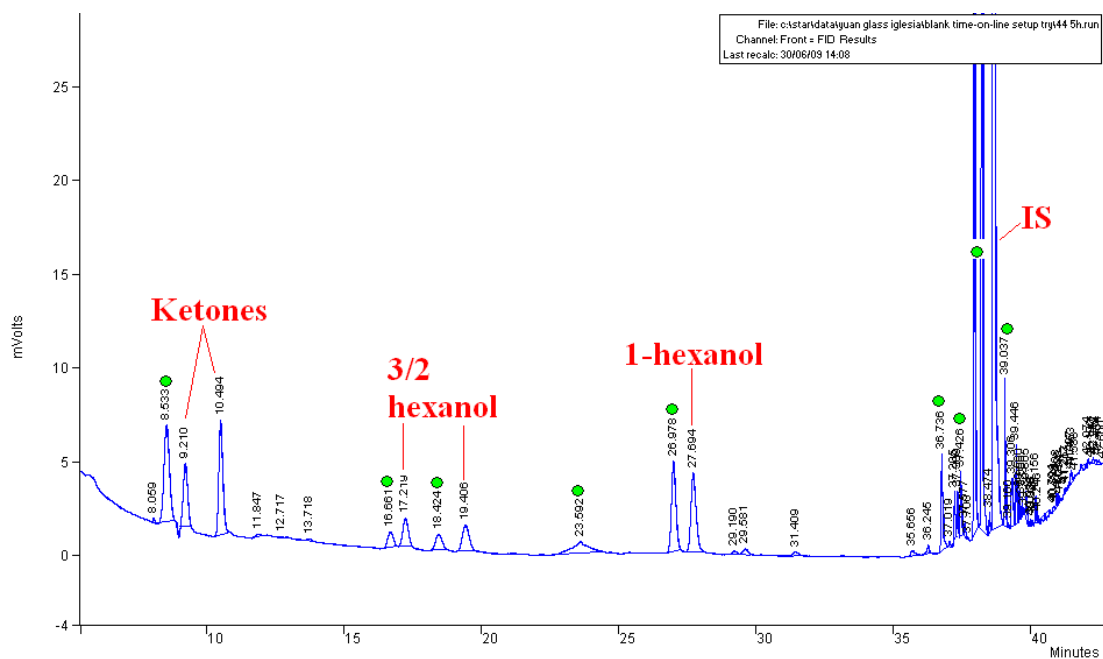


**Figure 3.2** The GC trace with the unknown products (marked with ●)

GC-MS analysis was then introduced to identify the known and unknown products. With a polar column in GC-MS, all the known products in hexane oxidation have been successfully identified, and a few the unknown products have been successfully analysed. **Table 3.7** showed the possible main unknown products. They are all named as ‘others’ in the following result tables.

**Table 3.7 List of suggested unknown products**

Possible main unknown Products	Retention time in GC-MS
2-pentanol, 2-methyl- $C_6H_{14}O$	3.68
3-pentanol, 3-methyl- $C_6H_{14}O$	3.84
4-methyl-2-pentacetate $C_8H_{16}O$	4.51
Propanoic acid	7.03
Nonanoic acid	18.43
$C_6H_{12}O_4$	20.05

#### 3.3.1.4 Application of aqua regia as washing agent

In the previous reactions, aqua regia was not always used as a washing agent. To check if this can influence the reaction results, reactions were carried out immediately after washing the reactors carefully with aqua regia (**Table 3.8**). Compared with the **Table 3.9** (without washing with aqua regia), the selectivity did not show much difference from the previous reactions which were not washed with aqua regia.

**Table 3.8 130 °C, 3 bar O<sub>2</sub>, 25 ml *n*-hexane, stir speed 2, single reaction (2 and 4 h)**

Time (h)	Reactor	Conv.(%)	Selectivity (%)				
			Ketones	Alcohols	Acid	Others	1-hexanol
0.5	A	0.010	37	25	3	35	8
1	A	0.019	27	29	2	42	9
2	B	0.022	13	61	2	26	9
3	A	0.060	29	16	1	54	10
4	B	0.064	22	15	1	60	9

**Table 3.9 130 °C, 3 bar O<sub>2</sub>, 25 ml *n*-hexane, modified time-on-line set-up, stir speed 2, 0.5 – 5 h, 0.15 ml 1,2,4-trichlorobenzene**

Time (h)	Reactor	Conv.(%)	Selectivity (%)				
			Ketones	Alcohols	Acid	Others	1-hexanol
0.5	A	0.013	39	23	3	35	8
1	A	0.023	28	28	1	43	9
2	A	0.037	31	20	1	48	10
3	A	0.061	27	18	1	54	10
4	A	0.089	21	16	1	62	9

### 3.3.1.5 Time-on-line reactions

Hexane oxidation reactions were performed with the Andrews glass reactor system; heating from room temperature to 130 °C takes 5 min to 4 h. The reaction conditions were equivalent to Iglesia's work: 25 ml hexane, 3 bar oxygen and 130 °C.

### Reactions with time-on-line modification

In order to investigate the time-on-line oxidation status during a reaction, a modification was made to one of the glass reactors. The modification consists of PTFE tubing being inserted into the reaction solution through the reactor top. The flow in the tubing can be controlled by two PTFE valves outside the reactor. Therefore samples can be taken while a reaction is running. The internal standard (1,2,4-trichlorobenzene, Sigma-Aldrich,  $\geq 99\%$ , 0,15 ml) was added to the solution before reaction. In this section, the reactions were all carried out in modified reactors with a time-on-line sampling port. Hexane oxidation reactions were still performed under conditions equivalent to Iglesia's work: 25 ml hexane, 3 bar oxygen and 130 °C, with varied time period. Reactions were repeated two times. The terminal selectivity (hexanoic acid + 1-hexanol) is around 5-9% (**Table 3.10** and **Table 3.11**).

**Table 3.10 130 °C, 3 bar O<sub>2</sub>, 25 ml *n*-hexane, modified time-on-line set-up, stir speed 2, 0.5 – 5 h, 0.15 ml 1,2,4-trichlorobenzene**

Time (h)	Reactor	Conv.(%)	Selectivity (%)				
			Ketones	Alcohols	Acid	Others	1-hexanol
0.5	A	0.003	44	21	2	33	7
1	A	0.018	16	13	1	70	5
2	A	0.057	14	10	0	76	5
3	A	0.094	13	11	0	76	6
4	A	0.163	14	11	0	75	6
5	A	0.247	11	11	0	78	6

**Table 3.11 130 °C, 3 bar O<sub>2</sub>, 25 ml *n*-hexane, stir speed 2, various times, 0.15 ml 1,2,4-trichlorobenzene, repeated**

Time (h)	Reactor	Conv.(%)	Selectivity (%)				
			Ketones	Alcohols	Acid	Others	1-hexanol
0.5	A	0.005	30	14	0	56	5
1	A	0.019	15	9	1	75	5
2	A	0.059	13	9	0	78	5
3	A	0.101	12	10	0	78	6
4	A	0.160	14	11	0	75	6
5	A	0.259	10	10	0	80	6

### 3.3.1.6 Discussion

**Figure 3.4** showed the conversion vs. selectivity in all the blank reactions in this project. They showed similar terminal selectivities to Iglesia's work (**Figure 3.5**) [8-9].

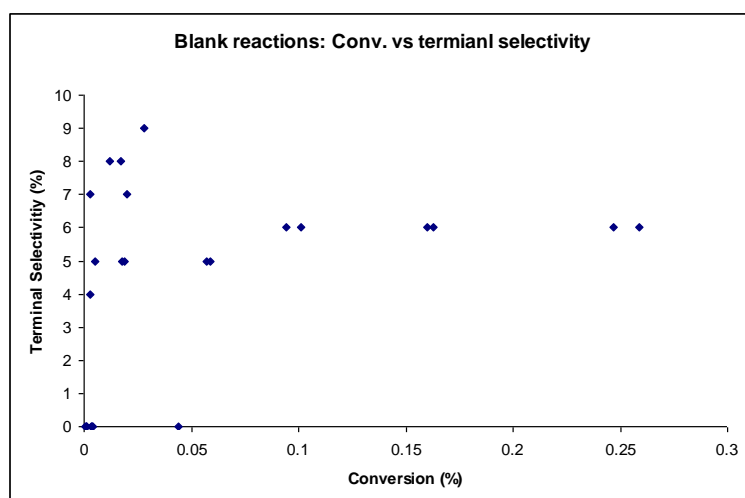


**Figure 3.4 Conversion vs. terminal selectivity in all the blank reactions**

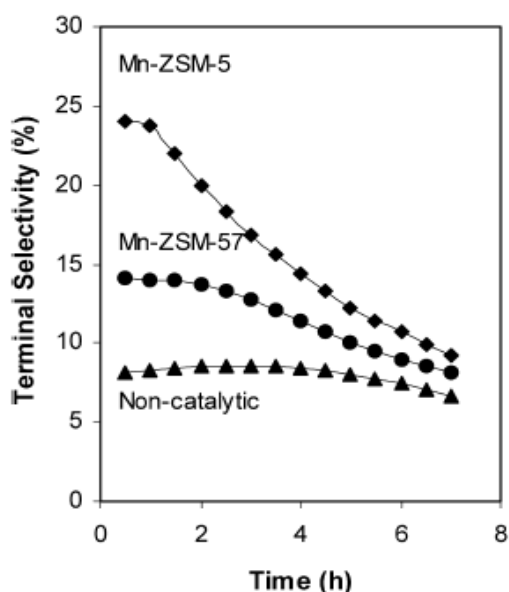


**Figure 3.5 Iglesia's results [8-9]**

### 3.3.2 Reaction with Mn-ZSM5 (from JM)

The Mn-ZSM5 catalyst as described in Iglesia's work was provided by Johnson Matthey, to investigate the activity and selectivity under the equivalent conditions. However it was found that both the conversion and terminal selectivity was extremely low (**Table 3.12**).

The Mn-ZSM5 catalyst was activated before each reaction, and then used in the reaction after cooling down to the room temperature. Therefore, it is possible that the sample absorbed moisture which could block the pore structure. Hence a time-on-line test reaction was performed to check this. In the reaction shown below, the Mn-ZSM5 was put into the hexane as soon as possible after being removed from the furnace. From the results (**Table 3.13**), the hot catalyst is still not very active and shows little difference in product distribution from the cool catalyst. The results are still different from Iglesia's.

**Table 3.12 130 °C, 3 bar O<sub>2</sub>, 25 ml *n*-hexane, stir speed 2, varied time, 1.00 g Mn-ZSM5, 0.15 ml 1,2,4-trichlorobenzene**

Time (h)	Reactor	Conv.(%)	Selectivity (%)				
			Ketones	Alcohols	Acid	Others	1-hexanol
0.5	A	0.007	15	1	0	84	0
1	A	0.010	10	0	0	90	0
2	A	0.015	12	1	0	87	0
3	A	0.018	16	2	0	82	0
4	A	0.021	18	2	0	80	0
5	A	0.0294	17	2	0	81	0

**Table 3.13 130 °C, 3 bar O<sub>2</sub>, 25 ml *n*-hexane, stir speed 2, time-on-line, 1 g Mn-ZSM5**

Time (h)	Reactor	Conv.(%)	Selectivity (%)				
			Ketones	Alcohols	Acid	Others	1-hexanol
30min	A	0					
1h	A	0					
4h	A	0.02	29	12	0	59	2

### 3.4 Conclusion

Comparison between the Andrews glass reactor and Parr stainless steel reactor showed that the blank reactions got higher conversion but lower terminal selectivity in the stainless steel reactor than the glass reactor, which indicates the stainless steel reactor itself may have some activity in the oxidation reaction.

The time on-line blank reaction results showed similar terminal selectivities to Iglesia's work in autoxidation [8-9], with the terminal selectivity 5%-9%. However, the terminal selectivity with Mn-ZSM5 was still very low (~0). Iglesia's results cannot be reproduced.

Except the linear alcohol and acids calibrated and listed in the experimental section in **Chapter 2**, further analysis found a few unknown products after the oxidation reaction. GC-MS analysis was performed and some of the unknown products were identified as the acids and other C6 alcohols.

### 3.5 References

- [1] J.M. Thomas, R. Raja, G. Sankar, R.G. Bell, *Nature*, (1999), 227.
- [2] R. Raja, J.M. Thomas, *Chemical Communications*, (1998), 1841.
- [3] R. Raja, G. Sankar, J.M. Thomas, *Journal of the American Chemistry Society*, 121, (1999), 119.
- [4] J.M. Thomas, R. Raja, G. Sankar, R. G. Bell, *Studies in Surface Science and Catalysis*, 130, (2000), 887.
- [5] R. Raja, G. Sankar, J.M. Thomas, *Angewandte Chemistry*, 39, (2000), 231.
- [6] J.M. Thomas, R. Raja, G. Sankar, R.G. Bell, *Accounts of Chemical Research*, 34, (2001), 191.
- [7] R. Raja, J.M. Thomas, *Journal of Molecular Catalysis A*, 3, (2002), 181.

[8] B. Mod n, B. Zhan, J. Dakka, J. G. Santiesteban, E. Iglesia, *Journal of Physical Chemistry*, 111, (2007), 1402.

[9] B. Zhan, B. Mod n, J. Dakka, J.G. Santiesteban, E. Iglesia, *Journal of Catalysis* 245, (2007), 316.

# CHAPTER 4

## *Catalytic Investigation for Teabag Coating*

---

# CATALYTIC INVESTIGATION

## FOR TEABAG COATING

---

### 4.1 Introduction

The aim of the project is to realise the terminal oxidation of long chain *n*-alkanes, for example, using *n*-decane and *n*-hexane as model compounds to produce 1-decanol, decanoic acid or 1-hexanol and hexanoic acid (**Figure 4.1**) in liquid phase reactions. There are two challenges in this study: how to enhance the activity of the reaction and how to control the regioselectivity of the oxidation. To overcome the challenges, various catalysts were introduced into the project.

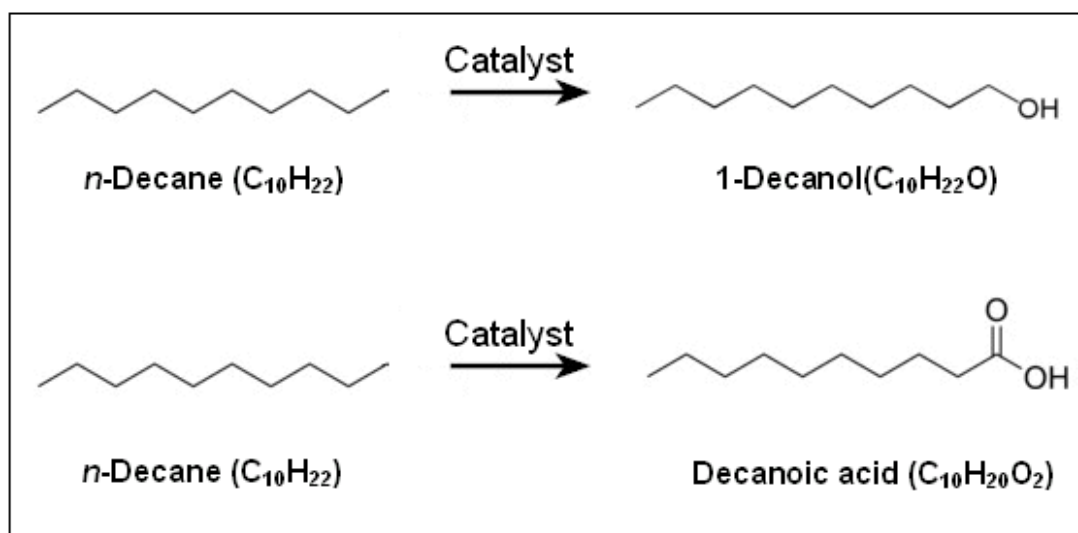


**Figure 4.2 Aim of the thesis – terminal oxidation of decane**

As introduced in **Chapter 1**, teabag technology involves two components: the active supported catalyst substrate, and the shape selective coating. In this chapter, the focus is to find the relatively active and selective substrate catalysts.

## 4.2 Experimental

### 4.2.1 Metal/support catalysts

A series of metal/support catalysts were prepared in the project by the impregnation method.

In the case, Pd, Au and Pt were employed. The synthesis method is shown as below [1]:

#### Preparation method for the 5 w.t.% Pd/TiO<sub>2</sub>

- i. Dissolve 0.5 g PdCl<sub>2</sub> in 10 ml deionized water. Stir and heat at 85°C for 30 min.
- ii. Place 1.9 g TiO<sub>2</sub> in a Petri dish. Dropwise add the PdCl<sub>2</sub> solution to the Petri dish. Shake the dish until the powder and solution mix well.
- iii. Dry the paste at 110°C for 16 h. Grind the paste and then calcine at 400°C for 3 h.

#### Preparation method for the 5 w.t.% Au/TiO<sub>2</sub>

- i. Prepare the HAuCl<sub>4</sub> solution which includes 0.1 g Au<sup>3+</sup>.
- ii. Place 1.9 g TiO<sub>2</sub> in a beaker. Dropwise add the HAuCl<sub>4</sub> solution to the beaker. Stir 30 min until the powder and solution mix well.
- iii. Dry the paste at 110°C for 16 h. Grind the paste and then calcine at 400°C for 3 h.

#### Preparation method for the 5 w.t.% Pt/TiO<sub>2</sub>

- i. Use 0.2655g H<sub>2</sub>PtCl<sub>6</sub>·6H<sub>2</sub>O and 10g deionized water to prepare the solution which includes 0.1g Pt<sup>4+</sup>.
- ii. Place 1.9g TiO<sub>2</sub> in a beaker. Dropwise add the H<sub>2</sub>PtCl<sub>6</sub> solution to the beaker. Stir until the powder and solution mix well.
- iii. Dry the paste at 110°C overnight. Grind the paste and then calcine at 500°C for 6h.

Parts of the prepared catalysts were reduced in H<sub>2</sub>. To prepare the reduced catalysts, the

catalysts were calcined in flowing H<sub>2</sub> at 300°C for 3 h.

Other supports were also employed, such as activated carbon (Aldrich G60, Waterlink Sutcliffe Carbons Activated Carbon Grade: 207A, Mesh: 12 \*20), graphite, SiO<sub>2</sub> (Grace, >99 %, 60-100 mesh) and alumina.

The reaction conditions taken for the powder form catalysts usually are: 200 psi O<sub>2</sub>, 600 rpm, 100 °C/110 °C, 10 g *n*-decane and 0.05 g catalyst.

#### 4.2.2 Rh/Ru loaded catalysts

##### Synthesis of catalyst

1 w.t.% and 3 w.t.% Rh/ $\alpha$ -Al<sub>2</sub>O<sub>3</sub>, Rh/ $\gamma$ -Al<sub>2</sub>O<sub>3</sub>, Ru/ $\gamma$ -Al<sub>2</sub>O<sub>3</sub> were prepared by the incipient wetness method and deposition precipitation (DP) method separately. The incipient wetness method was carried out as before. Taking the 1 wt.% Rh/ $\gamma$ -Al<sub>2</sub>O<sub>3</sub> as an example, to prepare 1 g 1 w.t.% Rh/ $\gamma$ -Al<sub>2</sub>O<sub>3</sub>, 0.99 g  $\gamma$ -Al<sub>2</sub>O<sub>3</sub> was dispersed in a solution of 0.025 g RhCl<sub>3</sub> · xH<sub>2</sub>O (Alfa Aesar). The water amount in the solution was the least amount to form a paste. The paste was dried overnight at 110 °C and then calcined at 400 °C for 3 h. The DP preparation is carried out as followed (taking the 3 wt.%Rh/ $\gamma$ -Al<sub>2</sub>O<sub>3</sub> as an example): to prepare 1 g 3 wt.% Rh/ $\gamma$ -Al<sub>2</sub>O<sub>3</sub>, 0.99 g  $\gamma$ -Al<sub>2</sub>O<sub>3</sub> was first dispersed in an aqueous solution of 0.075 g RhCl<sub>3</sub> · xH<sub>2</sub>O. A quantity of 1 M Na<sub>2</sub>CO<sub>3</sub> was slowly added to the RuCl<sub>3</sub> solution until the pH value of the mixture reached 10.5. The suspension was then maintained at the same pH for 1 h during the precipitation process. The resulting solid was washed with deionized water several times until no chloride ion was detected by addition of silver nitrate solution to the filtrate. All the catalysts were dried at 110 °C (12 h) in air. Finally they were calcined at 500 °C for 5 h in air [2].

Alumina (Saint-Gobain, surface area 0.25 m<sup>2</sup>/g) spheres have been tested in this project to date. The vacuum incipient wetness method was employed in the preparation of sphere catalysts. To

prepare 1 g catalyst, 1 g alumina sphere was placed into a sealed two necked round bottom flask. The flask was heated to 80 °C with an oil bath and evacuated by a vacuum pump for 1 h. The calculated amount of metal solution was added into the flask through a syringe. The flask was shaken until all the metal solution was absorbed into the spheres. Then the spheres were dried at 110 °C overnight and then calcined at 400 °C for 3 h.

### Reactions

The reaction conditions taken for the powder form catalysts usually are: 15 bar O<sub>2</sub>, 600 rpm, 110 °C, 10 g *n*-decane and 0.05 g catalyst. With the sphere supports, different from the previous work, the reaction system has to be adjusted, as single sphere is much heavier (e.g. the mass of a single silica sphere  $\approx$  0.09 g) than the catalysts used in the previous reactions (0.05 g in each reaction).

## **4.3 Results**

### **4.3.1 Pd, Au, Pt loaded supported catalysts**

The metal loaded catalysts and reduced catalysts were used in reactions under the conditions: 100°C, 200 psi O<sub>2</sub>, 24 h, 0.05 g catalyst and 600 rpm.

**Table 4.1 100°C, 200 psi O<sub>2</sub>, 24 h, 10 g *n*-decane, 0.05 g catalyst and 600 rpm**

Catalyst	Conv. (%)	Selectivity (%)													
		5/4 one	3 one	2 one	5/4 ol	3 ol	2 ol	C <sub>5</sub> OOH	Di- one	C <sub>6</sub> OOH	Di- one	Di- one	C <sub>7</sub> OOH	C <sub>8</sub> OOH	C <sub>10</sub> OOH
Pd/TiO <sub>2</sub>	0.09%	0	0	3	17	20	19	0	0	0	0	0	6	2	1
Reduced Pd/TiO <sub>2</sub>	0	0	0	0	0	0	0	0	0	0	0	0	0	0	0
Au/TiO <sub>2</sub>	0.17%	0	0	0	16	2	26	0	13	0	2	2	5	3	4
Au/TiO <sub>2</sub>	0.25%	0	0	15	18	0	22	0	9	0	3	2	10	2	9
Reduced Au/TiO <sub>2</sub>	0.005%	0	0	0	0	0	100	0	0	0	0	0	0	0	0
Pt/TiO <sub>2</sub>	0	-	-	-	-	-	-	-	-	-	-	-	-	-	-
Pt/TiO <sub>2</sub>	0	-	-	-	-	-	-	-	-	-	-	-	-	-	-
Reduced Pt/TiO <sub>2</sub>	0	-	-	-	-	-	-	-	-	-	-	-	-	-	-

These results (**Table 4.1**) show very low conversion, and are in fact lower than those for a blank reaction (0.1-0.3%), demonstrating an inhibition of some part of the reaction by the Pd/TiO<sub>2</sub>. With Au/ TiO<sub>2</sub> it was found in the product distribution that a number of C10 ketones formed in the reaction. Pd/TiO<sub>2</sub> inhibits the auto-oxidation reaction.

Initial results indicated poor activities with Pd/TiO<sub>2</sub>, Au/TiO<sub>2</sub> and Pt/TiO<sub>2</sub> for decane oxidation in both liquid reactions at 100 °C.

### 4.3.2 Higher temperature reactions

With the intention of obtaining higher conversion, it was decided to increase the reaction temperature to 110 °C. More catalysts were prepared and tested at 100 °C and 110 °C. The conversion and product distribution results were shown in Table 4.2 and Table 4.3. It was still found that none of the catalysts showed good activity at 100 °C. However the Au catalysts appear to be better than others on TiO<sub>2</sub> and SiO<sub>2</sub> supports.

**Table 4.2 100 °C, *n*-decane 10 g, catalyst 0.05 g, 200 psi O<sub>2</sub>, 24 h**

Catalyst	Conv. (%)	Selectivity (%)											
		5/4 one	3 one	2 one	5/4 ol	3 ol	2 ol	C <sub>5</sub> OOH	Di- one	C <sub>6</sub> OOH	C <sub>7</sub> OOH	C <sub>8</sub> OOH	C <sub>10</sub> OOH
Blank	<b>0.30</b>	22	13	18	7	6	10	4	11	0	6	2	1
TiO <sub>2</sub>													
TiO <sub>2</sub>	<b>0.10</b>	34	22	8	10	3	8	9	7	0	0	0	0
Au/TiO <sub>2</sub>	<b>0.25</b>	15	18	0	22	0	9	5	10	2	9	0	0
Pt/TiO <sub>2</sub>	<b>0</b>	-	-	-	-	-	-	-	-	-	-	-	-
Pd- Au/TiO <sub>2</sub>	<b>0.04</b>	37	6	6	5	3	2	7	34	0	0	0	0
Carbon													
Carbon	<b>0.02</b>	13	0	0	65	0	0	0	22	0	0	0	0
Au/Carbon	<b>0</b>	-	-	-	-	-	-	-	-	-	-	-	-
SiO <sub>2</sub>													
Au/SiO <sub>2</sub>	<b>0.17</b>	34	28	2	3	11	0	11	7	0	1	3	0
Au- Pd/SiO <sub>2</sub>	<b>0.29</b>	17	13	9	9	11	26	5	8	0	2	1	0

Table 4.3 110 °C, *n*-decane 10 g, catalyst 0.05 g, 15 bar O<sub>2</sub>, 24 h

Catalyst	Conv. (%)	Selectivity (%)											
		5/4 one	3 one	2 one	5/4 ol	3 ol	2 ol	C <sub>5</sub> OOH	Di- one	C <sub>6</sub> OOH	C <sub>7</sub> OOH	C <sub>8</sub> OOH	C <sub>10</sub> OOH
Blank*	<b>1.44</b>	26	7	8	17	2	2	4	12	8	6	1	2
TiO <sub>2</sub>													
TiO <sub>2</sub>	<b>3.68</b>	19	10	16	13	8	9	6	10	0	6	1	1
Au/TiO <sub>2</sub>	<b>5.71</b>	24	15	4	4	2	13	7	20	1	4	2	2
Repeat Au/TiO <sub>2</sub>	<b>2.88</b>	15	13	13	11	8	11	5	8	0	7	7	1
Pt/TiO <sub>2</sub>	<b>0.05</b>	0	0	0	52	0	0	0	48	0	0	0	0
SiO <sub>2</sub>													
SiO <sub>2</sub>	<b>1.21</b>	27	18	13	6	4	5	7	10	8	3	0	0
Au/SiO <sub>2</sub>	<b>2.02</b>	27	18	21	6	2	2	5	13	2	1	2	0
AuPd/SiO <sub>2</sub>	<b>1.87</b>	14	15	16	10	8	11	6	5	5	7	1	1
Al <sub>2</sub> O <sub>3</sub>													
Al <sub>2</sub> O <sub>3</sub>	<b>0.39</b>	26	14	6	18	5	4	7	8	10	1	0	0
Au/Al <sub>2</sub> O <sub>3</sub>	<b>1.04</b>	15	11	12	21	6	3	7	15	5	3	2	1
Carbon													
Au/Carbon	<b>0.01</b>	0	0	0	0	0	0	0	100	0	0	0	0

\*Blank reactions have been repeated and got conversions range from 1.44-2.02%.

### 4.3.3 Discussion

**Table 4.4** shows the comparison of the conversions at 100 °C and 110 °C. The increase of the reaction temperature from 100 °C to 110 °C resulted in an increase in the conversions observed. At the temperature of 110 °C, a number of catalysts showed some activity, but it must also be remembered that there is also a considerable rise in auto-oxidation through a temperature increase. Therefore, a radical scavenger was introduced.

**Table 4.4 Conversion at 100 °C and 110 °C**

Catalyst	Conv. at 100 °C(%)	Conv. at 110 °C(%)
Blank	0.30	1.44
TiO <sub>2</sub>	0.10	3.68
Au/TiO <sub>2</sub>	0.25	5.71 (2.88)
Pt/TiO <sub>2</sub>	0	0.05
Au/SiO <sub>2</sub>	0.17	2.02
AuPd/SiO <sub>2</sub>	0.29	1.87
Au/Carbon	0	0.01

### 4.3.4 Use of a radical scavenger

In order to identify the real activity of the catalyst, Tempo has been employed in the reactions to kill the auto-oxidation by acting as a radical scavenger. The TEMPO form used was stabilized on a polymer support.

**Table 4.5 110 °C, *n*-decane 10 g, catalyst 0.05 g, TEMPO 0.005 g, 15 bar O<sub>2</sub>, 24 h**

Catalyst	Conv. (%)	Selectivity (%)											
		5/4 one	3 one	2 one	5/4 ol	3 ol	2 ol	C <sub>5</sub> OOH	Di- one	C <sub>6</sub> OOH	C <sub>7</sub> OOH	C <sub>8</sub> OOH	C <sub>10</sub> OOH
Blank	<b>0</b>	-	-	-	-	-	-	-	-	-	-	-	-
TiO <sub>2</sub>													
TiO <sub>2</sub>	<b>0.11</b>	30	13	4	9	10	22	7	5	0	0	0	0
Au/TiO <sub>2</sub>	<b>0.28</b>	17	14	15	8	15	14	7	6	1	1	2	0
SiO <sub>2</sub>													
SiO <sub>2</sub>	<b>0.86</b>	21	13	13	5	3	2	4	30	4	6	1	1
Au/SiO <sub>2</sub>	<b>0.99</b>	21	14	18	8	7	8	5	9	4	4	4	1
Al <sub>2</sub> O <sub>3</sub>													
Au/Al <sub>2</sub> O <sub>3</sub>	<b>0.62</b>	15	10	17	7	12	13	5	10	5	4	1	0

**Table 4.6 Conversions without and with TEMPO**

Catalyst	Conv. without TEMPO(%)	Conv. with TEMPO(%)
Blank	1.44	0
SiO <sub>2</sub>	1.21	0.86
Au/SiO <sub>2</sub>	2.02	0.99
TiO <sub>2</sub>	3.68	0.11
Au/TiO <sub>2</sub>	5.71/2.88	0.28
Au/Al <sub>2</sub> O <sub>3</sub>	1.04	0.62

The results show a greater drop in conversion for the TiO<sub>2</sub> based samples than for the SiO<sub>2</sub> and Al<sub>2</sub>O<sub>3</sub> samples. This decrease is most marked as the TiO<sub>2</sub> samples have the greatest conversion without TEMPO and become those with the lowest conversion once the radical scavenger is added. The level of conversion obtained from catalytic processes still remains too low at this stage to develop further with a coating, so the search for a suitable material/conditions was continued.

#### **4.3.5 Development of the catalyst preparation method**

The impregnation method used previously within this work used a large excess of water. It was thought that this may be leading to disadvantageous distribution of metal particles, both in terms of size and distribution within the pores of the material. An alternative method of preparation using the incipient wetness method to only fill the pores of the material was therefore used and compared to the previous method. The support materials were exposed to the same preparation conditions (acid/heat treatments) so that the effects of these could be negated. Please note that from here the modified GC program and column are used to analyse the products. **Table 4.7** reports the results from a catalyst tested by both the old and new methods. A higher conversion is reported with the new method and an increase in acid selectivity.

**Table 4.7 Comparison between GC analysis methods**

Catalyst	Conv. (%)	Selectivity (%)												
		5/4 one	3 one	2 one	5/4 ol	3 ol	2 ol	C <sub>5</sub> OOH	1 ol	C <sub>6</sub> OOH	C <sub>7</sub> OOH	C <sub>8</sub> OOH	C <sub>9</sub> OOH	C <sub>10</sub> OOH
Al <sub>2</sub> O <sub>3</sub> (Old)	<b>0.39</b>	26	14	18	6	5	4	7	-	10	1	0	-	1
Al <sub>2</sub> O <sub>3</sub> (New)	<b>0.69</b>	21.7	15.0	17.6	6.0	4.3	7.4	7.2	1.4	6.1	9.0	2.0	0.6	1.5

**Table 4.8 24h, 110 °C, 600 rpm, 15 bar Oxygen, *n*-decane (10 g), 0.05 g catalyst**

Catalyst	Conv. (%)	Selectivity (%)												
		5/4 one	3 one	2 one	5/4 ol	3 ol	2 ol	C <sub>5</sub> OOH	1 ol	C <sub>6</sub> OOH	C <sub>7</sub> OOH	C <sub>8</sub> OOH	C <sub>9</sub> OOH	C <sub>10</sub> OOH
TiO <sub>2</sub>	<b>1.96</b>	18.2	10.9	13.5	7.6	4.8	7.8	11.4	1.0	12.2	7.9	0.9	1.9	1.7
Au/TiO <sub>2</sub>	<b>3.43</b>	27.5	12.7	3.2	9.6	7.0	5.2	8.3	0.9	10.9	11.2	1.1	0.5	1.9
SiO <sub>2</sub>	<b>1.61</b>	26.2	17.2	18.3	4.3	3.3	5.8	7.3	1.0	6.3	6.8	1.0	0.4	2.1
Au/SiO <sub>2</sub>	<b>2.18</b>	17.8	13.5	13.2	5.4	3.5	6.8	8.2	1.1	11.5	12.5	3.6	0.5	2.2
Graphite	<b>2.81</b>	17.7	13.3	15.0	9.5	6.1	9.3	8.2	1.1	6.7	8.7	1.5	0.6	2.2
Au/Graphite	<b>3.87</b>	14.5	10.6	11.0	7.3	4.8	7.4	8.7	1.5	11.1	13.3	6.7	1.0	2.2
G60	<b>0</b>	-	-	-	-	-	-	-	-	-	-	-	-	-
Au/G60	<b>0</b>	-	-	-	-	-	-	-	-	-	-	-	-	-

Graphite was tried as the support this time and was the catalyst with the highest conversion so far. The conversion and selectivity of products are shown graphically in **Figure 4.2** to **Figure 4.7**.

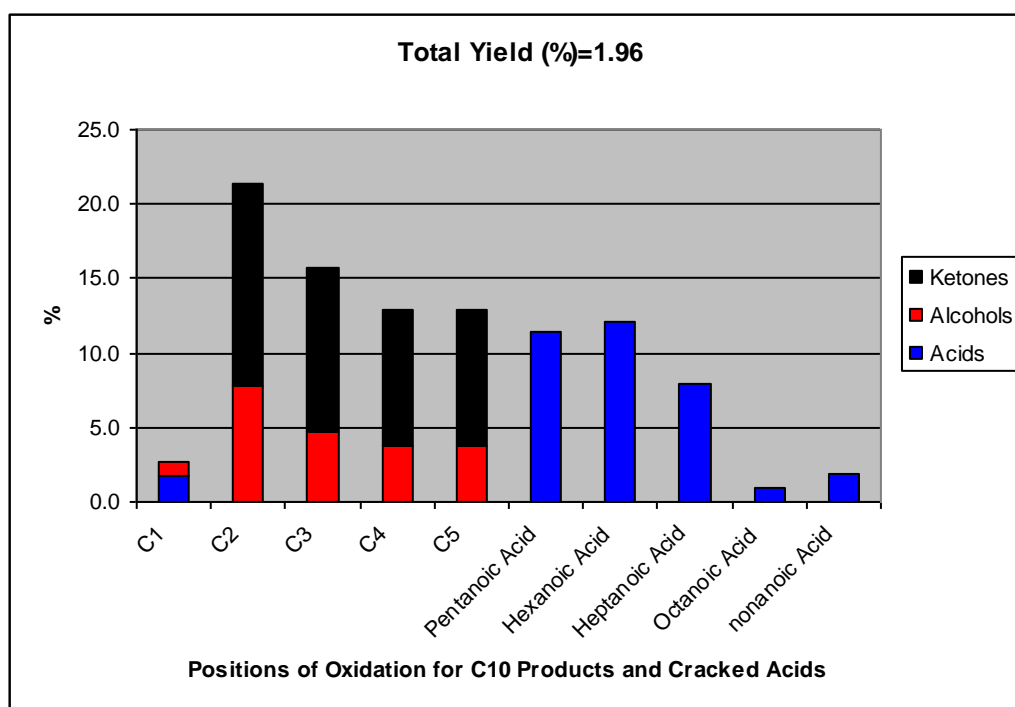


**Figure 4.2 24 h, 110 °C, 600 rpm, 15 bar Oxygen, 0.05 g TiO<sub>2</sub>**

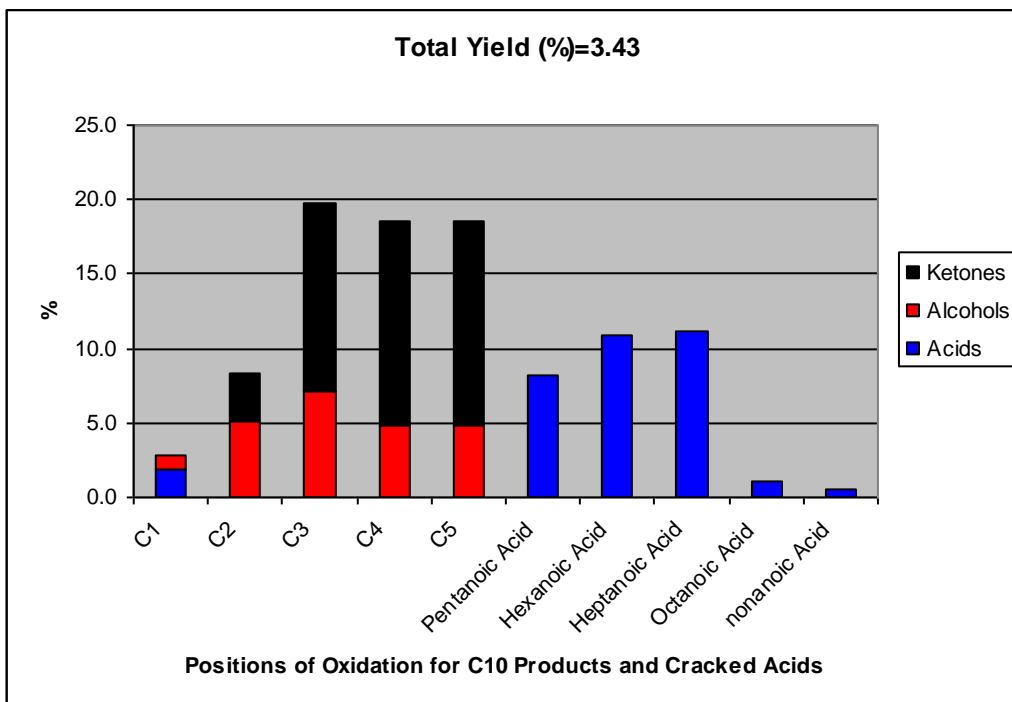


**Figure 4.3 24h, 110 °C, 600 rpm, 15 bar Oxygen, 0.05 g Au/TiO<sub>2</sub>**

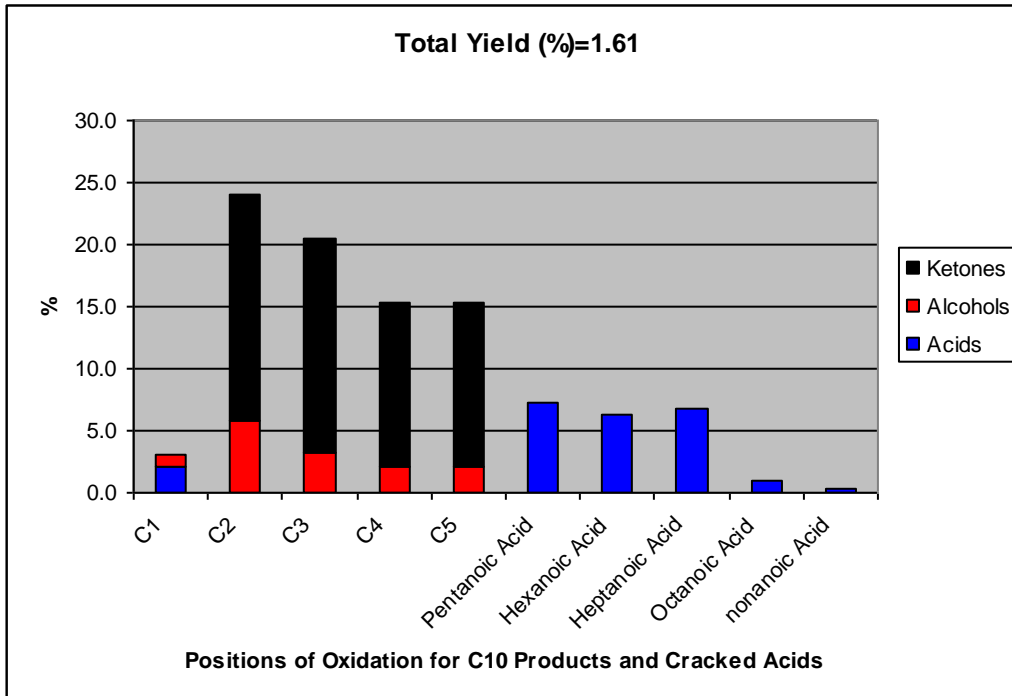


**Figure 4.4 24h, 110 °C, 600 rpm, 15 bar Oxygen, 0.05 g SiO<sub>2</sub>**

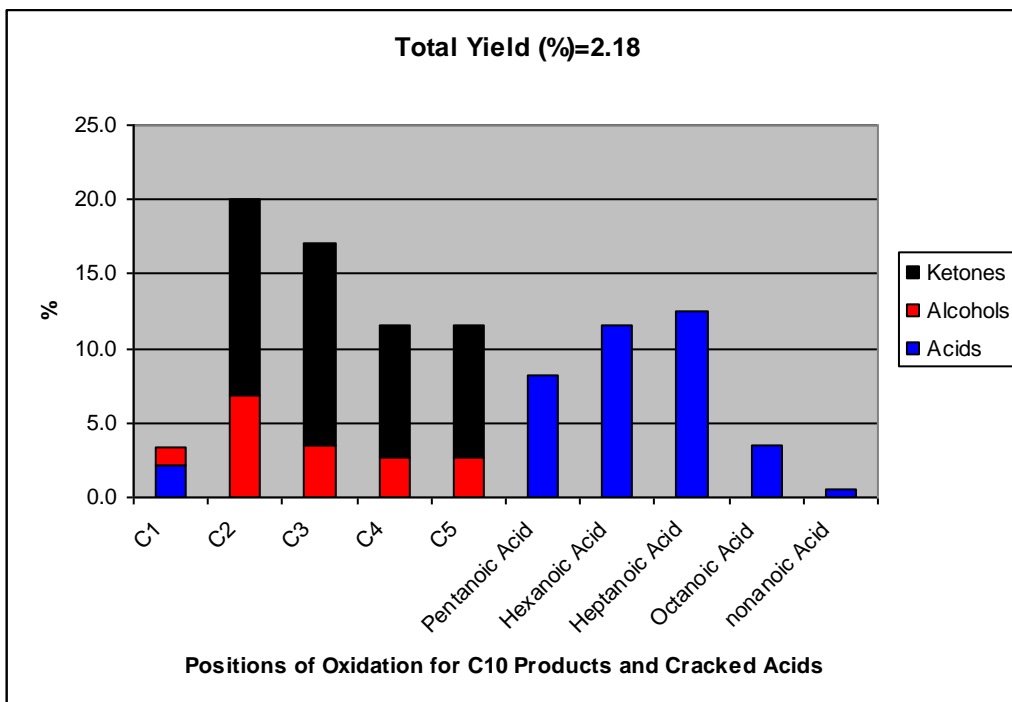


**Figure 4.5 24 h, 110 °C, 600 rpm, 15 bar Oxygen, 0.05 g Au/SiO<sub>2</sub>**

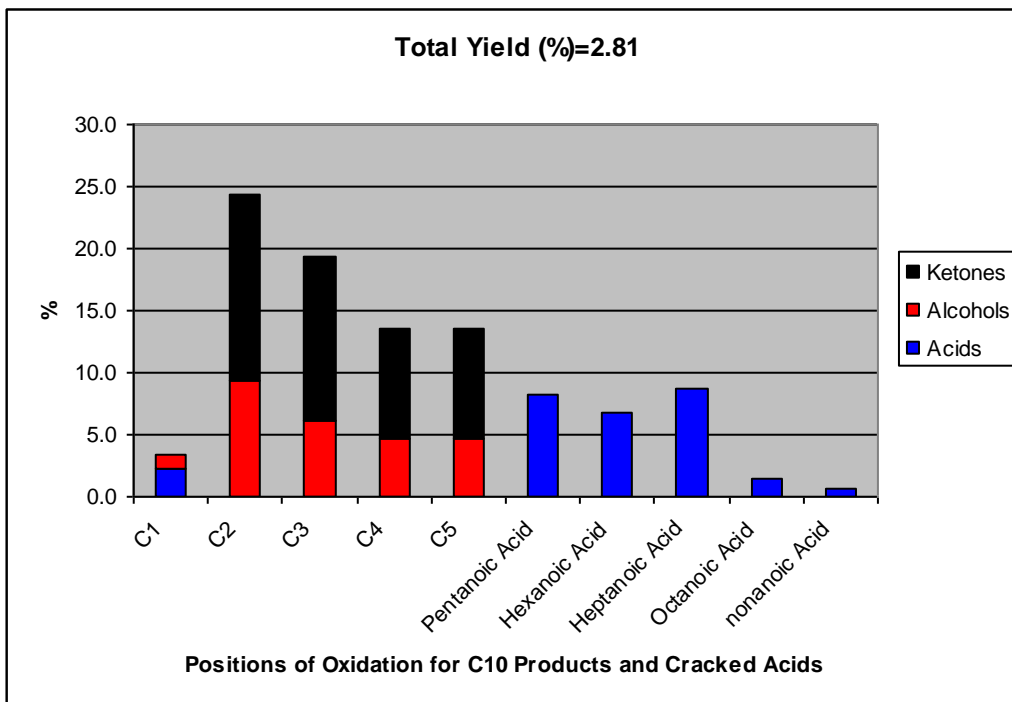


**Figure 4.6 24 h, 110 °C, 600 rpm, 15 bar Oxygen, 0.05 g graphite**

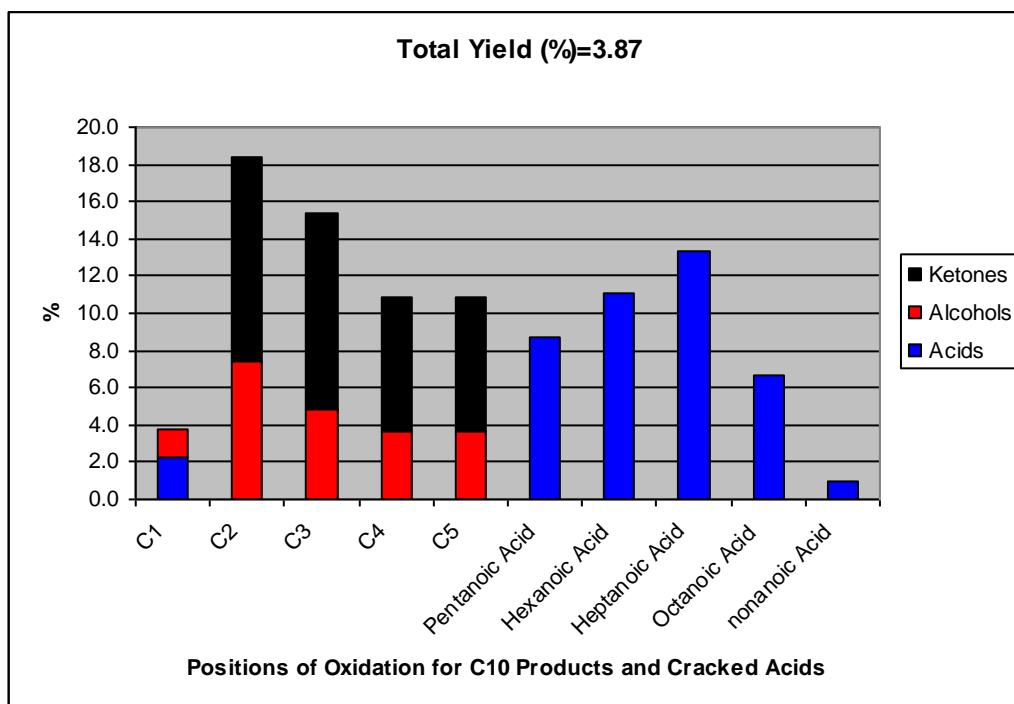


**Figure 4.7 24 h, 110 °C, 600 rpm, 15 bar Oxygen, 0.05 g Au/Graphite**

#### 4.3.6 Ru and Rh loaded catalysts

From the literature, the  $\alpha$ - and  $\gamma$ -alumina supports are two of the most widely used supports for the preparation of Ru/Rh catalysts and zeolite coating. It should be noted that from the previous results with gold, the alumina powder support showed less activity than the titania and silica powder supports; however, titania support does not suit the coating conditions; therefore, several different types of alumina supports were selected and tested in this section.

### 4.3.6.1 $\alpha$ -phase alumina powder support

The 5 w.t.% Rh/Al<sub>2</sub>O<sub>3</sub> used in the test was prepared by the incipient wetness method using: Al<sub>2</sub>O<sub>3</sub> - calcined, powder, primarily  $\alpha$ -phase, 100-325 mesh, and RhCl<sub>3</sub> xH<sub>2</sub>O (Rh 40 w.t. %)

The 5 w.t.% Rh/Al<sub>2</sub>O<sub>3</sub> powder catalyst have been tested at 100 °C and 110 °C. Table 4.9 shows the results for the 6 h oxidation at 100 °C. The result for the blank reaction at the same temperature was given as a comparison.

**Table 4.9 100 °C, 15 bar, 10 g *n*-decane, 0.05 g catalyst, 6 h**

Catalyst	Conv. (%)	Selectivity (%)													
		5/4 one	3 one	2 one	5/4 ol	3 ol	2 ol	1 ol	C <sub>5</sub> OOH	C <sub>6</sub> OOH	C <sub>7</sub> OOH	C <sub>8</sub> OOH	C <sub>9</sub> OOH	C <sub>10</sub> OOH	
Blank	<b>0.02</b>	20.6	13.4	17.3	6.7	4.8	8.7	1.9	15.0	4.1	5.2	0.8	0.4	1.2	
$\alpha$ -Al <sub>2</sub> O <sub>3</sub>	<b>0.008</b>	20.2	13.5	21.1	8.4	6.2	10.4	2.4	14.5	1.8	1.5	0	0	0	
5%Rh/ $\alpha$ - Al <sub>2</sub> O <sub>3</sub>	<b>0.02</b>	20.4	13.8	20.2	8.4	6.4	10.2	2.4	13.8	1.8	2.2	0.2	0.2	0	

**Table 4.10 110 °C, 15 bar, 10 g *n*-decane, 0.0 5g catalyst, 6 h**

Catalyst	Conv. (%)	Selectivity(%)												
		5/4 one	3 one	2 one	5/4 ol	3 ol	2 ol	1 ol	C <sub>5</sub> OOH	C <sub>6</sub> OOH	C <sub>7</sub> OOH	C <sub>8</sub> OOH	C <sub>9</sub> OOH	C <sub>10</sub> OOH
Blank	<b>0.07</b>	28.7	17.2	23.2	3.5	2.4	4.1	1.0	15.4	2.2	1.9	0.2	0.1	0
$\alpha$ -Al <sub>2</sub> O <sub>3</sub>	<b>0.06</b>	22.2	14.1	19.5	5.2	3.9	7.0	1.3	18.6	4.3	2.9	0.4	0.2	0.1
5%Rh/ $\alpha$ -Al <sub>2</sub> O <sub>3</sub>	<b>0.06</b>	22.1	13.8	18.5	5.8	4.4	7.1	1.4	21.0	2.5	2.7	0.2	0.2	0.1

It is found the 5 w.t.% Rh/Al<sub>2</sub>O<sub>3</sub> did not show activity above that observed for the autoxidation at 100 °C, while the product distribution between the Al<sub>2</sub>O<sub>3</sub> with and without the addition of 5%Rh is very similar. At a raised temperature, 110 °C, it is again found that there is no change in the activity and product distribution between the autoxidation, and Al<sub>2</sub>O<sub>3</sub> with and without the addition of 5%Rh (**Table 4.10**). According to the results at 100 °C and 110 °C, it seems that the Rh did not help the oxidation on the Al<sub>2</sub>O<sub>3</sub> support. This may be due to the fact that the 5 w.t.% loading of Rh is too high a concentration for the Al<sub>2</sub>O<sub>3</sub> support. A later BET analysis showed that the surface area of this kind of Al<sub>2</sub>O<sub>3</sub> powder is 1m<sup>2</sup>/g, which means the 5 w.t.% loading of Rh is too concentrated for the  $\alpha$ -Al<sub>2</sub>O<sub>3</sub>. Therefore a less loading of Rh should be tested.

The reaction results with a 0.1 w.t.% Rh loading at 110°C are given in **Table 4.11**. From this table it is found that both the conversion and selectivity are quite similar between the blank  $\alpha$ -Al<sub>2</sub>O<sub>3</sub> and the metal added catalyst, which means the 0.1 w.t.% Rh/ $\alpha$ -Al<sub>2</sub>O<sub>3</sub> powder catalyst is inactive. The  $\alpha$ -Al<sub>2</sub>O<sub>3</sub>, with a low surface area, is not a suitable support for the project.

**Table 4.11 110 °C, 15 bar, 10 g *n*-decane, 0.05 g catalyst, 6 h**

Catalyst	Conv. (%)	Selectivity (%)													
		5/4 one	3 one	2 one	5/4 ol	3 ol	2 ol	1 ol	C <sub>5</sub> OOH	C <sub>6</sub> OOH	C <sub>7</sub> OOH	C <sub>8</sub> OOH	C <sub>9</sub> OOH	C <sub>10</sub> OOH	
Blank	<b>0.07</b>	28.7	17.2	23.2	3.5	2.4	4.1	1.0	15.4	2.2	1.9	0.2	0.1	0	
$\alpha$ -Al <sub>2</sub> O <sub>3</sub>	<b>0.06</b>	22.2	14.1	19.5	5.2	3.9	7.0	1.3	18.6	4.3	2.9	0.4	0.2	0.1	
0.1%Rh/ $\alpha$ -Al <sub>2</sub> O <sub>3</sub>	<b>0.06</b>	22.1	13.8	18.5	5.8	4.4	7.1	1.4	21.0	2.5	2.7	0.2	0.2	0.1	

#### 4.3.6.2 $\gamma$ -phase alumina powder support

In order to allow a higher loading of Rh on the support, the  $\gamma$ -Al<sub>2</sub>O<sub>3</sub> with a surface area of 140 m<sup>2</sup>/g was employed at this time. A 3 w.t.% Rh was added to the  $\gamma$ -Al<sub>2</sub>O<sub>3</sub> as an initial test (**Table 4.12**). The product distribution for blank and the  $\alpha$ -Al<sub>2</sub>O<sub>3</sub> based catalyst reactions under the same conditions are given as a comparison.

According to **Table 4.12**, there is no difference between the blank  $\alpha$ -Al<sub>2</sub>O<sub>3</sub> support and the 0.1 w.t.% Rh added catalyst; however there is a definite increase in the activity with a 3% Rh addition on the  $\gamma$ -Al<sub>2</sub>O<sub>3</sub>. As well as the conversion increase, the product distribution changes – compared with the blank  $\gamma$ -Al<sub>2</sub>O<sub>3</sub> support, the selectivity for the ketones decreased while the cracked acids increased. It is clear that the particle size and concentration of active centre on the supports significantly influence the activity of the catalyst. Therefore, a further investigation was carried out. A lower loading of Rh on the same support and other catalyst preparation technique was tried to gain a best performance.

**Table 4.12 110 °C, 15 bar, 10 g *n*-decane, 0.05 g catalyst, 6 h**

Catalyst	Conv. (%)	Selectivity (%)													
		5/4 one	3 one	2 one	5/4 ol	3 ol	2 ol	1 ol	C <sub>5</sub> OOH	C <sub>6</sub> OOH	C <sub>7</sub> OOH	C <sub>8</sub> OOH	C <sub>9</sub> OOH	C <sub>10</sub> OOH	
Blank	<b>0.07</b>	28.7	17.2	23.2	3.5	2.4	4.1	1.0	15.4	2.2	1.9	0.2	0.1	0	
$\alpha$ -Al <sub>2</sub> O <sub>3</sub>	<b>0.06</b>	22.2	14.1	19.5	5.2	3.9	7.0	1.3	18.6	4.3	2.9	0.4	0.2	0.1	
0.1%Rh/ $\alpha$ -Al <sub>2</sub> O <sub>3</sub>	<b>0.06</b>	22.1	13.8	18.5	5.8	4.4	7.1	1.4	21.0	2.5	2.7	0.2	0.2	0.1	
$\gamma$ -Al <sub>2</sub> O <sub>3</sub>	<b>0.03</b>	21.4	13.8	24.5	9.0	6.7	12.5	2.7	6.8	0.4	0.5	0	0	0.3	
3%Rh/ $\gamma$ - Al <sub>2</sub> O <sub>3</sub>	<b>1.02</b>	15.5	10.9	13.1	9.1	5.7	8.4	1.3	15.8	10.1	6.4	1.4	0.3	2.1	

Different loadings of Rh by different preparation technique on  $\gamma$ -Al<sub>2</sub>O<sub>3</sub>

1 w.t.% and 3 w.t.% Rh/ $\gamma$ -Al<sub>2</sub>O<sub>3</sub> were prepared by incipient wetness method and deposition precipitation method respectively and the reaction results are given below.

**Table 4.13 110 °C, 15 bar, 10 g *n*-decane, 0.05 g catalyst, 6 h (by incipient wetness method)**

Catalyst	Conv. (%)	Selectivity (%)													
		5/4 one	3 one	2 one	5/4 ol	3 ol	2 ol	1 ol	C <sub>5</sub> OOH	C <sub>6</sub> OOH	C <sub>7</sub> OOH	C <sub>8</sub> OOH	C <sub>9</sub> OOH	C <sub>10</sub> OOH	
Blank	<b>0.07</b>	28.7	17.2	23.2	3.5	2.4	4.1	1.0	15.4	2.2	1.9	0.2	0.1	0	
untreated $\gamma$ -Al <sub>2</sub> O <sub>3</sub>	<b>0.03</b>	21.4	13.8	24.5	9.0	6.7	12.5	2.7	6.8	0.4	0.5	0	0	0.3	
1%Rh/ $\gamma$ - Al <sub>2</sub> O <sub>3</sub>	<b>0.62</b>	16.3	11.3	13.9	7.3	4.9	7.7	1.4	17.7	9.6	7.0	1.0	0.2	1.6	
3%Rh/ $\gamma$ - Al <sub>2</sub> O <sub>3</sub>	<b>0.93</b>	15.5	10.9	13.1	9.1	5.7	8.4	1.3	15.8	10.1	6.4	1.4	0.3	2.1	

**Table 4.14 110 °C, 15 bar, 10 g *n*-decane, 0.05 g catalyst, 6 h (by deposition precipitation method)**

Catalyst	Conv. (%)	Selectivity (%)													
		5/4 one	3 one	2 one	5/4 ol	3 ol	2 ol	1 ol	C <sub>5</sub> OOH	C <sub>6</sub> OOH	C <sub>7</sub> OOH	C <sub>8</sub> OOH	C <sub>9</sub> OOH	C <sub>10</sub> OOH	
Blank	<b>0.07</b>	28.7	17.2	23.2	3.5	2.4	4.1	1.0	15.4	2.2	1.9	0.2	0.1	0	
Untreated $\gamma$ -Al <sub>2</sub> O <sub>3</sub>	<b>0.03</b>	21.4	13.8	24.5	9.0	6.7	12.5	2.7	6.8	0.4	0.5	0	0	0.3	
1%Rh/ $\gamma$ - Al <sub>2</sub> O <sub>3</sub>	<b>0.32</b>	17.4	12.1	16.3	7.0	4.9	8.1	1.5	18.2	7.2	5.8	0.7	0.3	0.7	
3%Rh/ $\gamma$ - Al <sub>2</sub> O <sub>3</sub>	<b>0.30</b>	16.2	11.0	15.6	8.5	5.8	9.6	1.6	17.6	6.8	5.5	0.7	0.4	0.8	

Having a cross comparison among the results a few conclusions can be drawn: a) with the incipient wetness method, the different loading of Rh makes a difference in the activity, however the difference in selectivity is limited; b) with the DP method, the activity with different loading can be regarded as the same within the experimental error; the catalysts prepared by DP are less active than by the incipient wetness method c) with higher Rh loading, the selectivity of ketones decreased while the internal alcohol increased in comparison with the autoxidation, untreated  $\gamma$ -Al<sub>2</sub>O<sub>3</sub> and less loading of Rh catalyst, but the changes between the two different loading samples were not significant: the total cracked acids selectivity does not change, for both the two preparation technique.

Using the 3 w.t.% Rh/ $\gamma$ -Al<sub>2</sub>O<sub>3</sub> from the same batch, four parallel reactions were done to confirm the results (**Table 4.15**). According to the table, reaction 1 and reaction 2 were done when the batch was new, and the quite similar conversion and product distribution was reached; however the reaction 3 and 4, which were done days later, different product distributions and similar conversion was reached with the same loading catalyst prepared by DP method. This probably means the Rh formed by the incipient wetness method is not stable in air and became inactive in the storage.

**Table 4.15 110 °C, 15 bar, 10 g *n*-decane, 0.05 g 3 w.t.%Rh/ $\gamma$ -Al<sub>2</sub>O<sub>3</sub>, 6 h (by incipient wetness method)**

Reaction	Conv. (%)	Selectivity (%)													
		5/4 one	3 one	2 one	5/4 ol	3 ol	2 ol	1 ol	C <sub>5</sub> OOH	C <sub>6</sub> OOH	C <sub>7</sub> OOH	C <sub>8</sub> OOH	C <sub>9</sub> OOH	C <sub>10</sub> OOH	
1	<b>0.93</b>	15.5	11.1	13.6	9.1	5.7	8.6	1.2	16.1	9.4	6.2	1.3	0.3	2.1	
2	<b>1.02</b>	15.5	10.9	13.1	9.1	5.7	8.4	1.3	15.8	10.1	6.4	1.4	0.3	2.1	
3	<b>0.32</b>	17.6	12.4	17.1	9.1	5.9	9.5	1.3	12.6	6.5	5.1	1.0	0.3	1.5	
4	<b>0.41</b>	15.9	11.4	15.3	9.4	6.1	9.6	1.5	13.7	7.6	6.1	1.2	0.4	1.5	

Different metal on the same support

Ru is also a metal with suggested possible activity in the system. Therefore, the 3 w.t.% Ru/ $\gamma$ -Al<sub>2</sub>O<sub>3</sub> was prepared by the incipient wetness method and DP method as well. 3 w.t.% Rh, Au, and Ru were added to  $\gamma$ -Al<sub>2</sub>O<sub>3</sub> support respectively and then compared in **Table 4.16**. It looks that by the incipient wetness prep, the Rh is the most active system, while the Ru is not working. The 3 w.t.% Ru/ $\gamma$ -Al<sub>2</sub>O<sub>3</sub> prepared by DP method showed no activity at all.

**Table 4.16 110 °C, 15bar, 10g *n*-decane, 0.05g catalyst, 6h (by incipient wetness method)**

Catalyst	Conv. (%)	Selectivity (%)												
		5/4 one	3 one	2 one	5/4 ol	3 ol	2 ol	1 ol	C <sub>5</sub> OOH	C <sub>6</sub> OOH	C <sub>7</sub> OOH	C <sub>8</sub> OOH	C <sub>9</sub> OOH	C <sub>10</sub> OOH
$\gamma$ -Al <sub>2</sub> O <sub>3</sub>	<b>0.03</b>	21.4	13.8	24.5	9.0	6.7	12.5	2.7	6.8	0.4	0.5	0	0	0.3
3%Rh/ $\gamma$ -Al <sub>2</sub> O <sub>3</sub>	<b>1.02</b>	15.5	10.9	13.1	9.1	5.7	8.4	1.3	15.8	10.1	6.4	1.4	0.3	2.1
3%Au/ $\gamma$ -Al <sub>2</sub> O <sub>3</sub>	<b>0.36</b>	14.2	10.2	14.5	9.7	7.3	12.0	2.0	13.9	6.2	8.4	0.5	0.3	0.7
3%Ru/ $\gamma$ -Al <sub>2</sub> O <sub>3</sub>	<b>0.004</b>	35.1	15.9	19.2	12.7	6.4	10.8	0	0	0	0	0	0	0

#### 4.3.6.3 Loading with alumina spheres

To allow the addition of zeolite coating, the metal added sphere catalyst needs to be tested. With a very low surface area of the alumina sphere (diameter = 5 mm, surface area = 0.25 m<sup>2</sup>/g), only a very low loading is allowed on it, or the metal on the surface would be too concentrated to react with the alkanes. **Table 4.17** shows the reaction results with 0.1wt.% Au and Rh added alumina spheres. However, it was found that such low loadings do not help the activity; the conversion with the addition of metal is even lower than the blank spheres. But the 0.1%Rh/alumina sphere can achieve a quite different product distribution – the selectivity of the cracked acids is quite low.

As we know a low surface sphere is better for the zeolite coating; however it limits the performance of the active centre. This is an incompatible problem which needs to be solved.

As a trial to add more active centres on the support for zeolite coating, a smaller alumina sphere was also employed. This type of alumina sphere is with 1mm diameter and 203 m<sup>2</sup>/g surface area. An experiment with the addition of 3 w.t.% Au proves the active centre on it works better than the low surface area alumina sphere (**Table 4.18**). As nobody used a high surface area alumina support in the zeolite coating before, we did not know what would happen when it is coated. A test was carried out and discussed in **Chapter 6**.

**Table 4.17 110 °C, 15 bar, 10 g *n*-decane, 6 h, 600 rpm, 2 spheres (low surface area Al<sub>2</sub>O<sub>3</sub> sphere)**

Catalyst	Conv. (%)	Selectivity (%)													
		5/4 one	3 one	2 one	5/4 ol	3 ol	2 ol	1 ol	C <sub>5</sub> OOH	C <sub>6</sub> OOH	C <sub>7</sub> OOH	C <sub>8</sub> OOH	C <sub>9</sub> OOH	C <sub>10</sub> OOH	
Untreated Al <sub>2</sub> O <sub>3</sub> spheres	<b>0.21</b>	20.7	13.1	16.8	6.4	4.5	7.3	<b>1.8</b>	19.0	4.9	4.4	0.3	0.2	<b>0.6</b>	
0.1% Au Al <sub>2</sub> O <sub>3</sub> spheres	<b>0.12</b>	14.2	12.9	19.6	7.7	5.4	8.8	<b>1.8</b>	18.8	4.6	5.3	0.3	0.2	<b>0.4</b>	
0.1% Rh Al <sub>2</sub> O <sub>3</sub> spheres	<b>0.04</b>	23.3	15.9	24.9	8.7	6.9	11.1	<b>3.0</b>	11.1	0.5	0.7	0	1.1	<b>0.3</b>	

**Table 4.18 110 °C, 15 bar, 10 g *n*-decane, 6 h, 600 rpm, 0.05 g spheres (high surface area Al<sub>2</sub>O<sub>3</sub> sphere)**

Catalyst	Conv. (%)	Selectivity (%)													
		5/4 one	3 one	2 one	5/4 ol	3 ol	2 ol	1 ol	C <sub>5</sub> OOH	C <sub>6</sub> OOH	C <sub>7</sub> OOH	C <sub>8</sub> OOH	C <sub>9</sub> OOH	C <sub>10</sub> OOH	
untreated Al <sub>2</sub> O <sub>3</sub> spheres	<b>0.04</b>	21.5	13.8	21.6	9.2	6.4	10.6	<b>2.5</b>	10.2	1.4	2.0	0.2	0.4	<b>0.4</b>	
3% Au Al <sub>2</sub> O <sub>3</sub> spheres	<b>0.26</b>	23.5	14.8	18.8	5.4	3.8	6.0	<b>1.5</b>	15.8	4.9	4.4	0.4	0.1	<b>0.7</b>	

#### 4.4 Conclusion

Both decane and hexane oxidation have been studied as model reactions. The reactions were carried out using either a Parr stainless steel reactor or an Andrews glass reactor under a range of conditions. Various catalysts have been tested for decane oxidation at the beginning of the project, e.g. 5 w.t.% Au/TiO<sub>2</sub>, 2.5 w.t.% Au-2.5 w.t.% Pd/SiO<sub>2</sub>. Most of the catalysts showed very low conversion and very poor terminal selectivity. Increasing the temperature leads to higher conversion but results to more cracked products and less selectivity for oxygenated C<sub>10</sub> products. **Figure 4.8** shows the activity of the auto-oxidation and the catalysts activity. From this figure it can be seen that the most active catalyst was 5 w.t.% Au/TiO<sub>2</sub>. However, these catalysts did not show good terminal alcohol selectivity, whereas the cracked acid selectivity was high (32.0%) (**Figure 4.9**).

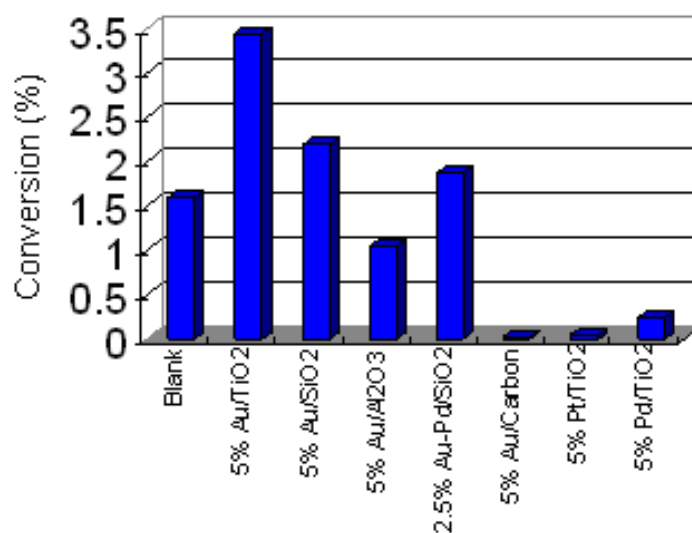


Figure 4.8 Conversion with different catalysts (reaction conditions: 110°C, 10 g *n*-decane, 0.05 g catalyst, 15 bar O<sub>2</sub>, 600 rpm, stainless steel reactor).

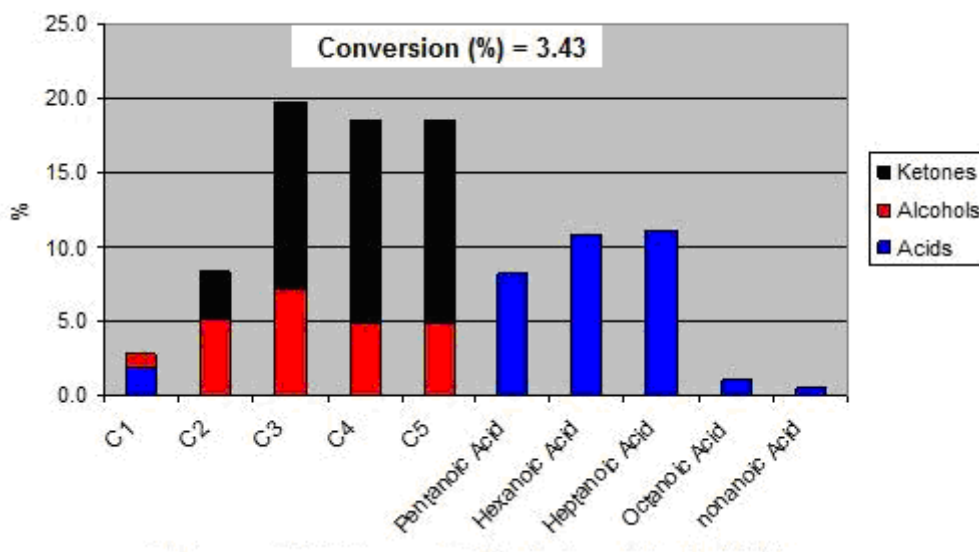


Figure 4.9 Product distribution with 5 wt.% Au/TiO<sub>2</sub> (reaction conditions: 110°C, 10 g *n*-decane, 0.05 g catalyst, 15 bar O<sub>2</sub>, 600 rpm, stainless steel reactor).

#### 4.5 References

[1] J. K. Edwards, B. E. Solsona, P. Landon, A. F. Carley, A. Herzing, C.J. Kiely and G.J. Hutchings, *Journal of Catalysis*, 235, (2005), 69.

[2] P. Siva Sankar Reddy, N. Pasha, M.G.V. Chalapathi Rao, N. Lingaiah, I. Suryanarayana, P.S. Sai Prasad, *Catalysis Communications*, 8, (2007), 1406

# CHAPTER 5

## *Cyclodextrin Covered Catalysts*

---

# CYCLODEXTRIN COVERED CATALYSTS

---

## 5.1 Introduction

Cyclodextrins (CDs) are cyclic oligosaccharides composed of six (alpha), seven (beta), or eight (gamma) glucopyranose units linked by  $\alpha(1-4)$ -glycosyl bonds that have the shape of hollow truncated cones. They have a central cavity of 6-10 nm, which can form complexes with various organic compounds in aqueous solution inside their hydrophobic cavities [1]. Due to their unusual properties, cyclodextrins have been widely investigated and utilized in pharmacy, biology, the food industry, analytical chemistry, separation science and various other areas [2-9].

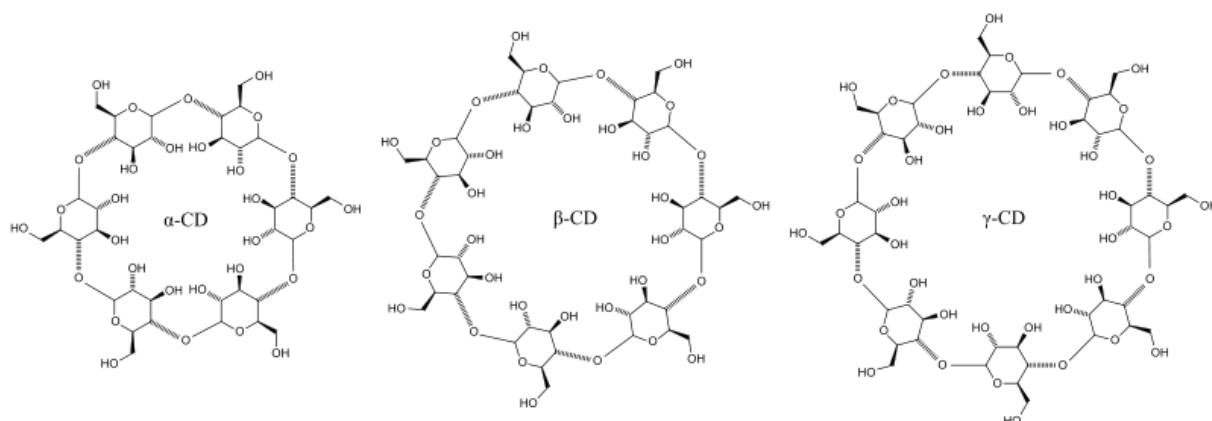


**Figure 5.3 Chemical structure of  $\alpha$ - and  $\beta$ -CDs**

Although the application of cyclodextrins as a shape-selective material has been widely reported, the number of reports focusing on their application to the oxidation of linear alkanes is limited. The first literature concerning alkane oxidation with cyclodextrins was published in 1972 by Lammers [10]. Lammers *et al.* proposed that  $\alpha$ -CD derivatives can encapsulate one *n*-hexane molecule in its stretched conformation in the interior of the cavity, whereas  $\beta$ -CD derivatives can encapsulate one *n*-hexane molecule in a compact coil form (but only loosely

bound). Based on this, Otsuka published an article in 1991 on the application of CDs for the terminal oxidation of *n*-hexane in a H<sub>2</sub>-O<sub>2</sub> fuel cell [11]. In 2000, Otsuka and Yamanka used FeCl<sub>3</sub>/graphite as the host cathode to study the effect of cyclodextrin additives on the selective oxygenation at the primary carbon of *n*-hexane [12]. They demonstrated that when *n*-hexane was introduced to the cavity of the cyclodextrin, the methylene C–H bonds of *n*-hexane are blocked by the walls of the cyclodextrins from an attack by the active oxygen species, so oxygenation occurs exclusively at the terminal carbons. As a result, they reported that when  $\alpha$ - and  $\beta$ -CDs were added to the FeCl<sub>3</sub>/graphite cathode, the selectivity for terminal oxygenation increases (selectivity for 1-hexanol ~12%) compared with that of the normal FeCl<sub>3</sub>/graphite cathode.

Based on these studies, it is clear that cyclodextrins can be an effective shape-selective material in the hexane oxygenation reactions by the electrochemistry system. However, it would be interesting to see if there is a less expensive and easier method to apply cyclodextrins to alkane oxidation. In this project, the possibility of using cyclodextrins as an organic shape selective coating over catalysts for the oxidation of long chain alkanes was investigated.

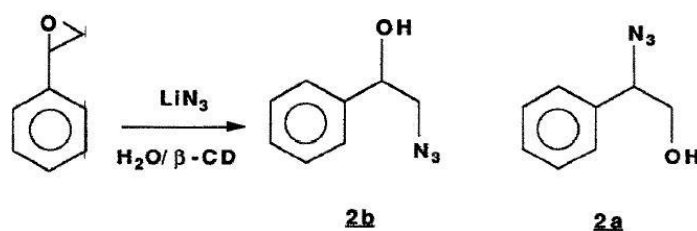
The idea of using CDs as catalyst coatings is that they may allow only the primary C–H bonds of alkanes to interact with active oxygen species present at the catalyst surface, thus forcing oxygenation exclusively at the terminal carbon. The diameters of cyclodextrin cavities are 0.47–0.53 nm ( $\alpha$ -CD), 0.60–0.65 nm ( $\beta$ -CD), and 0.78–0.83 nm ( $\gamma$ -CD). The common depth of the cavities is about 0.79 nm [12]. The width of linear alkanes is typically 0.4–0.5 nm. Due to the molecular size of the long chain alkanes, the cavities of  $\alpha$ - and  $\beta$ -CDs are considered to be more preferable for the selective oxidation of long chain alkanes. Several different

cyclodextrin modified catalysts have been prepared and are discussed in this chapter.

## 5.2 Cyclodextrins as catalyst modifiers

There are no previous studies on how to apply cyclodextrins as a direct coating material for catalysts applied to long chain alkane oxidation. However, CDs have been applied as regioselective catalysts or catalyst modifiers in various other chemical reactions [13-19].

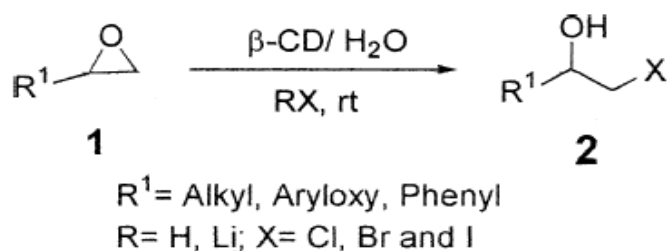
Guy *et al.* [13] reported some preliminary results obtained on the effects of CDs during the ring-opening reaction of epoxides with  $\text{LiN}_3$  in aqueous media. The experiment was carried out by stirring a mixture of epoxide,  $\text{LiN}_3$  and  $\beta\text{-CD}$  in water at room temperature. They observed an ‘increase in the regioselectivity of the ring-opening process’. A regioselectivity of 59% could be obtained for compound **2b** (**Scheme 5.1**) when the reaction was performed in the presence of  $\beta\text{-CD}$ , compared to 8.6 % without the use of  $\beta\text{-CD}$ . Although a good selectivity can be reached with the use of  $\beta\text{-CD}$  as a mediator, a decrease in the regioselectivity was observed as the conversion of styrene oxide was increased; and after 43 hours of reaction the selectivity had dropped to 20%.



**Scheme 5.1.** The ring- opening reaction of epoxides with  $\text{LiN}_3$  in aqueous media in the presence of  $\beta\text{-CD}$  [14]

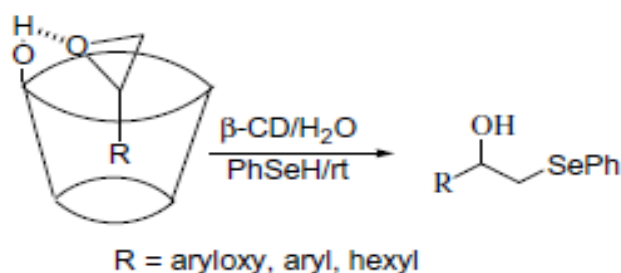
Reddy *et al.* [14] reported the regioselective ring opening of epoxides to halohydrins with hydrogen and lithium halides in the presence of  $\beta\text{-CD}$  using water as solvent. The reaction was

carried out by the *in situ* formation of a  $\beta$ -CD - epoxide complex followed by the addition of hydrogen halide or lithium halide (**Scheme 5.2**). Stirring at room temperature results in the formation of the corresponding halohydrin without the formation of any side products or rearrangements. The CDs appeared not only to activate the epoxides but also to promote the highly regioselective formation of halohydrins due to the formation of an inclusion complex.



**Scheme 5.2. The ring opening of epoxides to halohydrins in the presence of  $\beta$ -CD [14]**

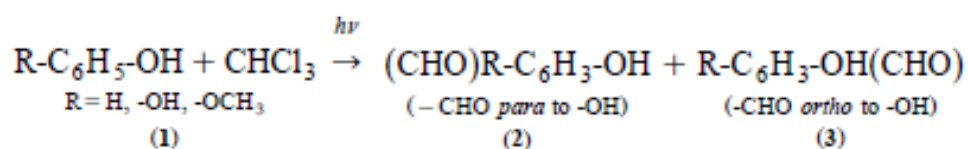
Similar research has been reported by Sridhar *et al.* [15] for the regioselective ring opening synthesis of  $\beta$ -hydroxy selenides from benzeneselenol and epoxides (**Scheme 5.3**). The reaction was found to proceed at room temperature in presence of  $\beta$ -CDs in water.



**Scheme 5.3. The ring opening synthesis of  $\beta$ -hydroxy selenides from benzeneselenol and epoxides in the presence of  $\beta$ -CD [15]**

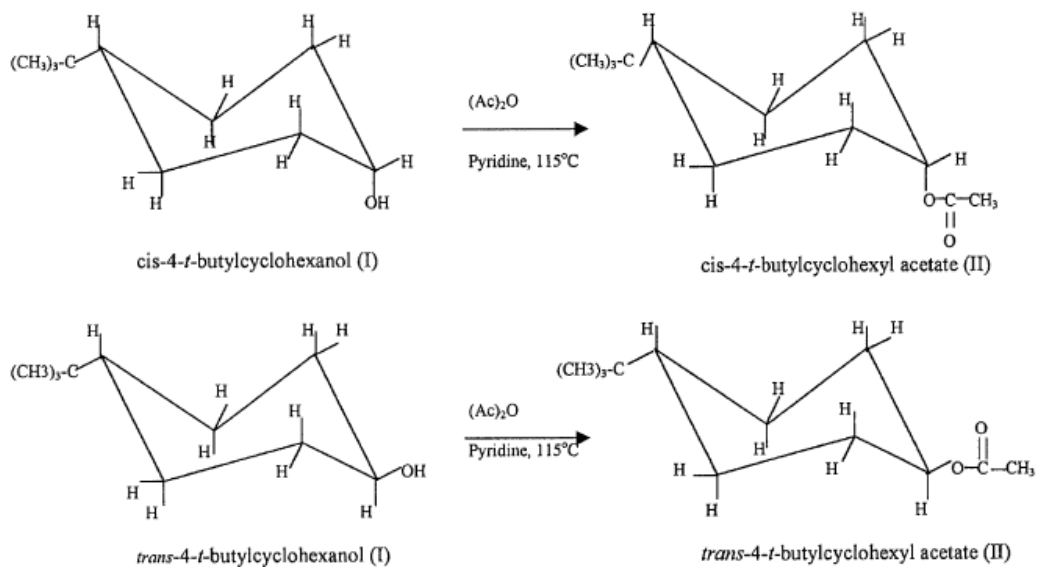
Ravichandran [16] found that, in the presence of  $\beta$ -CD and its derivatives, the photo-Reimer–

Tiemann reaction of phenols with chloroform proceeds with high selectivity for the formation of 4-hydroxy benzaldehydes. The  $\beta$ -CDs were reported to have two effects on the reaction (**Scheme 5.4**). Firstly, both the yield of the aldehyde and the reaction rate were enhanced. Secondly, the position of formylation was altered, i.e. the ratio of 2/3 (*para/ortho* attack) was increased. The presence of  $\beta$ -CD showed an enhanced yield up to 74% with 82.4% selectivity for the formation of 4-hydroxy benzaldehyde against a yield of up to 62% with 66.6% selectivity for the same compound without the presence of  $\beta$ -CD.



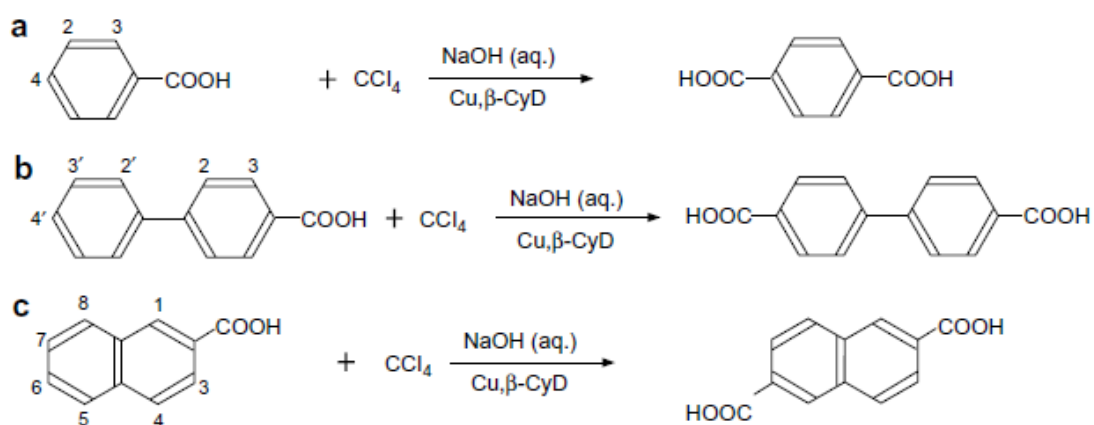
**Scheme 5.4. The formation of 4-hydroxy benzaldehydes [16]**

Pattekhan and Divakar reported the regioselective acetylation of 4-*t*-butylcyclohexanol in the presence of  $\beta$ -CD [17]. The experiment was carried out with 10–20 times excess of acetic anhydride. At a molar ratio of 1:10 of 4-*t*-butylcyclohexanol:acetic anhydride (**Scheme 5.5**), they reported a conversion of 99.0% to 4-*t*-butylcyclohexyl acetate with a *trans/cis* ratio of 3.48 with very little unreacted alcohol present (*trans/cis* ratio 2.5). They also found that with an increase in the concentration of  $\beta$ -CD (although the ester yield was less than the control) the *trans/cis* ratio increased steadily from 3.46 for 1:0.1 (yield 57.7%) to 5.49 for 1:1 eq. (yield 74.4%) of 4-*t*-butylcyclohexanol to  $\beta$ -CD. However, the *trans* ester yield was comparable to the control (76.9%) in the presence of 1 eq. of  $\beta$ -CD. They concluded that the results showed that the selectivity in esterification between the *trans* and *cis* alcohols was due to inclusion complex formations within the  $\beta$ -CD cavity.



**Scheme 5.5 4-*t*-butylcyclohexanol to acetic anhydride [17]**

Hirai and Shiraishi [18] reported their study of regioselective carboxylation of aromatic compounds using CDs as catalysts under mild conditions, producing terephthalic acid, 4,4'-biphenyldicarboxylic acid and 2,6-naphthalene-dicarboxylic acid (**Scheme 5.6**). In their opinion, it is the inclusion complex formations of  $\beta$ -CD with the aromatic hydrocarbon and carbon tetrachloride, in the reaction mixture that promotes the yield and selectivity of the target dicarboxylic acids. The high selectivity was ascribed to the conformation of the  $\beta$ -CD–aromatic monocarboxylate inclusion complexes.



**Scheme 5.6. The formation of terephthalic acid, 4,4'-biphenyldicarboxylic acid and 2,6-naphthalene-dicarboxylic acid [18]**

Ji *et al.* [19] reported how the amount of  $\beta$ -CD can affect the oxidation of sulfides to sulfoxides and sulfones with aqueous hydrogen peroxide in the presence of  $\beta$ -CD. In their operation, 1 mmol of  $\beta$ -CD was dissolved in 25 ml of deionised water at 45 °C and then the methyl phenyl sulfide was added under stirring, and hydrogen peroxide was slowly added as well. They found that a rise in the amount of  $\beta$ -CD strongly increases the conversion of methyl phenyl sulfide from 56% to 93% at 45 °C.

From the literature survey, in various reactions CDs can be effective catalyst modifiers and work at room temperature or very low reaction temperature, and are easy to apply and low cost. According to this, the method to create CD covered catalysts were developed as in the **Experimental** section below.

## 5.3 Experimental

### 5.3.1 Preparation of CD covered catalysts

The main method of catalyst preparation was impregnation. The porous catalysts were

impregnated in the CDs solution to leave adsorbed CDs on the surface. Using CD covered Au/SiO<sub>2</sub> as an example; the detailed steps of the preparation were as follows:

1. BET surface area of the Au/SiO<sub>2</sub> determined.
2. Assuming CD molecules cover the catalyst surface one by one without gaps and create a monolayer (**Figure 5.2**), the required mass of CDs to completely cover the surface of catalysts was calculated (e.g. to cover 1 g of Au/SiO<sub>2</sub>, 0.37 g of  $\alpha$ -CDs or 0.35 g of  $\beta$ -CDs is needed).
3. The calculated amount of CDs was then dissolved in 25 ml of deionised water by heating to 45°C and stirring.
4. 5 ml of the CDs solution was added to 1 g of Au/SiO<sub>2</sub> and the mixture heated to 45°C and stirred for 30 min and then put into an oven to dry overnight at 110°C.

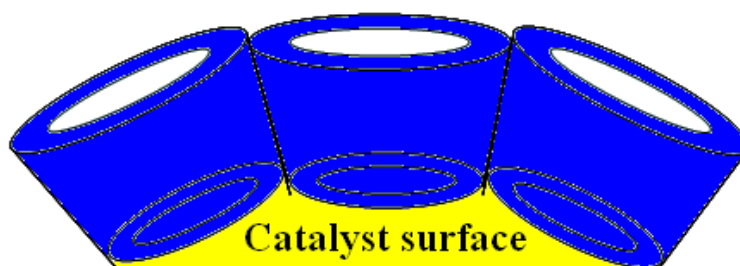


**Figure 5.2 Ideal catalyst surface covered by cyclodextrin molecules**

### 5.3.2 Catalyst testing

Reactions were carried out in a high-pressure stainless steel autoclave with a nominal volume of 45 ml and a magnetic PTFE stirrer. In each experiment, the reaction unit was flushed once with O<sub>2</sub> to remove the air. And then the pressure was increased to 15 bar O<sub>2</sub> at room temperature. Normally the prepared catalysts were tested in the unit using the following conditions: 15 bar O<sub>2</sub>, 600 rpm stirring speed, 110°C, 10 g *n*-decane and 0.05 g catalyst, 16 h.

In most cases the tested catalysts were modified following the method described in Section 5.3.1 to create fully covered catalysts. However, in some cases, the catalysts were modified by less than a monolayer of cyclodextrins (samples denoted 1/4  $\alpha$ -CDs covered Au/SiO<sub>2</sub> for catalysts with a coverage of 1/4 monolayer). Samples were not able to be fully recycled after reactions; therefore each experiment was performed with fresh catalyst. In addition, some reactions were carried out with addition of PS-TEMPO (2,2,6,6-Tetramethyl-1-piperidinyloxy, provided by Johnson Matthey) as a radical scavenger.

0.2  $\mu$ l. samples of the reaction mixtures were analysed after reaction using a gas chromatograph (Varian 3380) fitted with a CP-WAX52 CB column and an FID detector. An internal standard (0.150 ml, 1,2,4-trichlorobenzene) was added to the product mixture to quantify the results.

## 5.4 Results

### 5.4.1 BET analysis

The BET surface area of the catalysts covered by different amounts of cyclodextrins was determined as shown in Table 5.1.

**Table 5.1 The BET surface area of the different catalysts**

Catalysts	Surface Area (m <sup>2</sup> /g)
5 wt.%Au/SiO <sub>2</sub>	254
1/4 $\alpha$ -CDs covered Au/SiO <sub>2</sub>	222
$\alpha$ -CDs fully covered Au/SiO <sub>2</sub>	155
1/4 $\beta$ -CDs covered Au/SiO <sub>2</sub>	189
$\beta$ -CDs fully covered Au/SiO <sub>2</sub>	96

It was observed that with an increasing amount of cyclodextrins, the surface area of the

catalysts decreased. For example, for the  $\alpha$ -CD series, the standard Au/SiO<sub>2</sub>, the specific surface area was decreased by 12% with 1/4  $\alpha$ -CD coverage, and 39% with the fully covered Au/SiO<sub>2</sub>. According to Poncheal *et al.* [20], this reduction in surface area correlates with the covering of the nitrogen adsorption sites by the cyclodextrin on the substrate catalyst surface, which hinders the nitrogen molecules access to the binding sites. Therefore, the decrease of the surface area is an evidence of the successful loading of cyclodextrin on the surface of Au/SiO<sub>2</sub>.

## 5.4.2 Activity of CDs

### 5.4.2.1 Activity of CDs under reaction conditions

At the beginning of the research, it was important to establish the activity of CD themselves under the reaction conditions. Therefore, reactions with only CD and no catalyst were carried out. Two different amounts of CDs were used (0.05 g and 1.00 g). An average of two blank reactions (no catalysts, only decane and oxygen) is also given for comparison. The results were shown in **Table 5.2**.

**Table 5.2 Activity of CDs**

Catalyst	Conv.(%)	Selectivity (%)				
		C10 Ketones	C10 Alcohols	Cracked Acids	Others	Terminal
Blank	<b>0.66</b>	58.6	6.6	12.0	23.6	<b>2.6</b>
0.05g $\alpha$ -CDs	<b>0.30</b>	47.4	6.3	10.7	35.5	<b>2.7</b>
1.00g $\alpha$ -CDs	<b>0.11</b>	22.4	12.6	16.0	48.9	<b>2.1</b>
0.05g $\beta$ -CDs	<b>0.32</b>	42.2	7.5	12.8	37.4	<b>1.7</b>
1.00g $\beta$ -CDs	<b>0.17</b>	18.7	13.1	15.2	53.0	<b>3.1</b>

Reaction conditions: 16 h, 110°C, 15 bar O<sub>2</sub>, 10 g *n*-decane, 0.05 g or 1.00 g CDs, stainless steel reactor.

The addition of both  $\alpha$ - and  $\beta$ -CDs leads to a decrease of conversion, when compared to the blank reaction under the same conditions. In the product distribution, there was a definite decrease in the selectivity to ketones, and an increase in the selectivity to alcohols and acids. The unknown other products increased as well, especially with 1.00 g of CD.

In the CD structures there are a number of OH groups (Figure 5.1), therefore it could be possible that the CDs are being oxidized rather than decane. It has been reported that without tethering them to a catalyst, cyclodextrins can be oxidized and yield ketones and carboxylic acids [21]. It is also possible that the CDs react and produce some of the unknown products.

To determine whether the cyclodextrins were stable under the reaction conditions, they were added into another solvent, performing the reaction under the decane reaction conditions. Reactions were performed with  $\alpha$ - or  $\beta$ -CDs (0.05 g) in water (10 g) keeping the other conditions the same as for the reaction using decane (stainless steel reactor, 15 bar O<sub>2</sub>, 600 rpm stirring speed, 110°C, 16 h). After the reaction, no products were observed in the GC trace (**Figure 5.3**), which indicates that the CDs are not reacting under the reaction conditions. The product distribution changes observed are due to modifying the catalyst.

However, no trend in terminal selectivity with the additions of CDs is observed (**Table 5.5**) and the range of terminal selectivities observed is considered to be within the experimental errors. Therefore it is assumed that, without a catalyst, the CDs are not shape-selective catalysts for the oxidation of decane.

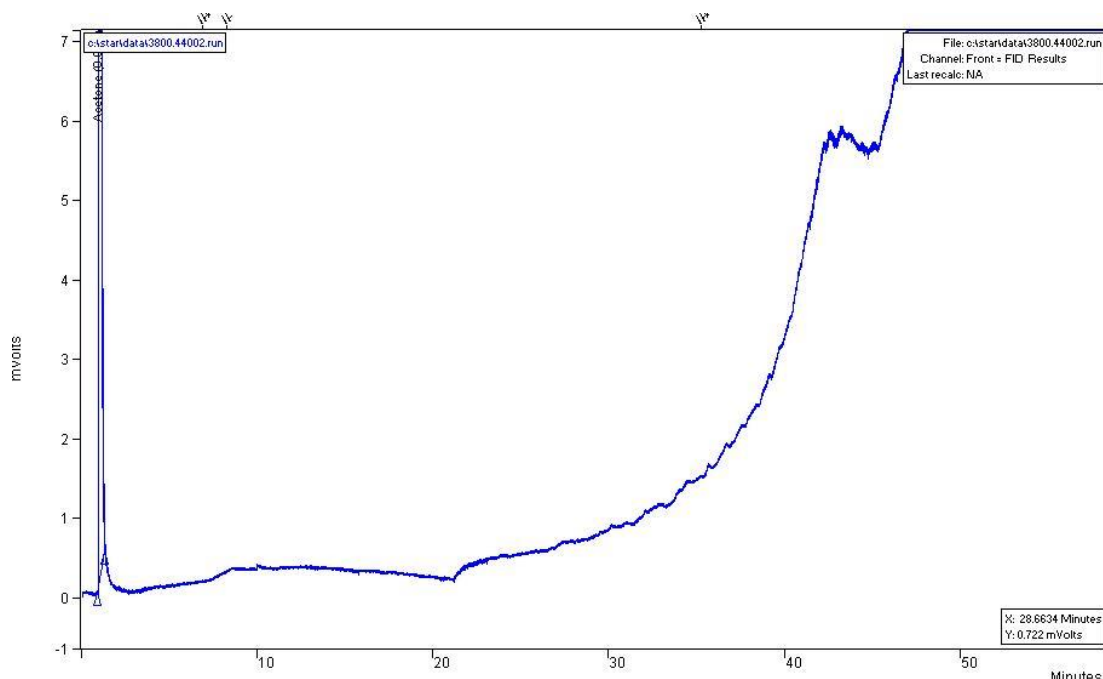


**Figure 5.3 GC analysis:  $\beta$ -CDs reacting with water**

#### 5.4.2.2 Activity of CDs with the addition of radical scavenger

A radical scavenger – PS-TEMPO was added to the reaction. Previously it has been shown that that 0.005 g PS-TEMPO can suppress the radical reaction in blank reactions (**Chapter 4**). Therefore, 0.005 g PS-TEMPO was added into the reaction, in order to observe the non-radical catalytic reaction with CDs.

The results are given in **Table 5.3**. It was found that the conversion decreased with the addition of PS-Tempo. For all the reactions with PS-TEMPO a 0.05% conversion was observed and the selectivity of the other products increased. However, an increase in selectivity for alcohols and acids was still observed when the amount of  $\alpha$ -CDs is increased from 0.05 g to 1.00 g. The terminal selectivities were very low (around 0.5%-0.8%).

**Table 5.3 Activity of CDs with PS-TEMPO**

Catalyst	Conv.(%)	Selectivity (%)				
		C10 Ketones	C10 Alcohols	Cracked Acids	Others	Terminal
0.05g $\alpha$ -CDs	<b>0.30</b>	47.4	6.3	10.7	35.5	2.7
With PS-TEMPO	<b>0.05</b>	2.6	2.2	3.2	92.0	0.5
1.00 g $\alpha$ -CDs	<b>0.11</b>	22.4	12.6	16.0	48.9	2.1
With PS-TEMPO	<b>0.05</b>	3.4	2.9	4.9	88.8	0.7
0.05g $\beta$ -CDs	<b>0.32</b>	42.2	7.5	12.8	37.4	1.7
With PS-TEMPO	<b>0.05</b>	2.6	2.2	3.8	90.4	0.8

Reaction conditions: 16 h, 110°C, 15 bar O<sub>2</sub>, 10 g *n*-decane, 0.05 g or 1.00 g CDs, 0.005 g PS-TEMPO, stainless steel reactor.

### 5.4.3 Activity of CD modified Au/SiO<sub>2</sub>

#### 5.4.3.1 The fully covered Au/SiO<sub>2</sub>

In **Chapter 4**, it is reported that Au/SiO<sub>2</sub> is one of the best catalysts for decane oxidation. Therefore, the CDs were impregnated onto Au/SiO<sub>2</sub> to prepare CD modified catalysts and the results are shown in **Table 5.4**.

It was found that the conversion was higher with the Au/SiO<sub>2</sub> without having being modified by the addition of CDs. This could be because of the CD on the surface covering some of the active sites on the Au/SiO<sub>2</sub>, leading to the decreased conversion. It was also found the terminal selectivity was increased slightly from 2.7% to around 3.2% with CDs. Repeating the reaction showed the same results, although this increase is considered to be within the experimental errors.

**Table 5.4 Activity of CD modified Au/SiO<sub>2</sub>**

Catalyst	Conv.(%)	Selectivity (%)				
		C10 Ketones	C10 Alcohols	Cracked Acids	Others	Terminal
Blank	<b>0.68</b>	58.6	6.6	12.0	23.6	<b>2.6</b>
Au/SiO <sub>2</sub>	<b>1.00</b>	49.7	10.6	14.5	25.2	<b>2.7</b>
0.05g $\alpha$ -CDs	<b>0.30</b>	47.4	6.3	10.7	35.5	<b>2.7</b>
$\alpha$ -CD modified Au/SiO <sub>2</sub>	<b>0.53</b>	29.0	16.7	16.2	38.2	<b>3.1</b>
0.05g $\beta$ -CDs	<b>0.32</b>	42.2	7.5	12.8	37.4	<b>1.7</b>
$\beta$ -CD modified Au/SiO <sub>2</sub>	<b>0.70</b>	32.5	17.3	15.8	34.4	<b>3.2</b>

Reaction conditions: 16 h, 110°C, 15 bar O<sub>2</sub>, 10 g *n*-decane, 0.05 g catalyst, stainless steel reactor.

#### 5.4.3.2 Different level of CD coverage over catalysts

When preparing the CD covered Au/SiO<sub>2</sub>, the amount of CD needed to fully cover the surface area of Au/SiO<sub>2</sub> was calculated. However, tests were performed to investigate if different levels of coverage can affect the terminal selectivity, which is also a potential way to prove if the CDs are shape selective. A quarter of the amount of CD was added to the catalyst which was tested under the same reaction conditions as previously, and the results are shown in **Table 5.5**.

**Table 5.5 Activity of CD modified Au/SiO<sub>2</sub>**

Catalyst	Conv.(%)	Selectivity (%)				
		C10 Ketones	C10 Alcohols	Cracked Acids	Others	Terminal
Au/SiO <sub>2</sub>	<b>1.00</b>	49.7	10.6	14.5	25.2	2.7
$\alpha$ -CD 1/4 covered Au/SiO <sub>2</sub>	<b>0.71</b>	29.1	15.0	17.9	38.0	2.9
$\alpha$ -CD fully covered Au/SiO <sub>2</sub>	<b>0.53</b>	29.0	16.7	16.2	38.2	3.1
$\beta$ -CD 1/4 covered Au/SiO <sub>2</sub>	<b>0.50</b>	32.0	16.0	16.0	36.0	2.9
$\beta$ -CD fully covered Au/SiO <sub>2</sub>	<b>0.70</b>	32.5	17.3	15.8	34.4	3.2

Reaction conditions: 16 h, 110°C, 15 bar O<sub>2</sub>, 10 g *n*-decane, 0.05 g catalyst, stainless steel reactor.

According to **Table 5.1**, it was found that different amounts of CDs lead to a different coverage level of CDs on the catalyst surface. However, from **Table 5.5**, it can be seen that with different level of CD coverage, the difference between product distributions was very limited. The trend of BET surface area change and terminal selectivity change for the  $\alpha$ -CD covered Au/SiO<sub>2</sub> is shown in **Figure 5.4**.

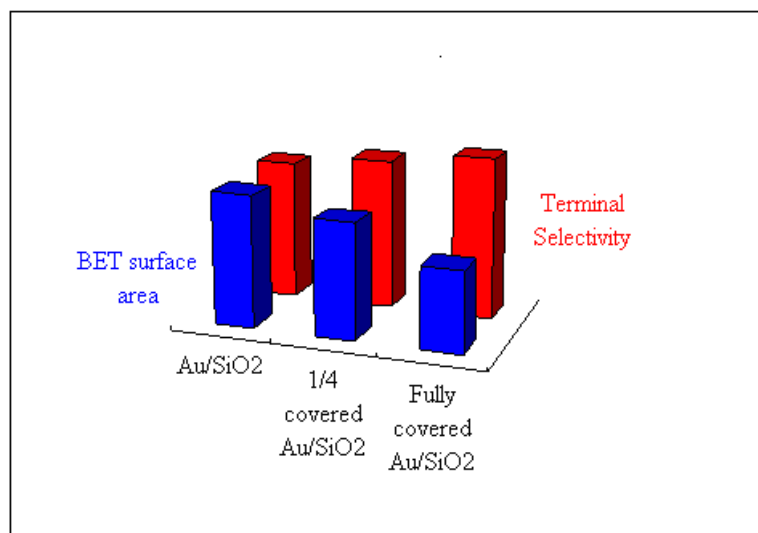


**Figure 5.4 The trend of BET surface area change and terminal selectivity change**

There was a 0.2-0.3% increase in the terminal selectivity between the 1/4 covered sample and the fully covered sample. Thus there is a general trend in increasing terminal selectivity with increase CD content. This increase is however also considered to be within the experimental error. Therefore, from these experiments, it cannot be concluded if the CDs worked as a shape-selective coating in the reaction.

#### **5.4.3.3 Cyclodextrin modified catalyst recycling**

To check the stability of CDs on the modified catalysts, decane oxidation reactions with  $\alpha$ - and  $\beta$ -CD covered Au/SiO<sub>2</sub> were performed, then the catalysts were recycled and reused. However, it should be noticed that the full repeat was impossible as there was a loss of catalyst during the recycle, and for 0.05 g catalyst, only 0.02 g was recovered after recycling.

**Table 5.6 Reaction with recycled CD modified Au/SiO<sub>2</sub>**

Catalyst	Conv.(%)	Selectivity (%)				
		C10 Ketones	C10 Alcohols	Cracked Acids	Others	Terminal
$\alpha$ -CD covered Au/SiO <sub>2</sub>	<b>0.668</b>	31.5	19.2	30.0	19.2	<b>2.4</b>
Recycled $\alpha$ -CD covered Au/SiO <sub>2</sub>	<b>0.100</b>	38.3	19.1	20.3	21.0	<b>2.3</b>
$\beta$ -CD covered Au/SiO <sub>2</sub>	<b>0.556</b>	34.5	16.1	31.2	17.2	<b>2.4</b>
Recycled $\beta$ -CD covered Au/SiO <sub>2</sub>	<b>0.053</b>	32.3	19.8	27.5	19.1	<b>2.6</b>

Reaction conditions: 16 h, 110°C, 15 bar O<sub>2</sub>, 10 g *n*-decane, 0.05 g catalyst, stainless steel reactor.

Although there was a huge decrease in the conversion, the change in the terminal selectivity was minor (**Table 5.6**). This result may indicate that the Au/SiO<sub>2</sub> was deactivated after the reaction. As no decrease in terminal selectivity was found with the recycled catalyst, it is thought that CDs still covered the catalyst after the reaction. However, due to the large loss of catalysts in the recycling process and the experimental error at low conversion, the results are not clear.

#### **5.4.4 CD modified Au/HCl treated SiO<sub>2</sub>**

In **Chapter 4**, it was found that the acid treated silica support did not show a difference from the silica support without acid treatment in terminal selectivity. However, it was considered worth determining if there is any difference with the cyclodextrin coatings. Therefore, Au/HCl treated SiO<sub>2</sub> was also modified with CDs and tested under the same reaction conditions (**Table**

5.7).

**Table 5.7 Activity of CD covered Au/HCl treated SiO<sub>2</sub>**

Catalyst	Conv.(%)	Selectivity (%)				
		C10 Ketones	C10 Alcohols	Cracked Acids	Others	Terminal
Au/HCl treated SiO <sub>2</sub>	<b>0.90</b>	44.5	11.3	15.8	28.4	2.9
$\alpha$ -CD covered	<b>0.80</b>	31.1	15.9	18.3	34.7	3.0
$\beta$ -CD covered	<b>0.50</b>	28.6	15.1	16.4	39.9	2.8

Reaction conditions: 16 h, 110°C, 15 bar O<sub>2</sub>, 10 g *n*-decane, 0.05 g catalyst, stainless steel reactor.

A decrease in conversion was again observed when CDs were added to the reaction. The terminal selectivity of the treated Au/HCl treated SiO<sub>2</sub> is slightly higher than the non-treated Au/SiO<sub>2</sub> and the conversion slightly lower. The difference in conversion and terminal selectivity are both considered to be within the experimental errors. With CDs on Au/HCl treated SiO<sub>2</sub> no changes in terminal selectivity were detected in the reaction, however the conversion decreases. This may be because the CDs are not selective in the reaction. However it could also be possible that the H<sup>+</sup> remained on the surface of the Au catalyst and then reacts with the –OH bond on the CDs.

## 5.5 Conclusions

The aim of the project was to synthesize coatings onto active catalysts which can effectively oxidize long chain alkanes in the primary position. In this chapter, cyclodextrins were investigated as an organic shape-selective material to coat the Au/SiO<sub>2</sub> catalysts. Addition of CDs without the catalyst decreased the conversion but no trend in terminal selectivity was observed. With the CD covered Au/SiO<sub>2</sub> catalyst, a decrease in conversion is seen compared to the blank reaction; however the changes in terminal selectivities are still limited and considered to be within the experimental errors. To conclude, the CD covered catalysts, which were prepared by the direct impregnation method, did not play an important role in increasing the terminal selectivity.

## 5.6 References

- [1] G.A. Signorell, T.C. Kaufmann, W. Kukulski, A. Engel, H. Remigy, *Journal of Structural Biology*, 157, (2007), 321
- [2] J. Haggin, *Chemical Engineering News*, 70, (1992), 25.
- [3] J. Szejtli, *Cyclodextrin Technology*, Kluwer Academic Publishers, Dordrecht, (1988).
- [4] R. Dagani, *Chemical Engineering News*, 71, (1993), 4.
- [5] H. Parrot-Lopez, H. Galons, A.W. Coleman, J. Mahuteau, M. Miocque, *Tetrahedron Letters*, 33, (1992), 209.
- [6] D.W. Armstrong, W. Li, A.M. Stalcup, H. V.Secor, R.R. Izac, J.I. Seeman, *Analytical Chemistry Acta*, 234, (1990), 365.
- [7] D.W. Armstrong, A.M. Stalcup, M.L. Hilton, J.D. Duncan, J.R. Faulkner, S. Chang, *Anal. Chem.*, 62, (1990), 1610
- [8] J. Szejtli, *Cycloakxtrin Technology*. Kluwer Academic, Dordrecht, (1988)

- [9] M.L. Bender and M. Komiyama, *Cyclodextrin Chemistry* .Springer, Berlin, (1978).
- [10] J.N.J.J. Lammers, *Recueil*, 91, (1972), 1135
- [11] K. Otsuka, K. Furuka, *Electrochimica Acta*, 37 (6), (1992), 1135
- [12] K. Otsuka, I. Yamanaka, *Catalysis Today*, 57, (2000), 71
- [13] A. Guy, J. Doussot, R. Garreau, A. Godefroy-Falguieres, *Tetrahedron:Asymmetry*, 3, (1992), 247
- [14] M.A. Reddy, K. Surendra, N. Bhanumathi, K.R. Rao, *Tetrahedron*, 58, (2000), 6003
- [15] R. Sridhar, B. Srinivas, K. Surendra, N.S. Krishnaveni, K.R. Rao, *Tetrahedron Letters*, 46, (2005), 8837
- [16] R. Ravichandran, *Journal of Molecular Catalysis A: Chemical*, 130, (1998), 205
- [17] H.H. Pattekhan, S. Divakar, *Journal of Molecular Catalysis A: Chemical*, 184, (2002), 79
- [18] H. Hirai, Y. Shiraishi, *Reactive & Fuctional Polymers*, 67, 2007, 1115
- [19] H. Ji, X.Hu, D. Shi, Z. Li, *Russian Journal of Organic Chemistry*, 42 (7), (2006), 959
- [20] A. Ponchel, S. Abramson, J. Quartararo, D. Bormann, Y. Barbaux, E. Monflier, *Microporous and Mesoporous Materials*, 75, (2004), 261
- [21] M.E. Deary, D.M. Davies, *Carbohydrate Research*, 317(1-4), (1999), 10
- [22] K. Otsuka, I. Yamanaka, *Catalysis Today*, 57, (2000), 71

# CHAPTER 6

## *Teabag Technology*

---

# TEABAG TECHNOLOGY

---

## 6.1 Introduction

The aim of this research project is to realize the selective oxidation of long chain alkanes to alcohols and acids at the terminal position. Therefore various selective materials can be considered. Zeolites, known as one of the most popular shape-selective catalysts, is the focus of the chapter. Zeolites can be synthesized as membranes for the purpose of separation, adsorption or for the selective reaction. An ideal zeolite membrane combines the general advantages of inorganic membranes (temperature stability, solvent resistance) with shape selectivity. Small aggregates of zeolite crystals as a coating on the surface of a catalyst can improve external mass transfer characteristics especially in fast liquid phase and gas/liquid phase reactions [1]. A continuous zeolite membrane can discriminate the components of gaseous or liquid mixtures dependent on their molecular size. Hence, in this chapter, the aim is to utilize zeolite membrane as coatings outside the metal/support catalysts, to realise the selectivity of the terminal long chain alkane oxidation product. This technology is called teabag technology. Specifically, teabag technology is an idea that zeolite coatings work as the teabag to control the diffusion of reactants to the active sites in a specific configuration that only allows the oxidation of the terminal position. This chapter aims to find a zeolite with the suitable pore size, so that only the wanted reactant and product can pass through the outer coating to an oxidation catalyst underneath.

## 6.2 The teabag technology project

‘Teabag technology’ was first named by Johnson Matthey (JM), which is one of the sponsors and co-operating companies of the research project. The key work in this area has been carried

out by Paul Collier (JM) who used zeolite A as the coating material on the catalyst (e.g. Pt-Fe/SiO<sub>2</sub>, Pd-Fe/SiO<sub>2</sub>) for the CO oxidation in the presence of butane [2, 3]. The zeolite A coating synthesis process they used was as follows: 5 g catalyst spheres were added into a 5 w.t.% solution of polyelectrolyte (Percol 1697 from Allied Colloids Ltd.) containing dilute ammonia to adjust the pH value between 10 and 11. The solution was stirred at room temperature for 20 minutes. Subsequently the spheres were separated from the solution and washed with demineralized water. Then the spheres were rapidly added to a zeolite gel which was composited with a solution of 6.07 g sodium aluminate in 52 g demineralized water to a solution of 15.51 g sodium metasilicate in 52 g demineralized water. The gel was stirred at room temperature for 2 hours and then hydrothermally crystallized at 100°C for 24 hours. The zeolite coated catalyst spheres were separated from the crystallization solution and washed with demineralized water, dried at 105°C, and then calcined at 500°C for 2 hours. The oxidation experiment results showed with the coated catalyst, carbon monoxide is selectively oxidized at temperature between 150°C and 400°C (**Figure 6.1**).

However, this technique cannot be applied in this project in exactly the same way, because the pore size of zeolite A is too small (pore size ranges from 3-4.5 Å: K/NaA: 3 Å, NaA: 4 Å, Ca/NaA: 4.5 Å) for the long chain alkane diffusion. Therefore, other zeolite membrane needs to be explored to fit the long chain alkanes. Considering the molecule size of hexane and decane, MFI type zeolite (including silicalite-1 and ZSM-5), zeolite X and mordenite are all possible candidates (pore size ranges from 8-10 Å).

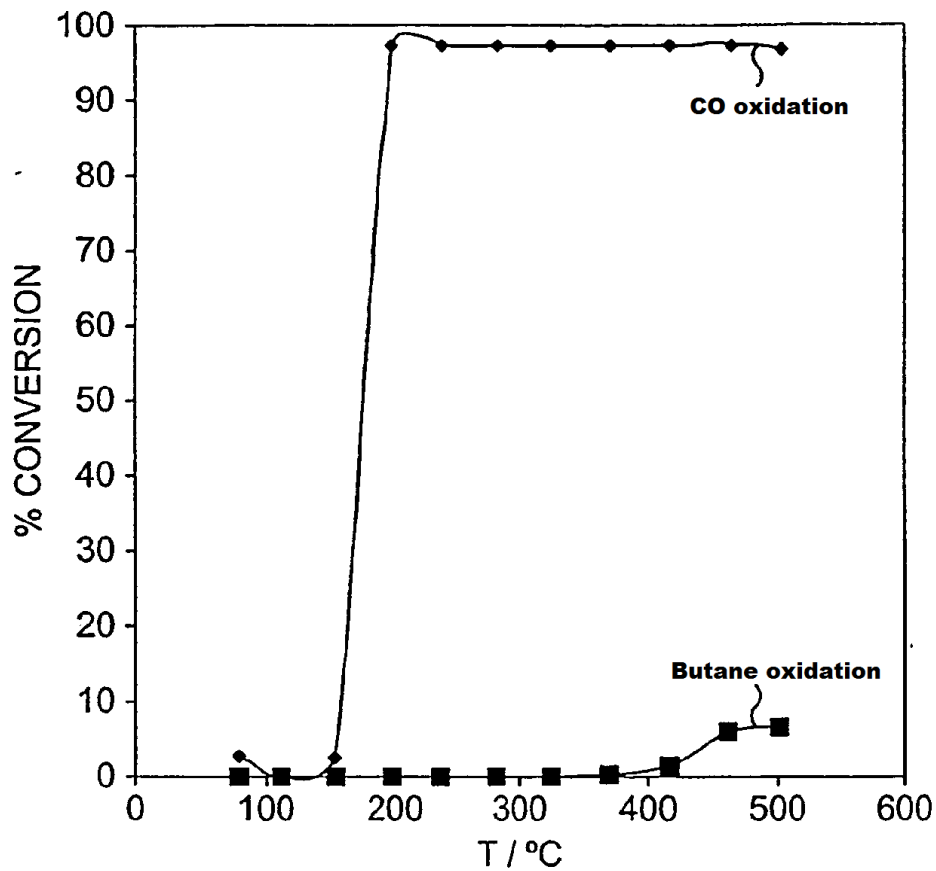


**Figure 6.1 CO and butane conversion comparison, with the presence of zeolite A coated catalyst**

### 6.3 Zeolite membrane synthesis

In order to create a typical zeolite membrane coating for this project, it is important to understand the current research stage of zeolite membrane synthesis and the parameters that influence the synthesis.

#### 6.3.1 Preparation method

The methods for the preparation of the zeolite coatings recorded in the literature can be generally catalogued into three different ways:

- 1) Slurry coating or wash-coating, in which the zeolite is brought onto the support from a wash-coat solution, containing precursors of binders based on alumina, zirconia, silica, titania or silica-alumina. The coatings are calcined to obtain bonding of the crystallites to the support surface [4].
- 2) Dry gel conversion, in which a gel containing the aluminosilicate precursor, water and template, is brought onto the support, dried and subsequently crystallized by contacting with steam at 105-150°C [5].
- 3) *In situ* coating, in which the crystals are directly grown close to, or on the support either from a gel or a solution with the hydrothermal synthesis conditions [6-21].

The disadvantage of first and second methods is that the crystal layers created in those ways always show a low continuity and a limited accessibility; therefore, it is more common today to use the *in situ* hydrothermal method in dilute aluminosilicate systems in which the amorphous gel phase is not present. Zeolite coatings prepared in this way have a high continuity and can be optimized for use as either a membrane or a catalyst.

The first hydrothermal method system that produced zeolite NaA was reported at the International Zeolite Association (IZA) meeting in Tokyo in 1986 by Wenqin *et al.* [6]. The batch composition in it formed the starting point of the present work in clear solution. Another advantage of the clear solution method is that it permits the use of *in situ* observations using light scattering techniques to study the synthesis [7], especially the nucleation and crystal growth processes occurring within the solution phase. After Wenqin *et al.* [6] published the system, almost all syntheses of zeolite A coatings were accomplished using the clear solution system with the composition:  $x\text{Na}_2\text{O}:y\text{Al}_2\text{O}_3:1\text{SiO}_2:200\text{H}_2\text{O}$ , where  $x$  ranges from 5 to 13 and

y ranges from 0.1 to 0.2.

Cetin *et al.* [8] used a small difference in their batch composition: they used the aluminosilicate solution with a composition of  $10\text{Na}_2\text{O}:\text{Al}_2\text{O}_3:\text{SiO}_2:200\text{H}_2\text{O}$ . The same ratio was also utilized in the research of Andac *et al.* [9]. Anhydrous NaOH pellets were dissolved in deionised water and granular sodium aluminate and sodium silicate were added to the solution. Additions were made to solutions cooled to below  $27^\circ\text{C}$  and the final reaction mixture was stirred for 15 min at the temperature prior to the syntheses. Hydrothermal crystallization was carried out in a stainless steel reaction vessel at  $60^\circ\text{C}$  for various periods of time ranging from 1 to 10 h. It was reported that a zeolite film with a thickness of about  $1.5\ \mu\text{m}$  could be obtained after a synthesis time of 10 h.

Different compositions have also been reported in the literature for the zeolite A coatings. Wang *et al.* [10] employed a solution with  $0.3\text{Na}_2\text{O}:\text{Al}_2\text{O}_3:3.4\text{SiO}_2:4.2\ (\text{TMA})_2\text{O}: 237\text{H}_2\text{O}$ . The experiments were run at a higher temperature of  $100^\circ\text{C}$  for 24 h, coatings were successfully applied to a porous  $\alpha\text{-Al}_2\text{O}_3$  support. The particle size of the zeolite crystallites was 250 nm by SEM.

As a development of the hydrothermal synthesis, a seeding method was introduced into the zeolite membrane preparation. For example, Sterte *et al.* [11] synthesized mono disperse silicalite-1 crystals and then used the crystals as seeds in the synthesis of coatings. Supports were seeded first and then zeolite membranes were grown by the hydrothermal method described in the other methods [6-10]. They showed that coatings synthesized by this method had better adhesivity, thermal stability and crystal orientation than those prepared by other

methodologies.

In a synthesis of ZSM-5 coatings on stainless steel, Tatlier *et al.* [12] used a substrate heating method, keeping the reaction mixture at temperatures below 100°C, while the metal plates were heated to a temperature above 100°C. It was demonstrated that continuous ZSM-5 coatings of different textures with different crystal morphologies and void fractions could be formed depending on the reaction conditions (**Table 6.1**). The mass of the coatings increased with the substrate temperature and the duration of synthesis, because of the effect of temperature on the rate of crystallization. The method was regarded to be beneficial in respect to the synthesis duration compared to the conventional procedures.

**Table 6.1 Mass and thickness of the coatings at an oil bath temperature of 90 °C**

<b>Resistance temperature ( °C)</b>	<b>Synthesis duration (days)</b>	<b>Coating mass (mg/cm<sup>2</sup>)</b>	<b>Actual coating thickness (µm)</b>	<b>Equivalent coating thickness (µm)</b>	<b>Void fraction</b>
200	3	0.1 <sup>a</sup>	–	–	–
240	3	0.2 <sup>a</sup>	–	–	–
280	3	0.5	4.0	2.9	0.28
240	5	1.7	12.0	9.7	0.20
240	8	2.7	27.0	15.3	0.43
280	5	3.3	38.0	18.8	0.51

<sup>a</sup> The coating is not crystalline.

### 6.3.2 Supports in zeolite coating

For the synthesis of zeolite coatings support materials should be chosen that are readily available, attrition resistant and chemically stable under the reaction conditions.

In **Table 6.2** various types of support are given together with their physical and chemical properties [13].

Supports such as  $\alpha$ -Al<sub>2</sub>O<sub>3</sub> [9, 14, 15], quartz [8] and stainless steel [8, 9] were reported in use for the zeolite A coating in the literature reviewed to date. And as reported in the US patent 2005/0032628 [2], the catalyst substrate comprises at least one platinum group metal, which are known as effective catalysts for the oxidation of a wide variety of chemical species, supported on a support material. The support materials are preferably oxidized materials including silica, alumina, titania and so on. It is possible that preparations using these supports could be adapted to introduce an active metal to the support before applying the zeolite coating.

It was reported that the formation of a continuous coating of zeolite is not easy to achieve over an alumina or stainless steel support using conventional hydrothermal crystallization techniques [9, 16]. The surface charge of zeolites is negative at basic pH (typical zeolite synthesis conditions), which means that there is an electrostatic barrier preventing the growth of zeolite coatings on supports. To overcome this, several methods of introducing positive charge to the supports were investigated.

**Table 6.2 Supports currently used in the preparation of zeolite coatings**

Support material	Nature	Surface area <sup>a</sup>	Amount of OH- groups <sup>b</sup>
<b>Spheres/extrudates</b>			
$\alpha$ -Al <sub>2</sub> O <sub>3</sub>	Hydrophobic	high	low
$\gamma$ -Al <sub>2</sub> O <sub>3</sub>	Hydrophilic	high	high
<b>Single crystal wafers</b>			
Si	Hydrophilic	low	high
TiO <sub>2</sub>	Hydrophilic	low	medium
Sapphire( $\alpha$ -Al <sub>2</sub> O <sub>3</sub> )	Hydrophobic	low	low
<b>Plates/disks</b>			
Stainless steel	Hydrophilic	low	high
Quartz	Hydrophilic	low	high
Vitreous glass	Hydrophilic	low	high
Pressed carbon	Hydrophobic	high	low
<b>Foams</b>			
$\alpha$ -Al <sub>2</sub> O <sub>3</sub>	Hydrophilic	high	low
<b>Fibres</b>			
Carbon	Hydrophobic	medium	low
Vegetal	Hydrophilic	medium	medium
Inorganic	Hydrophilic	medium	high
<b>Inserts</b>			
Gold	Hydrophobic	low	low
Teflon	Hydrophobic	low	low

<sup>a</sup> Low: < 1 m<sup>2</sup>g<sup>-1</sup>; medium: 1-10 m<sup>2</sup>g<sup>-1</sup>; high: > 10m<sup>2</sup>g<sup>-1</sup>

<sup>b</sup> Low: < 1 OH nm<sup>-2</sup>; medium: 1-2.5 OH nm<sup>-2</sup>; high > 2.5 OH nm<sup>-2</sup>

Collier *et al.* [16] reported a method using a copolymer of acrylamide and the methyl chloride quaternary salt of 2-(dimethylamino) ethyl acrylate. The polymer species are strongly adsorbed

on the support, by the electrostatic attraction between the quaternary ammonium groups of the adsorbate and the oxide ions at the support surface, resulting most probably in a flat conformation. The presence of excess quaternary ammonium groups imparts an overall positive charge to the polymer-covered support surface allowing the zeolite coating to stick.

Andac *et al.* [9] reported a treatment method for stainless steel to introduce positive charge to the surface. The stainless steel plates were first boiled in toluene for 30min and then held at 60°C for 15 min in a mixture of H<sub>2</sub>O<sub>2</sub>(30%), NH<sub>4</sub>OH(25%) and H<sub>2</sub>O in a 1:1:5 ratio by volume. In this way, NH<sub>4</sub><sup>+</sup> is attached to the support surface, creating the positive charge.

A typical method of preparation catalyst substrate was investigated by Nishiyama *et al.* [17].

In the report they prepared the silicalite-1 coating with Pt/TiO<sub>2</sub> by impregnation in two steps:

1) *Preparation of Pt/TiO<sub>2</sub> particles.* Platinum-loaded titania catalyst was prepared by the impregnation of spherical TiO<sub>2</sub> particles with Pt from a solution of hydrogen hexachloroplatinate (IV) hexahydrate. The impregnation solution was prepared by dissolving H<sub>2</sub>PtCl<sub>6</sub>·6H<sub>2</sub>O salt in deionised water. Then the slurry was dried at 120°C overnight and at 500°C for 6 h in air. Reducing in hydrogen for 3 h at 300°C is required before utilization

2) *Zeolite coating.* The surface of the Pt/TiO<sub>2</sub> particles was positively charged by treatment in a solution of 0.4 w.t.% polyethyleneimine in deionised water. Then the particles were immersed in a 1.0 w.t.% silicalite-1 solution. The crystallization was carried out in the closed vessel at 180°C for 24h (**Figure 6.2**). After washing with deionized water and drying the product at 90°C overnight, it was calcined in air at 500°C for 6 h.

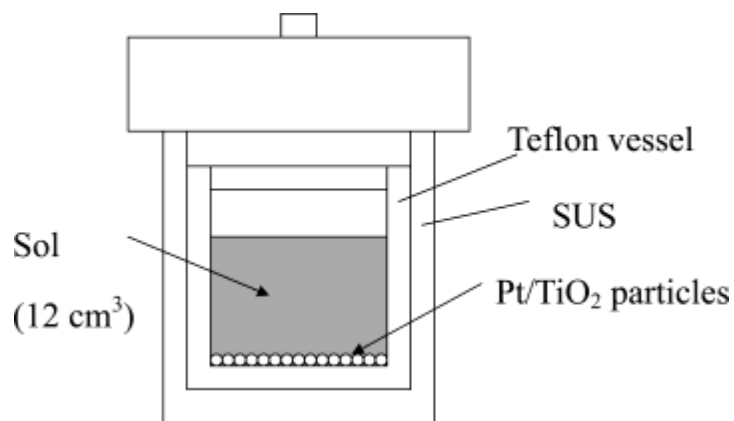


**Figure 6.2 Reaction vessel used for zeolite coating**

### 6.3.3 Other factors for preparation

Some other factors that would influence the production of zeolite coating have been investigated, including the operating temperature [1, 8, 9], the utilization of ultrasound [1, 9, 18], the role of water content [14] and the aging time [5].

#### Temperature

The preparation of continuous zeolite coatings is related to two competing phenomena occurring on the surface, nucleation and crystal growth. The thickness of the zeolite coating may be decreased in the case where a higher number of smaller crystals growing on the unit surface of the substrate are available. In this respect, temperature may be a significant factor for the property of the coating prepared.

Puil *et al.* [1] prepared samples coated in zeolite beta by a hydrothermal method for 18 h at 155°C. The autoclaves were then cooled to room temperature in air and the solids recovered by filtration, washed and dried at 120°C, before the coated particles were removed by a 500 µm sieve. The samples were then suspended in water and treated ultrasonically for 2-4 h to

remove any 'loose' crystals, after which the samples were again filtered, dried, sieved and calcined at 550°C for 12 h. The ion-exchange was carried out in aqueous 0.1 M NH<sub>4</sub>Cl at room temperature for 24 h, followed by drying at 120°C and calcining at 550°C. They reported after calcination and ion-exchange the supported zeolite beta coatings show activity in the reaction. The activity is similar to the intrinsic activity of commercial zeolite β samples.

Cetin *et al.* [8] reported that the temperature affected the thickness of the zeolite 4A layers. They found the thickness of closed zeolite 4A layers may be decreased at relatively lower synthesis temperatures when relatively longer synthesis times are employed. They suggested the possible reason might be that the rate of nucleation being less temperature sensitive than the rate of crystal growth. Zeolite 4A coatings of 1 and 0.7 μm thickness have been prepared on quartz and stainless steel substrates respectively at 45°C. No subsequent calcination of the material was reported in the paper.

In 2005 Andac *et al.* [9] successfully carried out the zeolite A hydrothermal crystallization on stainless steel plates at temperatures of 50°C and 60°C for various periods of time ranging from 2 to 15 h by using a heater and a temperature controller. The experiment was carried out in an ultrasonic water bath. And then the product was filtered using a filter paper with fine mesh size. The filtrate was then refiltered through a 0.1 μm PVDF membrane, before washing thoroughly with deionized water and drying overnight in an oven at 65°C.

### Ultrasound

Use of ultrasound in polymer synthesis is known to be helpful in providing rate and yield enhancements. In the zeolite coating synthesis, the effect of ultrasound was reported by a few

researchers [1, 9, 18], leading to a conclusion that the ultrasonic irradiation leads to acceleration of crystallization of zeolite coating and some other benefits. For example, Andac *et al.* [9] reported that in the presence of ultrasound, the thickness of the zeolite A coatings on stainless steel plates could be decreased from about 1.5  $\mu\text{m}$  to about 0.6  $\mu\text{m}$  and a closed layer was obtained after 3 h of synthesis, instead of 10 h at 60°C. The final roughness value was also smaller for the coating prepared in the presence of ultrasound.

This phenomenon is likely to be due to an increase in the nucleation rate, resulting in a higher number of particles forming on the substrate at earlier synthesis times in the presence of ultrasound. Hence with the ultrasound, lower temperature and shorter times than with the conventional preparation method can be expected.

#### Water Content

Kalipcilar *et al.* [14] found a relationship between the water content in the synthesis solutions and the thickness of the coating formed. They carried out the synthesis of silicalite layers on  $\alpha\text{-Al}_2\text{O}_3$  disks with a molar batch composition of  $6.5\text{Na}_2\text{O}:25\text{SiO}_2:\text{xH}_2\text{O}:6.9\text{TPABr}$  (6.9 g silicic acid, 7.9 g TPABr) by varying the water content from 500 to 2000 miles at 200°C. They found that the silicalite layer which was synthesized from the most concentrated batch was formed from crystals with an average size of 100  $\mu\text{m}$  and a thickness of 36  $\mu\text{m}$ . And the layer thickness and average crystal size decreased to about 8 and 7  $\mu\text{m}$ , respectively when the batch containing 1400 miles of water was used. As shown in **Figure 6.3**, the continuity of the layer and the crystal size was improved as the water content of the batch was increased from 500 to 1136 miles and decreased on further dilution of the batch to 1400 and 2000 miles.

Gavalas *et al.* [19] investigated the effect of the batch composition on the properties of ZSM-

5 layers on non-porous and porous  $\alpha$ -Al<sub>2</sub>O<sub>3</sub> supports. They found the dilution of the crystallization solution led to a partial coverage of the surface and poor growth of the crystals under the surface.

Sterte *et al.* [20] observed that decreasing amounts of water in the clear crystallization solution resulted in the formation of a continuous film. Thin oriented silicalite-1 films with thicknesses in the range of 180 nm to 1  $\mu$ m have been obtained by varying the contents of the reaction mixture

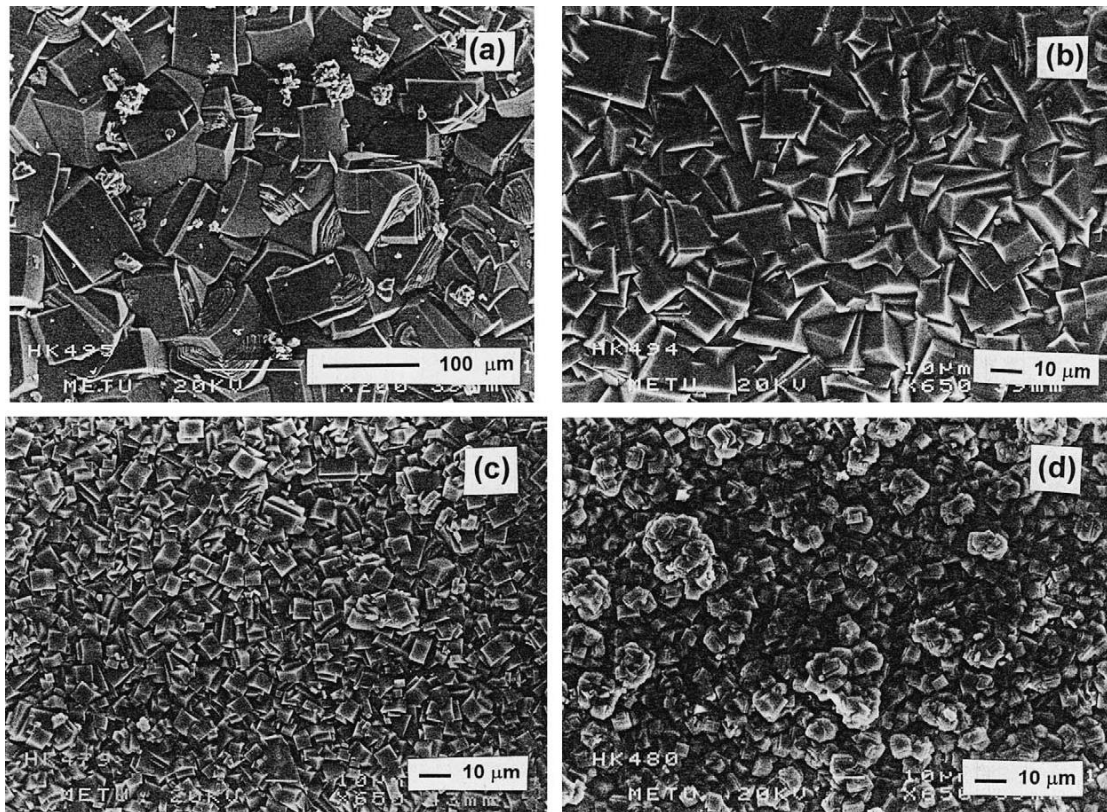


**Figure 6.3** Surface SEM images of silicalite-1 layers synthesized from the batch with a molar composition 6.5Na<sub>2</sub>O:25SiO<sub>2</sub>:xH<sub>2</sub>O:6.9TPABr at 200 °C. (a) 500 mol, (b) 800 mol, (c) 1136 mol and (d) 1400mol.

### Calcination Rate

In an early work of preparation of MFI membranes [21], it has been recommended that calcination of supported MFI membranes should be carried out in air at a maximum temperature of 400°C with a low heating rate of 1 °C/min. However no particular reason for using a low rate was given.

Hedlund *et al.* [22] that thin silicalite-1 films on asymmetric  $\alpha$ -Al<sub>2</sub>O<sub>3</sub> can be calcined at 500°C with a heating/cooling rate as high as 5°C/min without reducing the membrane quality. They also reported that films with different microstructure, thickness and on other types of supports may behave differently.

### Aging the solution

The formation of zeolite coatings and their properties, such as the thickness, continuity and orientation of the crystals, are related to the presence and macro-organization of a precursor phase. Based on this view, preshaped zeolite coatings can be prepared.

Gora *et al.* [5] especially emphasized the effect of aging in their report for the zeolite synthesis. In the experiment the aluminosilicate gel was aged for 38.5h at 25 °C. The solution was shown to be very effective as an initiator for nucleation. They found addition of even 2.7% of the solution to a reaction mixture (10Na<sub>2</sub>O: 0.2Al<sub>2</sub>O<sub>3</sub>:1SiO<sub>2</sub>:200H<sub>2</sub>O) increased the nucleation rate considerably, which means that aging the solution could accelerate the coating speed.

### **6.3.4 Deactivation**

Deactivation is a problem for all the catalysts. Due to the structure of the zeolite catalyst, coking

is the most common reason for the deactivation. However, in research on a silicalite-1 coating, Nishiyama *et al.* [17] reported that the deactivation of the coated catalyst was reduced compared with the uncoated one. They regarded the reason probably to be the protection against poisoning impurities in the feed.

## **6.4 Experimental**

### **6.4.1 Preparation of coated catalysts**

From the literature survey it can be concluded that the hydrothermal method is the most common way to prepare zeolite coatings, which was also the method taken in this project. However, the hydrothermal method can be divided into several kinds of different methods depending on the exact preparation procedure. According to the coating steps, the hydrothermal method can be divided into a direct synthesis method and a secondary synthesis method (the seeding method); according to the batch composition, it can be divided into the normal method (with template) and the template-free method. Different preparation methods have been attempted in this project as the research developed. The preparation methods of coated catalysts have been improved subsequently, also with different metal active centres, powder/sphere supports and zeolite membranes. The tested samples in this project have been listed in **Table 6.3**.

The details of synthesis and characterization for each sample are discussed in the following sections in chronological order.

**Table 6.3 List of synthesized zeolite coating samples**

<b>Zeolite coating type</b>	<b>Substrate catalyst theoretical w.t.% loadings</b>	<b>Support type</b>
Zeolite A	SiO <sub>2</sub> HCl treated SiO <sub>2</sub> 5 w.t.% Au/SiO <sub>2</sub> MgO $\alpha$ -Al <sub>2</sub> O <sub>3</sub> $\gamma$ -Al <sub>2</sub> O <sub>3</sub>	SiO <sub>2</sub> powder MgO powder SiO <sub>2</sub> spheres $\alpha$ -Al <sub>2</sub> O <sub>3</sub> spheres $\gamma$ -Al <sub>2</sub> O <sub>3</sub> spheres
Silicalite-1	3 w.t.% Au/ $\gamma$ -Al <sub>2</sub> O <sub>3</sub>	$\gamma$ -Al <sub>2</sub> O <sub>3</sub> spheres
ZSM-5	0.1 w.t.% Rh/ $\alpha$ -Al <sub>2</sub> O <sub>3</sub> 0.1 w.t.% Au/ $\alpha$ -Al <sub>2</sub> O <sub>3</sub>	$\alpha$ -Al <sub>2</sub> O <sub>3</sub> spheres
Zeolite X/Y	SiO <sub>2</sub>	SiO <sub>2</sub> spheres

**6.4.1.1 Zeolite A coated samples with silica powder support**

Powder form silica support was employed at the beginning of the coating attempts, unlike many of the literature reports of coatings where extended solids such as rod and sphere supports were used. The synthesis of 5 w.t.% Au/SiO<sub>2</sub> has been discussed in **Chapter 4**. The corresponding coated samples (coated SiO<sub>2</sub>, coated HCl SiO<sub>2</sub> and coated Au/SiO<sub>2</sub>) were prepared in two steps.

Preparation the substrate catalysts

To make a comparison, three kinds of substrate catalysts (SiO<sub>2</sub>, HCl treated SiO<sub>2</sub>, and 5 w.t.% Au/SiO<sub>2</sub>) were coated. Among them the HCl treated SiO<sub>2</sub> and Au/SiO<sub>2</sub> were prepared with the SiO<sub>2</sub> support (silica powder, Grace, >99 %, 60-100 mesh) and dilute HCl solution/HAuCl<sub>4</sub> 3H<sub>2</sub>O solution respectively by the incipient wetness method. The dilute HCl solution should be adjusted to the same pH value with the HAuCl<sub>4</sub> 3H<sub>2</sub>O solution. Using the 5 w.t.% Au/SiO<sub>2</sub> as an example, to prepare 1 g 5 w.t.% Au/SiO<sub>2</sub>, 0.95 g SiO<sub>2</sub> powder was impregnated by a solution with 0.1 g HAuCl<sub>4</sub> 3H<sub>2</sub>O. The samples were dried in the 110 °C oven and then calcined at 400 °C for 3 h at a heating rate of 20 °C /min.

### Synthesis of the zeolite A coatings

Substrate catalysts were washed with 0.1 M HCl in an ultrasonic bath for 20 min and then washed again with deionised water before drying at 110 °C overnight. Then a zeolite solution with the batch composition tetraethyl orthosilicate (TEOS) (Aldrich); Al<sub>2</sub>(SO<sub>4</sub>)<sub>3</sub> (Aldrich); NaOH; H<sub>2</sub>O was made. The molecular ratio is 80SiO<sub>2</sub>:1Al<sub>2</sub>O<sub>3</sub>:10Na<sub>2</sub>O:1500H<sub>2</sub>O. The solution was stirred for three hours before being mixed with the substrate and placed into autoclaves. The autoclaves were heated at 180 °C for 24 h. Finally, the products were washed in deionized water in the ultrasonic bath and dried at 110 °C overnight.

At the same time, in order to test if the catalysts still remain active after being treated in this way, the catalysts were treated in the same manner as the coating procedure, but without the coating solution. The products with coating solution are called the ‘coated products’; while the products without coating solution are called the ‘treated products’ in the following section.

#### **6.4.1.2. Zeolite 4A coated samples with sphere supports**

Silica spheres (Saint-Gobain, diameter 3.2 mm, surface area 0.25 m<sup>2</sup>/g) and alumina (Saint-Gobain, surface area 0.75 m<sup>2</sup>/g) spheres have been employed in the synthesis. The Au/SiO<sub>2</sub> and Au/Al<sub>2</sub>O<sub>3</sub> spheres were prepared by a vacuum incipient wetness method. The zeolite 4A coatings have been synthesized following the method reported by Collier *et al.* [2]. 5 g of 5 w.t.% Au/SiO<sub>2</sub> spheres or alumina spheres were added to a 5 w.t.% solution of the polyelectrolyte. Two kinds of polyelectrolyte have been tested: polydiallyl dimethyl ammonium chloride, and 2-propen-1-ammonium N,N-dimethyl-N-2-propenyl chloride (magnafloc It35) containing dilute ammonia and stirred at room temperature for 20 minutes. The spheres were subsequently separated from the solution and washed with demineralized

water, and then added to a zeolite solution which was prepared with rapid addition and stirring. The solution contained 6.07 g sodium aluminium oxide (Alfa Aesar) in 52 g demineralized water to a solution of 15.51 g sodium metasilicate (Alfa Aesar, anhydrous) in 52 g demineralized water. The mixture containing the spheres was stirred at room temperature for 2 hours and then hydrothermally crystallized at 100 °C for 24 hours. Finally the zeolite-coated spheres were separated from the crystallization solution and washed with demineralized water, dried at 105 °C and then calcined in air at 500 °C for 2 hours.

#### 6.4.1.3 Silicalite-1 coating with sphere supports

1 w.t.% and 3 w.t.% Rh/ $\alpha$ -Al<sub>2</sub>O<sub>3</sub>, Rh/ $\gamma$ -Al<sub>2</sub>O<sub>3</sub>, Ru/ $\gamma$ -Al<sub>2</sub>O<sub>3</sub> were prepared by the incipient wetness method and deposition precipitation (DP) method separately. The incipient wetness method was carried out as previously reported in **Chapter 4**. Taking the 1 w.t.% Rh/ $\gamma$ -Al<sub>2</sub>O<sub>3</sub> as an example, to prepare 1 g 1 w.t.% Rh/ $\gamma$ -Al<sub>2</sub>O<sub>3</sub>, 0.99 g  $\gamma$ -Al<sub>2</sub>O<sub>3</sub> had a solution of 0.025 g RhCl<sub>3</sub> · xH<sub>2</sub>O (Alfa Aesar) added. The water content was predetermined and was that required to form a paste with the alumina support. The paste was dried overnight at 110 °C and then calcined at 400 °C for 3 h. The DP preparation was performed as follows (taking the 3 w.t.%Rh/ $\gamma$ -Al<sub>2</sub>O<sub>3</sub> as an example): to prepare 1 g 3 w.t.% Rh/ $\gamma$ -Al<sub>2</sub>O<sub>3</sub>, 0.99 g  $\gamma$ -Al<sub>2</sub>O<sub>3</sub> was first dispersed in an aqueous solution of 0.075 g RhCl<sub>3</sub> · xH<sub>2</sub>O. A quantity of 1 M Na<sub>2</sub>CO<sub>3</sub> was slowly added to the RuCl<sub>3</sub> solution until the pH value of the mixture reached 10.5. The suspension was then maintained at the same pH for 1 h during the precipitation process. The resulting solid was washed with deionized water several times until no chloride ion was detected by silver nitrate solution in the filtrate. All the catalysts were dried at 110 °C (12 h) in air. Finally they were calcined at 500 °C for 5 h in air [23]. Alumina (Saint-Gobain, surface area 0.25 m<sup>2</sup>/g) spheres have also been tested.

The vacuum incipient wetness method was employed in the preparation of sphere catalysts. To prepare 1 g catalyst, 1 g alumina spheres were placed into a sealed two neck round bottom flask. The flask was heated to 80 °C with an oil bath and connected to a vacuum pump for 1 h. The calculated amount of metal solution was added into the flask through a syringe. The flask was shaken until all the metal solution was absorbed into the spheres. The spheres were then dried at 110 °C overnight, before calcination at 400 °C for 3 h.

Coatings have been applied to Au/Al<sub>2</sub>O<sub>3</sub> and Rh/Al<sub>2</sub>O<sub>3</sub> based spheres. The silicalite-1 precursor solution consisted of TEOS (98%, Aldrich), tetrapropylammonium hydroxide (TPAOH) (1 M solution in water, Aldrich), ethanol (EtOH) (Fluka) and deionized water with the molar ratios of 0.5TPAOH: 120H<sub>2</sub>O: 8EtOH: 2SiO<sub>2</sub>. Approximately 1.0 g of catalyst sphere was immersed in 15 g of the precursor solution. The crystallization was carried out under hydrothermal conditions at 180 °C for 24 h in a stainless steel vessel with agitation. The coating procedure was repeated twice. The products were rinsed repeatedly with deionized water, separated by filtration and dried at 90 °C overnight, then calcined in air at 600 °C for 5 h with a heating rate of 1 °C/min [24].

#### **6.4.1.4 ZSM-5 coating with $\alpha$ - and $\gamma$ -Al<sub>2</sub>O<sub>3</sub>**

Synthesis of ZSM-5 coatings on both  $\alpha$ - and  $\gamma$ -Al<sub>2</sub>O<sub>3</sub> was attempted. Synthesis were carried out in Teflon-lined 60 ml autoclaves. Teflon liners were cleaned before and after each synthesis in NaOH solution for 24 h under the synthesis conditions. Supports were cleaned by boiling in toluene for 1 h and dried overnight at 110 °C before being immersed in the zeolite precursor solution. The zeolite precursor solution was prepared by adding tetrapropylammonium hydroxide (TPAOH, Aldrich, 1 M solution in water), sodium aluminate (NaAlO<sub>2</sub>, Aldrich, Al

50-56%) to tetraethyl orthosilicate (TEOS, Aldrich, 98%) in a PTFE beaker. The molar ration of the precursor solution was: 1 Al<sub>2</sub>O<sub>3</sub>: 40 SiO<sub>2</sub>: 10 TPAOH: 800 H<sub>2</sub>O.

The precursor solution was stirred for 10 h at room temperature as an aging process before filling the autoclaves. In all experiments 1 g of support was added to the autoclaves. The volume of precursor solution was varied (32 ml or 15 ml) to observe the influence of the amount of precursor. Syntheses were carried out at 160 °C for 24 h. Then the coated samples and the extra synthesized powder for the same batch were washed with deionized water and dried overnight at 110 °C. Finally the samples were calcined at 550 °C for 12 h using a heating rate of 5 °C/min.

#### **6.4.2 Reaction conditions**

The reaction conditions taken for the powder form catalysts in this project usually are: 15 bar O<sub>2</sub>, 600 rpm, 110 °C, 10 g *n*-decane and 0.05 g catalyst. Therefore the zeolite A coated SiO<sub>2</sub>, HCl treated SiO<sub>2</sub>, and 5 w.t.% Au/SiO<sub>2</sub> were tested under the same conditions.

With the sphere supports, the reaction system was adjusted. They have been tested both in stainless steel autoclaves and the Andrews glass reactor according to Iglesia's work [25]. In addition, as a single sphere is much heavier (e.g. the mass of a single silica sphere ≈ 0.09g) than the catalysts used in the previous reactions (0.05g in each reaction), in the experiment, 1 g sphere catalysts have been used in each reaction at 110 °C. Other conditions used in the stainless steel reactor are the same as before: 15 bar O<sub>2</sub>, 60 0rpm, and 10 g *n*-decane. In the Andrews glass reactor the conditions are: 3 bar O<sub>2</sub>, 600 rpm and 25 ml *n*-hexane.

### **6.4.3 Characterization**

In the coating experiments, the weight of the samples before and after coating was recorded to determine the coverage of the coating/m<sup>2</sup> support.

The uncoated and coated spheres were crushed into powders to perform XRD analysis. XRD patterns of both the supports and the coated samples were analysed by a PANalytical X'pert MPD X-ray diffractometer with a monochromatic CuK $\alpha$  source at 40 KeV and 40 mA. The morphology of the coated spheres was analysed by a Zeiss Evo-40 series scanning electron microscopy. EDX mapping was carried out by the same instrument in conjunction with an INCAx-sight EDX detector. Reaction samples were analysed by gas chromatography, with a CP Wax 52CB column, 25 m, 0.53 mm, 2.0 microns using a programmed temperature ramp. Each sample was injected at least twice.

## **6.5 Results**

### **6.5.1 Zeolite A coating with powder support**

Coating of SiO<sub>2</sub> and MgO based catalysts was attempted using the direct template-free method, in which powder form SiO<sub>2</sub> and MgO supports were employed. It is important to ascertain the effects of treatment on the bulk catalyst. Hence the 'treated' catalysts were tested in this section as well. As the SiO<sub>2</sub> based catalysts works better in the liquid phase while the MgO based catalysts proved to be more active in the gas phase, the coated and treated SiO<sub>2</sub> and MgO based catalysts were separately tested in the corresponding phase.

#### **6.5.1.1 Coated SiO<sub>2</sub> in liquid phase reaction**

The SiO<sub>2</sub> based catalysts were analysed by the BET, XRD, SEM&EDX before testing in

reactions.

### BET

When studying the data on surface area (**Table 6.4**) it is quite obvious that after being coated, the surface area of the sample is dramatically reduced. There is also a slight increase in the surface area of the samples when treated but not coated. SEM images have been taken to check the morphology of the samples and to see if reasons can be ascribed for the changes in surface area.

**Table 6.4 BET results for the SiO<sub>2</sub> based catalysts**

Catalysts	Surface Area(m <sup>2</sup> g <sup>-1</sup> )
SiO <sub>2</sub>	268
HCl SiO <sub>2</sub>	277
Au/SiO <sub>2</sub>	255
Coated SiO <sub>2</sub>	14
Coated HCl SiO <sub>2</sub>	7
Coated Au/SiO <sub>2</sub>	6
Treated SiO <sub>2</sub>	270
Treated HCl SiO <sub>2</sub>	286
Treated Au/SiO <sub>2</sub>	315

### SEM & EDX

According to the SEM images (**Figure 6.4**), it can be seen that both the untreated catalysts and the treated catalysts show similar morphologies under the microscope. The coated samples present a much different morphology, clearly showing a roughened overlayer, both attached to the large macroscopic particles and also unattached and separate. For the coated SiO<sub>2</sub> catalyst (**Figure 6.4 b**), it can be seen that the coating does not cover the whole surface and a large presence of the smoother SiO<sub>2</sub> support is visible. In contrast, following acid and disposition of gold (**Figure 6.4 e and h**), the covering seems more complete, although there is clearly still a

large amount of unattached coating present. The Au particle distribution on the support is clear shown in the BSD detector in **Figure 6.5**.

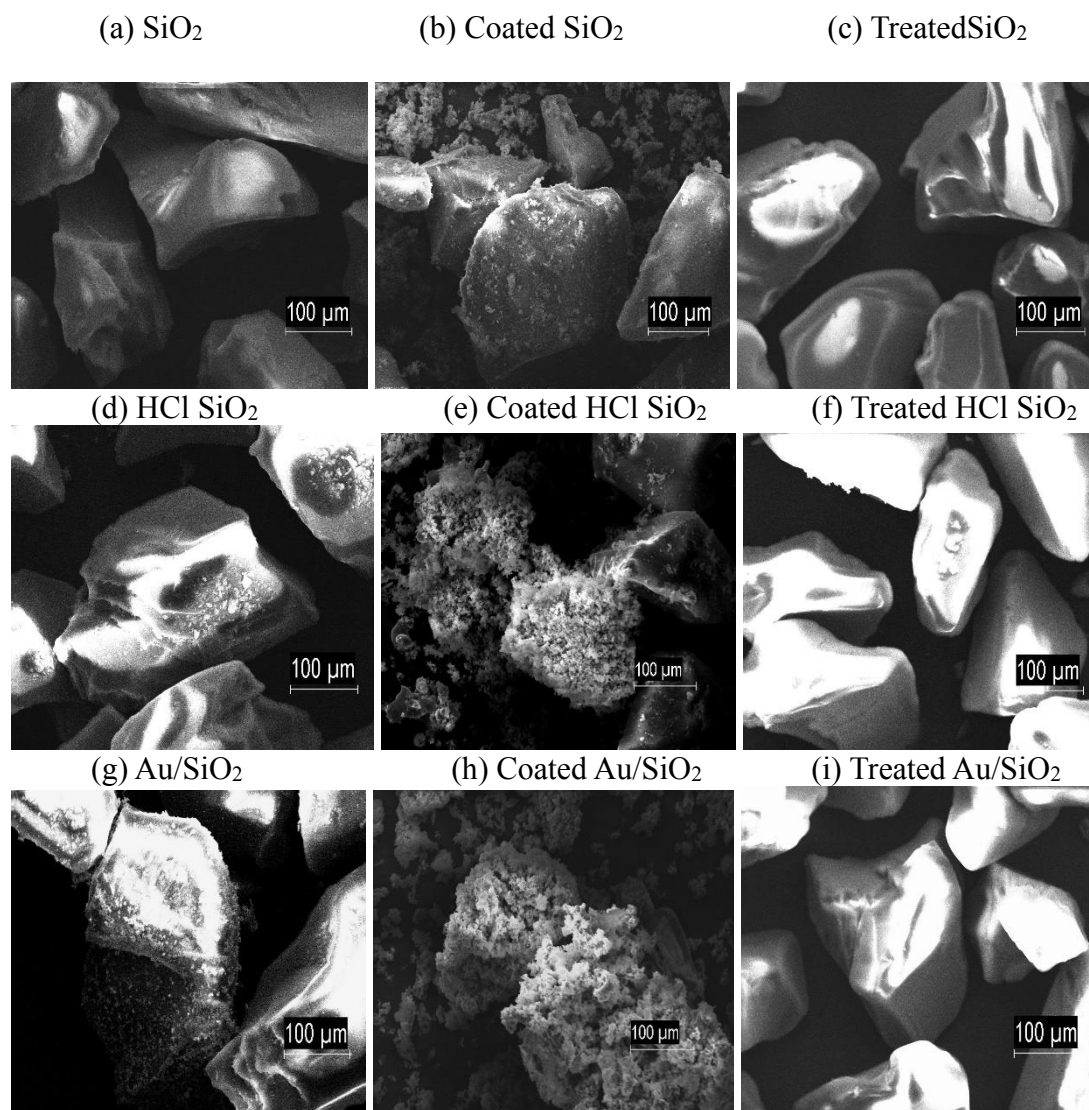


**Figure 6.4 Comparison of SEM Images of the SiO<sub>2</sub> Catalysts**  
Each image is approximately 550 μm wide

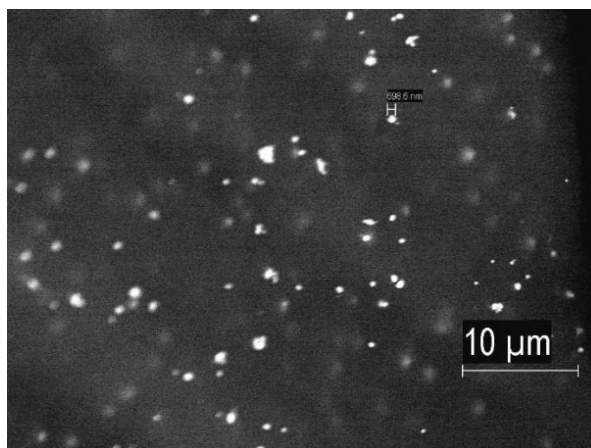


**Figure 6.5 Au particles in BSD detector**

Compared with the coated catalysts, it was known the surface area had been massively decreased with the addition of the coating, so it was expected that at a high magnification image a difference should be observed. This is indeed the case (**Figure 6.6**), with the untreated silica presenting a smooth appearance while the surface of the coated samples show a large degree of roughness. It is likely that the surface area decrease is caused by the coating blocking a large amount of the pore structure of  $\text{SiO}_2$ .

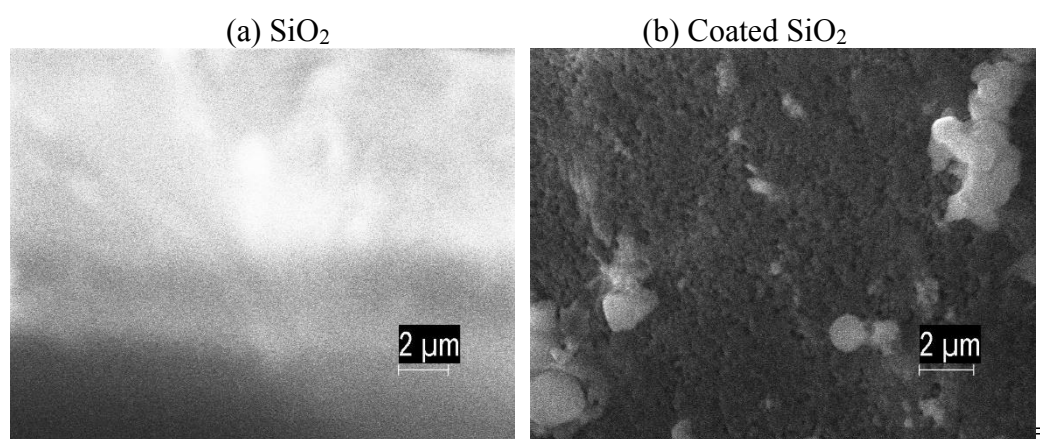


**Figure 6.6 Surface of the uncoated and coated  $\text{SiO}_2$  samples**

According to the EDX results (**Table 6.5**), the treated  $\text{Au}/\text{SiO}_2$  appeared to show a decrease in the Au present, which probably means that the Au was lost in the treatment (most likely in the

ultrasonic bath). However in the SEM image of the treated Au/SiO<sub>2</sub> sample Au particles can still be observed (**Figure 6.7 b**). And the Au particles look less in number and smaller in size than before treatment (**Figure 6.7 a**). Therefore it is suggested that the apparent loss of Au might due to both the loss during the treatment and the detector limitation.

The EDX results (**Table 6.5**) also show that the coating contains an amount of sodium (except the coated SiO<sub>2</sub>) and that the coating is sufficiently thick and complete to mean that no gold is observed from under the coating. Importantly no aluminium is detected, showing the formed coating is not a zeolite but instead silica.

**Table 6.5 EDX results for SiO<sub>2</sub> based Catalysts**

Catalysts	O (Weight %)	Si (Weight%)	Other Element (Weight%)
SiO <sub>2</sub>	62.5	37.5	0
HCl SiO <sub>2</sub>	61.8	38.2	0
Au/SiO <sub>2</sub>	59.8	36.2	Au 4.0
Coated SiO <sub>2</sub>	64.2	35.8	0
Coated HCl SiO <sub>2</sub>	63.8	33.5	Na 2.7
Coated Au/SiO <sub>2</sub>	62.0	35.7	Na 2.3
Treated SiO <sub>2</sub>	61.0	39.0	0
Treated HCl SiO <sub>2</sub>	61.4	38.6	0
Treated Au/SiO <sub>2</sub>	62.2	37.4	Au 0.4

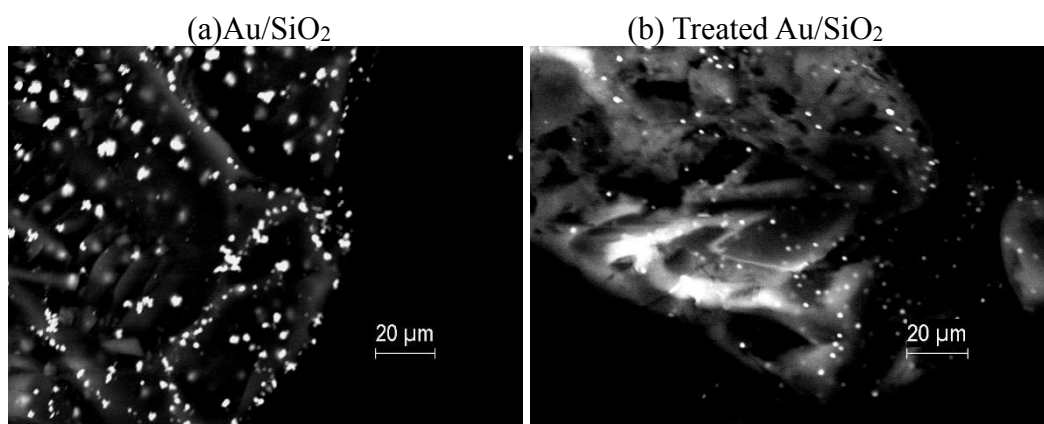


**Figure 6.7 Au particles on the AuSiO<sub>2</sub> and treated Au/SiO<sub>2</sub> with the BSD detector**

## XRD

Examining the bulk of the catalysts by XRD shows only two observable phases for all the catalysts. These are an amorphous silica and gold (in the relevant samples, **Figure 6.8**). There are no changes observed by the addition of the coating, which could mean it is too small to be observed, or it may be amorphous in nature. The large gold particles observed in the SEM are also confirmed by the XRD data where highly defined, sharp peaks are observed.

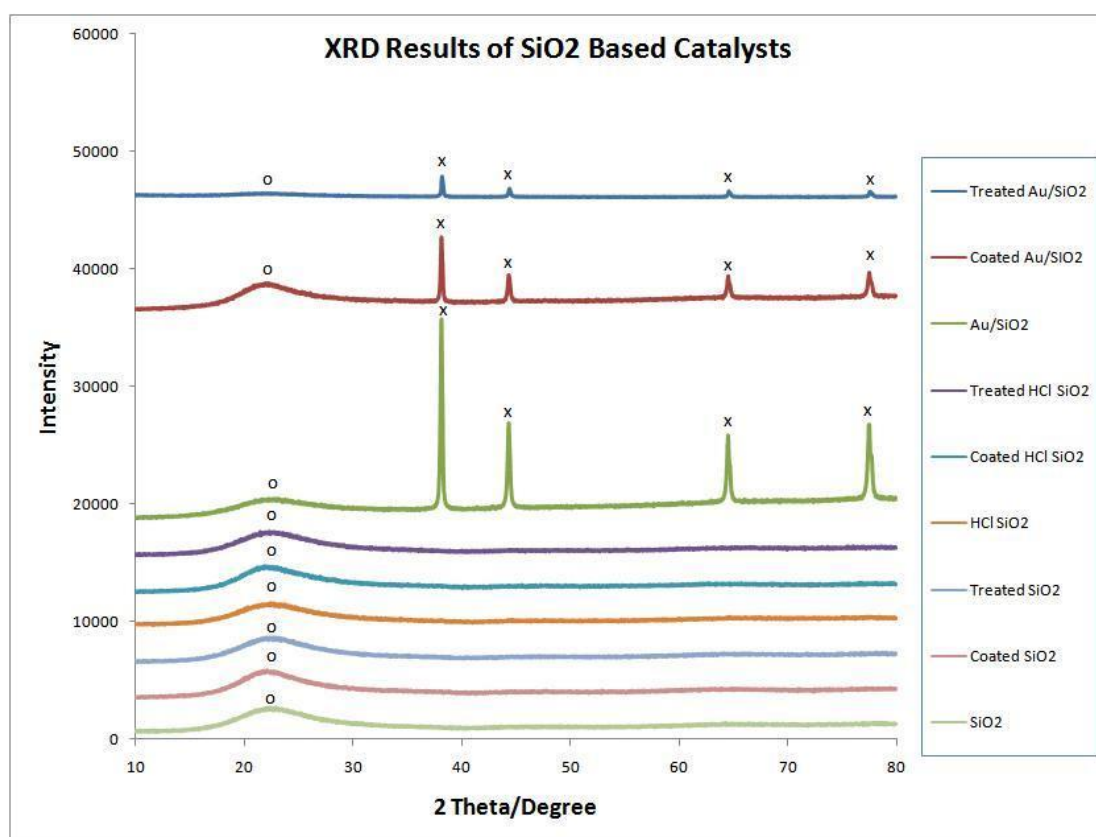


**Figure 6.8 XRD Analysis for the SiO<sub>2</sub> based catalysts**  
o - SiO<sub>2</sub> peak; x - Au peak.

## Liquid Phase Reactions

To check if the SiO<sub>2</sub> based catalysts are still active after being treated, the treated SiO<sub>2</sub> based catalysts were tested in reactions (**Figure 6.9-Figure 6.11, Table 6.6-Table 6.8**). According to the results below, after being treated in the coating procedure, the catalysts still remain active.

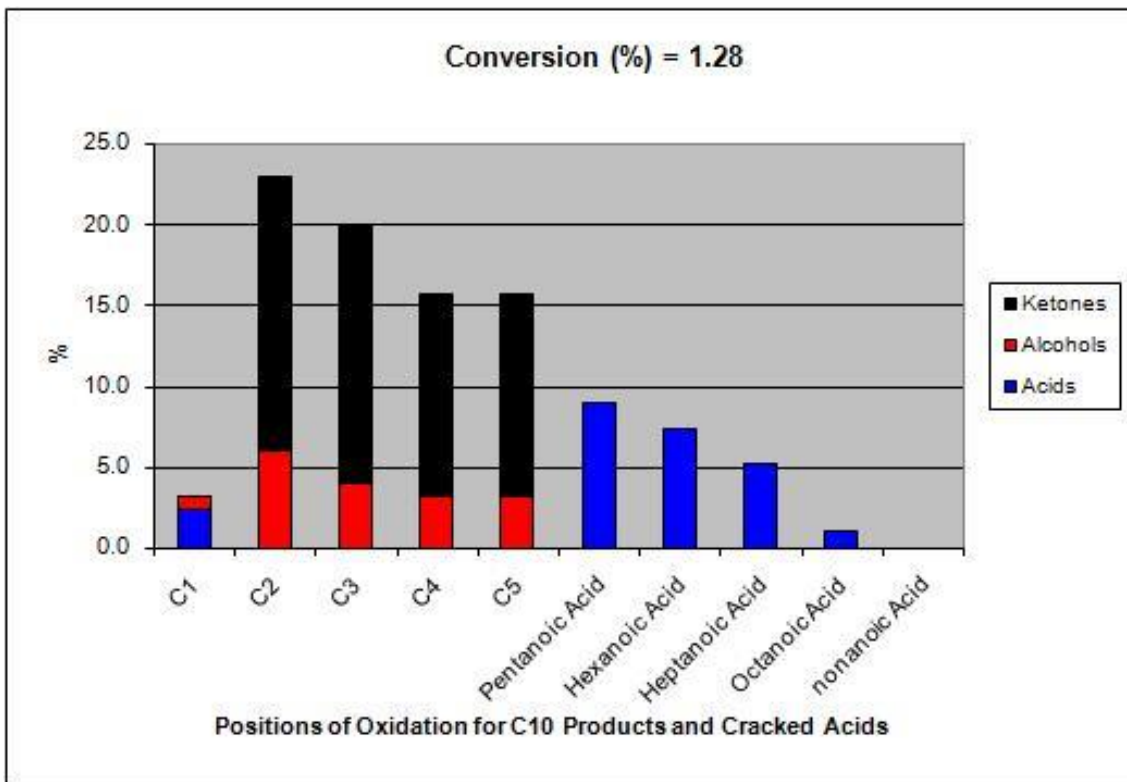


**Figure 6.9 24 h, 110°C, 600 rpm, 15 bar Oxygen, 10 g *n*-decane, 0.05 g Treated SiO<sub>2</sub>**

**Table 6.61 24 h, 110°C, 600 rpm, 15 bar Oxygen, 10g *n*-decane, 0.05g Treated SiO<sub>2</sub>**

Catalyst	Conv. (%)	Selectivity (%)													
		5/4 one	3 one	2 one	5/4 ol	3 ol	2 ol	1 ol	C <sub>5</sub> OOH	C <sub>6</sub> OOH	C <sub>7</sub> OOH	C <sub>8</sub> OOH	C <sub>9</sub> OOH	C <sub>10</sub> OOH	
Treated SiO <sub>2</sub>	<b>1.28</b>	25.0	16.0	17.0	6.4	4.0	5.9	0.9	9.0	7.3	5.2	1.0	0.1	2.3	

C<sub>10</sub> Terminal selectivity = 0.9%+2.3% = 3.2%

Cracked Acid selectivity = 9.0% + 7.3% + 5.2% + 1.0% + 0.1%= 22.6%

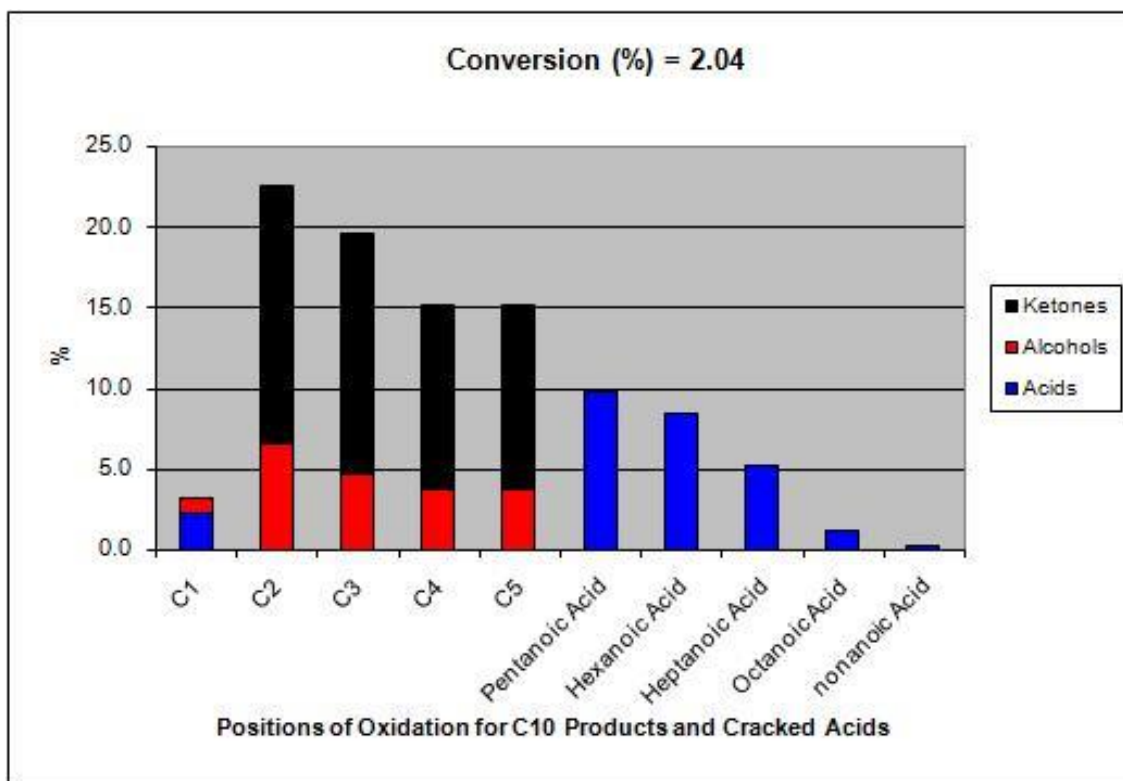


**Figure 6.10 24 h, 110°C, 600 rpm, 15 bar Oxygen, 10 g *n*-decane, 0.05 g Treated HCl SiO<sub>2</sub>**

**Table 6.7 24 h, 110°C, 600 rpm, 15 bar Oxygen, 10g *n*-decane, 0.05 g Treated HCl SiO<sub>2</sub>**

Catalyst	Conv. (%)	Selectivity (%)													
		5/4 one	3 one	2 one	5/4 ol	3 ol	2 ol	1 ol	C <sub>5</sub> OOH	C <sub>6</sub> OOH	C <sub>7</sub> OOH	C <sub>8</sub> OOH	C <sub>9</sub> OOH	C <sub>10</sub> OOH	
Treated HCl SiO <sub>2</sub>	<b>2.04</b>	22.9	15.0	16.0	7.3	4.6	6.5	0.9	9.7	8.3	5.1	1.1	0.2	2.2	

C<sub>10</sub> Terminal selectivity = 0.9%+2.2% = 3.1%

Cracked Acid selectivity = 9.7% + 8.3% + 5.1% + 1.1% + 0.2%= 24.4%

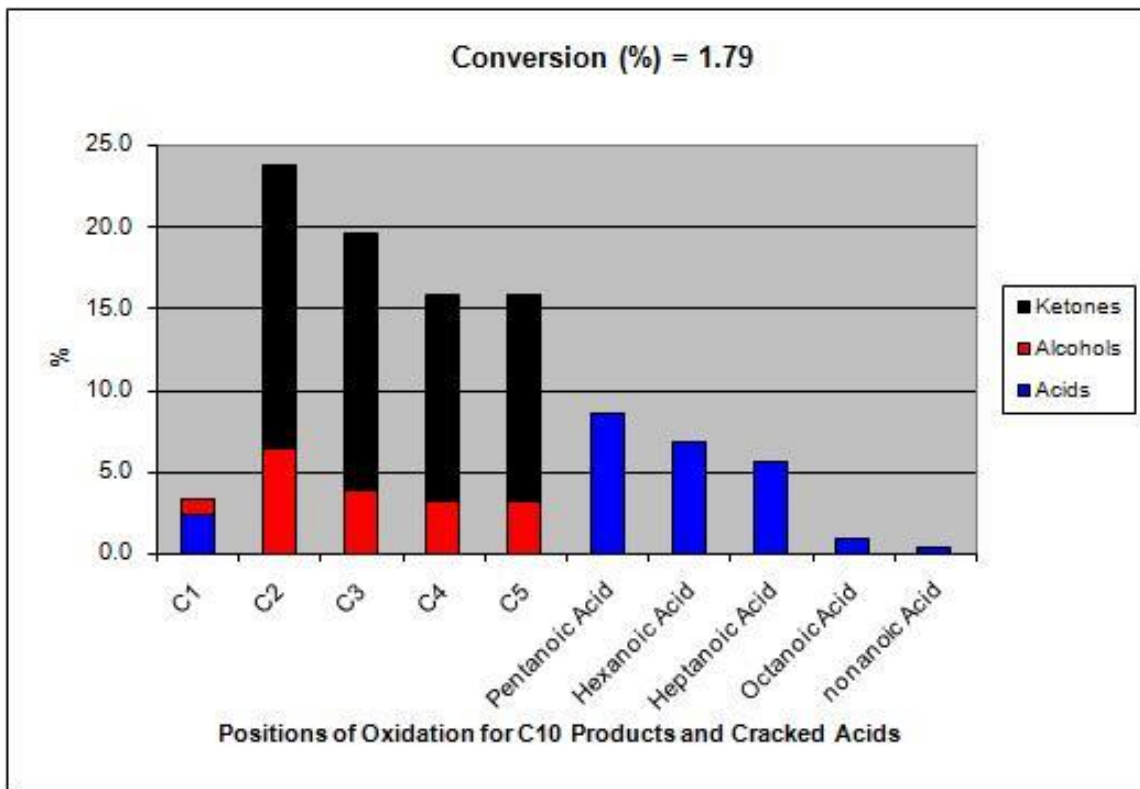


Figure 6.11 24 h, 110°C, 600 rpm, 15 bar Oxygen, 10 g *n*-decane, 0.05 g Treated 5 w.t.%Au/SiO<sub>2</sub>

Table 6.8 24 h, 110°C, 600 rpm, 15 bar Oxygen, 10 g *n*-decane, 0.05 g Treated 5 w.t.% Au/SiO<sub>2</sub>

Catalyst	Conv. (%)	Selectivity (%)													
		5/4 one	3 one	2 one	5/4 ol	3 ol	2 ol	1 ol	C <sub>5</sub> OOH	C <sub>6</sub> OOH	C <sub>7</sub> OOH	C <sub>8</sub> OOH	C <sub>9</sub> OOH	C <sub>10</sub> OOH	
Treated Au/SiO <sub>2</sub>	1.79	25.3	15.6	17.3	6.2	3.9	6.3	1.0	8.5	6.8	5.5	0.9	0.3	2.3	

C<sub>10</sub> Terminal selectivity = 1.0%+2.3% = 3.3%

Cracked Acid selectivity = 8.5% + 6.8% + 5.5% + 0.9% + 0.3%= 22.0%

Then the three coated catalysts were tested and results for them are given below (Figure 6.12 to Figure 6.14, Table 6.9 to Table 6.11). And the results are compared in Table 6.12.

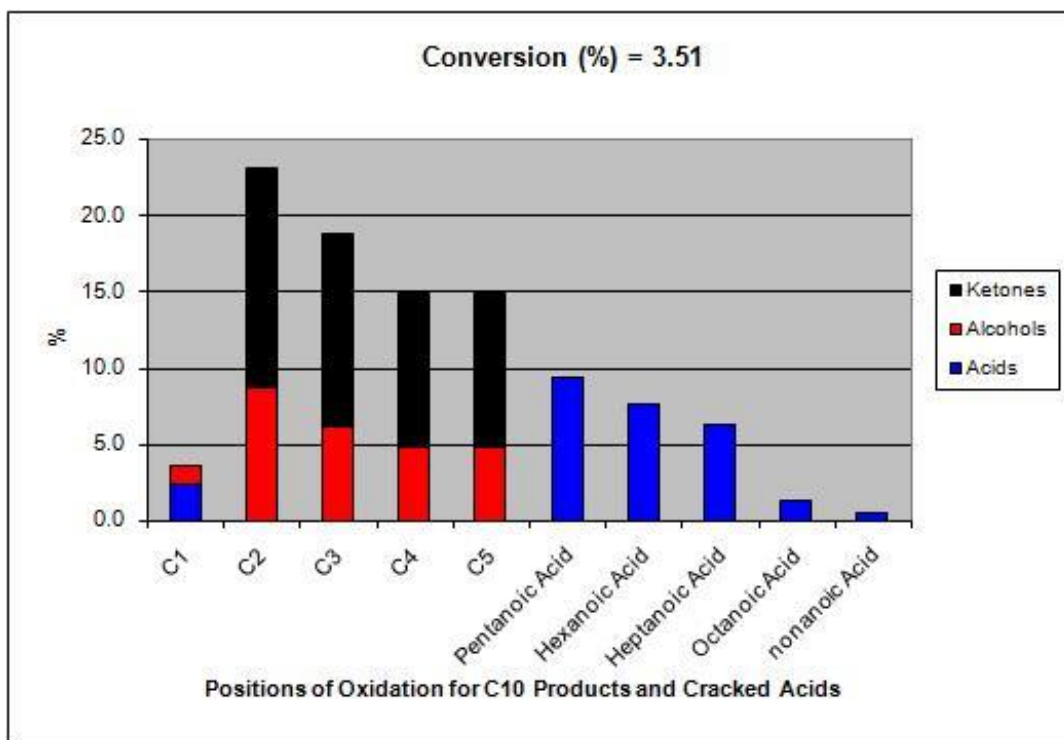


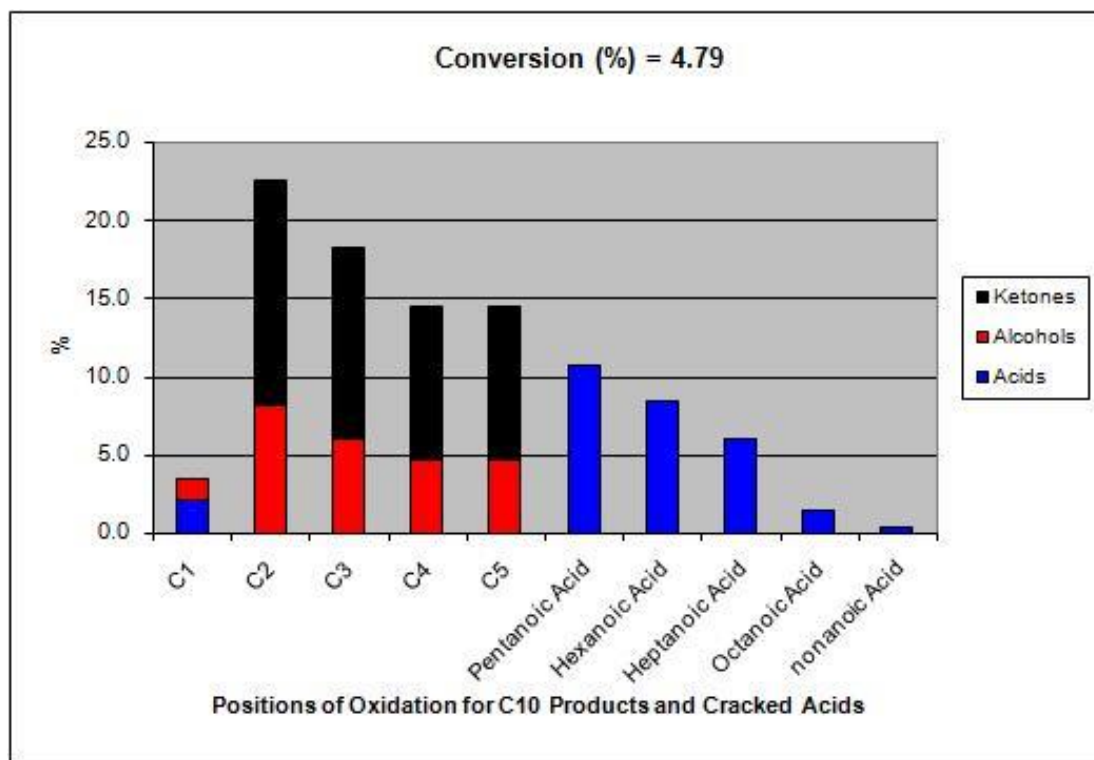
Figure 6.121 24 h, 110°C, 600 rpm, 15 bar Oxygen, 10g *n*-decane, 0.05 g Coated SiO<sub>2</sub>

Table 6.9 24 h, 110°C, 600 rpm, 15 bar Oxygen, 10 g *n*-decane, 0.05 g Coated SiO<sub>2</sub>

Catalyst	Conv. (%)	Selectivity (%)													
		5/4 one	3 one	2 one	5/4 ol	3 ol	2 ol	1 ol	C <sub>5</sub> OOH	C <sub>6</sub> OOH	C <sub>7</sub> OOH	C <sub>8</sub> OOH	C <sub>9</sub> OOH	C <sub>10</sub> OOH	
Coated SiO <sub>2</sub>	<b>3.51</b>	20.1	12.6	14.3	9.7	6.1	8.7	1.3	9.4	7.6	6.2	1.2	0.5	2.3	

C<sub>10</sub> Terminal selectivity = 1.3%+2.3% = 3.6%

Cracked Acid selectivity = 9.4% + 7.6% + 6.2% + 1.2% + 0.5% = 24.9%



**Figure 6.13** 24 h, 110°C, 600 rpm, 15 bar Oxygen, 10 g *n*-decane, 0.05 g Coated HCl SiO<sub>2</sub>

**Table 6.10** 24 h, 110°C, 600 rpm, 15 bar Oxygen, 10 g *n*-decane, 0.05 g Coated HCl Treated SiO<sub>2</sub>

Catalyst	Conv. (%)	Selectivity (%)													
		5/4 one	3 one	2 one	5/4 ol	3 ol	2 ol	1 ol	C <sub>5</sub> OOH	C <sub>6</sub> OOH	C <sub>7</sub> OOH	C <sub>8</sub> OOH	C <sub>9</sub> OOH	C <sub>10</sub> OOH	
Coated HCl SiO <sub>2</sub>	<b>4.79</b>	19.6	12.2	14.3	9.3	6.0	8.2	1.3	10.7	8.4	6.0	1.4	0.4	2.1	

C<sub>10</sub> Terminal selectivity = 1.3%+2.1% = 3.4%

Cracked Acid selectivity = 10.7% + 8.4% + 6.0% + 1.4% + 0.4% = 26.9%

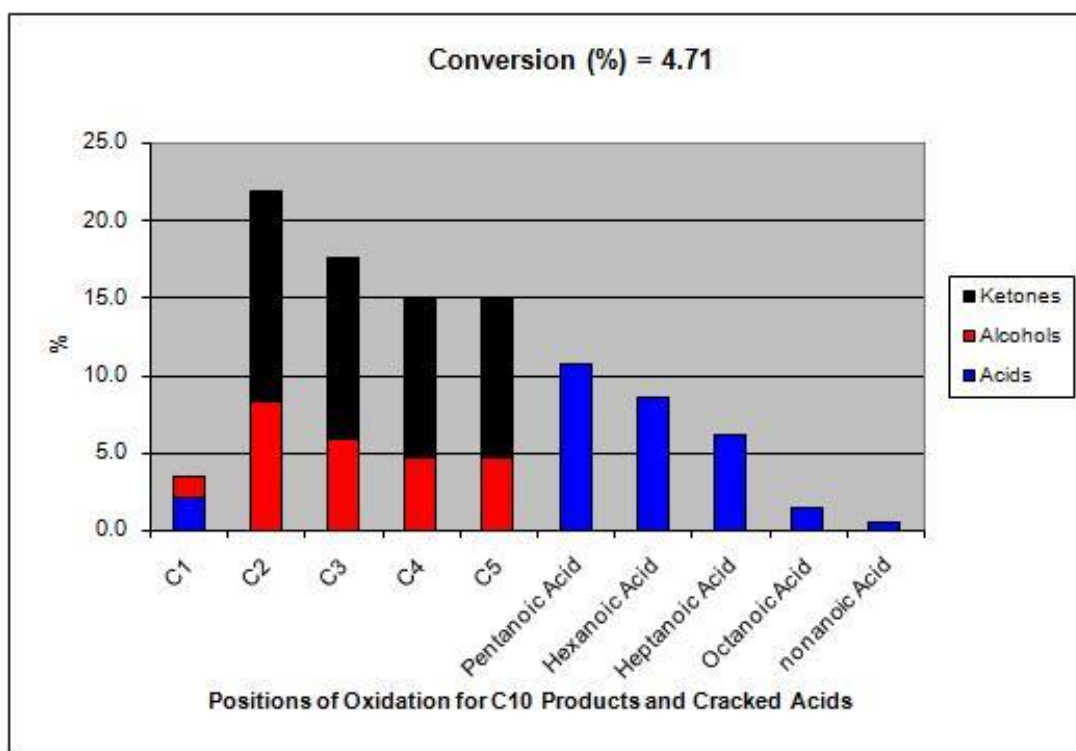


**Figure 6.14 24 h, 110°C, 600 rpm, 15 bar Oxygen, 10 g *n*-decane, 0.05 g Coated Au/SiO<sub>2</sub>**

**Table 6.11 24 h, 110°C, 600 rpm, 15 bar Oxygen, 10 g *n*-decane, 0.05 g Coated AuSiO<sub>2</sub>**

Catalyst	Conv. (%)	Selectivity (%)												
		5/4 one	3 one	2 one	5/4 ol	3 ol	2 ol	1 ol	C <sub>5</sub> OOH	C <sub>6</sub> OOH	C <sub>7</sub> OOH	C <sub>8</sub> OOH	C <sub>9</sub> OOH	C <sub>10</sub> OOH
Coated Au/SiO <sub>2</sub>	<b>4.71</b>	20.6	11.7	13.4	9.4	5.8	8.3	1.4	10.7	8.6	6.1	1.4	0.4	2.0

C<sub>10</sub> Terminal selectivity = 1.4%+2.0% = 3.4%

Cracked Acid selectivity = 10.7% + 8.6% + 6.1% + 1.4% + 0.4% = 27.2%

If a good zeolite coating is formed outside the catalysts, the activity of the catalysts will be limited. However, with the current coating, the conversion became higher than before (**Table 6.12**), while the product distribution of the systems remained similar. To this extent it seems that the coating may be promoting the reaction by acting as a radical initiator. The catalysts with the highest activity (Coated HCl SiO<sub>2</sub> and coated Au/SiO<sub>2</sub>) were then tested in the presence of TEMPO to try to scavenge the radical reaction (**Figure 6.15** and **Figure 6.16**).

**Table 6.12 Compare the SiO<sub>2</sub> Based Catalysts**

Catalyst	Conv. (%)	Selectivity (%)												
		5/4 one	3 one	2 one	5/4 ol	3 ol	2 ol	1 ol	C <sub>5</sub> OOH	C <sub>6</sub> OOH	C <sub>7</sub> OOH	C <sub>8</sub> OOH	C <sub>9</sub> OOH	C <sub>10</sub> OOH
SiO <sub>2</sub>	<b>1.61</b>	26.9	16.4	18.8	5.2	3.6	4.8	0.8	7.0	6.4	5.8	1.3	0.1	2.8
Au/SiO <sub>2</sub>	<b>2.42</b>	22.4	14.5	16.7	5.5	4.7	7.0	1.0	8.7	7.8	6.7	1.8	0.2	2.9
Treated SiO <sub>2</sub>	<b>1.28</b>	25.0	16.0	17.0	6.4	4.0	5.9	0.9	9.0	7.3	5.2	1.0	0.1	2.3
Treated HCl SiO <sub>2</sub>	<b>1.94</b>	22.9	15.0	16.0	7.3	4.6	6.5	0.9	9.7	8.3	5.1	1.1	0.2	2.2
Treated Au/SiO <sub>2</sub>	<b>1.79</b>	25.3	15.6	17.3	6.2	3.9	6.3	1.0	8.5	6.8	5.5	0.9	0.3	2.3
Coated SiO <sub>2</sub>	<b>3.51</b>	20.1	12.6	14.3	9.7	6.1	8.7	1.3	9.4	7.6	6.2	1.2	0.5	2.3
Coated HCl SiO <sub>2</sub>	<b>4.79</b>	19.6	12.2	14.3	9.3	6.0	8.2	1.3	10.7	8.4	6.0	1.4	0.4	2.1
Coated Au/SiO <sub>2</sub>	<b>4.71</b>	20.6	11.7	13.4	9.4	5.8	8.3	1.4	10.7	8.6	6.1	1.4	0.4	2.0

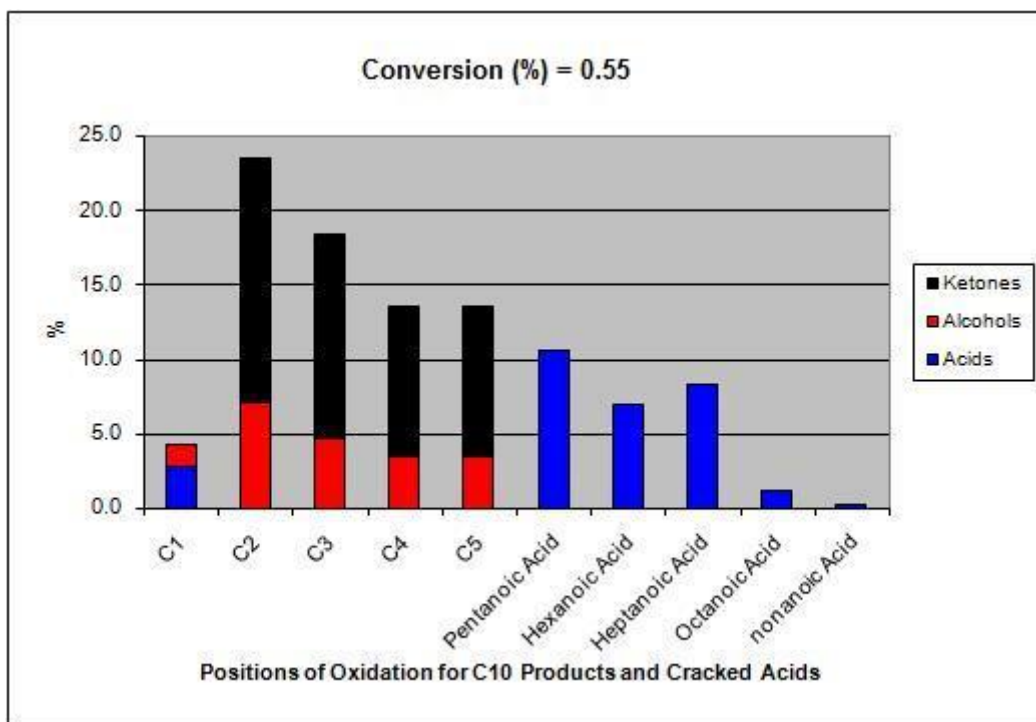


Figure 6.15 24 h, 110°C, 600 rpm, 15 bar Oxygen, 10 g *n*-decane, 0.05 g Coated HCl SiO<sub>2</sub>, 0.005 g TEMP

Table 6.13 24 h, 110°C, 600 rpm, 15 bar Oxygen, 10 g *n*-decane, 0.05 g Coated HCl SiO<sub>2</sub>, 0.005g TEMPO

Catalyst	Conv. (%)	Selectivity (%)												
		5/4 one	3 one	2 one	5/4 Ol	3 ol	2 ol	1 ol	C <sub>5</sub> OOH	C <sub>6</sub> OOH	C <sub>7</sub> OOH	C <sub>8</sub> OOH	C <sub>9</sub> OOH	C <sub>10</sub> OOH
Coated HCl SiO <sub>2</sub> + TEMPO	<b>0.55</b>	20.0	13.7	16.4	6.9	4.6	7.0	1.5	10.5	6.9	8.3	1.2	0.2	2.7

C<sub>10</sub> Terminal selectivity = 1.5%+2.7% = 4.2%

Cracked Acid selectivity = 10.5% + 6.9% + 8.3% + 1.2% + 0.2% = 27.1%

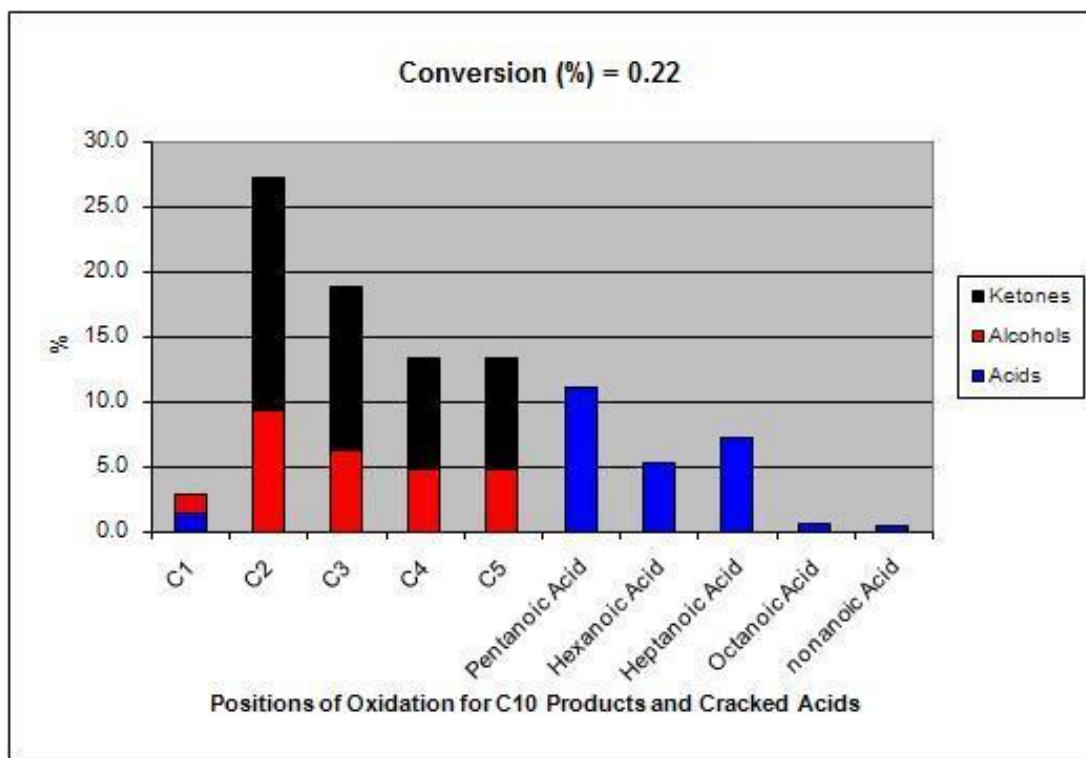


Figure 6.16 24 h, 110°C, 600 rpm, 15 bar Oxygen, 10 g *n*-decane, 0.05 g Coated Au/SiO<sub>2</sub>, 0.005 g TEMPO

Table 6.14 24h, 110°C, 600 rpm, 15 bar Oxygen, 10g *n*-decane, 0.05g Coated Au/SiO<sub>2</sub>, 0.005g TEMPO

Catalyst	Conv. (%)	Selectivity (%)													
		5/4 one	3 one	2 one	5/4 Ol	3 ol	2 ol	1 ol	C <sub>5</sub> OOH	C <sub>6</sub> OOH	C <sub>7</sub> OOH	C <sub>8</sub> OOH	C <sub>9</sub> OOH	C <sub>10</sub> OOH	
Coated Au/SiO <sub>2</sub> +TEMPO	0.22	17.3	12.6	18.0	9.4	6.2	9.2	1.4	11.1	5.3	7.2	0.6	0.4	1.4	

C<sub>10</sub> Terminal selectivity = 1.4% + 1.4% = 2.8%

Cracked Acid selectivity = 11.1% + 5.3% + 7.2% + 0.6% + 0.4% = 24.6%

Only very slight differences in product distribution was found between the reactions with and without TEMPO (Table 6.15), which are within experimental error. It is interesting to note though that the coated acid-treated SiO<sub>2</sub> catalyst is the most active observed in the presence of TEMPO, compared to the previous best of 0.45 % for Au/TiO<sub>2</sub>, while pure SiO<sub>2</sub> was inactive

in the presence of TEMPO. This shows that either the acid treatment or the coatings are helping to promote activity.

**Table 6.15 Compare the results with and without TEMPO**

Catalyst	Conv. (%)	Selectivity (%)												
		5/4 one	3 one	2 one	5/4 Ol	3 ol	2 ol	1 ol	C <sub>5</sub> OOH	C <sub>6</sub> OOH	C <sub>7</sub> OOH	C <sub>8</sub> OOH	C <sub>9</sub> OOH	C <sub>10</sub> OOH
Coated HCl SiO <sub>2</sub> +TEMPO	<b>0.55</b>	20.0	13.7	16.4	6.9	4.6	7.0	1.5	10.5	6.9	8.3	1.2	0.2	2.7
Coated HCl SiO <sub>2</sub>	<b>4.79</b>	19.6	12.2	14.3	9.3	6.0	8.2	1.3	10.7	8.4	6.0	1.4	0.4	2.1
Coated Au/SiO <sub>2</sub> + TEMPO	<b>0.22</b>	17.3	12.6	18.0	9.4	6.2	9.2	1.4	11.1	5.3	7.2	0.6	0.4	1.4
Coated Au/SiO <sub>2</sub>	<b>4.71</b>	20.6	11.7	13.4	9.4	5.8	8.3	1.4	10.7	8.6	6.1	1.4	0.4	2.0

A time-on-line study was then carried out to further investigate the activity of the coated samples. The comparison of results was shown in **Figure 6.17** to **Figure 6.19**. The three SiO<sub>2</sub> coated catalysts: coated SiO<sub>2</sub>, coated HCl SiO<sub>2</sub> and coated Au/SiO<sub>2</sub> have been tested time on-line without and with TEMPO. The conversion and terminal selectivity (C10 terminal selectivity and cracked acids selectivity) without and with TEMPO are compared.

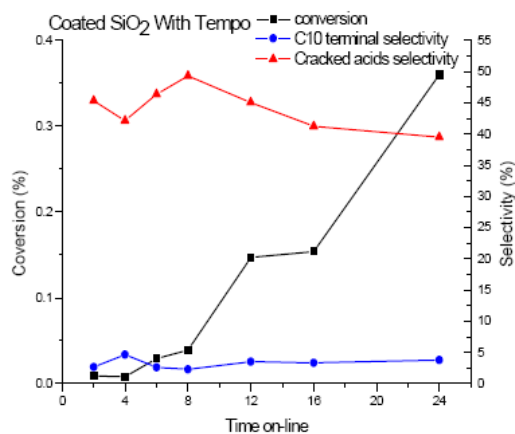
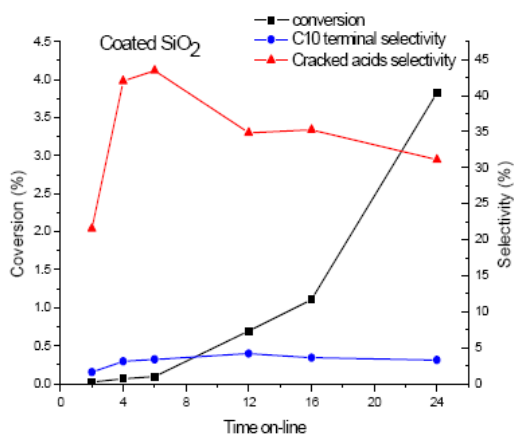


**Figure 6.17 Coated SiO<sub>2</sub> and coated SiO<sub>2</sub> with TEMPO**

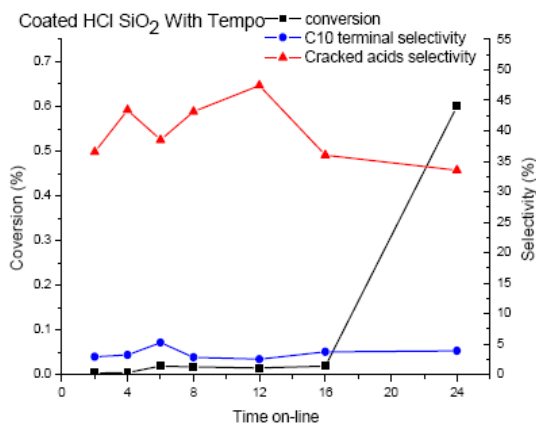
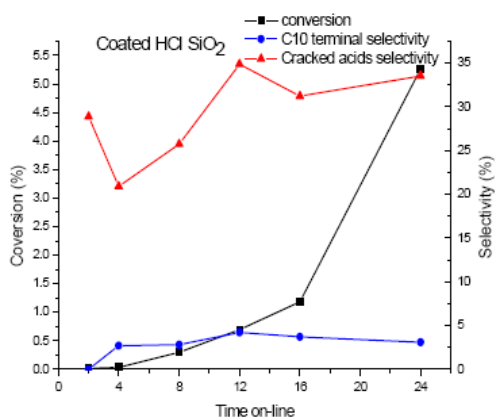


**Figure 6.18 Coated HCl SiO<sub>2</sub> and coated HCl SiO<sub>2</sub> with TEMPO**

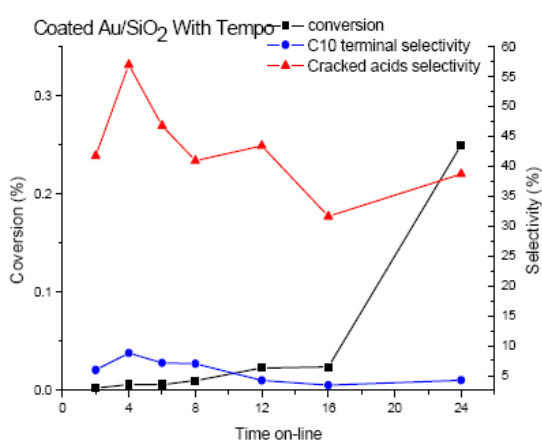
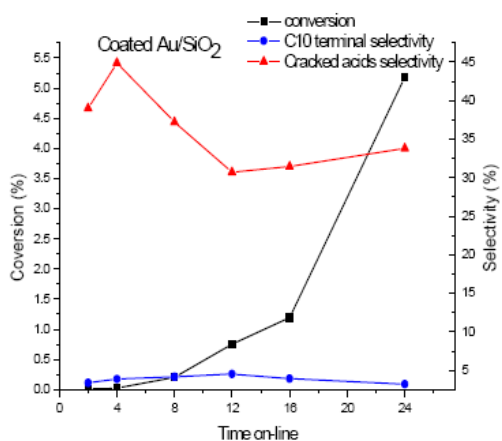


**Figure 6.19 Coated Au/SiO<sub>2</sub> and coated Au/SiO<sub>2</sub> with TEMPO**

### 6.5.1.2 Discussion

It can be seen that both conversion and selectivity for the reformation of shortened acids are quite different between the reactions without and with TEMPO. Though the conversion with TEMPO is much reduced (as would be expected), the selectivity for shortened acids is higher (typically ~10%) than when TEMPO is not present. The presence of increased selectivity for shortened acids seems to be at the expense of C<sub>10</sub> ketones; while little difference is seen in the C<sub>10</sub> terminal selectivity.

The results both in the presence and absence of TEMPO show a considerable induction period with a large increase in conversion only occurring after 16 hours of time on line. This is similar to work previously reported on the autoxidation of *n*-decane.

In the presence of TEMPO, the three coated samples have little difference in both conversion and selectivity. From this, it is suggested that in these reactions, the activity is due to the SiO<sub>2</sub> overlayer more than the catalyst underneath.

In order to test the activity of the coating formed, the coated MgO catalysts were also tested in liquid phase under the same conditions to make a comparison.

### 6.5.1.3 Coated MgO in gas phase reaction

MgO based Catalysts were analysed and tested in gas phase reactions discussed in this section.

#### BET

It is found in **Table 6.16** that after being coated or treated, the surface area increased. The situation is a little different from the SiO<sub>2</sub> samples. To have a good understanding of this, the

structure of the catalyst particles are shown in the SEM images (**Figure 6.20**).

**Table 6.16 BET results for the MgO based catalysts**

Catalysts	Surface Area(m <sup>2</sup> /g)
MgO	98
HCl MgO	74
Au/MgO	51
Coated MgO	39
Coated HCl MgO	110
Coated Au/MgO	169
Treated MgO	134
Treated HCl MgO	112
Treated Au/MgO	120

### SEM&EDX

According to the **Figure 6.20**, it can be found that before the treatment the blank catalysts are in very small particles; after being treated, the particles maintain their original size, however, some become stuck together to form large macroscopic particles (images c, f, i).

In a higher magnification image of the MgO without any treatment (**Figure 6.21 a**) and coated MgO (**Figure 6.21 b**). Obviously both the size and surface properties are quite different from SiO<sub>2</sub> crystals. And it can be clearly seen that something is covering the MgO substrate. The formed coating composition is discussed in the following XRD and XPS section.

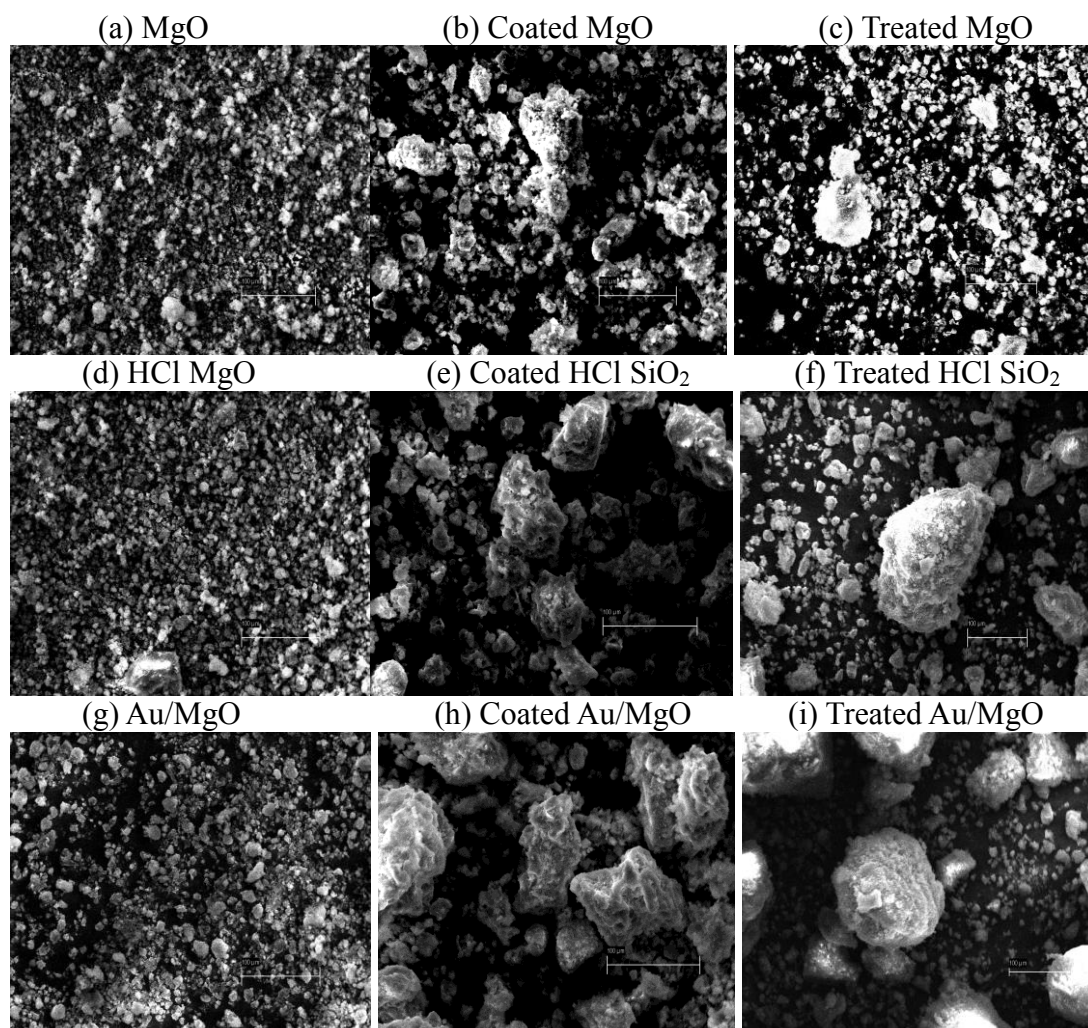


**Figure 6.20 Comparison of SEM Images of MgO Based Catalysts**  
Each image is approximately 550  $\mu\text{m}$  wide

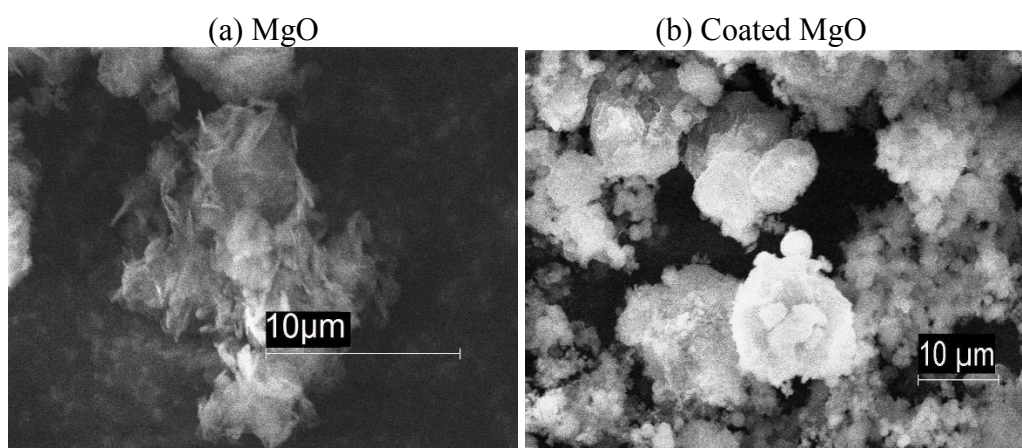


**Figure 6.21 SEM images of MgO and Coated MgO with a higher magnification**

**Table 6.17 EDX results for MgO Based Catalysts**

Catalysts	O (Weight %)	Mg (Weight%)	Si (Weight%)	Other Element (Weight%)
MgO	50.8	48.3	0	Ca 0.84
HCl MgO	46.5	52.1	0	Cl 0.8, Ca 0.6
Au/MgO	48.5	46.6	0	Cl 1.3, Ca 0.8, Au 2.8
Coated MgO	59.0	5.9	35.0	0
Coated HCl MgO	60.4	30.9	8.7	0
Coated Au/MgO	61.4	22.2	16.5	0
Treated MgO	62.3	37.7	0	0
Treated HCl MgO	62.8	37.2	0	0
Treated Au/MgO	61.2	35.8	0	Au 3.0

In the untreated blank catalysts some Cl and Ca are found, which corresponds with impurities in the magnesium carbonate (The starting material for the production of MgO). They disappear in the coated and treated samples, which is likely to be due to the treatment by ultrasonic bath and washing. It is clear that the O:Mg ratio is quite different among the original MgO based catalysts, the coated catalysts and the treated catalysts. If the increase of O ratio in the coated samples only comes from the coating formed, it would not be expected that the treated samples would also observe the O ratio increase. This will be discussed with the XRD results together below.

As above, the EDX analysis found the treated Au/SiO<sub>2</sub> lost some Au (Au became only 0.4% after being treated), but this did not occur with the treated Au/MgO. It is suggested that this is due to the different surface properties – as shown in the SEM, the SiO<sub>2</sub> support we employed

has a very smooth surface. It is also noticeable that again that the gold is no longer observed once the coating has been laid down.

Again no aluminium was observed after this preparation so further analysis was taken with XPS to test if the concentration of aluminium is only in the surface region.

### XPS

A small amount coated MgO sample was analysed in the XPS, with the elements seen below along with their binding energies (**Table 6.18**). As is visible from the data, there is a large presence of silicon but no aluminium is observed, again showing the coating to be more silica-like in nature. The low level of magnesium detected suggests that the coating is relatively thick (>5 nm).

**Table 6.18 Binding Energy of the Detected Element**

Detected Element	Binding Energy (eV)	Approximate Composition (Atom %)
O	532.9	54.3
C	284.7	10.2
Si	103.6	33.8
Mg	49.9	1.3
Ca	~350	0.5

### XRD

From the XRD results (**Figure 6.22**), we can clearly distinguish the MgO and Au peaks (circles and crosses respectively) in the untreated and coated samples. However for the coated and treated catalysts, there are some other peaks in the figure which are unmarked. A simple search and match on this data suggests that the treatments imposed have led to a bulk hydroxylation and the formation of Mg(OH)<sub>2</sub>. This explains the O increase in the treated MgO samples as seen by EDX (**Table 6.17**). Again the gold peaks observed by XRD are very sharp showing the

presence of relatively large gold particles, and no bulk structure is found for the coating.

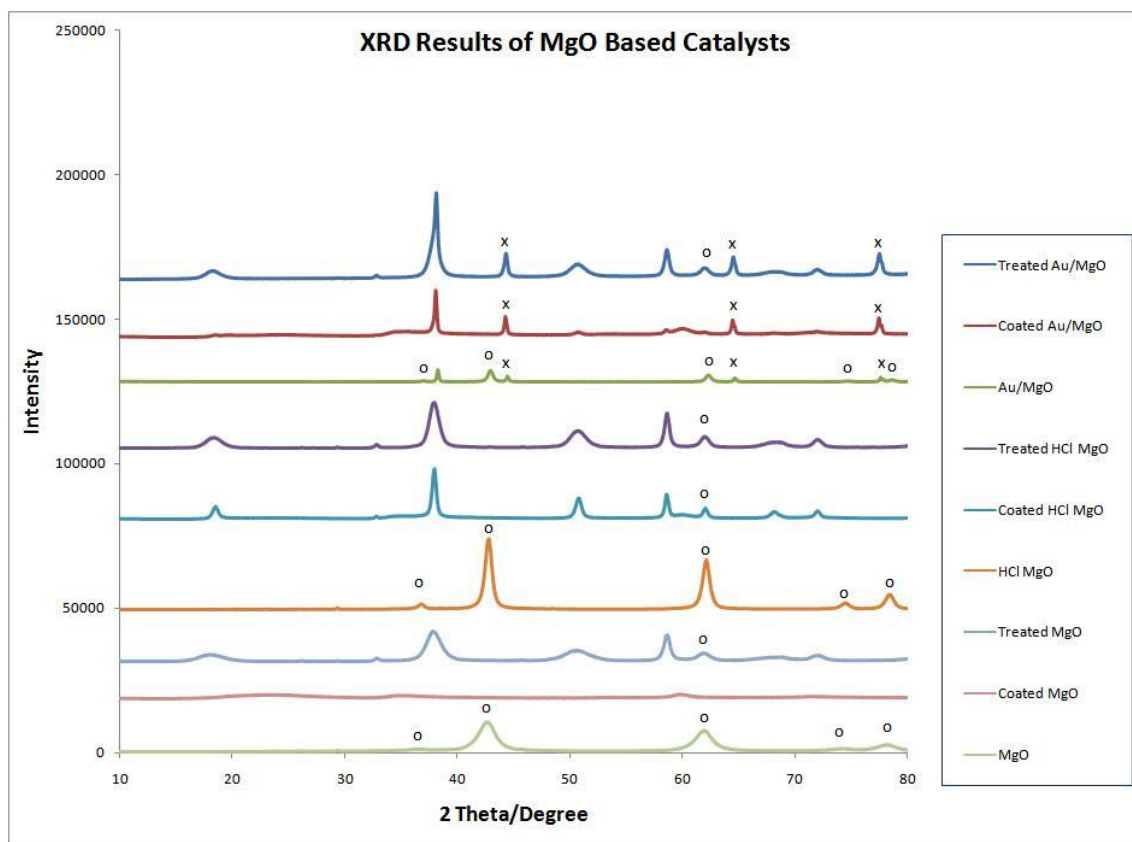


**Figure 6.22 XRD Analysis for MgO Based Samples**  
o -MgO; x - Au.

### Coated MgO in liquid phase reaction

MgO based catalysts were tested in the liquid phase reaction as shown in **Table 6.19**.

**Table 6.19 24 h, 110°C, 600 rpm, 15 bar Oxygen, 10 g *n*-decane, 0.05 g Catalyst**

Catalyst	Conv. (%)	Selectivity (%)													
		5/4 one	3 one	2 one	5/4 Ol	3 ol	2 Ol	1 ol	C <sub>5</sub> OOH	C <sub>6</sub> OOH	C <sub>7</sub> OOH	C <sub>8</sub> OOH	C <sub>9</sub> OOH	C <sub>10</sub> OOH	
MgO	<b>1.62</b>	21.1	14.5	17.5	7.1	4.8	8.5	1.8	6.7	6.1	8.6	0.8	0.4	1.9	
HCl MgO	<b>0.40</b>	19.4	11.9	16.3	10.4	7.3	14.3	2.5	4.4	5.2	5.6	0.2	1.2	1.2	
Au/MgO	<b>1.38</b>	21.5	15.5	20.0	9.4	6.5	13.7	2.3	2.6	2.4	3.6	1.3	0.6	0.6	
Coated MgO	<b>1.65</b>	23.2	15.0	16.0	8.5	5.4	7.4	1.1	7.4	5.9	5.6	1.4	0.6	2.4	
Coated HCl MgO	<b>0.60</b>	20.5	15.6	14.8	8.7	5.5	7.8	2.1	11.3	8.0	3.1	0.8	0.3	1.5	
Coated Au/MgO	<b>1.47</b>	20.6	13.1	14.1	8.9	5.6	8.4	1.5	9.9	8.2	6.4	0.8	0.1	2.4	

The high conversion that was observed for the coated SiO<sub>2</sub> based catalysts was not observed this time. This is somewhat surprising as previously it appeared that the coating was promoting the reaction, but may be explained by the different nature of the coating. In the next section the coating on the MgO samples is analysed and it can be seen that no sodium is present (**Table 6.17**), unlike the SiO<sub>2</sub> coated samples (**Table 6.12**).

### Coated MgO in Gas Phase Reaction

Both the coated and treated MgO samples have been tested in the gas phase reactions (**Table 6.20** to **Table 6.24**).

**Table 6.20 Conversions obtained with different catalysts in the gas phase reactor when varying the C:O ratio**

Catalyst	Temp (°C)	C:O	Conv. (%)	Cracked	Decene	C10 oxygenates	CO <sub>x</sub>
MgO	318	14:1	2.7	97	1	0.0	2
MgO	318	7:1	1.7	97	1	0.0	2
Au/MgO	275	14:1	1.1	96	1	0.0	3
Au/MgO	275	7:1	0.8	97	1	0.0	1

**Table 6.21 N<sub>2</sub>O oxidant, 14:1 C:O, 0.89 % *n*-decane, 1.33 s residence time.**

Catalyst	Temp (°C)	X	Cracked	Decene	C10 alcohol/ketones	CO
Coated MgO	239	0.3	76	5.2	0.0	19
	282	0.4	84	4.3	0.0	11
	305	0.6	94	2.4	0.0	4
	327	1.3	96	1.4	0.2	2
Coated Acid MgO	211	0.1	52	26.1	0.0	22
	253	0.2	59	10.9	0.0	30
	275	0.4	57	4.4	0.0	39
	295	0.6	91	3.2	0.0	6
Coated Au/MgO	210	0.9	84	1.3	0.0	15
	250	2.5	93	0.6	0.6	6
	270	2.2	94	0.7	1.6	4
	290	3.2	92	1.2	1.1	5

**Table 6.22 - O<sub>2</sub> oxidant, 14:1 C:O, 0.89 % *n*-decane, 1.33s residence time.**

Catalyst	Temp (°C)	X	Cracked	Decene	C10 alcohol/ketones	CO
Coated MgO	237	0.2	77	6.3	0.0	16
	259	0.6	72	2.5	0.0	26
	282	0.9	79	2.5	0.0	19
	307	1.5	87	1.4	0.2	11
	326	2.5	89	0.8	0.6	9
Coated Acid MgO	209	0.1	70	17.7	0.0	13
	230	0.2	78	8.4	0.0	13
	251	0.4	83	5.9	0.0	11
	275	0.6	94	0.0	0.0	6
	293	2.0	94	1.6	0.3	4
Coated Au/MgO	208	0.5	41	2.5	0.0	57
	229	0.4	93	2.4	0.0	5
	249	1.1	71	0.7	0.0	28
	270	2.0	85	2.1	0.6	12
	295	3.7	97	2.7	0.2	0

**Table 6.23 N<sub>2</sub>O oxidant, 14:1 C:O, 0.89 % *n*-decane, 1.33 s residence time.**

Catalyst	Temp (oC)	X	Cracked	Decene	C10 alcohol/ketones	CO
Treated MgO	238	0.3	90	4.9	0.0	5
	260	0.9	96	1.6	0.0	2
	282	1.9	97	0.8	0.5	1
	306	4.7	97	0.7	0.3	2
	329	8.4	97	0.6	0.9	1
Treated acid MgO	209	0.1	70	21.7	0.0	8
	229	0.3	91	5.0	0.0	4
	248	0.8	94	1.8	0.3	4
	270	2.4	98	0.6	0.4	1
	288	6.5	99	0.5	0.3	1
Treated Au/MgO	211	0.5	94	2.9	0.0	3
	249	1.1	91	1.4	0.0	8
	252	2.3	95	0.7	0.0	5
	274	4.8	97	0.4	0.1	2
	294	9.5	97	0.2	0.2	2

**Table 6.24 O<sub>2</sub> oxidant, 14:1 C:O, 0.89 % *n*-decane, 1.33 s residence time.**

Catalyst	Temp (°C)	X	Cracked	Decene	C10 alcohol/ketones	CO
Treated MgO	238	0.8	90	3.5	0.0	7
	260	1.7	90	2.2	1.3	6
	283	3.1	94	2.9	2.2	1
	304	4.7	92	2.6	2.9	2
Treated acid MgO	208	0.4	81	4.9	0.0	14
	228	0.8	85	10.8	0.9	4
	247	1.8	87	5.3	2.5	5
	266	3.1	87	3.5	3.0	7
	286	3.4	90	3.0	3.9	3
Treated Au/MgO	212	1.1	87	1.4	0.0	12
	232	2.6	87	0.8	0.0	13
	252	4.6	91	1.3	0.1	8
	274	7.0	92	1.3	0.2	7
	293	8.2	93	1.3	0.5	6

#### 6.5.1.4 Discussion

The XRD results of MgO-based catalysts were quite similar to that of the SiO<sub>2</sub>-based catalysts, in which only the peaks of SiO<sub>2</sub> substrate were detected for the coated samples. Thus it can be concluded the coating formed in the direct template-free method is perhaps some amorphous SiO<sub>2</sub>, which, according to the SEM images, covered the substrates to an extent where the gold was no longer observed by EDX. Although the coating is probably SiO<sub>2</sub>, it is unlikely the coatings formed on the SiO<sub>2</sub> and MgO are the same due to the quite different appearance in the characterization, and the presence of sodium is absent from those on MgO.

Combining all the liquid phase reaction results above it seems that, instead of a zeolite coating, some other product is produced in the procedure. And according to **Table 6.12**, the product, surprisingly, seemed to be more active in decane oxidation. As the phenomenon did not appear

again with the coated MgO based catalysts, two proposals may be made based on this. One is if it is the same coating, the activity should be not due to the coating only; the other is the coating formed on the SiO<sub>2</sub> and MgO supports is not the same coating - perhaps some factors influenced the coating formation which led to a different coating formed, which can be proved in the different appearance in the characterization in XRD. Further investigation on this is given in the following gas phase section.

From these gas phase reaction results it can be seen that both the coated and treated catalysts give an increased conversion in comparison to the untreated MgO-based systems. Combined with the characterization data this increase in activity is suggested to result from the conversion of MgO to Mg(OH)<sub>2</sub>. In terms of selectivity for C<sub>10</sub> oxygenated products, the treated samples show the best result, followed by the coated and then the untreated. It should be remembered that these catalysts were tested under long residence times, which was been shown to give lower C<sub>10</sub> oxygenation selectivity. The best results are obtained with the acid-washed and then the treated MgO, which gave 3.9% selectivity at 3.4% conversion. These selectivity increases are not as high as had been hoped for, so further development of the coating is required, while attempting to preserve the substrate in an unaltered form.

#### **6.5.1.5 Conclusion**

Although a significant increase of the C<sub>10</sub> terminal selectivity was not found with any of the powder formed coated catalysts, it is notable that many catalysts show a high terminal selectivity in the form of cracked acids. As the oxidation of decane is viewed as a model reaction for terminal products, this probably has some promise as we can expect that a wide range of terminally oxidized linear alkanes could be achieved.

In this section, SiO<sub>2</sub> and MgO based catalysts were synthesised with a zeolite coating, in which the direct template-free zeolite membrane preparation method was employed. From SEM, EDX, XRD and XPS data, it can be concluded that with this method the desired zeolite coating was not obtained. Instead, an amorphous SiO<sub>2</sub> overlayer was formed on the surface. The direct template-free method does not seem to produce the desired coating for our powder catalysts. Especially for the SiO<sub>2</sub> based catalysts, the SiO<sub>2</sub> membrane formed not only on the surface of catalyst substrates, but also some excess that was not tethered to the surface.

The coated samples do however show increased activity in both liquid and gas phase reactions. In the liquid phase, the coated SiO<sub>2</sub> based catalysts showed a conversion increase of 1-2%, however the terminal selectivity is not affected. As the coated SiO<sub>2</sub> based catalysts have low surface area (**Table 4**), it seems that the activity per unit area is quite high. The treated MgO based catalysts in the gas phase reactor showed some good activity. The work now needs to move on to study a system with an ordered pore structure.

### **6.5.2 Zeolite A Coating with sphere support**

From the previous experience, the final product after a successful coating is a mixture of coated samples, extra zeolite and water. Therefore, with the powder form of supports such as silica and alumina, it is difficult to separate the coated samples from the mixture. From a wide search in the literature, the conclusion is the same: zeolite coatings were reported to be synthesized on supports with big structures, e.g. stainless steel cell or plate, alumina spheres and silica spheres. In this section, zeolite 4A coatings with alumina spheres have been tested. The synthesis procedure for the catalysts is described in the experimental section.

### 6.5.2.1 Results

Coatings on the alumina spheres have been carried on the alumina spheres without any active centre only. The alumina spheres have also been treated by the two different polyelectrolytes, coated in the same way and then used in reactions. **Figure 6.23** shows the surface of one of the coated alumina spheres under the SEM. According to the image, there is a full coverage of zeolite on the sphere, while the pore structure is still clear.

The coated alumina spheres were then used in the liquid phase reaction at 100°C for 16 h to test the selectivity. The reaction product distribution is shown in **Table 6.25** and **Figure 6.24** to **Figure 6.26**.

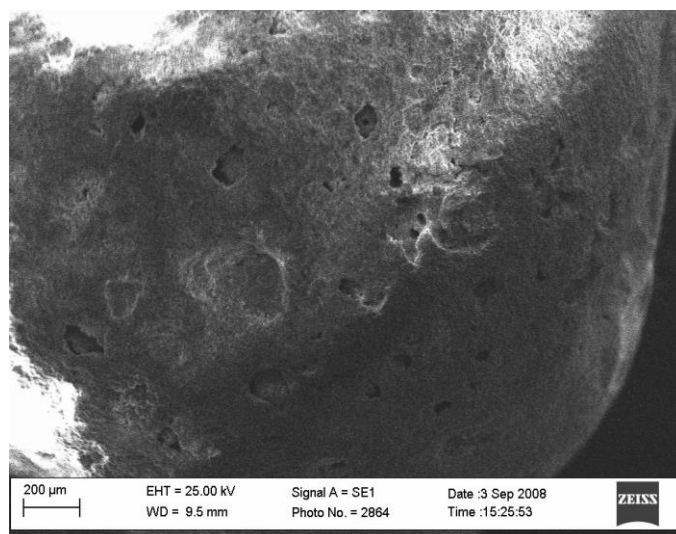


**Figure 6.23 Surface of the coated alumina spheres (treated by polydiallyl dimethyl ammonium chloride)**

**Table 6.25 100°C, 15 bar, 10 g *n*-decane, 3 Coated Al<sub>2</sub>O<sub>3</sub> spheres, 16 h**

Catalyst	Conv. (%)	Selectivity (%)												
		5/4 one	3 one	2 one	5/4 ol	3 ol	2 ol	1 ol	C <sub>5</sub> OOH	C <sub>6</sub> OOH	C <sub>7</sub> OOH	C <sub>8</sub> OOH	C <sub>9</sub> OOH	C <sub>10</sub> OOH
Blank	<b>0.18</b>	22.9	14.4	15.8	7.6	4.9	7.8	1.3	12.5	4.3	6.1	0.8	0.5	1.2
1*	<b>0.14</b>	19.0	11.9	16.6	10.1	7.1	11.3	2.1	16.2	2.0	2.8	0.5	0.3	0.2
2*	<b>0.07</b>	15.8	10.8	18.4	9.7	6.9	12.0	2.2	19.7	0.9	1.8	0.6	0.4	0.6

1- Treated by polydiallyl dimethyl ammonium chloride

2- Treated by magnafloc lt35

There must be some differences between different spheres, both in mass and coating status. To avoid problems caused by this, the reactions have been repeated to confirm the results. It was found that the conversions of the reactions were between 0.10- 0.14% for the spheres treated by polydiallyl dimethyl ammonium chloride, and 0.07-0.11% for the spheres treated by magnafloc. The C<sub>10</sub> terminal selectivity was always below 2.8%.

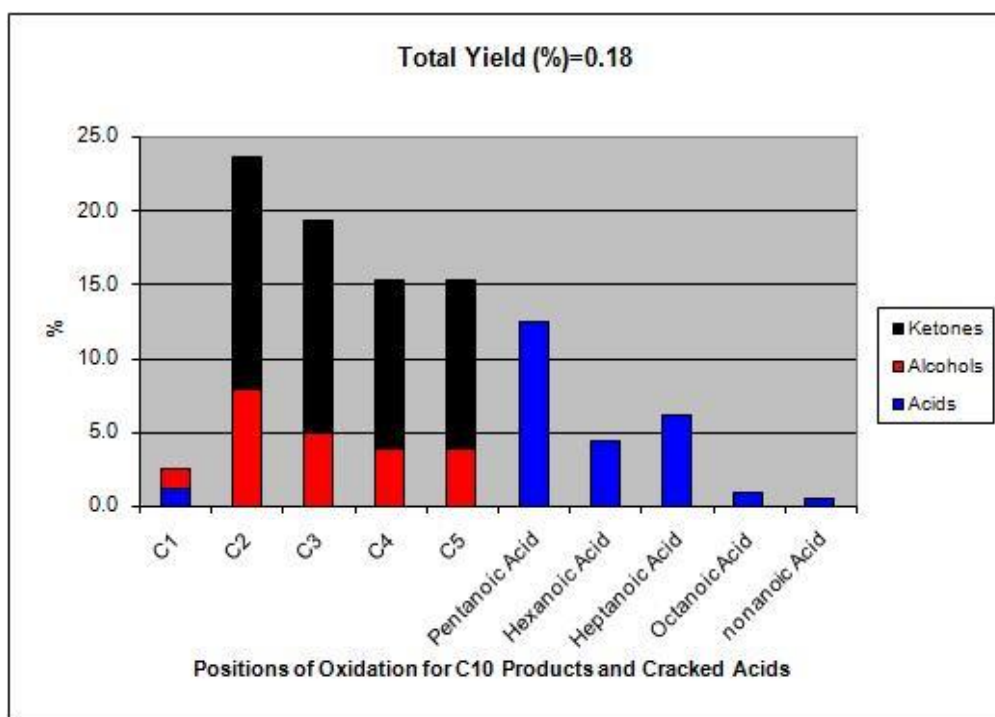


**Figure 6.24 100°C, 15 bar, 10 g *n*-decane, blank reaction, 16 h**

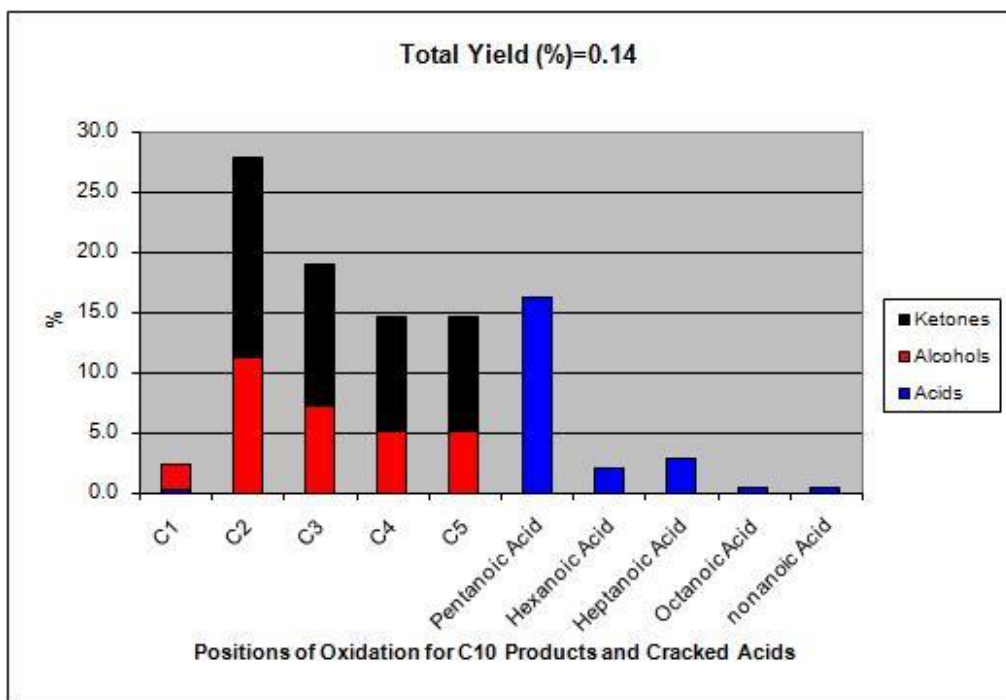


Figure 6.25 100°C, 15 bar, 10 g *n*-decane, 3 coated Al<sub>2</sub>O<sub>3</sub> spheres, 16 h

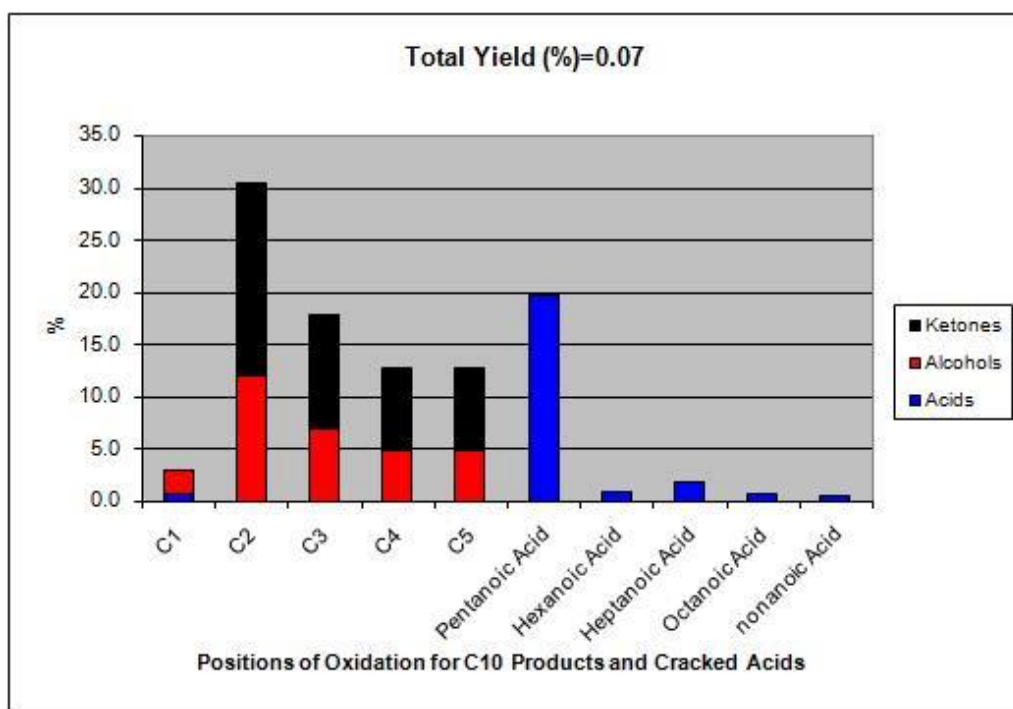


Figure 6.26 100°C, 15 bar, 10 g *n*-decane, 3 coated Al<sub>2</sub>O<sub>3</sub> spheres, 16 h

### 6.5.2.2 Discussion and conclusion

From the results, with the zeolite A coatings the conversion is almost the same as blank

reactions. However the coatings changed the product distribution (**Figure 6.24 to 6.26**), as compared to the blank reactions: there is a definite increase in the selectivity for decanols. Generally the selectivity for the shortened acids decreased, especially for the hexanoic acid and heptanoic acid, though the pentanoic acid increased. For the terminal position, there is not much change in total conversion, however the decanoic acid decreased. This means the zeolite A does not work for the primary position; instead, it seems it works in stopping the cracking in the position 3 and 4 and helping the decanol production in these positions. Probably the pore size of the zeolite A (around 4 Å) is a little bit small for the CH<sub>3</sub> groups (around 4.3 Å), while the smaller group CH<sub>2</sub> is more suitable in its pore size.

According to the above results, the zeolite 4A does not work for the terminal selectivity; other zeolites with larger pore sizes should be tried, such as mordenite and silicalite-1.

### **6.5.3 Silicalite-1 coating with sphere support**

In this section, silicalite-1 coating was applied to two different types of sphere supports, the  $\alpha$ -alumina sphere (diameter 5 mm) and the  $\gamma$ -alumina sphere (diameter 2 mm). It is well known the  $\alpha$ -Al<sub>2</sub>O<sub>3</sub> is a stable support for hydrothermal synthesis, while  $\gamma$ -Al<sub>2</sub>O<sub>3</sub> has less heat resistance. However,  $\gamma$ -Al<sub>2</sub>O<sub>3</sub> has a higher surface area (210 m<sup>2</sup>/g), it is therefore possible to load more active centres on it than on  $\alpha$ -Al<sub>2</sub>O<sub>3</sub> (0.82 m<sup>2</sup>/g), which is an attractive advantage.

#### **6.5.3.1 S1 coating with $\alpha$ -alumina spheres**

0.1 w.t.% Rh/alumina sphere and 0.1 w.t.% Au/alumina sphere were treated as the procedure described in the experimental section to synthesize silicalite-1 coated catalysts.

## Characterization

XRD analysis of the uncoated and coated samples was carried out to observe if the silicalite-1 layer was successfully synthesized. The results can be found in **Figure 6.27** and **Figure 6.28**.

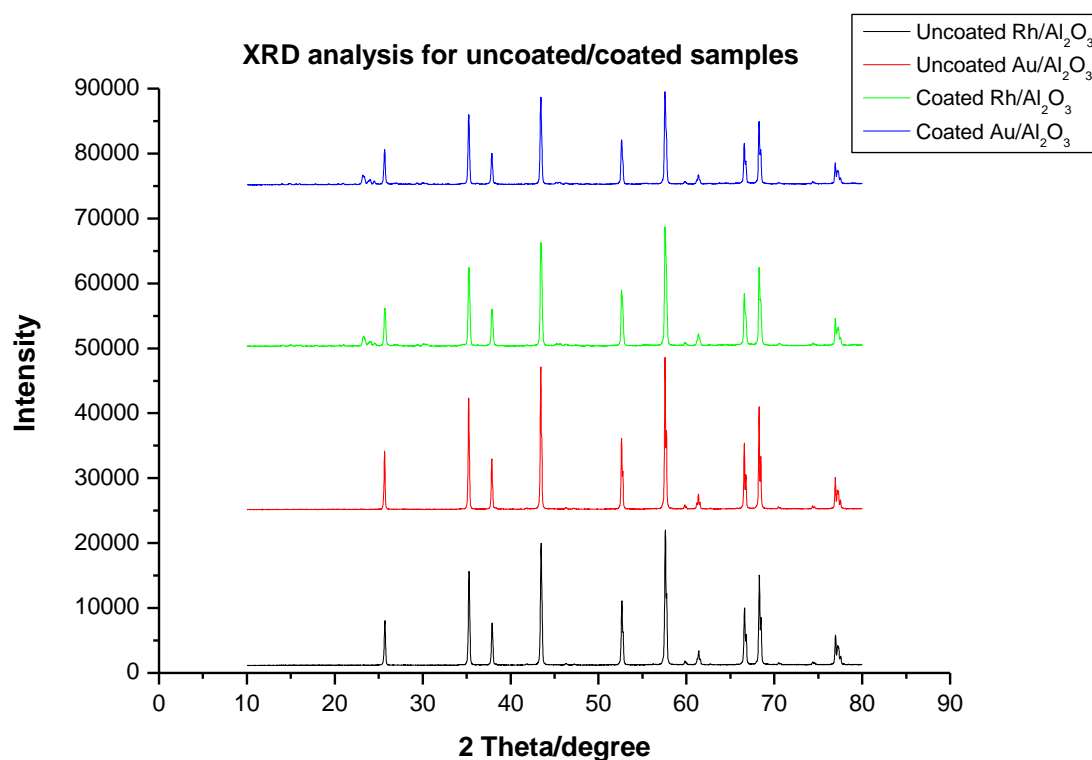


**Figure 6.27 XRD analysis for the uncoated and coated samples**

From **Figure 6.27** it is observed that the uncoated Rh and Au/Al<sub>2</sub>O<sub>3</sub> (black and red in the figure) show exactly the same peaks, which were identified as matched  $\alpha$ -Al<sub>2</sub>O<sub>3</sub>. No metal peaks were found, probably due to the very small metal particle size. In comparison with the uncoated samples, the two coated samples (green and blue in the figure) showed very similar peaks, expect a few small peaks around 23 °. These small peaks were searched and matched the MFI pattern; however it is not possible to distinguish between ZSM-5 and silicalite-1. A further investigation with a more accurate scan between the 5 ° and 40 ° in the XRD was carried out

and the results are shown in **Figure 6.28**. In **Figure 6.28**, the major peaks of MFI are marked with a cross. These peaks were found to match the MFI peaks very well. However, as the ZSM5 and silicalite-1 have very similar structures, we can still not identify if it is silicalite-1 through the XRD results; but an ordered structure was formed with the substrate catalysts.

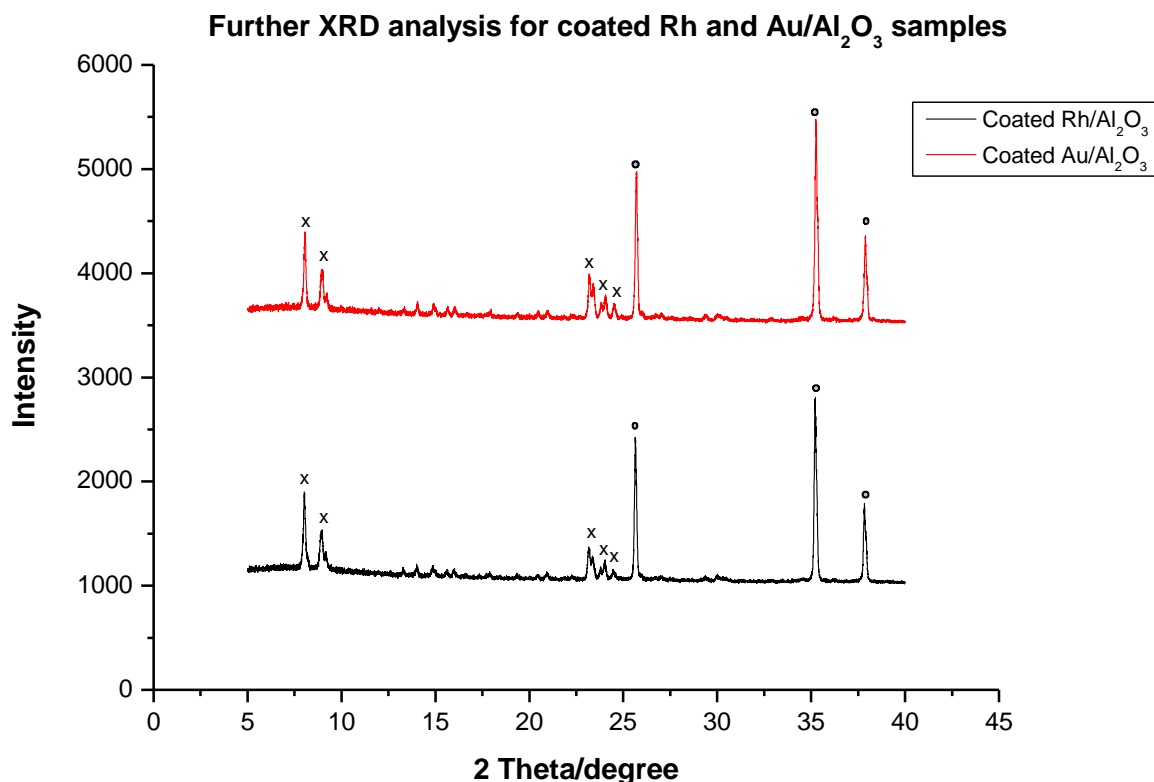


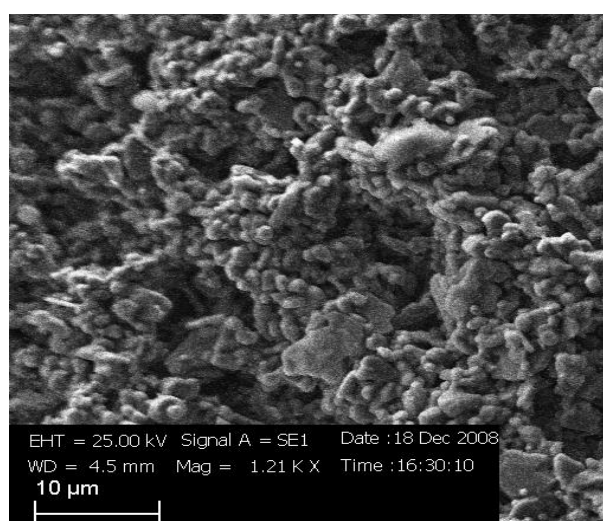
**Figure 6.28** Further XRD analysis for the coated samples

(x – MFI peaks; o -  $\alpha$ -Al<sub>2</sub>O<sub>3</sub> peaks)

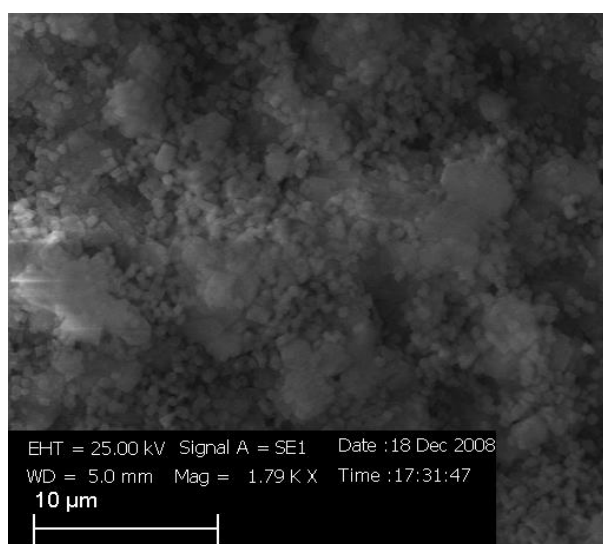
**Table 6.26** shows the surface area change before and after coating. **Figure 6.29** shows the morphology of the uncoated and coated spheres. At the same magnification, it was found that after being coated, the surface of catalyst spheres was covered by visible cubic particles, which are probably the accumulated silicalite-1 particles.

**Table 6.26 Surface area of the uncoated and coated catalysts**

Catalyst	Surface Area (m <sup>2</sup> /g)
0.1 w.t.% Rh/ $\alpha$ - Al <sub>2</sub> O <sub>3</sub> spheres	1
Coated 0.1 w.t.% Rh/ $\alpha$ - Al <sub>2</sub> O <sub>3</sub> spheres	43
0.1 w.t.% Au/ $\alpha$ - Al <sub>2</sub> O <sub>3</sub> spheres	1
Coated 0.1 w.t.% Au/ $\alpha$ - Al <sub>2</sub> O <sub>3</sub> spheres	48



(a) 0.1 w.t.% Au/ $\alpha$ -Al<sub>2</sub>O<sub>3</sub> sphere



(b) Coated 0.1 w.t.% Au/ $\alpha$ -Al<sub>2</sub>O<sub>3</sub> sphere

**Figure 6.29 Surface morphology of the uncoated and coated catalysts**

## Reaction

Although through the XRD results we cannot tell if the formed zeolitic material is ZSM5 or silicalite-1, it is highly possible it is silicalite-1, as in the precursor there is no Al source; the only Al in this system comes from the alumina support, which should be unable to dissolve in the zeolitic material synthesis procedure. Therefore in the following part we assume it is silicalite-1 coated catalysts formed and call it the ‘S1 coated’ samples.

The S1 coated samples were tested in the liquid phase reactions with *n*-decane at 110°C with 6h reactions. The corresponding results are given in the **Table 6.27**.

**Table 6.27 110°C, 15 bar, 10 g *n*-decane, 6 h, 600 rpm, 2 spheres**

Catalyst	Conv. (%)	Selectivity (%)												
		5/4 one	3 one	2 one	5/4 ol	3 ol	2 ol	1 ol	C <sub>5</sub> OOH	C <sub>6</sub> OOH	C <sub>7</sub> OOH	C <sub>8</sub> OOH	C <sub>9</sub> OOH	C <sub>10</sub> OOH
0.1% Rh/Al <sub>2</sub> O <sub>3</sub> spheres	<b>0.04</b>	23.8	15.1	22.3	6.5	4.8	8.2	<b>1.4</b>	14.3	1.7	1.6	0	0.2	<b>0.2</b>
Coated 0.1% Rh/Al <sub>2</sub> O <sub>3</sub> spheres	<b>0.12</b>	24.4	16.2	21.5	5.1	3.5	5.8	<b>1.3</b>	13.6	3.6	3.6	0.3	1.0	<b>0.2</b>
0.1% Au/Al <sub>2</sub> O <sub>3</sub> spheres	<b>0.12</b>	14.2	12.9	19.6	7.7	5.4	8.8	<b>1.8</b>	18.8	4.6	5.3	0.3	0.2	<b>0.4</b>
Coated 0.1% Au/Al <sub>2</sub> O <sub>3</sub> spheres	<b>0.16</b>	26.9	17.6	24.1	5.3	3.3	5.1	<b>1.1</b>	7.0	4.3	4.1	0.3	0.1	<b>0.9</b>

From the results in the **Table 6.27**, it is difficult to gain much understanding of the performance of the S1 coatings in the selective oxidation. Comparing the conversions in **Table 6.27**, it can be observed that both the samples with coatings obtained a higher conversion than those without coating. The two coated samples demonstrate a similar conversion, which might be

caused by the coatings themselves, instead of being caused from the active centres in the substrate catalysts. This may be due to the coated samples used in this trial having low activity (as described earlier); therefore the activity of the coatings cannot be covered. In comparison with the decanone and decanol products, it can be found that when without coatings, the selectivity for the decanone and decanols are very different for the Rh and Au catalysts; however after being coated, the selectivity for these two kinds of products became similar to each other. This is further evidence that the activities performed observed in these two reactions were caused by the coatings themselves. However on the two different catalysts, the coatings, which were analysed as the same type of coating in the XRD analysis, showed different acid selectivity, especially for pentanoic acid and decanoic acid.

### 6.5.3.2 S1 coating with $\gamma$ -alumina spheres

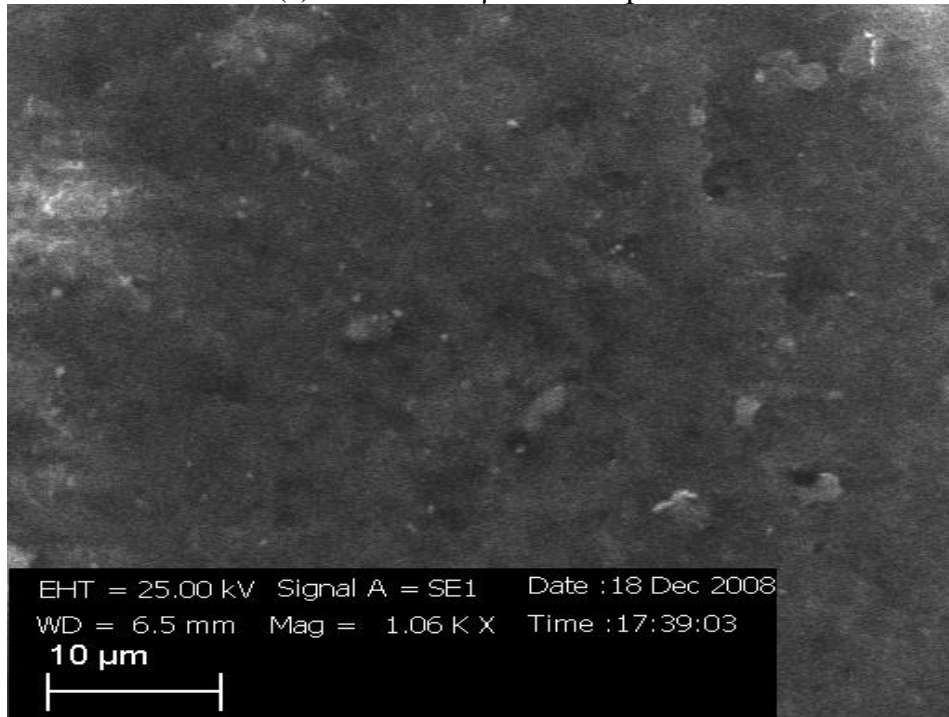
It is well known the  $\alpha$ - $\text{Al}_2\text{O}_3$  is a stable support for hydrothermal synthesis, while  $\gamma$ - $\text{Al}_2\text{O}_3$  has less heat resistance. However,  $\gamma$ - $\text{Al}_2\text{O}_3$  has a higher surface area ( $210 \text{ m}^2/\text{g}$ ); it is therefore possible to load more active centres on it than on  $\alpha$ - $\text{Al}_2\text{O}_3$  ( $0.82 \text{ m}^2/\text{g}$ ), which is an attractive advantage. In this section, the same coating synthesis procedure was again applied to the 3 w.t.% Au loaded smaller size  $\gamma$ -alumina spheres (diameter 2 mm) which have a surface area of  $210 \text{ m}^2/\text{g}$ . **Table 6.28** shows the surface area change before and after coating, while **Figure 6.30** shows the surface morphology of the uncoated and coated spheres. Similar to the coating with the  $\alpha$ - $\text{Al}_2\text{O}_3$  sphere, it was found that after being coated, the surface of catalyst spheres was covered by cubic particles, which should be the accumulated silicalite-1 particles. Further characterization by SEM and EDX has been performed to check if the coating layers are continuous and to determine their thickness (**Figure 6.31** to **Figure 6.33**).

SEM and EDX mappings analyses were performed for the coated samples, which indicated the thickness of the silicalite-1 layer of approximately 6-8  $\mu\text{m}$  (**Figure 6.31**). In the mapping images the silicon appears to be continuously distributed as a circle around the cross section of the sphere (**Figure 6.33**).

**Table 6.28 Surface area of the catalysts with and without coating**

Catalyst	Surface Area ( $\text{m}^2/\text{g}$ )
$\gamma\text{-Al}_2\text{O}_3$ spheres	<b>210</b>
3% Au/ $\gamma\text{-Al}_2\text{O}_3$ spheres	<b>184</b>
Coated 3% Au/ $\gamma\text{-Al}_2\text{O}_3$ spheres	<b>124</b>

(a) 3 w.t.% Au/ $\gamma$ -alumina sphere



(b) Coated 3 w.t.% Au/ $\gamma$ -alumina sphere

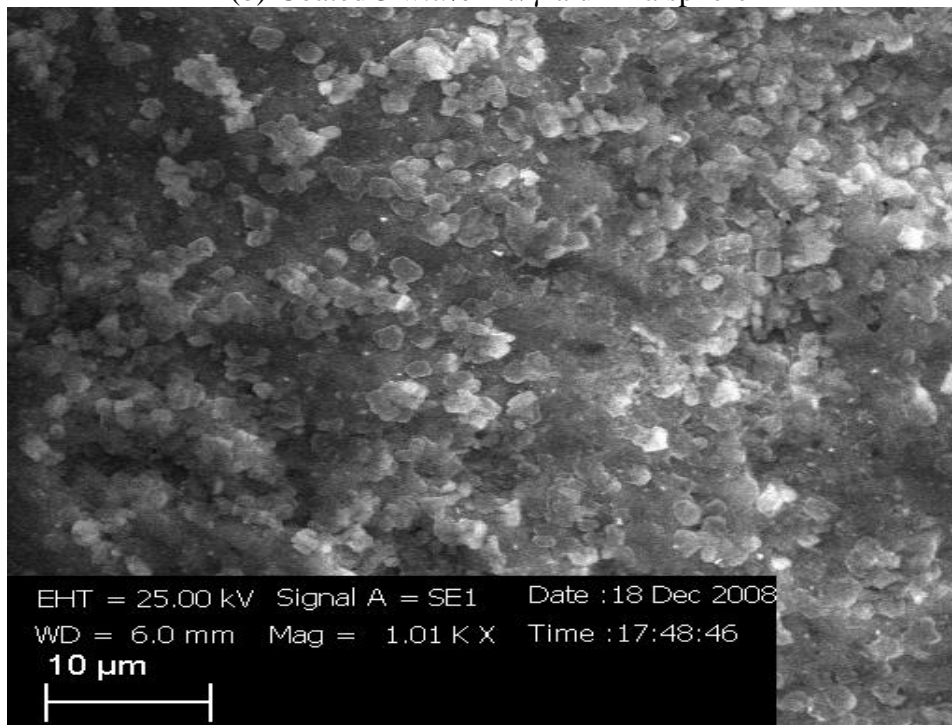
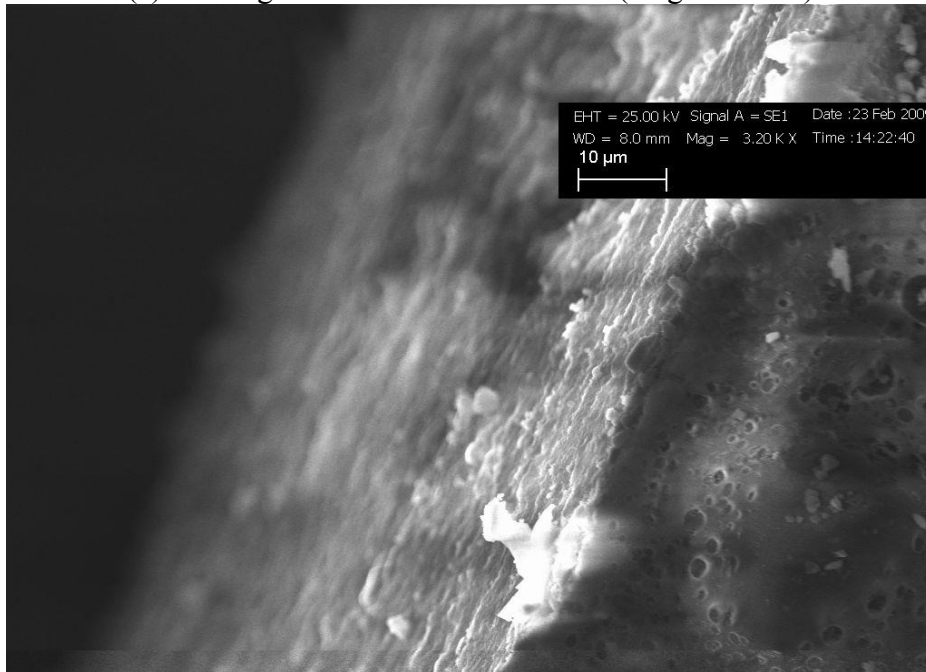


**Figure 6.30** Surface morphology of the uncoated and coated catalysts

(a) The edge of 1 mm 0.1% Au/Al<sub>2</sub>O<sub>3</sub> (mag= 3.2 KX)



(b) The edge of coated samples in higher magnification (mag =11.47 KX)

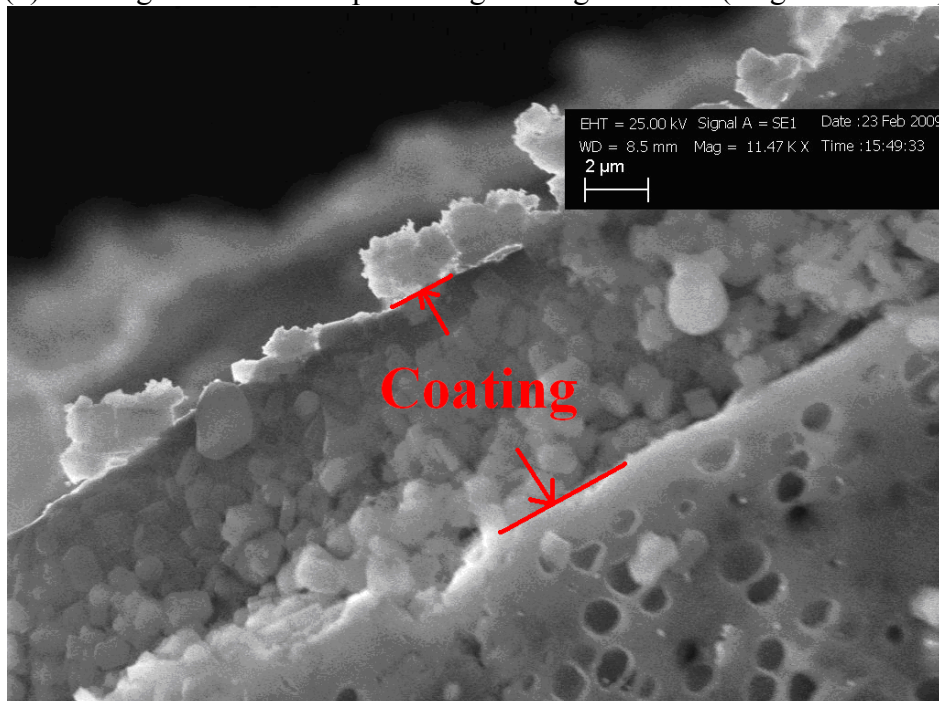
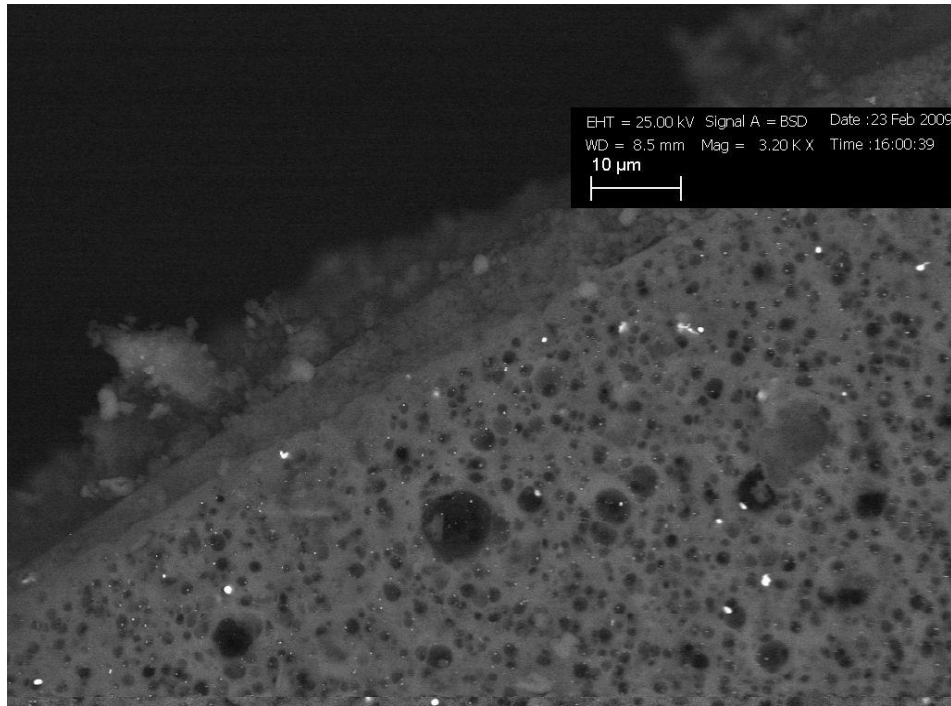
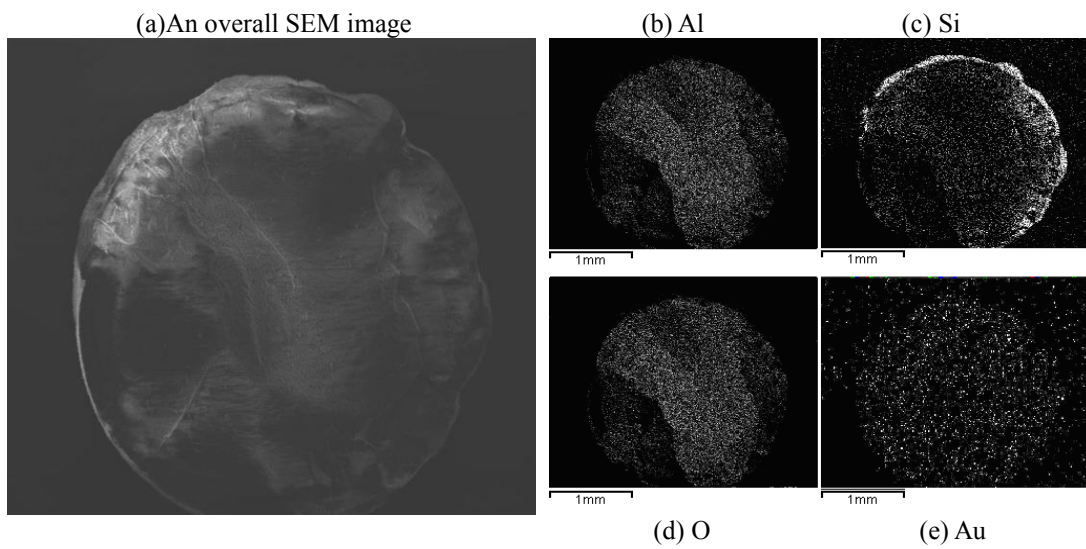


Figure 6.31 SEM images of the cross section of the S1 uncoated and coated 3 w.t.% Au/γ-Al<sub>2</sub>O<sub>3</sub> spheres



**Figure 6.32** The edge of the coated samples in BSD detector  
**EDX analysis: Au w.t.% = 2.2**



**Figure 6.33** EDX Mapping: the cross section of the S-1 uncoated and coated 3 wt.% Au/ $\gamma$ -Al<sub>2</sub>O<sub>3</sub> spheres

## Reaction

3 w.t.% Au/ $\gamma$ -Al<sub>2</sub>O<sub>3</sub> catalysts before and after coating were used in the reactions for a 6 h run as shown in **Table 6.29**.

**Table 6.29** 110°C, 15 bar, 10 g *n*-decane, 6 h, 600 rpm, 0.05 g catalysts (with  $\gamma$ -Al<sub>2</sub>O<sub>3</sub> sphere)

Catalyst	Conv. (%)	Selectivity (%)												
		5/4 one	3 one	2 one	5/4 ol	3 ol	2 ol	1 ol	C <sub>5</sub> OOH	C <sub>6</sub> OOH	C <sub>7</sub> OOH	C <sub>8</sub> OOH	C <sub>9</sub> OOH	C <sub>10</sub> OOH
3% Au/Al <sub>2</sub> O <sub>3</sub> spheres	<b>0.26</b>	23.5	14.8	18.8	5.4	3.8	6.0	<b>1.5</b>	15.8	4.9	4.4	0.4	0.1	<b>0.7</b>
Coated 3% Au/Al <sub>2</sub> O <sub>3</sub> spheres	<b>0.14</b>	16.8	11.5	17.4	9.8	7.1	11.3	<b>1.9</b>	9.3	4.7	7.8	0.6	0.4	<b>1.1</b>

### 6.5.3.3 Discussion and conclusion

The product distribution with the coated 3 w.t.% Au  $\gamma$ -alumina spheres (**Table 6.29**) is different from the results with the relatively bigger  $\alpha$ -alumina spheres (**Table 6.27**), which probably means the performance of this coated catalyst is not only the performance of the coating but also that of the underneath catalyst. This time the coating lowers the activity of the catalyst, with a small increase the terminal selectivity (though further experiments are needed to see if this is within experimental error): in comparison with the uncoated catalyst, the selectivity for ketones goes down and for the decanols and acids all go up, except the pentanoic acid, again. However, for the C10 terminal position, the increase is minimal.

Summarizing the section, it can be concluded a 6-8  $\mu$ m thick continuous silicalite-1 coating layer was successfully synthesized on the 3 w.t.%Au/ $\gamma$ -Al<sub>2</sub>O<sub>3</sub>. However, the sample was not found to work well as a teabag catalyst for the liquid phase oxidation of decane (**Table 6.29**),

which may be due to the activity of the silicalite-1 in the liquid phase. Therefore, other zeolite materials, which are not active themselves in the liquid phase would be useful as coatings in this study. As reported in Iglesia's work and our previous research, the H<sup>+</sup> form of the zeolite is not active for the liquid phase reaction; therefore, zeolite A and ZSM-5 can be considered possible options in the project. Given the pore size requirement for the decane molecules, it is suggested that ZSM-5 should be the better option. However the silicalite-1 coatings could still be useful materials to test in the gas phase where silicalite-1 is not active.

#### 6.5.4 ZSM-5 coating with alumina sphere support

The synthesis of ZSM-5 coatings was carried out only with the alumina supports, without any metal loadings. Experiments have been performed with both  $\alpha$ - and  $\gamma$ -Al<sub>2</sub>O<sub>3</sub>. To develop the optimized amount of the zeolite precursor solution for the hydrothermal synthesis, different volumes of solution with exactly the same molar composition have been used (32 ml and 15 ml). The results are shown below in sections for  $\alpha$ - and  $\gamma$ -Al<sub>2</sub>O<sub>3</sub> respectively.

##### 6.5.4.1 ZSM-5 coating with $\alpha$ -Al<sub>2</sub>O<sub>3</sub> spheres

###### With 32 ml zeolite precursor solution

Coverage of the coating was calculated by the weight of the coating per surface area of the support (0.82 m<sup>2</sup>/g), which was 0.0694 g/m<sup>2</sup> for this 32 ml zeolite precursor solution synthesis as shown in **Table 6.30** below. However, this is only a rough estimate as the weight change might be slightly affected by deposition of non-crystalline material.

**Table 6.30 Coverage of the coating on the  $\alpha$ -Al<sub>2</sub>O<sub>3</sub> support (32 ml solution)**

Support	Weight before coated (g)	Weight after coated (g)	Coverage (g/m <sup>2</sup> )
$\alpha$ -Al <sub>2</sub> O <sub>3</sub>	1.0491	1.1060	0.0694

With the normal scan by the XRD (**Figure 6.34**), it was found that the intensity of the coated sample is much less than uncoated one; this may be due to the coating or some crystallinity may be lost during the synthesis. Small ZSM-5 peaks are found in the diffractogram of the coated  $\alpha$ - $\text{Al}_2\text{O}_3$ .

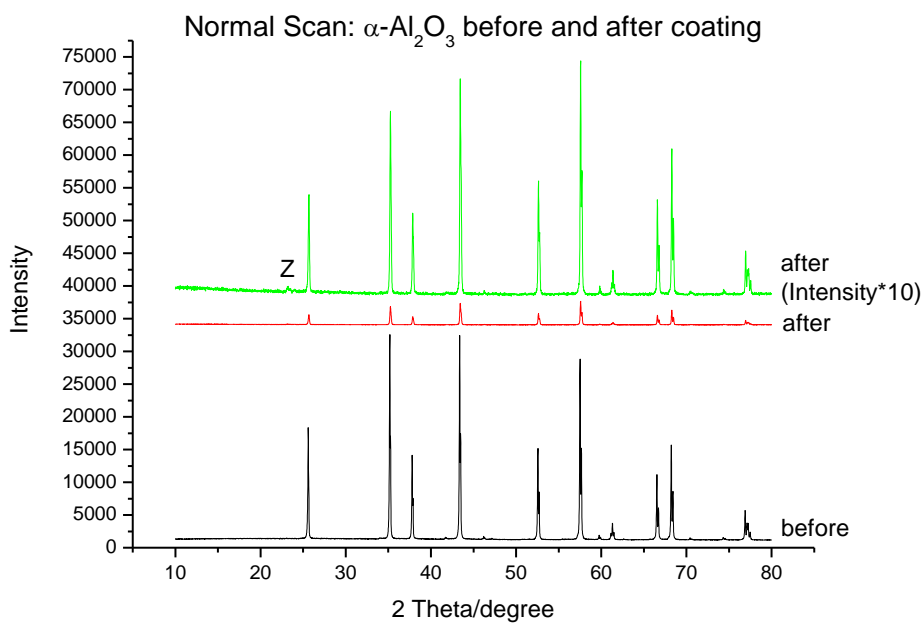


**Figure 6.34 Normal Scan:  $\alpha$ - $\text{Al}_2\text{O}_3$  before and after coating**  
z = likely ZSM-5 peaks

A low angle XRD scan for the coated samples showed more intense ZSM-5 peaks (**Figure 6.35**):

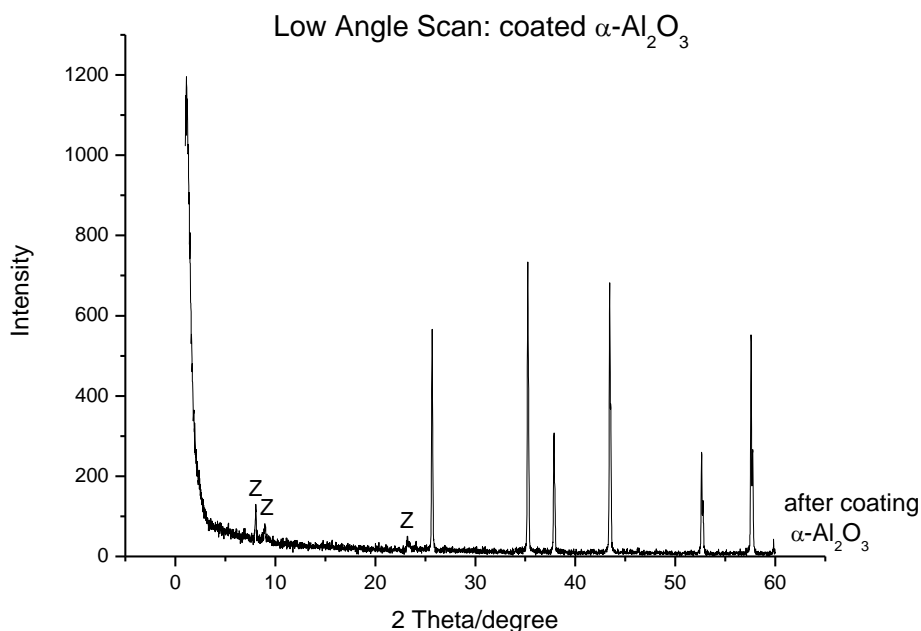


**Figure 6.35** Low angle scan: coated  $\alpha\text{-Al}_2\text{O}_3$

The coated  $\alpha\text{-Al}_2\text{O}_3$  under the SEM showed that the morphology of the surface was not homogeneous. Some of the surface was covered with faceted micron-sized agglomerates, while other parts of the surface were covered by the deposition of nano-sized particles (**Figure 6.36** and **Figure 6.37**).

EDX element mappings of the complete coated sphere and cross-sections of the coated sphere were performed. In **Figure 6.38**, as an example, 6.38(a) is the original whole coated  $\alpha\text{-Al}_2\text{O}_3$  sphere; 6.38(b), (c) and (d) are the distribution of Al, Si and O respectively in the blue, green and white colour. 6.38(e) is the mixture image of 6.38(b), (c) and (d). The mapping images of the cross sections, especially in **Figure 6.39**(c), showed the elements to be distributed as we

expected for a layer, with a silicon circle around the edge of the sphere. However, from the mixture image (**Figure 38(e)**) the elements do not appear to be distributed uniformly.

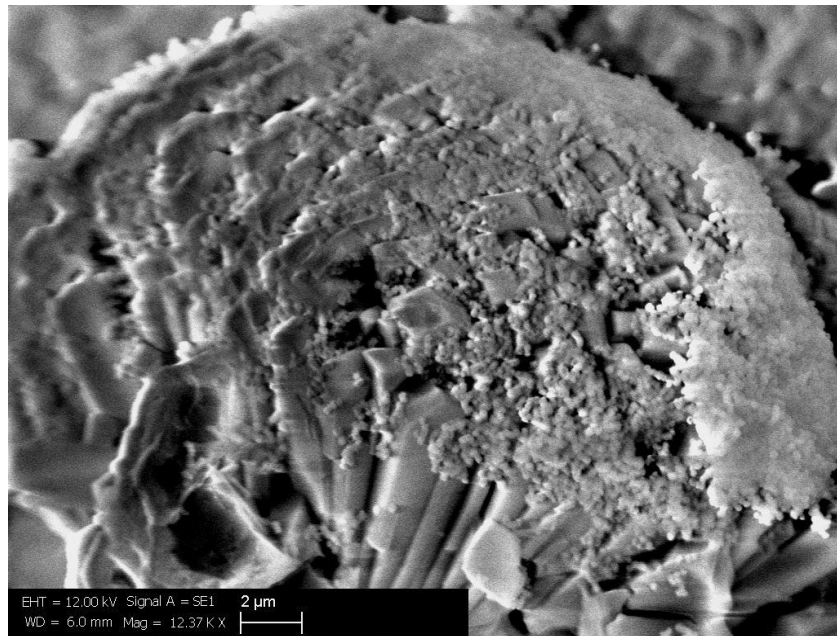


**Figure 6.36 Faceted micron-sized and nano-sized particles on the surface**

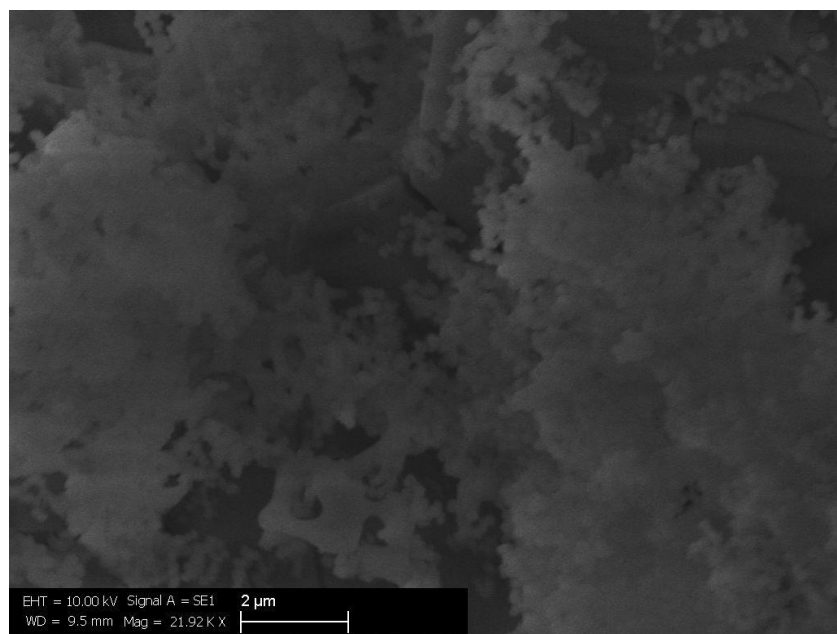


**Figure 6.37 Nano-sized particles**

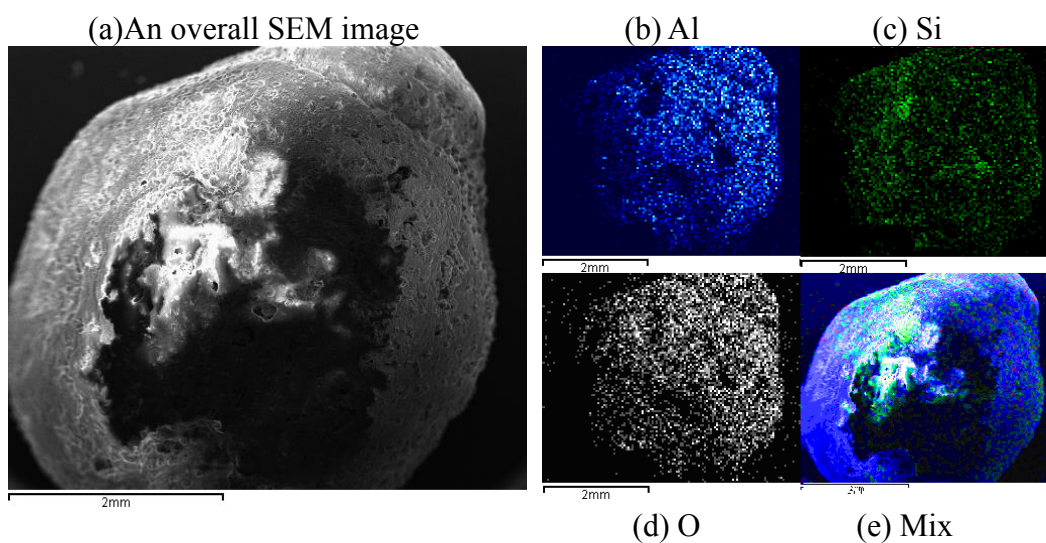


**Figure 6.38 Mapping for a whole coated  $\alpha$ - $\text{Al}_2\text{O}_3$  sphere**

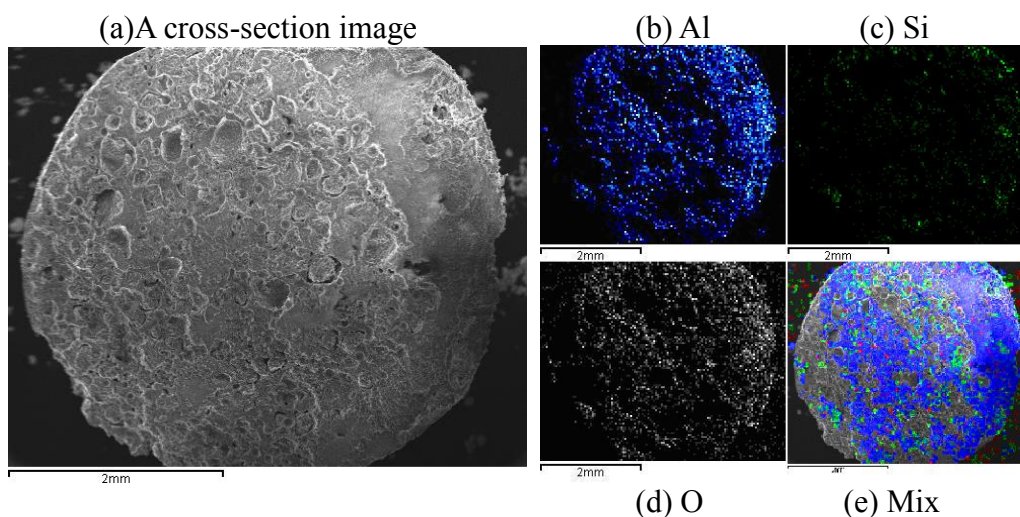


**Figure 6.39 Mapping for the cross-section of a coated  $\alpha$ - $\text{Al}_2\text{O}_3$  sphere**

With 15 ml zeolite precursor solution

The hydrothermal synthesis procedure was exactly the same as for the samples shown above, but with less zeolite precursor solution: 15 ml. The coverage of the coating with 15 ml zeolite precursor solution was calculated again as before. It was found that the coverage was 0.0693

g/m<sup>2</sup> (Table 6.31). Compared to the amount for the 32 ml solution synthesis (0.0694 g/m<sup>2</sup>), the coverage level was exactly the same. This showed that the ability of spheres to load coatings is limited; and in both the two syntheses the maximum loading was reached.

**Table 6.31 Coverage of the coating on the  $\alpha$ -Al<sub>2</sub>O<sub>3</sub> support (15ml solution)**

Support	Weight before coated (g)	Weight after coated (g)	Coverage (g/m <sup>2</sup> )
$\alpha$ -Al <sub>2</sub> O <sub>3</sub>	1.0486	1.1054	0.0693

With a low angle scan of the coated samples by XRD, the main peaks of ZSM-5 are still visible (Figure 6.40), which is similar to the 32 ml solution.

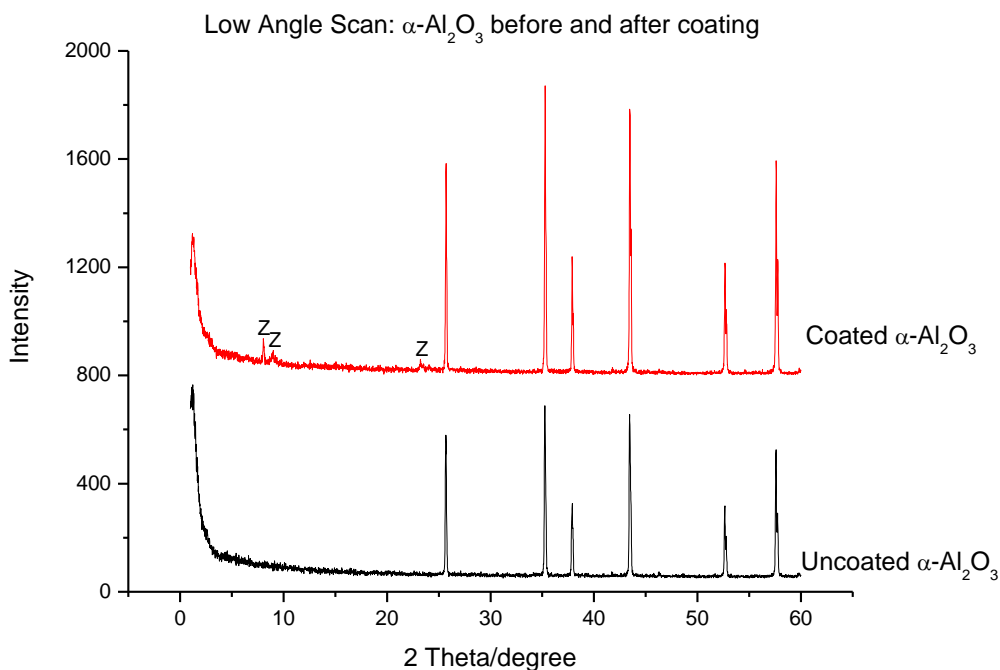


**Figure 6.40 Low angle scan:  $\alpha$ -Al<sub>2</sub>O<sub>3</sub> before and after coating**

In Figure 6.41 and Figure 6.42(a), there are clearly three different morphologies: fluffy nano-

sized particles; large faceted micron-sized particles and smaller micro-sized particles, the larger faceted micron-sized particles were also found in the results of the 32 ml solution synthesis. It appears as though the supports were fully covered. However, the thickness of the layer is difficult to identify, as in **Figure 6.42(b)**.

The EDX element mapping showed a homogeneous silicon distribution over the support sphere (**Figure 6.43 (c)**). However, the mixture image did not show the element distribution to be uniform (as for the 32 ml solution); this may be due to the different particles having differing compositions.

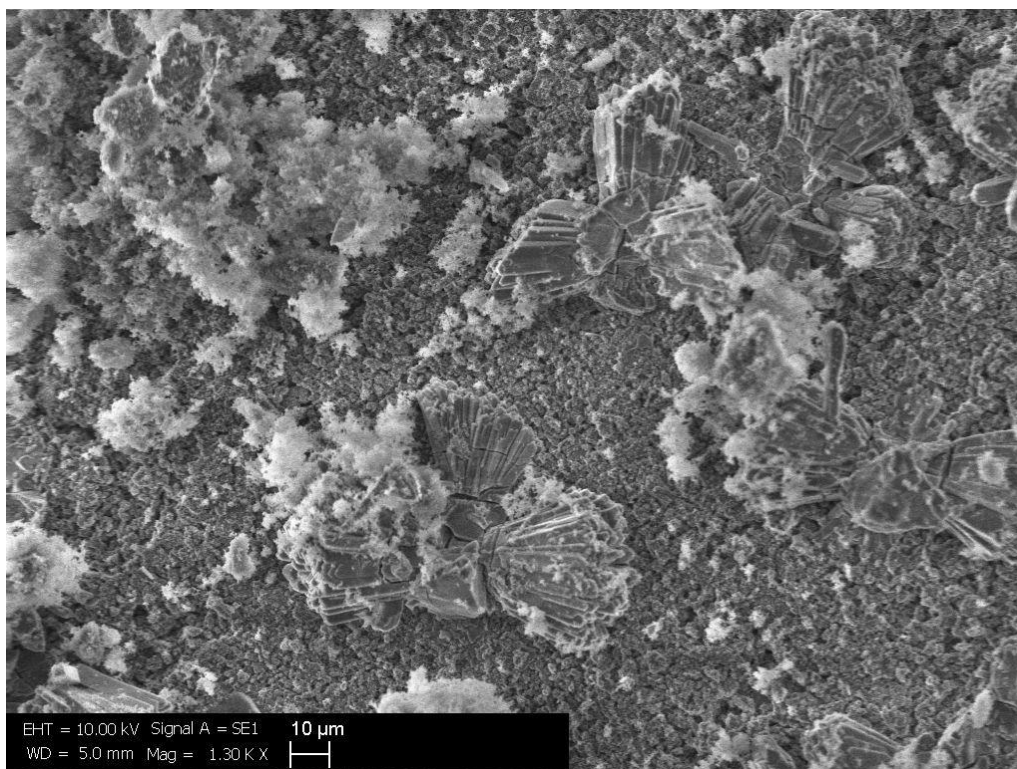
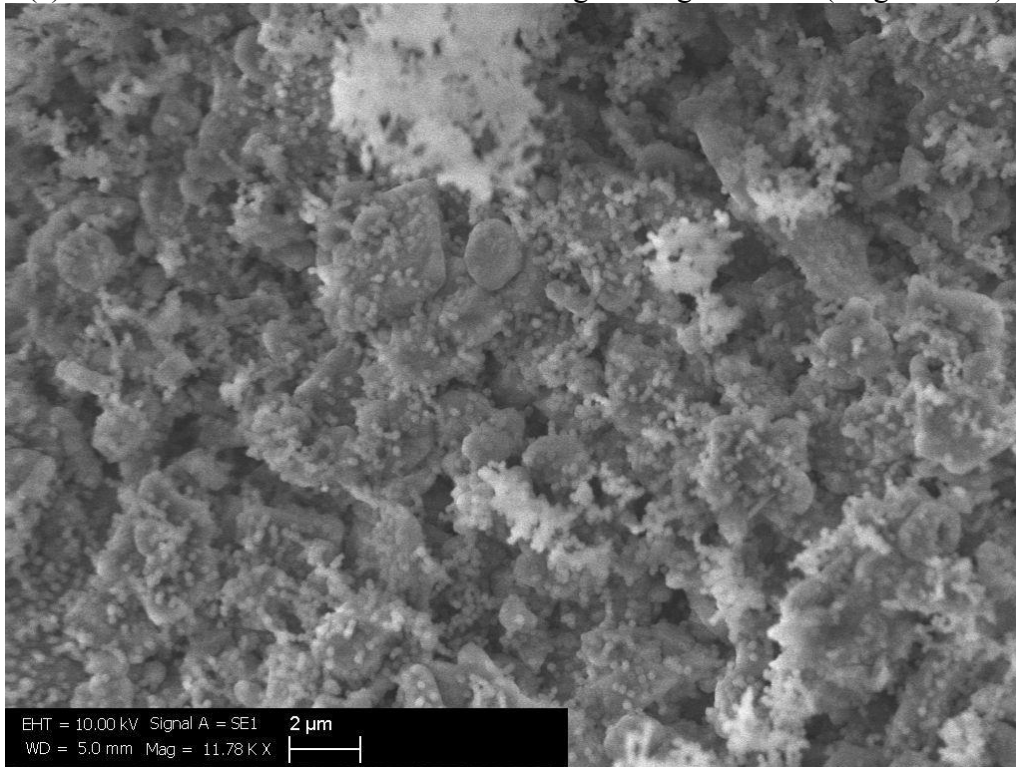


**Figure 6.41** Surface of the  $\alpha$ -Al<sub>2</sub>O<sub>3</sub> (mag = 1.30KX)

(a) Surface of the coated  $\alpha$ -Al<sub>2</sub>O<sub>3</sub> with a higher magnification (mag = 11.78)



(b) Cross-section of the coated  $\alpha$ -Al<sub>2</sub>O<sub>3</sub> (mag = 1.6KX)

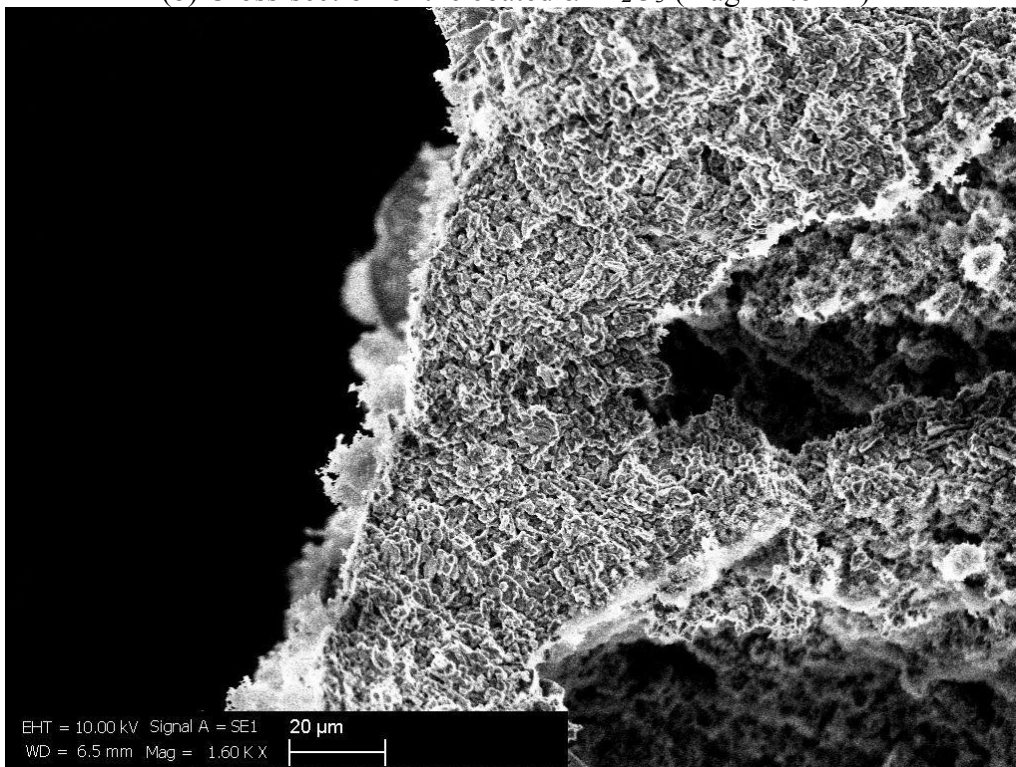


**Figure 6.42** Morphology of the coated  $\alpha$ -Al<sub>2</sub>O<sub>3</sub> (mag = 1.30KX)

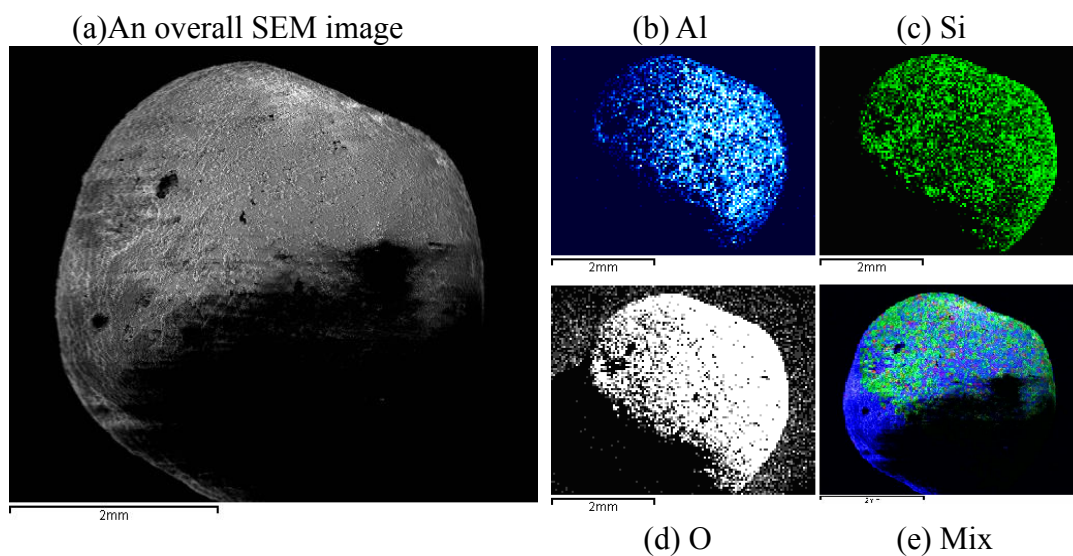


**Figure 6.43 Mapping of a whole coated  $\alpha$ -Al<sub>2</sub>O<sub>3</sub> sphere**

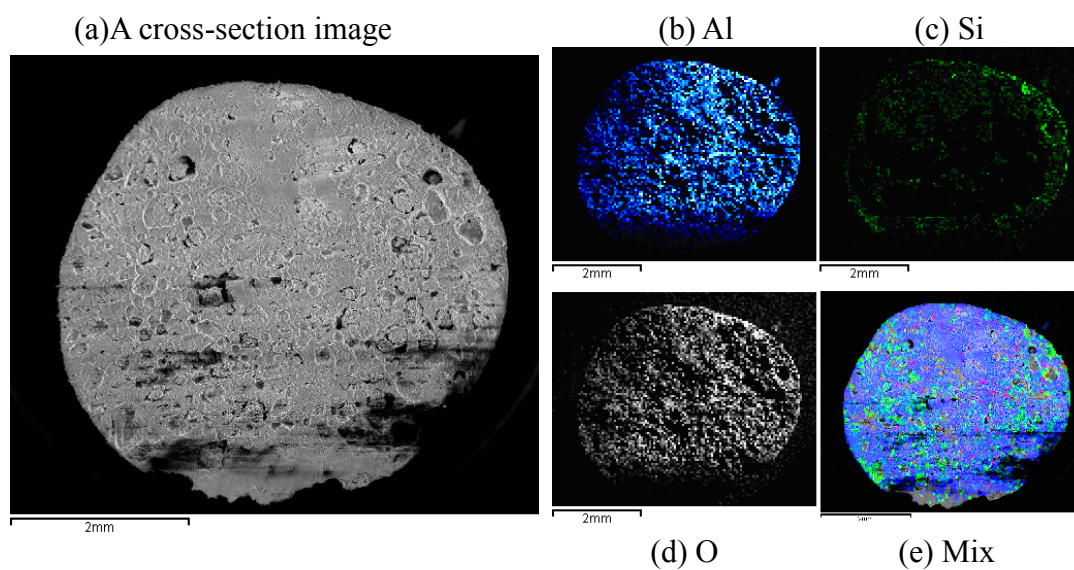


**Figure 6.44 Mapping of the cross-section of a coated  $\alpha$ -Al<sub>2</sub>O<sub>3</sub> sphere**

According to the above characterization, the ZSM-5 coating was successfully achieved on the  $\alpha$ -Al<sub>2</sub>O<sub>3</sub> spheres, although there were a few irregularly shaped micron sized particles. The next stage is to try to synthesize small crystals and a thinner layer ZSM-5.

#### 6.5.4.2 ZSM-5 coating with $\gamma$ -Al<sub>2</sub>O<sub>3</sub> spheres

##### With 32 ml zeolite precursor solution

The coverage level of the coating was unable to be calculated as some of the support spheres were found to be crushed after the hydrothermal synthesis. This may be because the  $\gamma$ -Al<sub>2</sub>O<sub>3</sub> heat resistance was reduced under the atmospheric conditions inside the autoclave. However in the previous synthesis of silicalite-1 layer (180°C), it was found that the 3% Au/ $\gamma$ -Al<sub>2</sub>O<sub>3</sub> was much more stable as compared the blank  $\gamma$ -Al<sub>2</sub>O<sub>3</sub> spheres used in the ZSM-5 synthesis (160°C). In the XRD low angle scan, no ZSM-5 peaks were found (**Figure 6.45**). This may be due to the coating not forming; or a thin coating layer which cannot be detected by XRD.

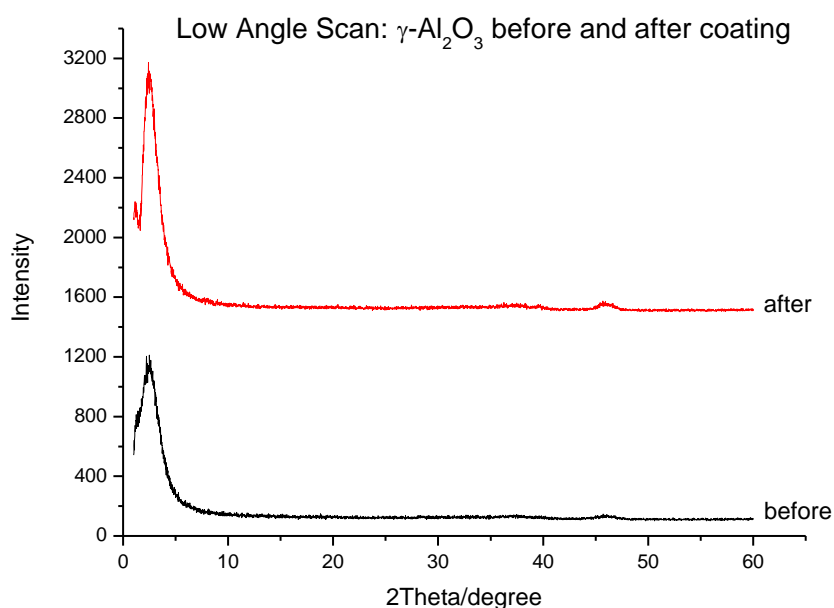


**Figure 2 Low angle scan:  $\gamma$ -Al<sub>2</sub>O<sub>3</sub> before and after coating**

From the same autoclave, the extra ZSM-5 powder was calcined separately with good heating rate control and identified as ZSM-5 (**Figure 6.46**):

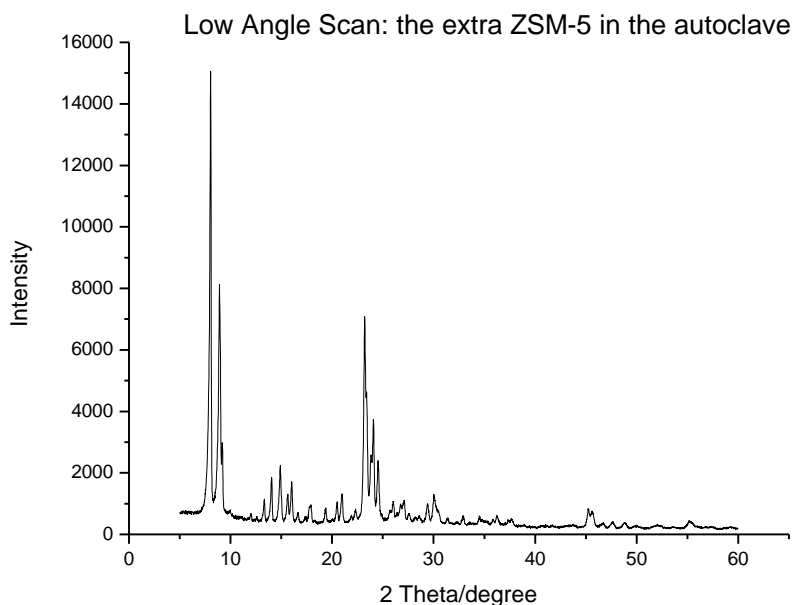


**Figure 6.46 Low angle scan: the extra ZSM-5 powders in the same batch with  $\gamma$ -Al<sub>2</sub>O<sub>3</sub>**

The SEM images further confirmed there are no visible layers on the  $\gamma$ -Al<sub>2</sub>O<sub>3</sub> surface. It is possible that a very thin layer or particles was synthesized, that is below the detection limits of the SEM; therefore catalytic results are required to see if there is any change in product distribution as compared with the un-treated  $\gamma$ -Al<sub>2</sub>O<sub>3</sub>. In **Figure 6.47(b)**, residues of carbon from the template are detected. In the mapping images it looks as though the silicon distribution is not a circle (**Figure 6.48**); however this could be an artefact due to the cutting of the spheres in the sample preparation for the SEM scan.

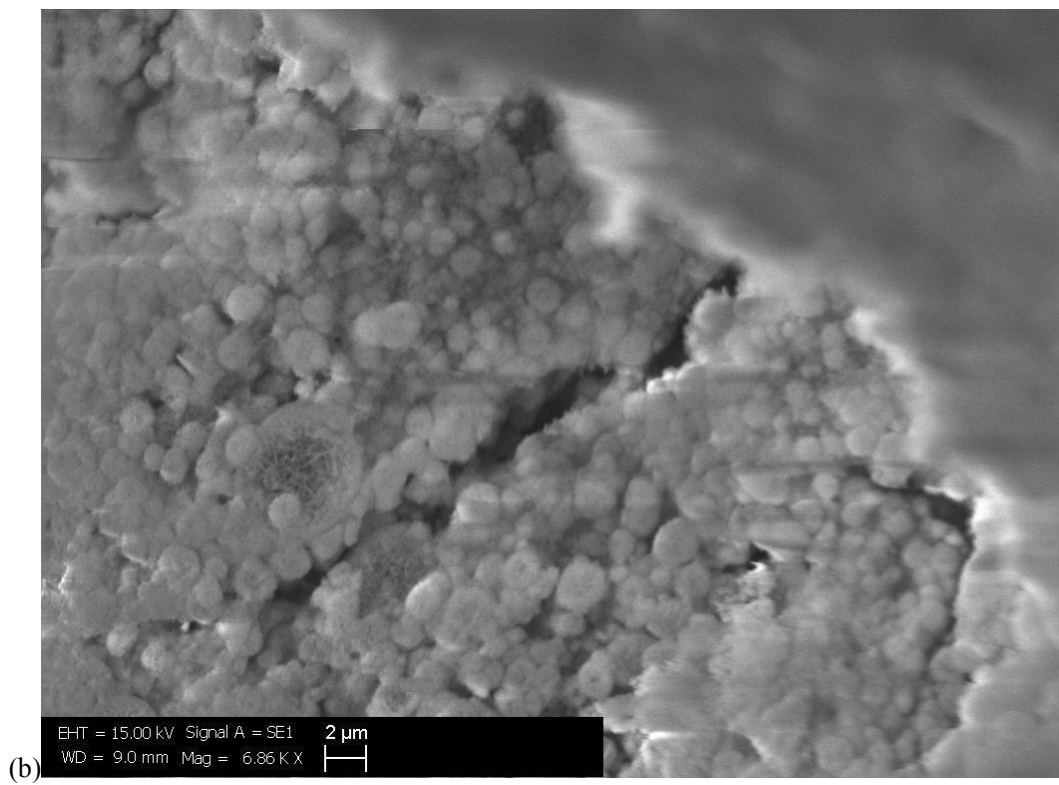
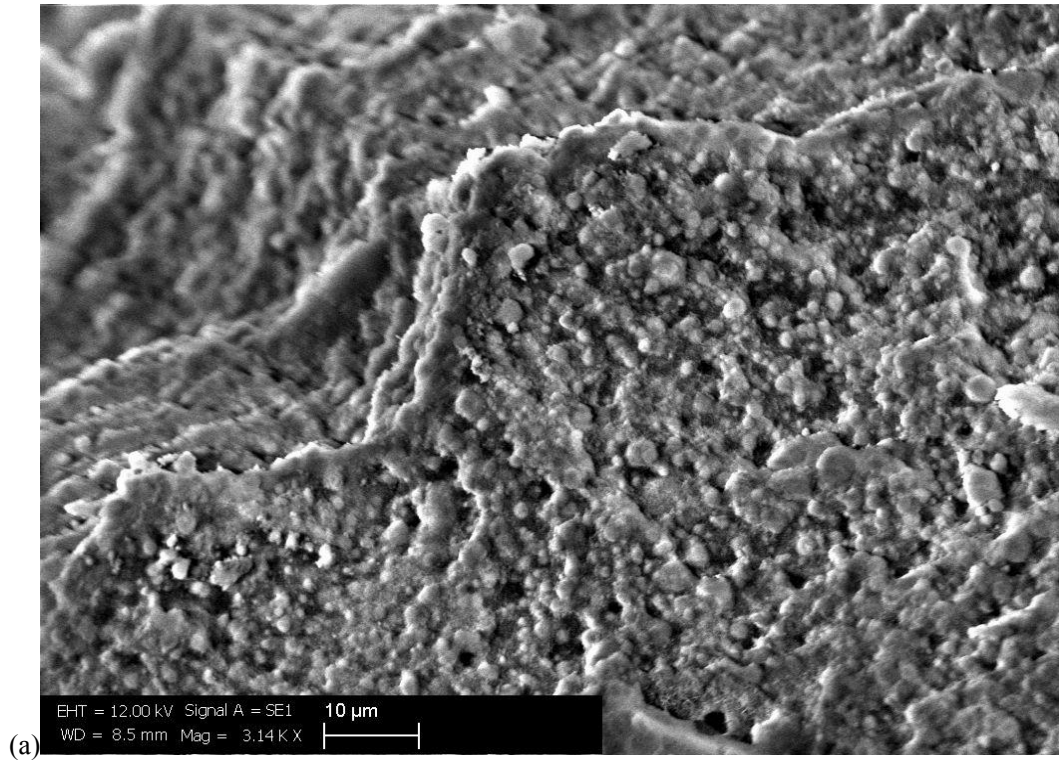


**Figure 6.47 SEM images of the surface of coated  $\gamma$ -Al<sub>2</sub>O<sub>3</sub>**

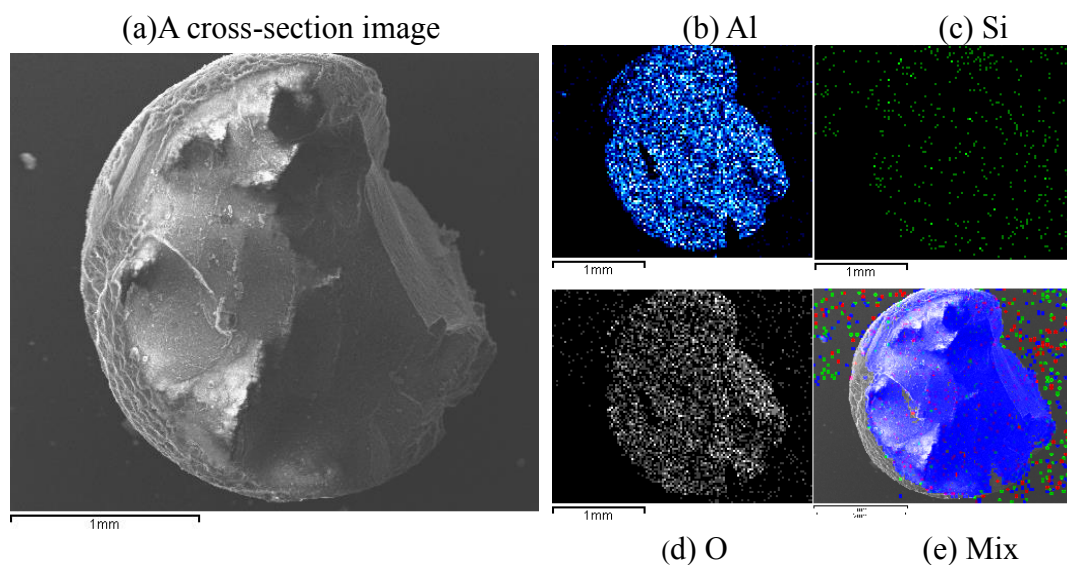


**Figure 6.48** Cross-section of a coated  $\gamma\text{-Al}_2\text{O}_3$  sphere

With 15 ml zeolite precursor solution

The hydrothermal synthesis procedure was performed as for the samples shown above, but with a less zeolite precursor solution: 15 ml.

The coverage level of the coating was again unable to be calculated. Low angle XRD revealed the coated sample to be different from the 32 ml solution. Several peaks in the measured diffractogram (**Figure 6.49**) are similar to the main peaks of ZSM-5 (marked with ‘o’); however the main peaks (marked with ‘x’) in this are more likely to be from silicon dioxide. However, the extra powder from the  $\alpha$ - and  $\gamma$ - batches is similar and both are identified as ZSM-5 after calcination (**Figure 6.50**). Combining all the XRD analyses, it is reasonable to conclude that  $\gamma\text{-Al}_2\text{O}_3$  itself has an influence on the synthesis of coatings at its surface.

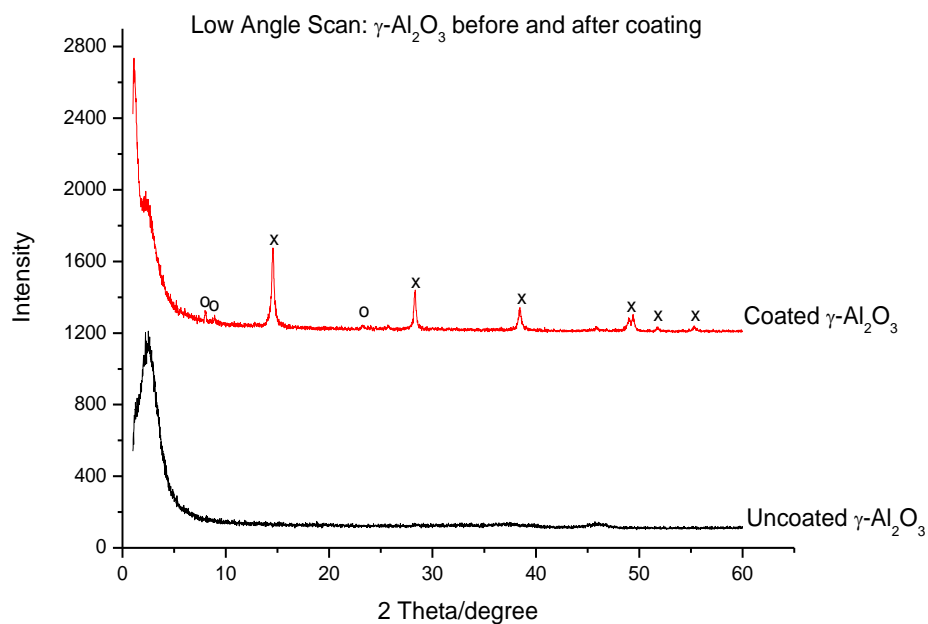


**Figure 6.49** Low angle scan: uncoated and coated  $\gamma$ - $\text{Al}_2\text{O}_3$  surface  
o – likely to be ZSM-5; x – might be silicon dioxide peaks

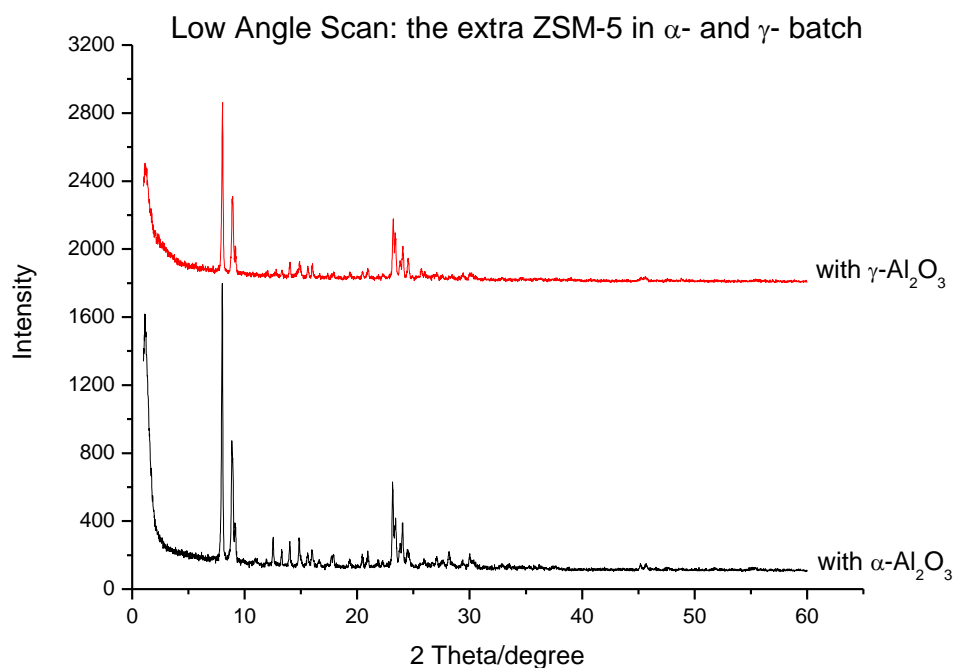


**Figure 6.50** Low angle scan: the extra powders with  $\alpha$ - and  $\gamma$ - batch

In the SEM images below (**Figure 6.51**), it is observed the coverage on the surface does not look like the regular ZSM-5 particles. The thick fluffy coating is probably silicon dioxide as

indicated from the more intense XRD peaks. Silicon dioxide might not have the same desired shape selectivity or radical scavenger properties as a zeolite.

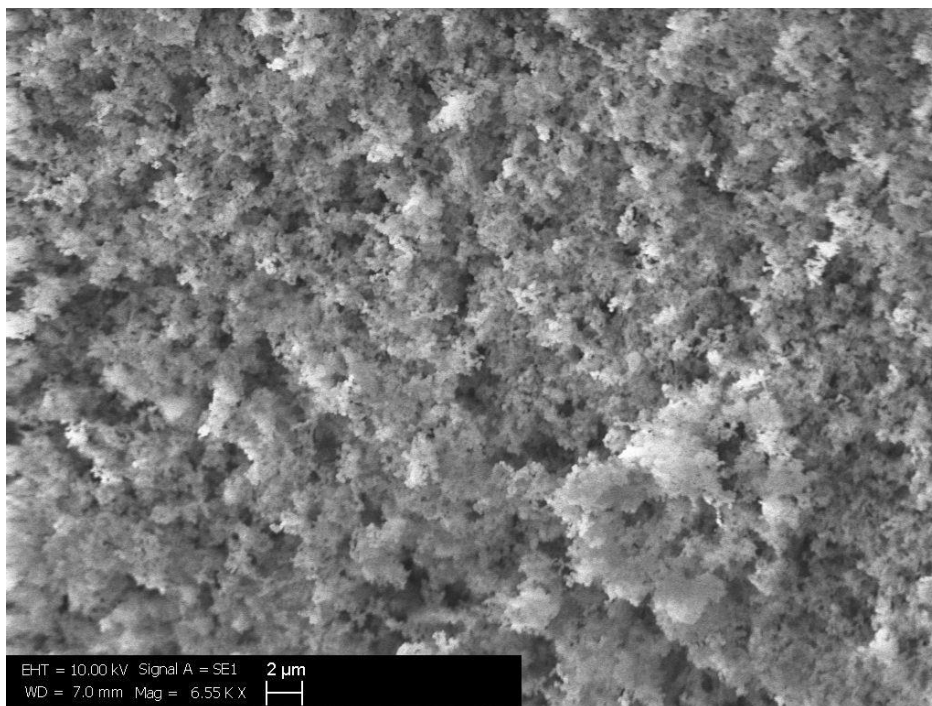


**Figure 6.51** Surface of the coated  $\gamma$ - $\text{Al}_2\text{O}_3$

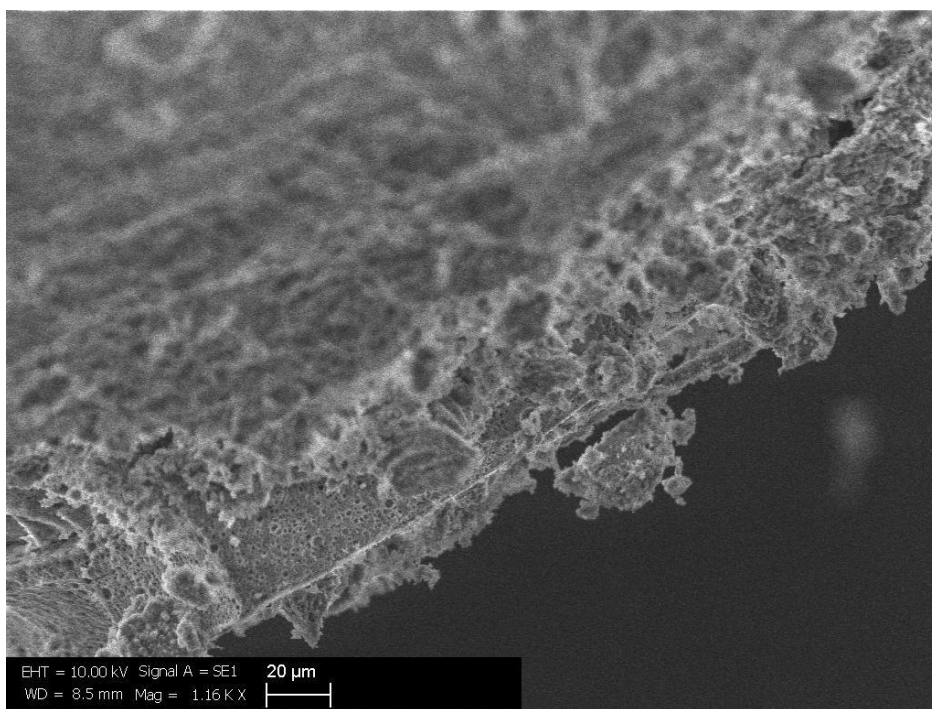


**Figure 6.52** the cross-section of the coated  $\gamma$ - $\text{Al}_2\text{O}_3$

The element mapping (Figure 6.53 and Figure 6.54) below showed a homogeneous silicon distribution both on the whole sphere and the cross-section images.

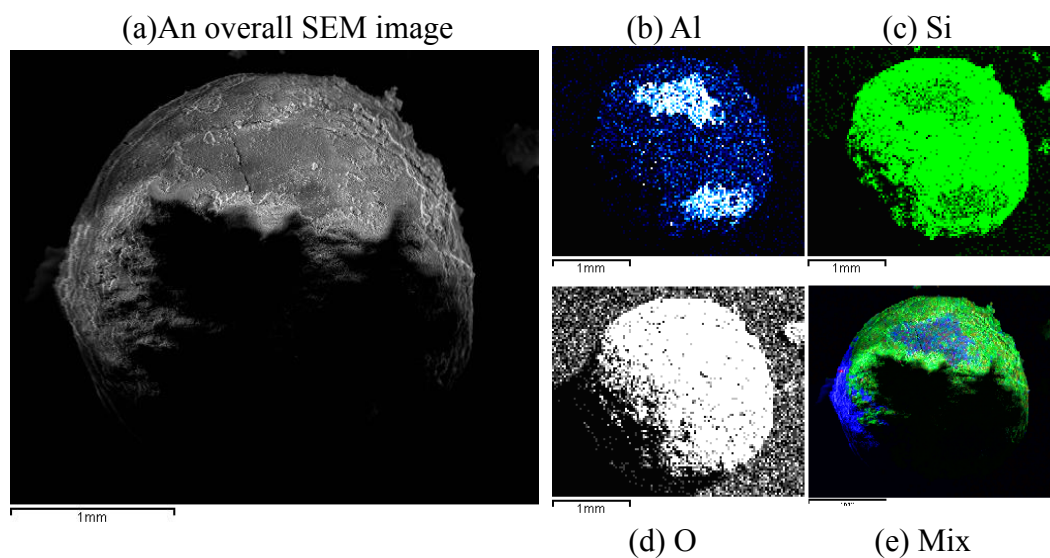


**Figure 6.53 Mapping of a whole coated  $\gamma\text{-Al}_2\text{O}_3$  sphere**

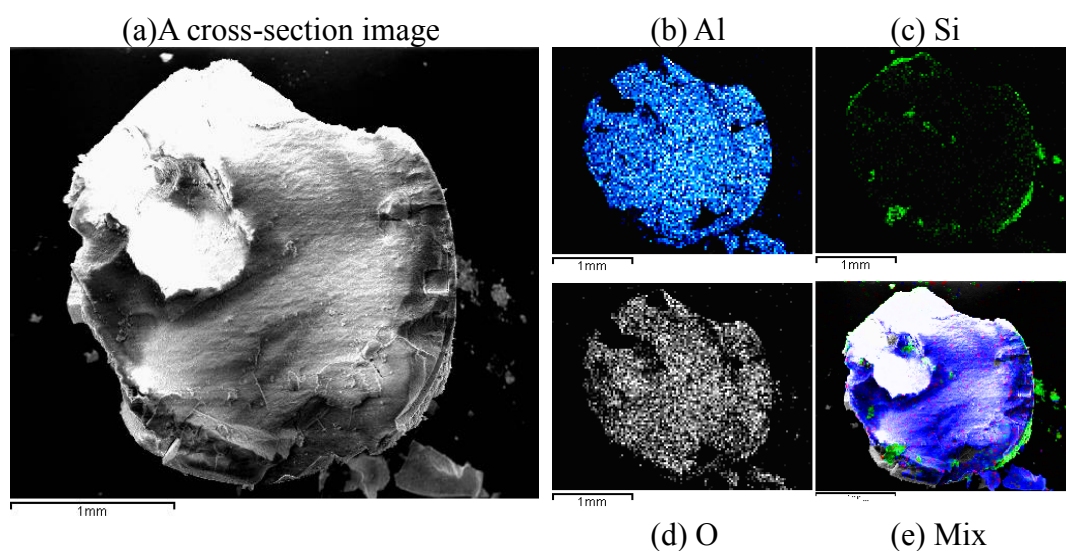


**Figure 6.54 Mapping of the cross-section of a coated  $\gamma\text{-Al}_2\text{O}_3$  sphere**

The two extra powders made from 15 ml precursor solutions ( $\alpha\text{-}$  and  $\gamma\text{-Al}_2\text{O}_3$ ) were observed and found to be different as well (Figure 6.55): in the  $\alpha\text{-Al}_2\text{O}_3$  batch, there are faceted micron-

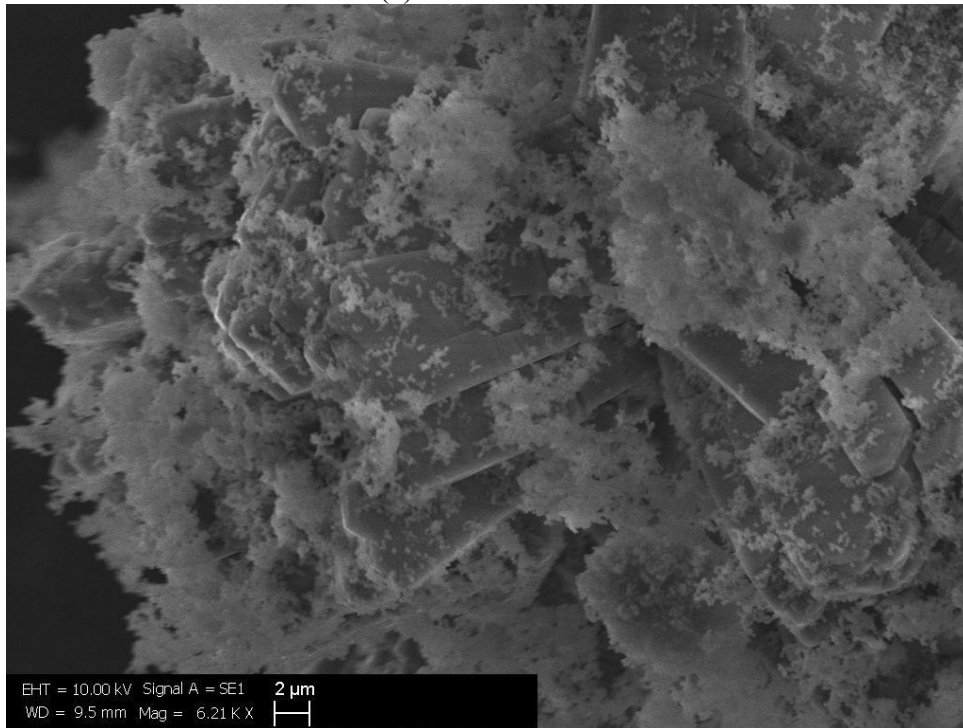
sized particles; while in the  $\gamma$ - $\text{Al}_2\text{O}_3$  batch, the morphology looked the same as the coated  $\gamma$ - $\text{Al}_2\text{O}_3$  surface.

From all of the analyses of the coated  $\gamma$ - $\text{Al}_2\text{O}_3$ , there is a large quantity of fluffy layers found, which are likely to be a kind of silicon dioxide. The catalytic application of coated  $\gamma$ - $\text{Al}_2\text{O}_3$  may not be successful because of it. Therefore it might not be a good option to use  $\gamma$ - $\text{Al}_2\text{O}_3$  for the ZSM-5 coating.

#### **6.5.4.3 Discussion**

According to the above characterization, the ZSM-5 coating was successfully achieved on the  $\alpha$ - $\text{Al}_2\text{O}_3$  spheres; although there were a few irregularly shaped ZSM-5 crystals. Coated  $\gamma$ - $\text{Al}_2\text{O}_3$  samples were found covered with a relatively large quantity of fluffy nano-sized particles which are likely to be a type of silicon dioxide, as detected by the XRD. ZSM-5 particles may be present, as indicated by very weak XRD peaks, but probably as a minority or with a very small crystal sizes and therefore not detected by XRD. The formation of different layers on the  $\alpha$ - and  $\gamma$ - $\text{Al}_2\text{O}_3$  may be because aluminum may leach from the support under the synthesis conditions. People reportedly to coat the  $\gamma$ - $\text{Al}_2\text{O}_3$  with a thin layer of mesoporous silica [26], which will reduce the risk of crack formation due to stress under the synthesis conditions. The  $\alpha$  and  $\gamma$ - $\text{Al}_2\text{O}_3$  supports clearly have an influence over the formation of coatings at their surface.

(a) From the  $\alpha$ -batch



(b) From the  $\gamma$ -batch

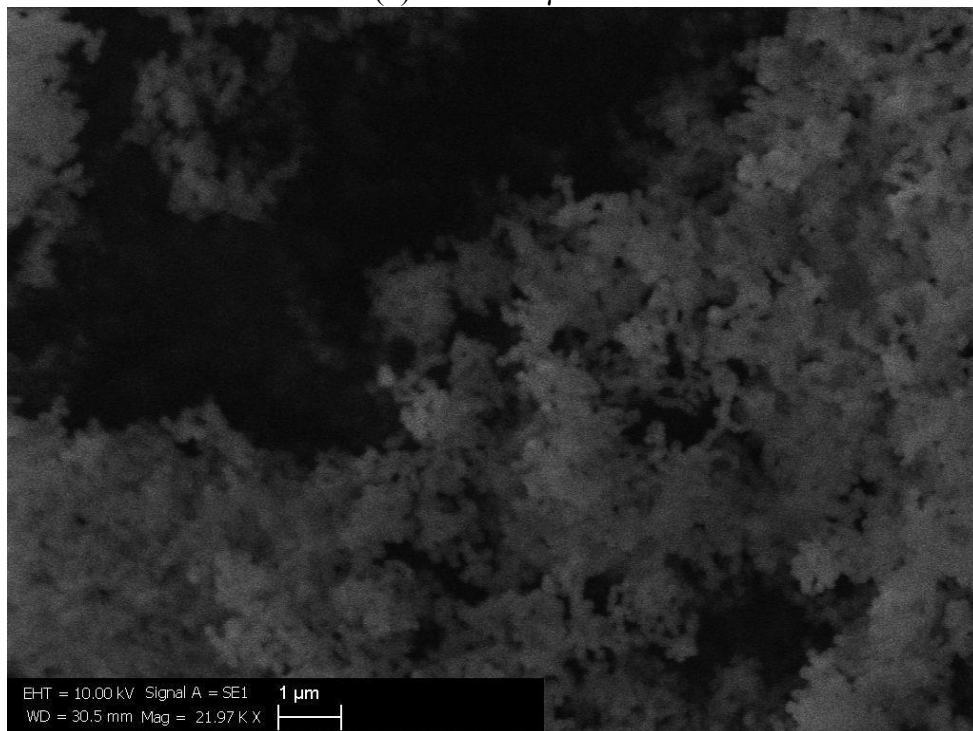


**Figure 6.55** the morphology of the extra powders from the  $\alpha$ - $\text{Al}_2\text{O}_3$  and  $\gamma$ - $\text{Al}_2\text{O}_3$  batches

## 6.5.5 Zeolite X/Y coating with silica spheres

### 6.5.5.1 Results

The zeolite X/Y coated silica samples were characterized by XRF and XRD (provided by JM). XRF results (**Table 6.33**) showed the silica to alumina ratio in the coated silica spheres and zeolite powder from batch 1 and 2. The XRD results identified the samples as quartz and cristabolite; sample 2 as faujasite, crystallite size 47.3 nm; sample 3 as quartz and sample 4 as faujasite, crystallite size 50.8 nm.

**Table 6.33 XRF analysis results**

	Sample 1	Sample 2	Sample 3	Sample 4
Si content	40.47%	18.64%	40.26%	18.50%
Al content	2.63%	13.41%	3.28%	13.39%
Na content	0.79%	11.23%	1.38%	11.13%
Calculated Si content	0.0144	0.0066	0.0143	0.0066
Calculated Al content	0.0005	0.0025	0.0006	0.0025
<b>Silica to alumina ratio</b>	<b>29.56</b>	<b>2.67</b>	<b>23.58</b>	<b>2.65</b>

Sample 1 - Silica spheres from batch 1  
Sample 2 - Zeolite powder from batch 1  
Sample 3 - Silica spheres from batch 2  
Sample 4 - Zeolite powder from batch 2

The two batches of zeolite X/Y coated silica spheres were tested in the hexane oxidation with short (30 min) and longer (4 h) reaction times respectively. The results were given in **Table 6.34**. As a comparison, according to **Table 6.35**, the terminal selectivity in a blank reaction in the same reaction time was 0 (30 min) and 4% (4 h).

**Table 6.34 Zeolite X coated silica, 130°C, 3 bar O<sub>2</sub>, 25 ml *n*-hexane, 600 rpm.**

Reaction Time	Conv. (%)	Selectivity (%)				
		Ketones	Alcohols	Hexanoic acid	Others	1-hexanol
Batch 1						
30 min	0.03	43	42	0	19	16
4 h	0.29	17	20	0	63	6
Batch 2						
30 min	0.04	36	40	0	22	13
4 h	0.60	11	21	0	68	7

**Table 6.35 Blank reactions, 130°C, 3 bar O<sub>2</sub>, 25 ml *n*-hexane, 600 rpm, single reaction**

Reaction Time (h)	Conv. (%)	Selectivity (%)				
		Ketones	Alcohols	Hexanoic acid	Others	1-hexanol
0.5	0					
4	0.074	23	17	0	60	4

### 6.5.5.2 Discussion

Comparing **Table 6.34** with **Table 6.35**, it was found that the terminal selectivity was much higher than the blank reaction, especially for short reaction times. In a 30 min reaction, the terminal selectivity was 16%, with batch 1, which was even higher than the highest terminal selectivity reported before (up to 13% ) with the zeolite A coated silica. With a longer reaction time, while the terminal selectivity decreased to 6-7%, the conversion was highly increased. The zeolite X/Y coated silica sample was active and selective, which indicates the zeolite X/Y coating works in the hexane oxidation.

### 6.5.6 Zeolite A in hexane oxidation

In section 6.5.1 and 6.5.2 it was concluded that, with 4Å pore size, zeolite A was not applicable for the decane molecule to pass through. However it is still worth trying in the smaller hexane molecule oxidation. In this section, coated samples with different synthesis times or amounts of supports were tested for hexane oxidation in the liquid phase. For comparison, some of the silica spheres were treated at the same pH and then calcined. The results of all the reactions are given below in Table 6.36.

**Table 6.36 130°C, 3 bar O<sub>2</sub>, 25 ml *n*-hexane, stir speed 2, single reaction (4 h), SiO<sub>2</sub> spheres and 24 h/1 g zeolite A coated SiO<sub>2</sub> spheres.**

Catalyst	Reactor	Conv.(%)	Selectivity (%)				
			Ketones	Alcohols	Acid	Others	1-hexanol
silica	C	0.38	20	13	0	67	5
Bases treated silica	B	0.52	13	17	0	70	5
8 h 1g silica	B	0.70	15	15	0	70	4
8 h 3g silica	C	0.53	14	15	0	71	6
12 h 1g silica	B	0.13	31	22	0	47	13
12 h 3g silica	C	0.24	24	18	0	58	10
24 h/1 g silica	B	0.61	14	12	1	73	4

From the above table, the 12 h/1 g batch shows some promise for terminal selectivity. And compared to the reaction result with only the silica sphere, it appears that the conversion with the coated sample was lower than with the silica spheres only. This is equivalent to the teabag technology principle. Therefore, the synthesis was repeated several times and tested again. All

the results are given in **Table 6.37**.

**Table 6.37 130°C, 3 bar O<sub>2</sub>, 25 ml *n*-hexane, stir speed 2, single reaction (4 h), SiO<sub>2</sub> spheres and zeolite-A coated SiO<sub>2</sub> spheres.**

Catalyst	Reactor	Conv.(%)	Selectivity (%)				
			Ketones	Alcohols	Hexanoic acid	Others	1-hexanol
Batch 1	B	0.26	17	14	1	68	7
Batch 2	B	0.13	31	22	0	47	13
Batch 3	B	0.11	28	23	0	49	11
Batch 4	B	0.46	12	13	0	75	5
Batch 5	B	0.50	10	12	0	78	5

It was found that some of the batches showed an interesting terminal selectivity. Some of the batches were analysed with XRD to check the structure of the samples. From **Figure 6.56**, it can be seen that the intensity ratios of first two major peaks are different for the three samples. **Figure 6.57** is a standard XRD pattern for the zeolite A structure; however, our products appear to have a additional peak at lower 2 Theta which does not seem to be from the zeolite A structure; all the other peaks observed are also present in the zeolite A structure. The source of the first strong peak is unknown. However, the ratio between the first and second peak changed in the three batches. It is notable that the batch 3, which showed 11% terminal selectivity, has a quite different 1<sup>st</sup>/2<sup>nd</sup> peak ratio from the others.

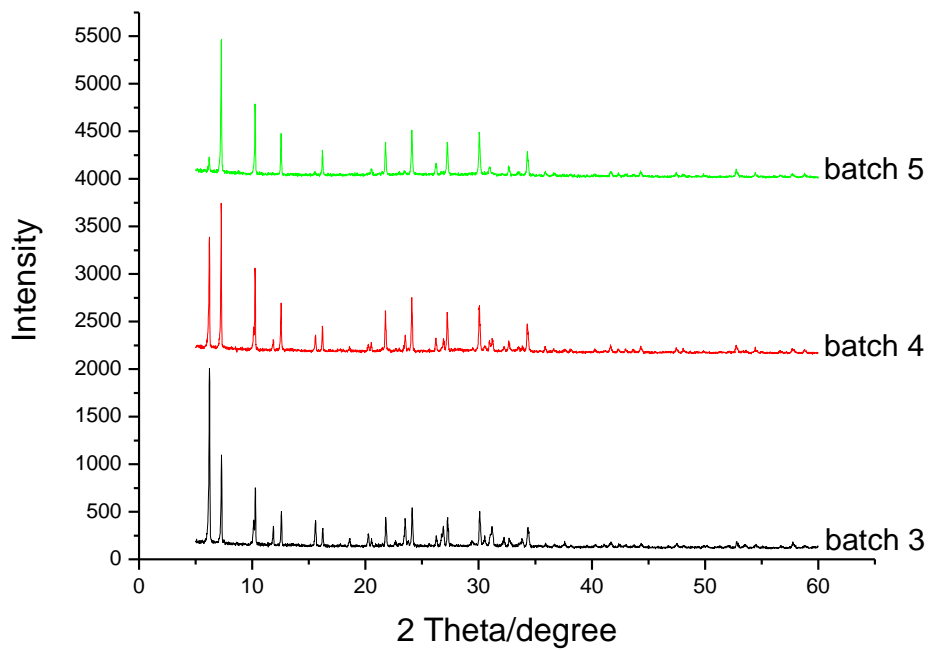


**Figure 6.56 XRD analysis for three batches of 12 h synthesized zeolite A powder**

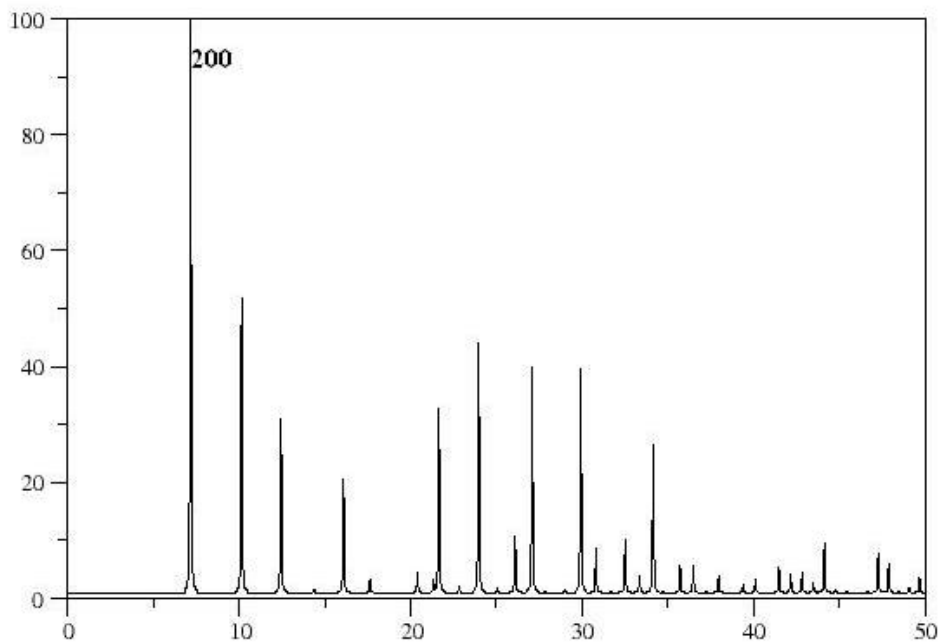


**Figure 6.57 The standard XRD pattern of zeolite A [27]**

## 6.6 Conclusions

This chapter showed the most focused work in this research, in which different types of zeolites and zeolitic material coatings were synthesized onto substrate catalysts, including zeolite 4A, silicalite-1, ZSM-5, zeolite X/Y. Characterization and catalytic tests were performed correspondingly with *n*-decane or *n*-hexane.

Application of zeolite A coating with silica powder support did not produce a significant increase of the C<sub>10</sub> terminal selectivity, but many catalysts show a high terminal selectivity in the form of cracked acids. This probably has some promise as it can be expected that a wide range of terminally oxidized linear alkanes could be achieved. SiO<sub>2</sub> and MgO based catalysts coated by a direct template-free zeolite membrane preparation method was concluded not with the desired zeolite coating. Instead, an amorphous SiO<sub>2</sub> overlayer was formed on the surface. However the coated samples do show increased activity in both liquid and gas phase reactions. In the liquid phase, the coated SiO<sub>2</sub> based catalysts showed a conversion increase by 1-2%, however the terminal selectivity is not affected. As the coated SiO<sub>2</sub>-based catalysts have low surface area (**Table 4**), it seems that the activity per unit area is quite high. The treated MgO-based catalysts in the gas phase reactor showed some good activity.

Zeolite A coated alumina catalysts showed a C<sub>10</sub> terminal selectivity always below 2.8%, with the conversion of reactions between 0.07% - 0.14%. The conversion is almost equivalent to the blank reactions. However the coatings changed the product distribution (**Figure 6.24 to 6.26**), as compared to the blank reactions. Generally the selectivity for the shortened acids decreased, especially for the hexanoic acid and heptanoic acid, though the pentanoic acid increased. For the terminal position, there is not much change in total, however the decanoic acid decreased,

while the selectivity for decanols increased slightly by 1%. This means that the zeolite A does not work for the primary position; instead, it seems it works in stopping the cracking in the position 3 and 4 and helping decanol production in these positions. Probably the pore size of the zeolite A (around 4 Å) is a little bit small for the CH<sub>3</sub> groups (around 4.3 Å), while the smaller group CH<sub>2</sub> is more suitable in its pore size.

Silicalite-1 coating was applied to both  $\alpha$ - and  $\gamma$ -alumina sphere supports with Rh or Au metal loaded as the active centres. It can be concluded that a 6-8  $\mu\text{m}$  thick continuous silicalite-1 coating layer was successfully synthesized on the 3%Au/ $\gamma$ -Al<sub>2</sub>O<sub>3</sub>. However, the sample was not found to work well as a teabag catalyst for the liquid phase oxidation of decane (**Table 6.29**). The terminal selectivity change was minimal. This may be due to the activity of the silicalite-1 in the liquid phase.

ZSM-5 coating was successfully achieved on the  $\alpha$ -Al<sub>2</sub>O<sub>3</sub> spheres, although there were a few irregularly shaped ZSM-5 crystals. Coated  $\gamma$ -Al<sub>2</sub>O<sub>3</sub> samples were found covered with a relatively large quantity of fluffy nano-sized particles which are likely to be a type of silicon dioxide, as detected by the XRD. ZSM-5 particles may be present, as indicated by very weak XRD peaks, but probably as a minority or with a very small crystal size and therefore not detected by XRD. The formation of different layers on the  $\alpha$ - and  $\gamma$ -Al<sub>2</sub>O<sub>3</sub> may be because aluminum may leach from the support under the synthesis conditions. It was found that the  $\alpha$  and  $\gamma$ -Al<sub>2</sub>O<sub>3</sub> supports clearly have an influence over the formation of coatings at their surface.

Zeolite X and Y coated silica catalysts tested with n-hexane liquid phase oxidation showed much higher terminal selectivity than the blank reaction, especially with a short reaction time.

In a 30 min reaction, the terminal selectivity was 16%, while the terminal selectivity for the blank reactions was 0-9%. With a longer reaction time, the terminal selectivity decreased to 6-7%.

Zeolite 4A coated silica spheres were also found to work in raising the terminal selectivity in hexane liquid phase oxidation. A stable 1-hexanol selectivity of >4% was observed with 4 h reaction. It was also observed that the synthesis time of the coating affected the reaction. With a coating synthesis time of 12 h, the maximum 1-hexanol selectivity could reach 13%.

## 6.7 References

- [1] N. van der Puil, F.M. Dautzenberg, H. van Bekkum, J.C. Jansen, *Microporous and Mesoporous Materials*, 27, (1999), 95.
- [2] Collier, Paul John, Golunski, Stanislaw Edmund, U.S. Patent No.0032628, 2005.
- [3] R.N. Devi, F.C. Meunier, T. Le Goaziou, C. Hardacre, P.J. Collier, S.E. Golunski, L.F. Gladden, M.D. Mantle, *Journal of Physical Chemistry C*, 112(29), (2008), 10968.
- [4] E.R. Geus, A.E. Jansen, J. Schoonman, H. van Bekkum, *Catalysis and Adsorption by Zeolites*, *Studies in Surface Science and Catalysis*, vol.65, Elsevier, Amsterdam, ( 1991), 451
- [5] M. Matsukata, *Chemical Communications*, (1996), 1441.
- [6] P. Wenqin, S.Ueda and M.Koizumi, *Proceedings of the 7<sup>th</sup> International Zeolite Conference* (Eds. Y. Murakami, A. Lijima and J.W.Ward), Elsevier, Tokyo, (1986), 177.
- [7] L. Gora, K. Streletzky, R.W. Thompson, G..D.J. Phillis, *Zeolites* 18, (1997), 119.
- [8] T. Cetin, M. Tatlier, A. Erdem-Senatalar, U. Demirler, M. Urgan, *Microporous and Mesoporous Materials*, 47, (2001), 1.

- [9] O. Andac, S.M. Telli, M. Tatlier, A. Erdem-Senatalar, *Microporous and Mesoporous Materials*, 88, (2006), 72.
- [10] Z. Zhou, J. Yang, Y. Zhang, L. Chang, W. Sun, J. Wang, *Separation and Purification Technology*, 55, (2007), 392.
- [11] Z. Wang, J. Hedlund, J. Sterte, *Microporous and Mesoporous Materials*, 52, (2002), 191.
- [12] M. Tatlier, M.Demir, B.Tokay, A.Erdem-Senatalar, L.Kiwi-Minsker, *Microporous and Mesoporous Materials*, 101, (2007), 274.
- [13] J.C. Jansen, J.H. Koegler, H. van Bekkum, H.P.A. Calis, C.M. van den Bleek, F. Kapteijn, J.A. Moulijn, E.R. Geus, N. van der Puil, *Microporous and Mesoporous Materials* 21, (1998), 213.
- [14] H. Kalipcilar, A. Culfaz, *Microporous and Mesoporous Materials* 52, (2002), 39
- [15] K. Aoki, K. Kusakabe, S.Morooka, *Journal of Membrane Science*, 141, (1998), 197.
- [16] P. Collier, S. Golunski, C. Malde, J. Breen, R. Burch, *Journal of the American Chemistry Society*, 125, (2003), 12414.
- [17] N. Nishiyama, K. Ichioka, D. Park, Y. Egashira, K. Ueyama, L. Gora, W. Zhu, F. Kapteijn, J.A. Moulijn, *Industrial Engineering Chemistry Research*, 43, (2004), 1211.
- [18] J. Park, B.C. Kim, S.S. Park, H.C. Park, *Journal of Materials Science Letters*, 20, (2001), 531.
- [19] Y. Yan, M.E. Davis, G.R. Gavalas, *Industrial Engineering Chemistry Research*, 34, (1995), 1652
- [20] B.J. Schoeman, A. Erdem-Senatalar, J. Hedlund, J. Sterte, *Zeolites*, 19, (1997), 21.
- [21] E.R. Genus, H.van Bekkum, *Zeolites*, 15(4), (1995), 333
- [22] F. Jareman, C. Andersson, J. Hedlund, *Microporous and Mesoporous Materials*, 79, (2005), 1.

- [23] P. Siva Sankar Reddy, N. Pasha, M.G.V. Chalapathi Rao, N. Lingaiah, I. Suryanarayana, P.S. Sai Prasad, *Catalysis Communications*, 8, (2007), 1406.
- [24] D.C. Vu, M. Miyamoto, N. Nishiyama, S. Ichikawa, Y. Egashira, K. Ueyama, *Microporous and Mesoporous Materials*, 115, (2008), 106
- [25] B. Modén, B. Zhan, J. Dakka, J. G. Santiesteban, E. Iglesia, *Journal of Physical Chemistry*, 111, (2007), 1402.
- [26] M.R. Othman, S.C. Tan, S. Bhatia, *Microporous and Mesoporous Materials*, 121, (2009), 138.
- [27] Web: database of zeolites, <http://www.iza-structure.org/databases/>.

# CHAPTER 7

## *Conclusions*

---

## CONCLUSIONS

---

This thesis describes the searching, preparation, characterization and catalytic evaluation of active catalysts for the terminal selectivity of long chain linear alkanes. The focus of the thesis is the preparation, characterization and catalytic evaluation of the shape-selective materials, including the organic material cyclodextrins, and the inorganic materials, zeolite and zeolitic membranes. Prepared catalysts were performed with *n*-decane or *n*-hexane as models to produce the terminal products 1-decanol, 1-hexanol, decanoic acid and hexanoic acid. The conclusions of the research to date were summarized as follows.

Firstly the studies with the Andrews glass reactor were presented for the purpose of reproducing the best selective results available in the literature published by Thomas [1-4] and Iglesia [5, 6] for the oxidation of *n*-hexane in liquid phase. However Thomas et al. did not calculate the autoxidation with the ALPO catalysts. Iglesia's work was more crucial in this area. The time on-line blank reaction results showed similar terminal selectivities to Iglesia's work in autoxidation, with the terminal selectivity stable at 5%-9%. However, the terminal selectivity with Mn-ZSM5 was still very low (~0). Iglesia's high terminal selectivity with Mn-ZSM5 could not be reproduced.

A comparison between the Andrews glass reactor and the Parr stainless steel reactor showed that the autoxidation reactions performed higher conversion but lower terminal selectivity in the stainless steel reactor than the glass reactor, which indicates the stainless steel reactor itself may have some activity in the oxidation reaction.

Various catalysts have been evaluated for decane oxidation in the project, e.g. 5 w.t.% Au/TiO<sub>2</sub>, 2.5 w.t.% Au - 2.5 w.t.% Pd/SiO<sub>2</sub>. Most of the catalysts showed very low conversion and very poor terminal selectivity. Increasing the temperature leads to higher conversion but results in more cracked products and less selectivity for oxygenated C<sub>10</sub> products. **Figure 7.1** showed the activity of the auto-oxidation and the activity of a range of catalysts. It was found that the most active catalyst was 5 w.t.% Au/TiO<sub>2</sub>. However, these catalysts did not show good terminal alcohol selectivity (<3%); whereas the cracked acid selectivity was high (32.0%).

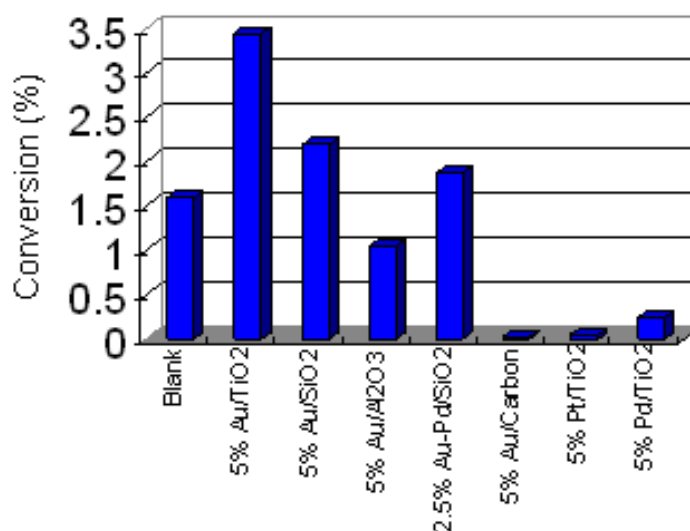


**Figure 7.1 – Conversion with different catalysts (reaction conditions: 110°C, 10 g *n*-decane, 0.05 g catalyst, 15 bar O<sub>2</sub>, 600 rpm, stainless steel reactor).**

Cyclodextrins were investigated as an organic shape-selective material to coat the Au/SiO<sub>2</sub> catalysts in **Chapter 5**. Addition of CDs alone without the catalyst decreased the conversion but no trend in terminal selectivity was observed. With the CD covered Au/SiO<sub>2</sub> catalyst, a decrease in conversion has been observed compared to the blank reaction; however the changes in terminal selectivities are still limited (1-2%) and considered to be within the experimental errors. To conclude, the CD covered catalysts, which were prepared by the direct impregnation method, did not play an important role in increasing the terminal selectivity.

Finally, the most important studies in the thesis was the synthesis of different types of zeolite coatings onto substrate catalysts, which was the so called 'teabag technology'. Zeolite 4A, silicalite-1, ZSM-5, zeolite X/Y were successfully synthesized. Characterization and catalytic evaluations were performed correspondingly with *n*-decane or *n*-hexane.

Application of zeolite A coating with silica powder support did not produce a significant increase of the C<sub>10</sub> terminal selectivity, but many catalysts show a high terminal selectivity in the form of cracked acids. This probably has some promise as it can be expected that a wide range of terminally oxidized linear alkanes could be achieved. SiO<sub>2</sub> and MgO based catalysts coated by a direct template-free zeolite membrane preparation method was concluded not with the desired zeolite coating. Instead, an amorphous SiO<sub>2</sub> overlayer was formed on the surface. However the coated samples do show increased activity in both liquid and gas phase reactions. In the liquid phase, the coated SiO<sub>2</sub>-based catalysts showed a conversion increase by 1-2%, however the terminal selectivity is not affected. As the coated SiO<sub>2</sub>-based catalysts have low surface area, it seems that the activity per unit area is quite high. The treated MgO based catalysts in the gas phase reactor showed some good activity.

Zeolite A coated alumina catalysts showed a C<sub>10</sub> terminal selectivity was always below 2.8%, with the conversion of reactions between 0.07% - 0.14%. The conversion is almost equivalent to the blank reactions. However the coatings changed the product distribution (**Figure 6.24 to 6.26**), as compared to the blank reactions. Generally the selectivity for the shortened acids decreased, especially for the hexanoic acid and heptanoic acid, though the pentanoic acid increased. For the terminal position, there is not much change in total, however the decanoic

acid decreased, while the selectivity for decanols increased slightly by 1%. This means the zeolite A does not work for the primary position; instead, it seems it works in stopping the cracking in positions 3 and 4 and helping the decanol production in these positions. Probably the pore size of the zeolite A (around 4 Å) is a little bit small for the CH<sub>3</sub> groups (around 4.3 Å), while the smaller group CH<sub>2</sub> is more suitable in its pore size.

Silicalite-1 coating was applied to both  $\alpha$ - and  $\gamma$ -alumina sphere supports with Rh or Au metal loaded as the active centres. It can be concluded that a 6-8  $\mu\text{m}$  thick continuous silicalite-1 coating layer was successfully synthesized on the 3%Au/ $\gamma$ -Al<sub>2</sub>O<sub>3</sub>. However, the sample was not found to work well as a teabag catalyst for the liquid phase oxidation of decane (**Table 6.29**). The terminal selectivity change was minimal. This may be due to the activity of the silicalite-1 in the liquid phase.

ZSM-5 coating was successfully achieved on the  $\alpha$ -Al<sub>2</sub>O<sub>3</sub> spheres; although there were a few irregularly shaped ZSM-5 crystals. Coated  $\gamma$ -Al<sub>2</sub>O<sub>3</sub> samples were found covered with a relatively large quantity of fluffy nano-sized particles which are likely to be a type of silicon dioxide, as detected by the XRD. ZSM-5 particles may be present, as indicated by very weak XRD peaks, but probably as a minority or with a very small crystal size and therefore not detected by XRD. The formation of different layers on the  $\alpha$ - and  $\gamma$ -Al<sub>2</sub>O<sub>3</sub> may be because aluminum may leach from the support under the synthesis conditions. It was found that the  $\alpha$  and  $\gamma$ -Al<sub>2</sub>O<sub>3</sub> supports clearly have an influence over the formation of coatings at their surface.

Zeolite X and Y coated silica catalysts tested with *n*-hexane liquid phase oxidation showed much higher terminal selectivity than the blank reaction, especially with a short reaction time.

In a 30 min reaction, the terminal selectivity was 16%, while the terminal selectivity for the blank reactions was 0-9%. With a longer reaction time, the terminal selectivity decreased to 6-7%.

Zeolite 4A coated silica spheres were also found to work in raising the terminal selectivity in hexane liquid phase oxidation. A stable 1-hexanol selectivity of >4% was observed with a 4 h reaction. It was also observed that the synthesis time of the coating affected the reaction. With the coating synthesis time of 12 h, the maximum 1-hexanol selectivity could reach 13%.

## References

- [1] J.M. Thomas, R. Raja, G. Sankar, R. G. Bell, *Studies in Surface Science and Catalysis*, 130, (2000), 887.
- [2] R. Raja, G. Sankar, J.M. Thomas, *Angewandte Chemistry*, 39, (2000), 231.
- [3] J.M. Thomas, R. Raja, G. Sankar, R.G. Bell, *Accounts of Chemical Research*, 34, (2001), 191.
- [4] R. Raja, J.M. Thomas, *Journal of Molecular Catalysis A*, 3, (2002), 181.
- [5] B. Modén, B. Zhan, J. Dakka, J. G. Santiesteban, E. Iglesia, *Journal of Physical Chemistry*, 111, (2007), 1402.
- [6] B. Zhan, B. Modén, J. Dakka, J.G. Santiesteban, E. Iglesia, *Journal of Catalysis* 245, (2007), 316.